NTNU

Norwegian University of
Science and Technology

Influence of Hole Trajectory and Direction on MWD Survey Errors

Syed Muhammad Reza Hassan

Petroleum Engineering
Submission date: January 2018
Supervisor: Sigbjørn Sangesland, IGP
Co-supervisor: Bjørn Astor Brechan, IGP

Norwegian University of Science and Technology
Department of Geoscience and Petroleum

Summary

Wellbore positioning is important to meet directional drilling objectives. Inaccurate wellbore surveys can lead to wellbore collision, failure to penetrate thin reservoir sections and drilling of relief wells etc. Such consequences make accurate wellbore positioning essential. Wellbore survey data needed to calculate wellbore position at any point is commonly obtained through MWD tools.

The measurement accuracy of frequently used MWD tools usually decreases with increasing hole inclination and depth. This introduces uncertainties in wellbore position estimates. The Industry Steering Committee for Wellbore Survey Accuracy (ISCWSA) has proposed several survey error models to estimate Wellbore Position Uncertainty (WPU) at any depth along the well. The parameters in model's sensitivity to direction and nature of trajectory has not been discussed before. Therefore, this thesis has analyzed the behavior of all major MWD survey error sources in vertical, build up and horizontal sections of the three wells drilled in North/South, North/East and East/West directions.

A software model has been developed to analyze the influence of various MWD survey error sources in different drilling directions. The model is based on mathematical equations presented in Non-mag and Mag-corr ISCWSA MWD error models. The error terms from both are modeled to study the impact of each error source on measurement and position uncertainties. Finally, a comparison of the two survey error models is presented.

As drilling progresses, various survey errors tend to push the well path away from the planned course. Some dominate the process while others hardly influence. For example, results in this thesis show that magnetic axial drill string interference is least effective in North/South well, but is the major uncertainty source in East/West well. Similarly, it has been observed that an error source can be least effective in the vertical section and dominate the total uncertainty budget in the deviated part, for example BHA sag. The third category of error sources has been observed to be completely independent of inclination or azimuth, for example declination error. This unique behavior of different error sources is totally governed by their respective weighting functions.

Results further show that the effect of an error source on measurement and position uncertainty is not necessarily the same. Large azimuth errors may not have an equally large impact on position uncertainty and vice versa. Also, the effectiveness of an error source is

typically dependent upon its effect on total measurement or position error budget. An error source can cause large individual position uncertainty without having any significant influence on total position uncertainty budget.

This thesis can be further extended to include the effects of magnetic mud on wellbore position uncertainty. Specific error terms for this purpose should be formulated to model this effect. Also, a similar analysis can be made for Gyroscopic tools utilizing its own error terms.

Acknowledgment

This thesis marks the successful completion of my Master's degree in Petroleum Engineering with specialization in Drilling Technology. It has been written at the Department of Geoscience & Petroleum, Norwegian University of Science & Technology (NTNU), Trondheim, during Autumn 2017 in close collaboration with the faculty at NTNU.

I thank my supervisor, Professor Sigbjørn Sangesland for providing the opportunity to work on this project. I am also grateful to my co-supervisor, Assistant Professor Bjørn Brechan for his continuous support and cooperation. His guidance was instrumental in meeting the thesis objectives. I also sincerely acknowledge Erik Nyrnes from Statoil for his valuable time in making this project a success. He deserves the credit for suggesting the problem statement of this thesis and staying involved in the technical discussions related to the project.

I extend my gratitude to my family and friends who have always supported me. This would not have been possible without the presence of these wonderful people in my life. Last but not the least, I thank the institute (NTNU) for providing the necessary facilities to write this thesis, especially the software package Landmark™ provided by Halliburton. It has been an excellent learning tool for students specializing in Drilling technology at NTNU.

Table of Contents

List of Figures

Nomenclature

EOU	Ellipse of Uncertainty
AMIL	Magnetic Axial Drillstring Interference
MAL	Misalignment
WPU	Wellbore Position Uncertainty
ISCWSA	Industry Steering Committee for Wellbore Survey Accuracy
BHA	Bottom Hole Assembly
MDI	Magnetic Dip Angle Intensity
MFI	Magnetic Field Intensity

Symbols

I	Inclination
A	Wellbore Azimuth
Am	Magnetic Azimuth
Θ	Dip Angle
B_t	Total Magnetic Field Strength
S	Systematic Propagation mode
R	Random Propagation mode
G	Global Propagation mode
ϕ	Dog Leg Severity
α	Tool Face Angle
φ	Latitude

Chapter 1. Introduction

Petroleum Industry's success in exploring remote reservoirs, controlling blowout wells, drilling multiple wells from a single offshore platform have all been made possible due to the developments in directional drilling. It has not only helped reduce offshore drilling cost but also enhanced reservoir production through horizontal drilling. One of the many challenges associated with directional drilling is the accurate estimation of directional wellbore's position which is usually more uncertain than vertical wells.

Measurement While Drilling (MWD) tools are very common in the Petroleum industry to obtain downhole measurements of drilling parameters. This thesis will be dealing with only magnetic MWD measurements, so MWD will implicitly refer to magnetic MWD from now onwards. A set of sensors in the complete MWD package reports wellbore position at the survey stations. This position is mostly not the actual wellbore position due to different MWD survey error sources.

The nature and effect of these error sources on measurements and position uncertainty depends on well's geographical location, trajectory, drilling direction etc. All these together contribute in adding to the total Wellbore Position Uncertainty (WPU). To properly address the concern of WPU, a comprehensive understanding of these error sources in different drilling conditions is necessary.

1.1 MWD Survey Error Modeling

To have a quantitative estimate of the effect of an error source, The Industry Steering Committee on Wellbore Survey Accuracy (ISCWSA) has proposed different tool specific survey error models. These error models are used to study the effect of different error sources through a set of mathematical equations. In addition to these equations, it consists of error magnitude along with its propagation mode. Magnetic MWD error model implemented in this thesis is based on the mathematical equations presented by Williamson in [6].

1.2 Objective

The objective of this thesis is to analyze the behavior of all major MWD error sources as a function of hole inclination and azimuth. First, the effect of an error source on measurement uncertainty [Depth, Inclination, Azimuth] will be analyzed followed by its influence on WPU.

1.3 Overview

The thesis presents a detailed theoretical background of MWD measurements, errors associated with them and their effect on measurement and position uncertainties respectively.

Chapter 2 introduces fundamental principles on which MWD measurements are based including the theory and mathematical equations involved in the process. It further presents the detailed process of calculating wellbore position coordinates from MWD measurements utilizing earth's gravitational and magnetic field.

Chapter 3 deals with the basic calculations and representation of Wellbore Position Uncertainty (WPU) followed by a detailed theoretical discussion on all major MWD survey error sources, their likely impact on wellbore position and ways to mitigate them.

The effect of the MWD survey error sources is modeled using survey error models. *Chapter 4* introduces the basic components of a standard survey error model and the mathematical principles followed in calculating the effect of these error sources on Wellbore Position Uncertainty (WPU).

Chapter 5 presents the methodology adopted to meet the thesis objectives. It also details the scheme of analysis followed to understand the behavior of these error sources in different hole sections and drilling directions.

Chapters 6,7 & 8 discuss the results. In Chapter 6, the effect of error sources is analyzed using the Non-mag error terms while in *Chapter 7* Mag-corr error terms have been implemented. *Chapter 8* then presents an overall comparison of the two error models. Finally, the results are concluded in *Chapter 9*.

Chapter 2. Introduction to MWD Directional Wellbore Surveying

The success of directional drilling is highly dependent on both the quality and frequency of measurements obtained. These measurements can either be obtained while drilling or by a Wire Line (WL). Wire Line will be less effective in avoiding collision since the measurement is often further behind the bit and the drill string has to be static while Measurement While drilling (MWD is continuous measurements during drilling. This method provides an effective way to not only avoid collision with neighboring wells, but also penetrate the target with required precision. Any compromise in the accuracy of the survey data can have severe consequences for the drilling operation. In normal drilling operations, a collision with any other well can be damaging for both wells. Similarly, if the reservoir is not penetrated at the planned target it can result into loss of recovery or if a relief well is not intersected at the desired target area, the objective of drilling a relief well might not be achieved.

The following chapter will discuss in detail the application of MWD survey measurements in predicting wellbore position. Section 2.1 will explain the basic measurement principles on which MWD tools operate. Section 2.2 explains all the direction notations used in expressing the wellbore position at a certain point. Section 2.3 presents an introduction to the measurements, and different models used to predict the time dependent behavior of earth's magnetic field. Section 2.4 introduces the principles of measuring earth's reference gravity field and its three vector components measured by an accelerometer. After the calculation of earth's magnetic and gravity components, section 2.5 explains how these measurements are converted to key wellbore surveying parameters i.e Inclination and Azimuth through the mathematical equations. Section 2.6 finally provides the details on the most common and accurate survey measurement method i.e Minimum Curvature. Utilizing the above information of inclination and azimuth, this method can be used to predict the position of a wellbore at a certain depth with its Northing, Easting and Vertical component.

2.1 MWD Measurement Principles

An MWD tool has a survey instrument mounted on a non-magnetic drill collar on purpose to avoid interference from the magnetic components in the Bottom Hole Assembly (BHA). The survey instrument that provides the relevant data for computing wellbore's position at a certain point contains a package of accelerometers and magnetometers. The data from this tool is

continuously transmitted using mud pulses and can be encoded using either positive mud pulse telemetry, negative mud pulse telemetry or continuous wave telemetry [1].

2.2 Wellbore Position Coordinate System

Wellbore position at any point can be expressed in an earth-centered coordinate system with its specific Northing, Easting and Vertical, commonly used as NEV. This coordinate system provides the position of a wellbore in latitudes, longitudes and depth either in absolute terms or relative to the surface location of the borehole [2]. The direction of the wellbore is defined by two parameters, Inclination and Azimuth. Inclination is defined as *"The vertical angle measured from the down direction- the down, horizontal and up directions have inclinations of 0°,90° and 180°* ". Where, Azimuth is defined as "*Angle measured clockwise from true north - the north, east, south and west directions have azimuths of 0°,90°,180° and 270°* [3]. Figure 2.1 displays how the inclination and azimuth are defined in the earth-centered coordinate system.

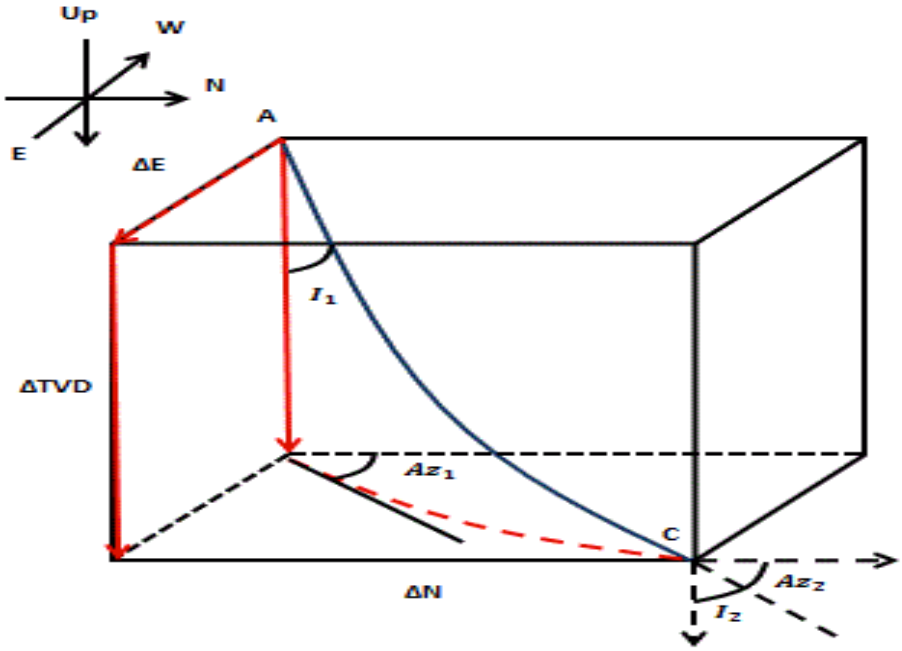

Figure 2.1 - Definition of Inclination and Azimuth in earth-centered coordinate system

Since the MWD tool continuously rotates as measurements are taken, therefore it is important to consider the amount of rotation while taking a measurement. High side direction is defined as "*The negative-V direction perpendicular to z-axis*" [2]. Whereas toolface angle is defined as "*The angle measured in a plane perpendicular to the drillstring between a reference direction*

on the drillstring and a fixed reference". This fixed reference in highly deviated wells is usually defined as the top of the borehole [3].

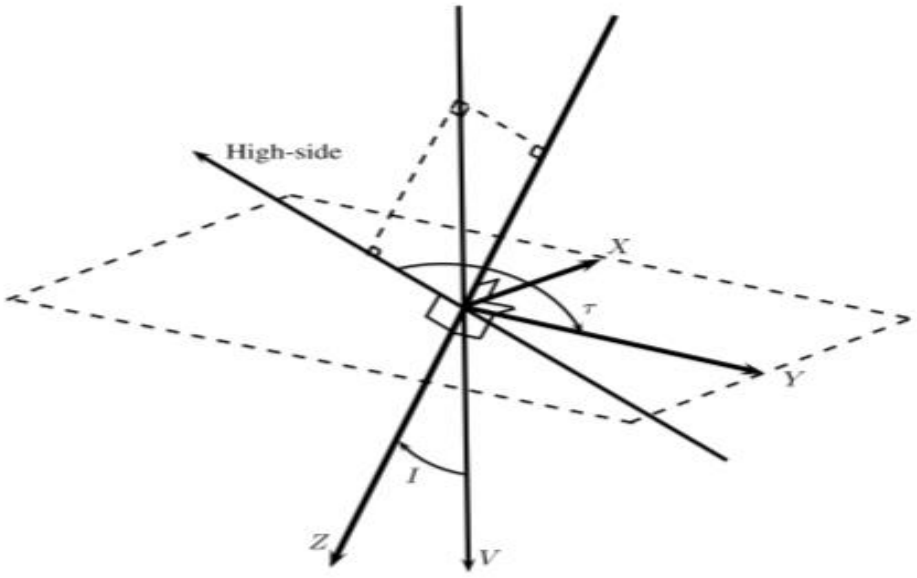

Figure 2.2 - Definition of High Side and Tool face angle [5]

2.3 Measurement of Earth's Magnetic Field

Earth's magnetic field originates from its core and serves as a reference for the compasses used. The magnetic field at any point can be completely defined by three vector components comprising of Declination angle, Dip angle and Field strength, also explained in Figure 2.3. Declination angle is measured clockwise from true north to magnetic north and is represented as **δ.** Dip angle **Θ** defines the attitude of magnetic field at any point and is measured as an angle between true north and magnetic field vector. The magnetic field strength **B** is usually measured in nano Teslas or micro Teslas, the greater is the Field strength the longer is the field vector **B** [1]**.** For calculation purpose, the vector is usually split into three orthogonal components pointing in x, y and z directions. The following three components can be calculated using the equations below [4].

$$B_x = B\cos\Theta\cos I\cos A_m\sin\alpha - B\sin\Theta\sin I\sin\alpha + B\cos\Theta\sin A_m\cos\alpha \qquad (2.1)$$

$$B_y = B\cos\Theta\cos I\cos A_m\cos\alpha - B\sin\Theta\sin I\cos\alpha - B\cos\Theta\sin A_m\sin\alpha \qquad (2.2)$$

$$B_z = B\cos\Theta\sin I\cos A_m + B\sin\Theta\cos I \qquad (2.3)$$

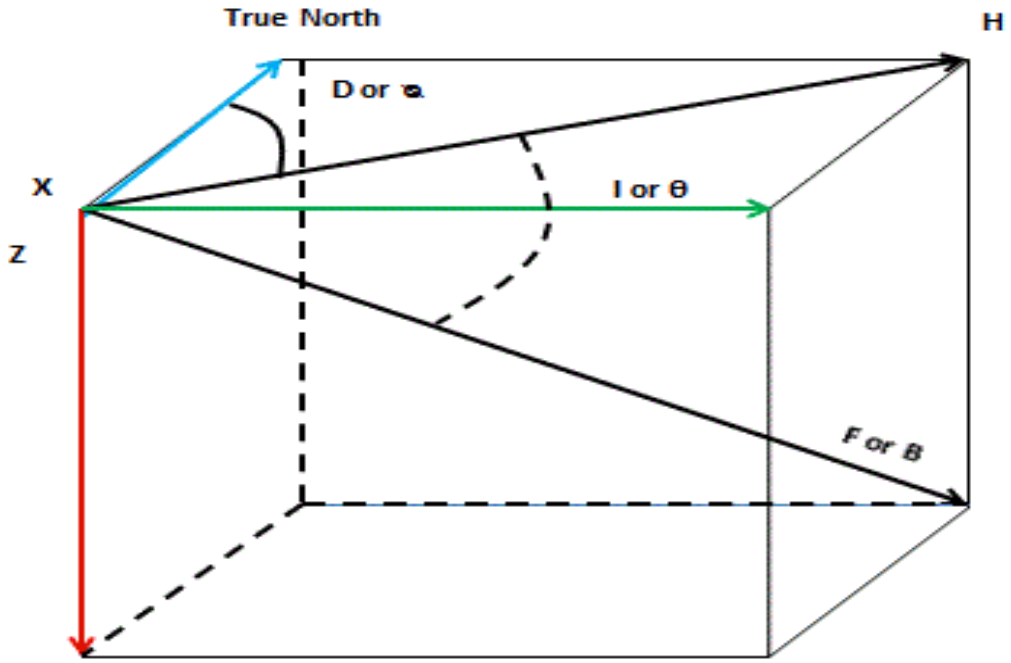

Figure 2.3 - Definition of Dip angle, Magnetic Field Strength and Declination

The estimation of above three vector components requires the strength of total magnetic field. Therefore, while calculating the total magnetic field strength at any point, it is important to be aware of the variations in earth's magnetic field over time and location. To incorporate the effect of these changes, different mathematical models are available to predict the geomagnetic field strength at a certain time and location. Some of these models and techniques for predicting the geomagnetic field are presented below.

2.3.1 BGGM

The BGS Global Geomagnetic Model (BGGM) is one of these models that gives an estimate of field strength generally based on main field from the earth's core, from its crust and other magnetic sources in the upper atmosphere. [5]

2.3.2 NOAA

Another higher order model produced by United States National Oceanic and Atmospheric Administration (NOAA) also considers the local crustal effects for modeling the variations in earth's magnetic field. [1]

2.3.3 IGRF

The International Association of Geomagnetism and Aeronomy (IAGA) has released a series of mathematical models known as International Geomagnetic Reference Field (IGRF) for modeling earth's magnetic field with its secular variations. The latest version of this series has been released in December 2014, known as "*12th Generation International Geomagnetic Reference Field" IGRF-12.* [8]

Both IGRF and WMM are lower order models and (relatively) less accurate compared to higher order models such as BGGM

2.3.4 WMM

The World Magnetic Model (WMM) is jointly developed by National Geophysical Data Center (NGDC,USA) and the British Geological Survey (BGS) and updated every 5 years [6]. WMM is primarily used to correct for magnetic declination and provides detailed geometry of the earth's magnetic field from 1km below to 850 km above the earth's surface. Beyond this range the model is not valid. For more details on the mathematical formulations and application, see reference [7].

2.3.5 In Field Referencing (IFR)

The above models in 2.3.1 - 2.3.4 are global. Both the higher and lower order models cannot precisely map out the variations in earth's magnetic field at a local level. The IFR technique is applied in circumstances when higher accuracy of MWD data is desired, especially when drilling close to the North pole where the results from global models are not much accurate. IFR along with BGGM or other models can be used to predict the Declination, Dip angle and Field strength for a specific site and the measurements for this can either be made aerially, on land or sea. Normally, these values are first estimated using BGGM or any other model and then the crustal variations measured from IFR is added to the original estimate. This final set of Declination, Dip angle and Field Strength values is usually used by the MWD.[1]

2.4 Measurement of Earth's Gravity Field

Earth's gravity field is relatively stable and does not vary much as its magnetic field. Similar to the magnetic field measurements, models for the measurement of earth's gravity field also exist. Utilizing the information from geographical coordinates, the formula below can be used to predict Earth's gravity field in mGal [8].

$$G = 978030 + 5186\sin^2\varphi + 0.309(D_v - h_o) - 0.084\rho D_v \quad (2.4)$$

Where,

φ Latitude (degrees)

D_v Vertical depth (meters)

h_o Height above Mean Sea Level (MSL) (meters)

ρ Drillstring's bulk density from top to D_v

The above formula can be divided into two different formulas for calculating field for offshore and onshore operations separately. Eq 2.5 can be used for offshore and Eq 2.6 for onshore operations respectively.

$$G = 978030 + 5186\sin^2\varphi + 0.14Dv \quad (2.5)$$

$$G = 978030 + 5186\sin^2\varphi + 0.10Dv - 0.31ho \quad (2.6)$$

Once a reference gravity value has been calculated from the above formula, the equations below can then be used to calculate the gravity components along all three axis x,y and z axis.

$$G_x = -G\sin I\sin A \quad (2.7)$$

$$G_y = -G\sin I\cos A \quad (2.8)$$

$$G_z = G\cos I \quad (2.9)$$

2.5 Application of Accelerometer and Magnetometer Measurements

The survey tool package consists of three accelerometers and three magnetometers mounted orthogonally to each other. The accelerometer package using the reference gravity field estimated in Eq 2.4 measures the three components of earth's gravity field from Eq's 2.7-2.9. Similarly, magnetometers using the total field strength can measure the magnetic field components along its three-axis using Eq's 2.1-2.3. The mathematics involved in the calculations of total magnetic field and gravity field along with their respective components has been discussed in detail in sections 2.3 and 2.4. The above tool measurements can now be

converted to the corresponding inclination and azimuth values for every survey station. These equations are provided below. [4]

$$I = \cos^{-1}\left[\frac{G_z}{\sqrt{G_x{}^2 + G_y{}^2 + G_z{}^2}}\right] \tag{2.10}$$

$$A_m = \tan^{-1}\left[\frac{(G_xB_y - G_yB_x)\sqrt{G_x{}^2 + G_y{}^2 + G_z{}^2}}{B_z(G_x{}^2 + G_y{}^2) - G_z(G_xB_x + G_yB_y)}\right] \tag{2.11}$$

2.6 Minimum Curvature Method

From sections 2.1-2.5 the mathematics and physics involved in MWD tool measurements has been discussed in detail, leading to the final calculation of inclination and azimuth, key inputs for wellbore position calculation.

The next and final step is to apply a survey calculation method for determining wellbore position. Among others, Minimum curvature method is regarded as the most accurate and commonly used survey calculation method for creating 3D well paths. The method considers the inclination and azimuth measurements both at the previous and new survey station to give a more accurate well path. Using the Ratio Factor from Eq 2.13, it approximates a circular arc instead of two tangent segments as in the Balanced Tangential Method. The ratio factor is calculated based on the dogleg between two survey points [9].

$$\phi = \cos^{-1}\left[\cos A_1 \cos A_2 + \sin A_1 \sin A_2 \cos(I_2 - I_1)\right] \tag{2.12}$$

$$F = \frac{2}{\phi}\left[\frac{180}{\pi}\right]\tan\frac{\phi}{2} \tag{2.13}$$

From the above relationships, the North, East and Vertical component (NEV) of the wellbore at a certain point can be estimated from Eq's 2.14-2.16 [9]. For more details on this method, refer to [10].

$$\Delta N = \frac{FL}{2}(\sin A_1 \cos I_1 + \sin A_2 \cos I_2) \tag{2.14}$$

$$\Delta E = \frac{FL}{2}(\sin A_1 \sin I_1 + \sin A_2 \sin I_2) \tag{2.15}$$

$$\Delta V = \frac{FL}{2}(\cos A_1 + \cos A_2) \tag{2.16}$$

Chapter 3. Error Sources in Wellbore Position Calculations

The wellbore position at any point is determined using MWD survey tools as explained in Chapter 2. However, the calculated wellbore position is usually not the actual position. This is because of the inaccuracy of the tools used for survey measurements, the environment in which measurements are taken, surveying procedures followed, and methods applied in the calculation of wellbore position. The contribution and impact of these different error sources varies depending upon the drilling conditions.

While calculating the wellbore position, the effect of these error sources must always be incorporated to understand and reduce uncertainty in wellbore position calculations. Properly addressing this aspect will lead to more reliable survey measurements, enhancing confidence to drill in close proximity with other wells or intersect smaller targets with precision. A standard industry practice is to define a path column at the panning phase as defined in figure 3.1. The well should be maintained within this tolerance while drilling for a safe operation. [11]

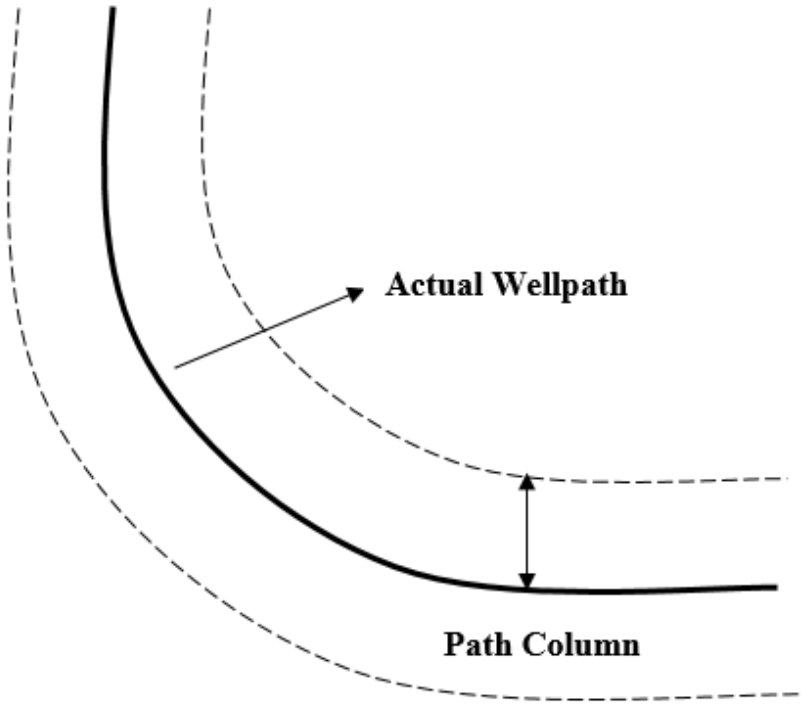

Figure 3.1 - Definition of Path Column

The following chapter will discuss different error sources contributing towards wellbore position uncertainty. Section 3.1 will explain how a wellbore position uncertainty is

represented using an Ellipse of Uncertainty (EOU). Section 3.2 will discuss the method applied to calculate te EOU at any point. Section 3.3 will present different error sources, primary reason why the error ellipse even exists.

3.1 Description of Position Uncertainty Ellipse

Wellbore position uncertainty at any depth is expressed through a position uncertainty ellipse. The size of this Ellipse of Uncertainty (EOU) will be directly proportional to the magnitude of position uncertainty because the well is assumed to lie somewhere within this EOU at a certain depth. Therefore, a large sized EOU will mean that the well path might be highly deviated from its planned course and vice versa.

The EOU at a certain depth can result from uncertainty in either two (2-D) or three dimensions (3-D). The uncertainty in azimuthal part of measurements is proportional to the length of lateral axis of the ellipse and the length of high side axis depends on inclination error. The third axis, along the hole is a result of relative depth error [1, 12]. Figure 3.2 represents the EOU along the well.

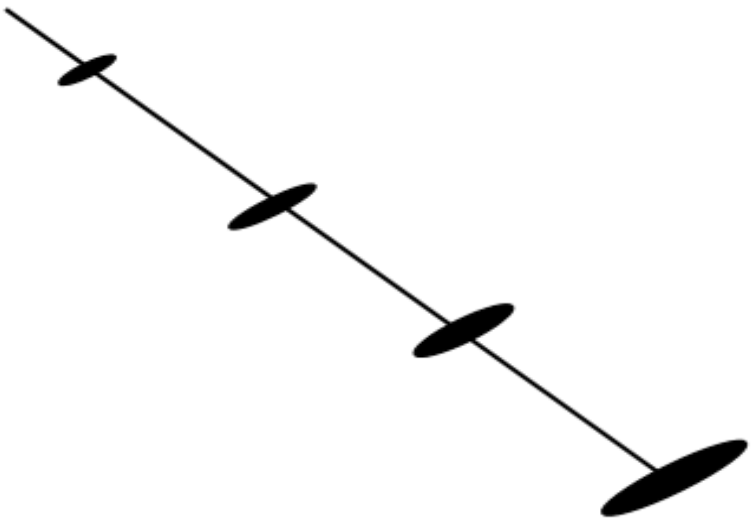

Figure 3.2 – Representation of Position Uncertainty through Ellipses of Uncertainty EOU

The position uncertainty ellipse at a single survey station is a result of total contribution from all error sources at this survey station. It is important to clarify that being statistically independent all error sources should be statistically summed together for the calculation of total error at a particular survey station [4]. However, when calculating the total position error along a well from an individual error source, error propagation mode must be followed for appropriate error summation. The error propagation mathematics presented by Williamson has

been provided in Appendix A. The final result of all error summations at a survey station is the following Variance-Covariance matrix.

$$\begin{pmatrix} \sigma^2{}_N & \sigma_N\sigma_E & \sigma_N\sigma_V \\ \sigma_N\sigma_E & \sigma^2{}_E & \sigma_E\sigma_V \\ \sigma_N\sigma_V & \sigma_E\sigma_V & \sigma^2{}_V \end{pmatrix}$$

Where,

$\sigma^2{}_N$ $\sigma^2{}_E$ $\sigma^2{}_V$ variance along North, East and Vertical axis

$\sigma_N\sigma_E$ covariance of North and East component

$\sigma_N\sigma_V$ covariance of North and Vertical component

$\sigma_E\sigma_V$ covariance of East and Vertical component

To calculate the dimensions of position uncertainty ellipse, the above Variance-Covariance matrix is further converted to its Eigen vectors and Eigen values through simple matrix manipulation. Eigen vectors define the direction of the ellipse of uncertainty whereas the Eigen values define their magnitudes. The details for calculating Eigen values and Eigen vectors is provided in Appendix B.

3.2 Error Sources

This section will in detail present various sources of errors in wellbore surveying that eventually lead to WPU. The errors vary from human errors, tool specification errors, contaminated drilling fluid, incorrect referencing etc. Identification of these error sources is the first step towards reducing uncertainty in survey results. All these errors can together highly impact the quality of survey data leading to unreliable wellbore position predictions. Some of these error sources will be presented below.

3.2.1 Drilling Fluid Contamination

Drilling fluids can impact the magnetic measurements usually obtained while drilling (MWD). This is because of the presence of various magnetic particles in the drilling mud which influence the measurements. The source of this magnetic material can be magnetized geological formations and eroded steel from casing or drillstring components mainly in the BHA [13]. These magnetic particles can significantly alter the magnetic properties of drilling mud and can cause the azimuth to deviate upto 5°, displacing the wellbore to almost 50 meters for one of the survey sections being analyzed. [14]

It has been found that drilling fluids act as a shield and tend to distort the transverse component of the earth's magnetic field due to their magnetic susceptibility. Previously only Drilling BHA was suspected as the source of this magnetic distortion rather than the drilling mud, but despite of applying the necessary corrections for it the problem persisted. Later, various laboratory and field tests revealed that the drilling mud attenuates the magnetic measurements and must be accounted for when correcting survey data. [15]

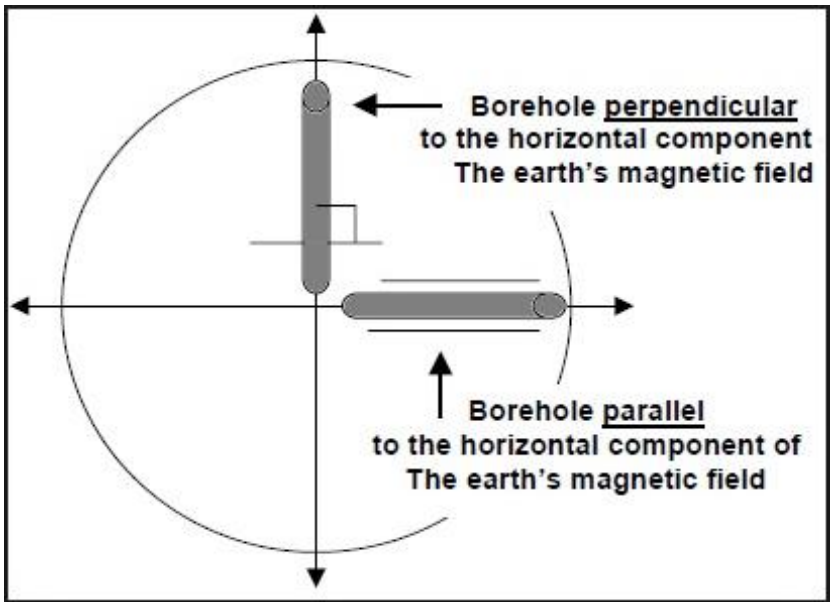

Figure 3.3 - Description of Earth's Magnetic Field with respect to Borehole [16]

3.2.2 Sensor Errors

Magnetic MWD tools and Gyro, employing different sensors for survey measurements are frequently used as survey tools. The construction and principle of measurement for the two tools varies, with each associated with its corresponding sensor errors. It is therefore important to be aware of these error sources so relevant corrections can be applied to correct for them and reduce WPU caused by these errors.

3.2.2.1 Accelerometer & Magnetometer Errors

Magnetic MWD tools utilize accelerometers and magnetometers for gravity and magnetic field measurement respectively. Accelerometer is simply a transducer that converts mechanical acceleration into electrical signal. The sensitivity of this sensor is dependent on the proportion of this mechanical acceleration converted to electrical output, also known as '**scale factor**' [17]. These sensors measure the gravity components along the three axes as well as inclination and toolface angles. Therefore, any errors in accelerometer sensors will impact inclination and toolface measurements. A study has shown that the impact of systematic accelerometer errors

such as scale factor, bias and sensor misalignment is not only limited to the accuracy of accelerometers but also upon their respective specifications [18]. Accelerometer errors originate due to tool string's acceleration and can be reduced through a technique known as "Filtering'' which is best to apply when the tool string speed remains constant. [13]

Similarly, any magnetic interference in the surrounding of MWD tool string will impact the magnetometer readings. Magnetic effects are either due to the magnetization in the tool string or local formations with iron contaminating the drilling mud with magnetic material. Magnetization is a result of using ferromagnetic material while making the tool string and usually has a constant magnitude and direction relative to the instrument. Whereas, contamination of the drilling mud with magnetic material produces hotspots [13].

3.2.2.2 Gyro Errors

A gyroscope is basically used to measure rotational velocity in one, two or three directions. They have evolved from simplest of the constructions involving axles, rotors and gimbals to more sophisticated electronic and optical devices [19]. Although, measurements taken with a gyro are more reliable compared to magnetic instruments, but they are still associated with several errors. For example, gyros must be referenced to a point of known direction before and after running in the hole. This can be done either by referencing it with topographical means which is relatively more accurate compared to when referencing with magnetic compasses [12].

In addition to this, while taking surveys with gyros, they may drift a few degrees. Since the drift is not constant throughout the run, it is difficult to account for this error. A calculated drift curve is constructed by monitoring the drift continuously. The difference between this calculated and observed drift is defined as closure. The smaller its value (both positive or negative), the greater is the reliability of gyro measurements. Similarly the gimbal construction of gyro limits the maximum inclination at which gyro can be used with confidence and hole inclinations exceeding 70° cannot be reliably surveyed using gyros [12]**.**

Considering the above errors, gyros will require corrections to improve the quality of survey data obtained through them. Most significant of these include gyro noise correction, scale factor, mass unbalance and tool misalignment which have also been specified in the gyro error model [20]**.** To reduce uncertainty in the results from gyro tools they are first corrected for these errors at master calibration facility and later in the field. It has been found that except mass unbalance and X & Y gyro biases, most of these error terms remained constant [21]**.**

Another approach followed to check the validity of gyro surveys is comparing both inrun and outrun azimuth values. If the difference is less than 1° in holes which have an inclination greater than 70°, gyro results can be regarded as reliable. [12]

3.2.3 Depth Measurement Errors

The wellbore position errors are first and foremost wrong pipe tally. Despite of spending billions of dollars on instruments, still huge uncertainty exists while measuring pipe accurately [22] . This wrong depth measurement can be consequential and affect other measurements too. All significant wellbore surveying parameters including, Inclination, Azimuth, Northing and Easting are attributed to a specific depth, assuming the depth is accurately measured. However, if that is not the case, then all these survey parameters will be assigned to a different depth leading to incorrect wellbore position estimates.

The source of these depth measurement errors is mostly associated with tool limitations. For example, depth measured using a wireline might be inaccurate because of wire stretching, drill pipes and casing joints are measured to nearest centimeter and tool friction can result in different depths while running in and out of the hole. In addition, for offshore wells, tides and different Rotary Kelly Bushing (RKB) elevations introduce uncertainty in depth measurements. All these factors can together make the depth measurements uncertain.

3.2.4 Tool Misalignment Errors

Practically, it is not possible for the drill string to remain perfectly aligned with the borehole axis in long deviated holes with complex trajectories. Both the drillstring and survey tools attached to it will be misaligned with respect to the borehole axis under the influence of gravity and hole trajectory. The error model for directional MWD presented in [4] has introduced two different sources leading to this misalignment, one in the BHA referred to as BHA Sag and the other as radially symmetric misalignment.

3.2.4.1 BHA Sag

The projection of the BHA misalignment in the vertical plane at a point of inclination measurement is defined as BHA Sag [23]**.** It is observed to dominate the total inclination error budget with almost 60% of contribution [4]. Due to this, the resulting TVD error because of BHA sag can be significant, disabling the access to small geological targets and accurate well placement in the reservoir. For example, incorrect TVD measurements can land a well in the water zone which can result in huge recovery losses. Considering its consequences, it becomes essential to correct for this error source and reduce the EOU at target depth due to BHA sag.

The magnitude of sag error among various other factors depends upon the BHA type, its geometry and sensor placement. According to ISCWSA, when the BHA sag correction has not been applied, a typical value for the sag error magnitude can be 0.2° with a weighting function of *(0, sin I ,0)* which is reduced to 0.08° after the correction is applied [4]. However, the following weighting function only considers the effect of gravity on sag which is not always true.

An investigation has been made into factors that can cause sag error in addition to gravity and a 3D BHA model has been constructed with different BHA configurations for analyzing the impact of sag error [23]. According to this study, the ISCWSA weighting function is applicable for well stabilized BHA's without any bend and in gauge holes. However, for curved and washed out holes with BHA's having a bend, the BHA Sag is not entirely dependent on inclination. The referred paper can be consulted for more details on the correction strategy and results.

3.2.4.2 Radially Symmetric misalignment

This is another form of tool misalignment described by Williamson which is dependent on the tool face measurement. Estimates made by John Turvil about its magnitude have been shared in the literature, with a combined value of 0.094° resulting from various misalignment sources including misalignment of sensor package in housing, sensor housing in drill collar, collar body in the borehole, and collar bore in the collar body.

Horizontal misalignment is another source of misalignment identified, which is defined as the "*projection of the BHA misalignment along the borehole, at the point of azimuth measurement on the lateral plane"* [23]**.** It is primarily due to distortion of MWD collar outside the vertical plane under the influence of bending forces. Magnitude of this error is sufficiently small, 0.004° and therefore lumped with the other radially symmetric misalignments.

The impact of tool misalignment can however be reduced by rotation of the tool. Also, when run in vertical cased holes, gyro surveys comprise of less uncertainty compared to magnetic surveys. The reason for this is obviously better centralization in the cased holes and the misalignment of the gyro tool can be measured and correspondingly adjusted for. Contrary to this, in inclined holes, because of gravity and nonaxial wireline pull, the tool might not be at the same inclination as the hole [12].

3.2.5 Human Errors

The error sources described above are modeled through mathematical relationships having a specific error magnitude and weighting function which indicates its impact on inclination, azimuth or depth measurement. In addition to these, there can still be certain error sources which cause uncertainty in wellbore position measurements, but cannot be modeled. For example, the shortcomings in the formulated survey management plan or incorrect implementation of survey procedures as prescribed in the plan can cause errors in wellbore position estimates. Also, incorrect application of survey error models, not using updated error models for every hole section and wellpath construction without analyzing all necessary information during anticollision analysis fall among common human errors [1]. All these factors can cause additional WPU other than modeled error sources and therefore must be considered for accurate wellbore positioning.

3.2.6 Geographical Location

The challenges pertaining to wellbore positioning also vary depending on the geographical location of the well. The depth and inclination measurements are made independent of the latitude, so it is mainly the azimuthal part of measurements that is influenced with changing geographical location for both magnetic and gyroscopic tools.

The magnetic tools utilize earth's magnetic field as a reference and measure tool's direction relative to this. When drilling in the auroral zones, magnetic storms cause variations in the magnitude and direction of this reference field further increasing the azimuth uncertainty. Also, while approaching the magnetic poles, the magnetic dip angle increases and the horizontal component of earth's magnetic field decreases. A relationship between azimuth uncertainty and magnetic dip angle Θ with k_1 as constant is provided in [24].

$$\Delta A_{magn} \sim \frac{k1}{\cos(\Theta)} \tag{17}$$

Gyroscopic tools on the other hand measure tool rotation in 3D space through gyroscopic sensors and use geographical north as a reference. For this reason, gyro measurements are not influenced by magnetic storms as in the case of magnetic sensors. However, while approaching the geographical poles the horizontal component of earth rotation decreases, thus distorting gyro measurements. This enhances the azimuth uncertainty which is dependent on the latitude according to the following relationship [24]

$$\Delta A_{gyro} \sim \frac{k_2}{\cos(\varphi)} \tag{3.2}$$

Where,

φ is latitude in degrees

3.2.7 Other Errors

Besides the error sources mentioned above, there can still be several other reasons which if not properly handled may cause uncertainty in wellbore position estimates. For example, the correct application of top hole position uncertainty is important which requires that the radius dimension of the well should be included when calculating position uncertainty for these sections. Also, the uncertainty in surface locations of the well should be used in calculating wellbore position uncertainty when scanning multiple sites. Similarly, at the planning stage all future wells which are likely to be drilled in the proximity of the planned well must be considered in anticollision scanning, else it may put restrictions on drilling them in future [1].

Chapter 4. Structure of an Error Model

An error model is defined by several components which are used to model the effects of various physical factors inducing survey errors. Combining these components, the size of EOU demonstrating Wellbore Position Uncertainty can be calculated at any point. A brief introduction of these components extracted from [1] has been presented below.

4.1 Error Source

An error source defines the primary origin of an error, which can be from an accelerometer or magnetometer bias for example, magnetic sources in the drilling mud or others mentioned in the previous chapter. Therefore, the identification of an error source is important for its further corrections.

4.2 Error Code

Every error source is abbreviated by its corresponding code, which makes it simpler for specifying different error sources in the error model. For example, the uncertainty arising from magnetometer bias along z axis is expressed through an error code as (MBZ). Usually, these error codes are used to represent different error sources in the error model.

4.3 Weighting Function

Weighting function of an error source expresses the effect of an error source on inclination, azimuth or depth. These functions can help predict the behavior of an error source in different wells or drilling environments. In addition to that, these equations are used to establish a link between uncertainty from an error source and its corresponding impact on survey measurements.

4.4 Error Magnitude

All survey error model have a number of scalar magnitudes associated with their different error sources. It is the product of this error magnitude and the weighting function which results in final error from a specific error source at a single survey station. These magnitudes are derived from the standard deviation of the whole set of possible output values expected from the error source over a certain sample. The value of this error magnitude may vary depending on the local conditions and different survey techniques. For example, the error magnitude for declination error reduces to almost 50% when IFR corrections are applied.

4.5 Propagation Mode

The primary equation that first explains how an error propagates from an error source to ultimately the survey measurement error is provided below [2].

$$e_i = \sigma_i \frac{dr}{dp} \frac{\partial p}{\partial \varepsilon_i} \tag{3.3}$$

e_i = size of an error in NEV axis due to an error source i

σ_i = error magnitude

$\frac{\partial p}{\partial \varepsilon_i}$ = weighting function for the error source i

$\frac{dr}{dp}$ = effect of survey errors on wellbore position

Once the effect of an error source has been calculated at all survey stations in all survey legs of a well, they must be added together. Whether this addition is arithmetic or Root Sum Squared (RSS) is decided based on the error propagation mode. For example, sensor errors will most likely remain the same at every survey station if a similar tool is used and will thus be considered to exhibit a systematic propagation mode. Similarly, the declination error usually remains the same across a certain geographical area and will be dealt as Global error. Based on this, four error propagation modes have been defined as following:

- **i.** Random (R)
- **ii.** Systematic (S)
- **iii.** Well by Well (W)
- **iv.** Global (G)

Chapter 5. Methodology

The objective of this thesis is to understand the impact of different MWD survey error sources on measurement (Depth, Inclination, Azimuth) and wellbore position (North, East, TVD) uncertainty. The toolface independent error terms representing these error sources have been selected from the ISCWSA MWD error model. The analysis has first been made for the Non-mag error model consisting of error terms not corrected for magnetic axial drillstring interference followed by those corrected for this interference. Finally, a comparison has been made between the error terms having different weighting functions in the two models. This will help understand the effectiveness of applying magnetic axial drillstring interference correction. However, it is important to mention that IFR and sag corrected error magnitudes have been used in both error models.

Most of the errors are a function of hole inclination and azimuth. Therefore, some errors are dominant when drilling in North/South direction while others in East/West direction. Similarly, some errors are most effective in the deviated part of the well while being least effective in vertical and near vertical part of the well. To investigate this further, three well paths have been constructed in Landmark's engineering program Compass™ in three different directions. The first one is drilled absolutely North/South, the second at 45° North and the third 75° North close to East/West direction. In this thesis. the well drilled at 0° azimuth has been referred as the North-South well, the one drilled at 45° azimuth is the North-East well and at 75° azimuth has been termed as the East-West well. Well paths along with their complete survey data have been provided in Appendix (C).

The Non-mag and Mag-corr error models have a total of 38 and 40 error terms respectively. Given this large number of error terms, it is preferred to group these error terms together depending upon the error source and then analyze the impact of each error source separately. The error terms for Non-mag error model have been grouped into following nine categories.

i) Depth Measurement errors
ii) Tool Misalignment errors
iii) BHA Sag error
iv) Declination error
v) Axial Drill string Interference
vi) Accelerometer Bias
vii) Accelerometer Scale

viii) Magnetometer Bias

ix) Magnetometer Scale

It is worth mentioning that depth measurement, tool misalignment, sag and declination errors have the same weighting functions in the Non-mag and Mag-corr error models. Therefore, in addition to a few new error terms, only the error terms having different weighting functions have been mentioned below for the Mag-corr error model. The error terms for the Mag-corr error model have been grouped into following categories.

i) Magnetic dip angle uncertainty

ii) Magnetic field uncertainty

iii) Accelerometer Bias

iv) Accelerometer Scale

v) Magnetometer Bias

vi) Magnetometer Scale

5.1 Calculation of Position Uncertainty Ellipse in Compass

After the categorization of the error terms, the size of position uncertainty ellipse for each error source has been derived from Compass™. This is achieved by including all error terms representing an error source in the Instrument Performance Model (IPM) file in Compass™. Details on how this position uncertainty is actually calculated has been explained in section 3.2.

5.2 Calculation of Measurement Uncertainties

Compass™ only provides position uncertainty estimates without any account of uncertainty in the components of measurement vector (Depth, Inclination, Azimuth). Since an error might affect the measurement and position uncertainty differently, therefore it becomes important to understand the effect of each error source on measurement uncertainty along with position uncertainty.

As explained in the introduction of this chapter, every error source consists of several error terms. The weighting function and error magnitude of individual error terms are used to calculate the measurement error from each error term. The final measurement error from an error source at a single survey station is then calculated by a statistical sum (Root Sum squared) of these measurement errors. An example calculation is presented in Appendix F. Whether this measurement error affects depth, inclination or azimuth will be determined from the weighting function. For example, measurement error calculated using declination error terms will only

add to the total azimuthal uncertainty while sag error will only affect the inclination uncertainty.

5.3 Analysis Breakup

Utilizing the measurement uncertainties from Excel model and position uncertainties from Compass™, the results from both are combined to study the effect of each error source along the hole in three wells, North-South, North-East and East-West.

The analysis has been made at different levels. First, the impact of each error source on measurement and position uncertainty will be analyzed in each well as a function of hole inclination and depth respectively. Based on these results, the behavior of each error source will then be compared between corresponding hole sections of different wells. This will help understand the effect of azimuth on measurement and position uncertainty. At the third level, the effect of each error source on total measurement and position uncertainty budget will be analyzed as a function of inclination and depth for all three wells separately.

For measurement uncertainty, the uncertainties caused by a particular error source will be compared with the total measurement uncertainties from all error sources combined. To study the effect on total position error budget, the total position uncertainty will be first calculated using all error sources combined and then calculating the position uncertainty considering all error sources except the error source being currently analyzed. Ignoring the error source actually reduces the total position uncertainty, and the extent to which it has been reduced determines the effectiveness of a particular error source towards total position uncertainty. Finally, to check if the error source has a similar impact on measurement and position uncertainty or not, a comparison of two will be made for each well.

.

Chapter 6. Error Analysis of Non-mag Error Model

This chapter will discuss the effect of general and Non-mag error sources on measurement and position uncertainty. The general error sources have the same error terms for both Non-mag and Mag-corr error models. These consist of Depth Reference errors, BHA Sag, Tool Misalignment and Declination error. A total of 38 error terms are used to represent the effect of these different error sources, which have been placed into total nine different categories based on the error source.

Using the error terms from the Non-mag error model, the scheme of analysis will be followed as explained in the analysis breakup of previous chapter. Each error source has been discussed separately by first analyzing its impact on measurement uncertainty and then position uncertainty through a set of plots.

6.1 Depth Reference Errors

The ISCWSA Error Model has proposed a total of five error terms to incorporate the effect of depth measurement errors for land and offshore drilling operations. In this thesis however, depth errors relevant to a floating platform have been used. The sections below will explain the effect of these error terms on depth and position uncertainty.

6.1.1 Effect on Depth Uncertainty

The weighting functions used for calculating depth uncertainty have been listed as equations 6.1-6.3. The equations below show that depth errors only depend on well's TVD and MD and are independent of drilling direction (azimuth). Apparently from the weighting functions above, depth errors also seem to be independent of hole inclination. But in reality, this is not true since TVD is affected by hole inclination. However, in the current study where all three wells have the same inclination throughout the well therefore the effect of depth error is expected to be the same in each well.

Figure 6.1 represents the combined effect of depth error in the three wells. The depth errors remain constant upto almost 500m MD and then continuously increase with depth to a maximum of almost 1.8 m at TD, which is also interestingly close to the size of position uncertainty ellipse at TD provided in Appendix E. Error magnitudes for these error terms have also been listed in Appendix D.

$$drfs = \begin{pmatrix} 1 \\ 0 \\ 0 \end{pmatrix} \tag{6.1}$$

$$dstg = \begin{pmatrix} tmd \times tvd \\ 0 \\ 0 \end{pmatrix} \tag{6.2}$$

$$dsfs = \begin{pmatrix} tmd \\ 0 \\ 0 \end{pmatrix} \tag{6.3}$$

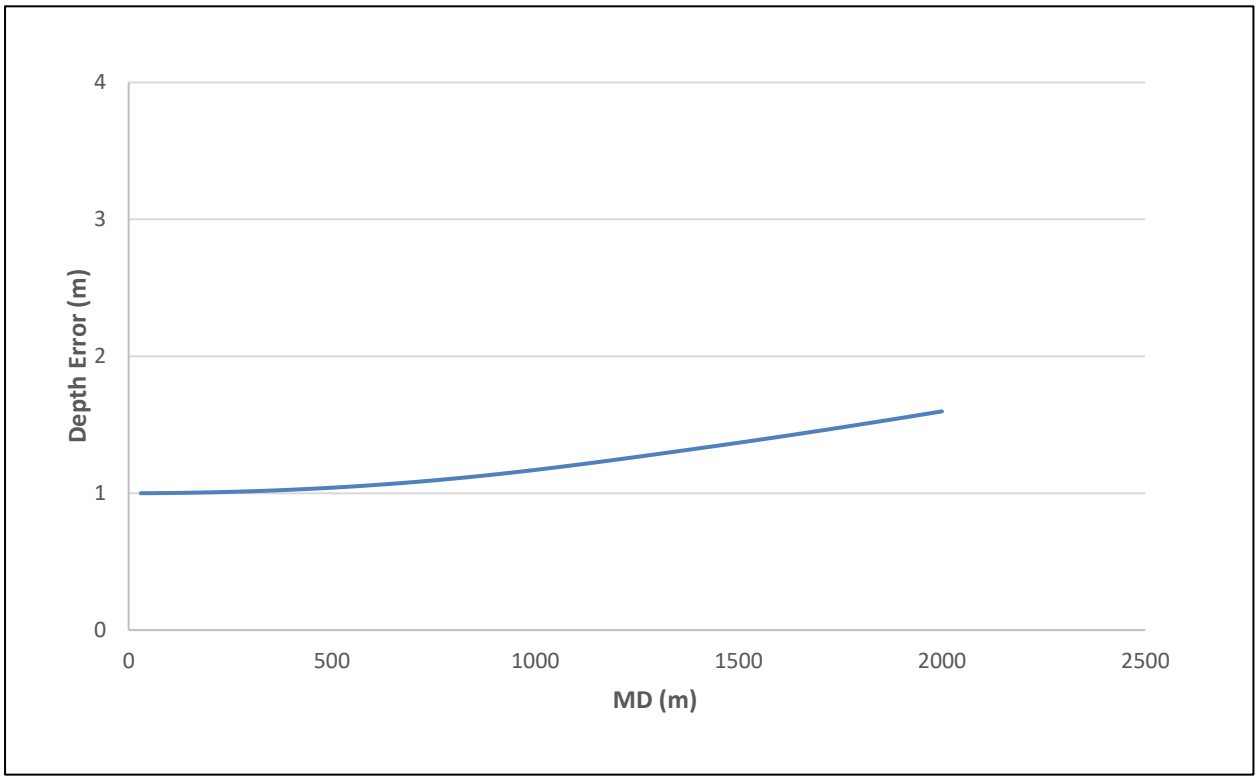

Figure 6.1 – Effect of Depth Errors on Depth Uncertainties

6.1.2 Effect on Total Position Uncertainty

The purpose of Figure 6.2 is to understand the effect of Depth errors on total position uncertainty and whether excluding the depth error terms from the error model will have any influence on total position uncertainty or not. Lengths of semi major and semi minor axis of ellipse of uncertainty have been plotted for the two cases. The first case calculates the size of

ellipse of uncertainty by including all error terms from different error sources in the Non-Mag error model. The second case calculates the size of ellipse of uncertainty due to all error sources except the depth errors. Thus, the difference in semi major axis for the two cases is indistinguishable throughout the well, but the semi minor axis for the two cases separate in the horizontal section.

The length of semi minor axis actually increases in the horizontal section when depth error terms are included, while it remains to a relatively lower constant value when the depth error terms are excluded. This is because semi minor axis represents the TVD errors and an increase in its length indicates the effect this error source has on TVD measurements in a well. Based on this understanding and the results below, depth error will mainly affect the TVD errors in the horizontal section of a well.

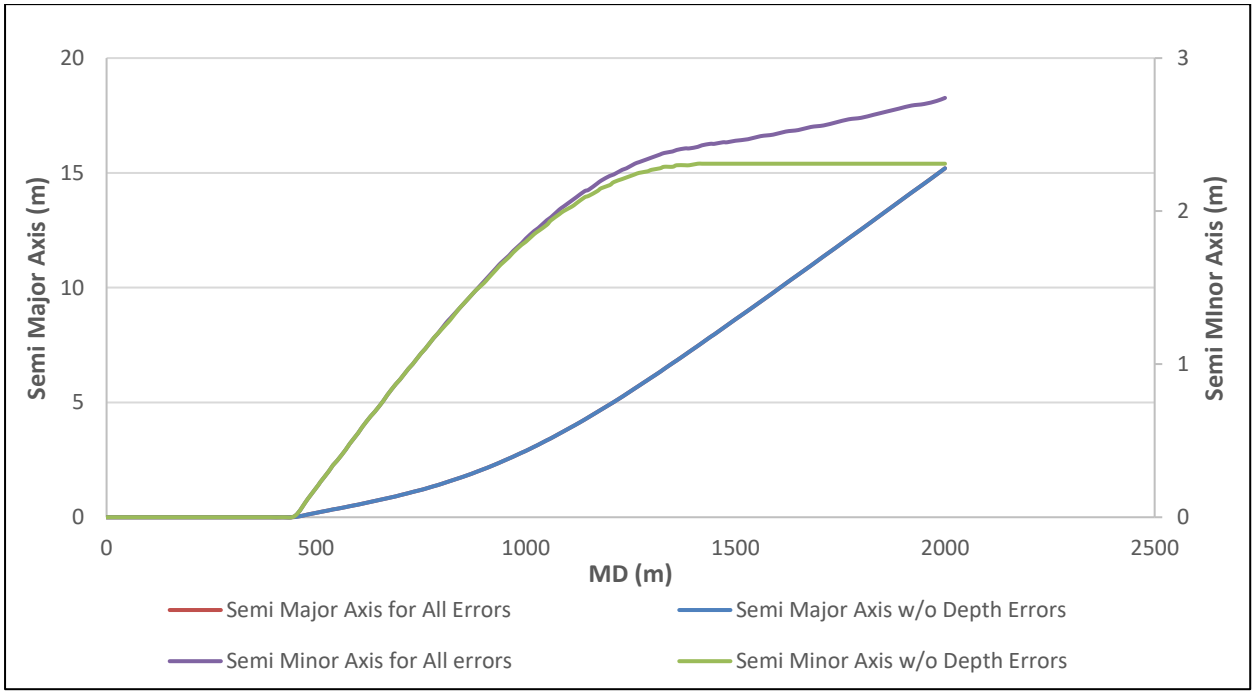

Figure 6.2 - Effect of Depth Errors on Total Position Uncertainty

6.2 BHA Sag

BHA Sag contributes towards the total inclination uncertainties only. The ISCWSA error model has proposed the following weighting function to account for uncertainties due to sag. Assuming BHA Sag correction has been applied, the error magnitude used in this study has been listed in Appendix D.

$$sag = \begin{pmatrix} 0 \\ \sin(I) \\ 0 \end{pmatrix} \tag{6.4}$$

6.2.1 Effect on Inclination Uncertainty

From the weighting function above, sag is also independent of drilling direction. Therefore, it will have the same impact in all three wells due to identical well profiles irrespective of their different directions. However, being a function of inclination, the effect of sag is minimum in the vertical and near vertical section. But as the inclination builds up it increases sharply and attains a maximum value of 0.08° in the horizontal section.

When comparing the inclination uncertainties only due to sag with the total inclination uncertainties, the separation between the two curves can be observed to narrow down gradually in the buildup section and reaching to a minimum in the horizontal section. This shows that sag will be most effective in the deviated and horizontal part of the well, while being least effective in the vertical and near vertical part.

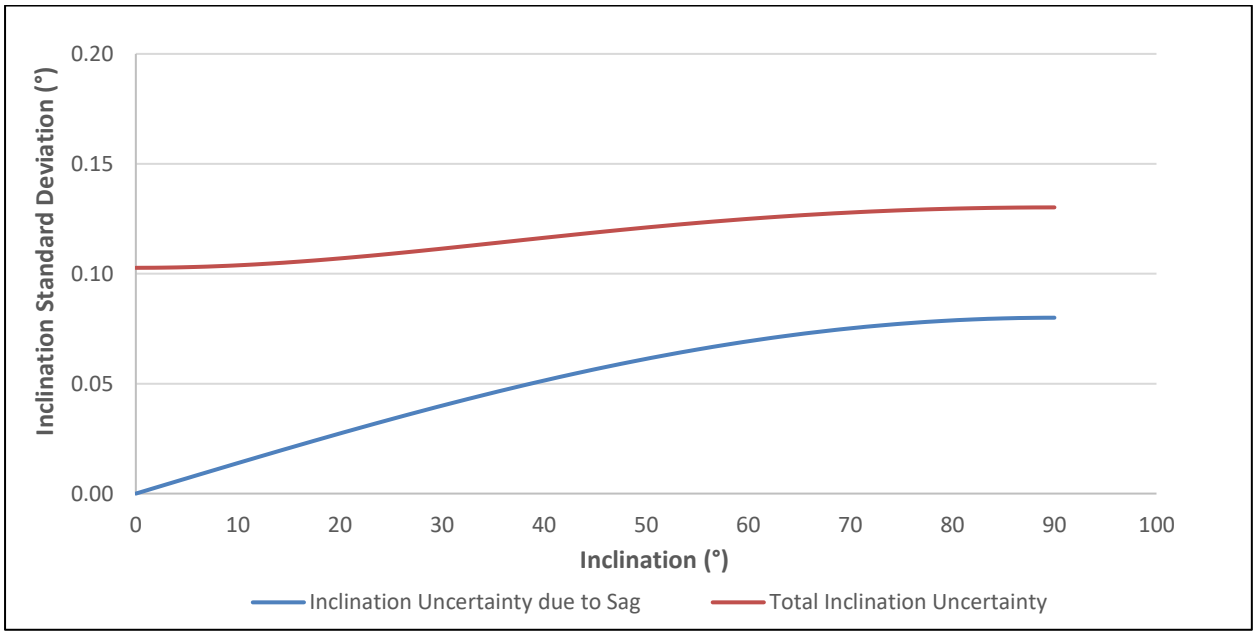

Figure 6.3 - Effect of BHA Sag on Inclination Uncertainties

6.2.2 Effect on Total Position Uncertainty

The purpose of Figure 6.4 is also to understand the effect of sag on total position uncertainty. Similar to the analysis of depth error, two cases have been considered in understanding the effect of sag on total position uncertainty, with and without considering sag error term in the

error model. Again, the difference is observed only in the lengths of semi minor axis in the horizontal section. Therefore, BHA Sag is also inducing TVD errors in the horizontal section and consequently adding to the total position uncertainty.

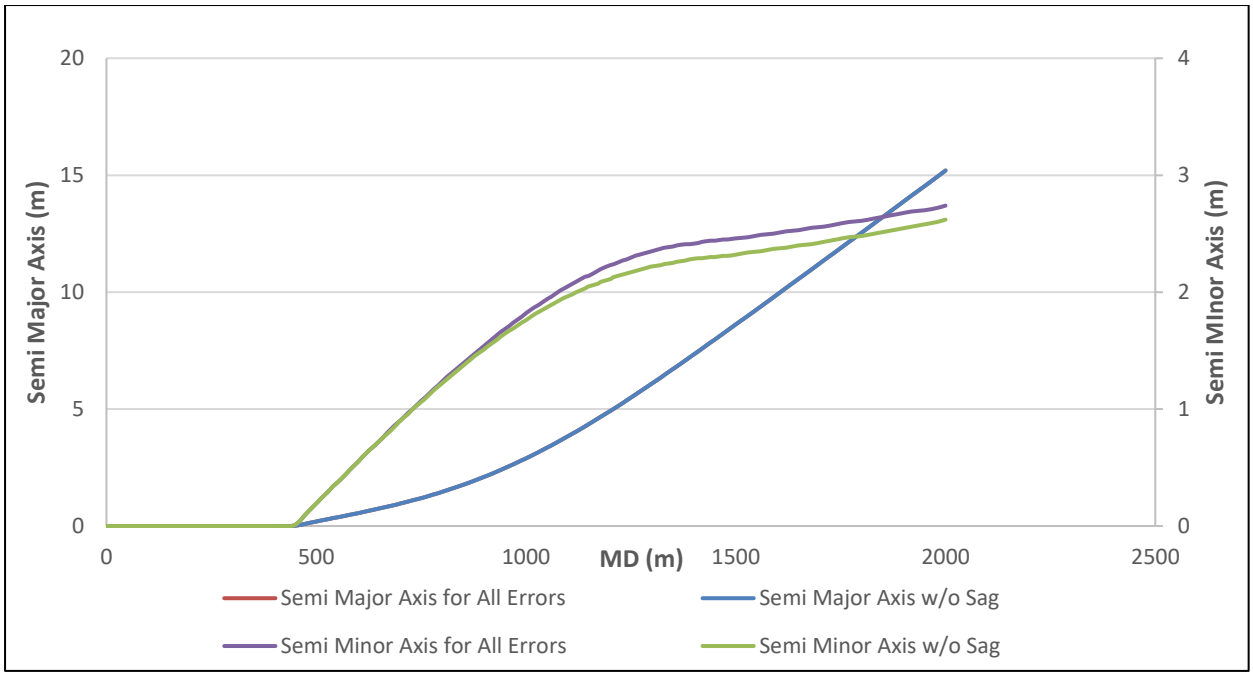

Figure 6.4 - Effect of BHA Sag on Total Position Uncertainty

6.3 Total Declination Error

ISCWSA error model has a set of four error terms to account for azimuth uncertainty due to declination error. Two of them consider the impact of constant declination error with random and global propagation modes. The other two error terms, also available in both global and random propagation modes incorporate the effect of uncertainties introduced during the measurement of earth's magnetic field components. However, in the current study both constant and B_h dependent declination errors with only global propagation modes have been used. The RSS of the measurement error from these two error terms has been considered as a total declination error. Also, the error magnitudes provided in Appendix D and used to calculate the effect of declination error are corrected for In Field Referencing (IFR). The weighing functions for the two error terms are provided below.

$$dec = \begin{pmatrix} 0 \\ 0 \\ 1 \end{pmatrix} \tag{6.5}$$

$$dbh = \begin{pmatrix} 0 \\ 0 \\ \dfrac{1}{B\cos\Theta} \end{pmatrix} \tag{6.6}$$

6.3.1 Effect on Azimuth Uncertainty

The weighting functions above can best describe the behavior of declination error. They clearly show that declination error is independent of hole inclination or direction and is rather influenced by only well location. Based on the error magnitude and weighting function for constant declination error, it will induce a constant 0.1° of azimuth error.

While the effect of B_h dependent declination error will depend upon the magnetic field strength and dip angle. If the well location is moved further south, the dip angle is expected to decrease causing a resultant increase in the cos (Θ) function and a possible reduction in magnetic field strength. Therefore, at any specific location, a combination of these two parameters will determine the total declination error. Assuming typical North-sea conditions in this study, using a dip angle of **70°** and magnetic field strength of **51000** nT the effect of B_h dependent declination error has been calculated to be approximately 0.15°. Finally, the statistical sum of these two error terms results in total declination error of 0.18°.

To analyze the contribution of this declination error to the total azimuth uncertainties, it is important to understand the behavior of the total azimuth uncertainties in the three wells. Since the declination error is constant in each well so the magnitude of total azimuth uncertainties will determine the impact of declination error towards the total azimuth error budget. The total azimuth uncertainties are extremely high in the vertical and near vertical section of all three wells. However, above approximately 20° inclination, the behavior is different. The total azimuth error increases in the North-East and East-West wells above this inclination and reaches to a maximum in the horizontal section, but that in North-South well, it maintains a constant trend.

Based on the behavior of total azimuth uncertainties, the declination error least influences the total azimuth uncertainties in the vertical and near vertical section of all three wells. Its impact however varies in the buildup and horizontal section. For the North-South well, it has a constant impact on total azimuth uncertainties in these hole sections. In the North-East and East-West well, since the total azimuth uncertainties increase but those due to declination remain constant, therefore the relative contribution of this error source drops. Based on this, among three wells

in Figure 6.5, the declination error seems to have relatively greatest effect in the buildup and horizontal sections of the North-South well and minimum in the East-West well.

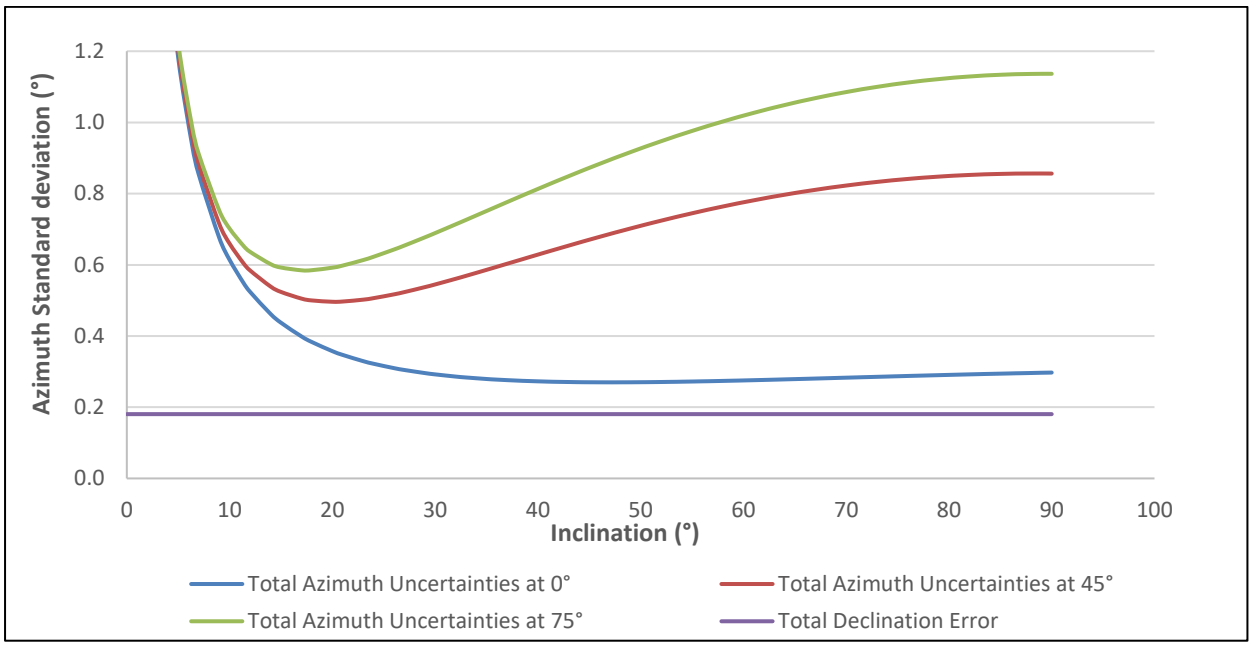

Figure 6.5 - Effect of Declination Error on Azimuth Uncertainties

6.3.2 Effect on Total Position Uncertainty

This section will explain the effect of declination error on total position uncertainty. The objective is to see if removing declination error terms from the error model has any influence on total wellbore position uncertainty or not. The three plots demonstrate that declination error does not have any influence on total position uncertainty at shallow depths of all wells. However, even at higher depths declination error affects total position uncertainty only in the horizontal section of North-South well and has no influence at all for the entire North-East and East-West wells.

From the results above, it can be concluded that declination error has a uniform impact on measurement and position uncertainties in the three subject wells. It is seen to have the greatest impact on total azimuth and position error budget in and close to the horizontal section of North-South well while least influencing the total azimuth and position uncertainties for almost entire North-East and East-West wells.

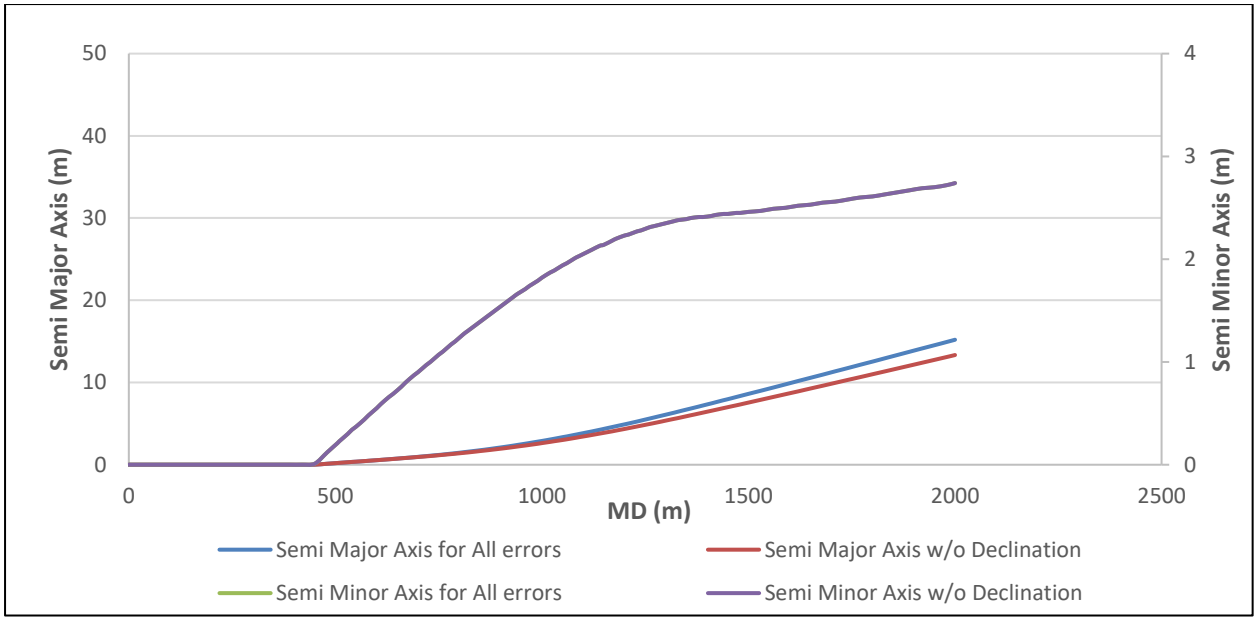

Figure 6.6 - Effect of Declination Error on Total Position Uncertainty at Azimuth = 0°

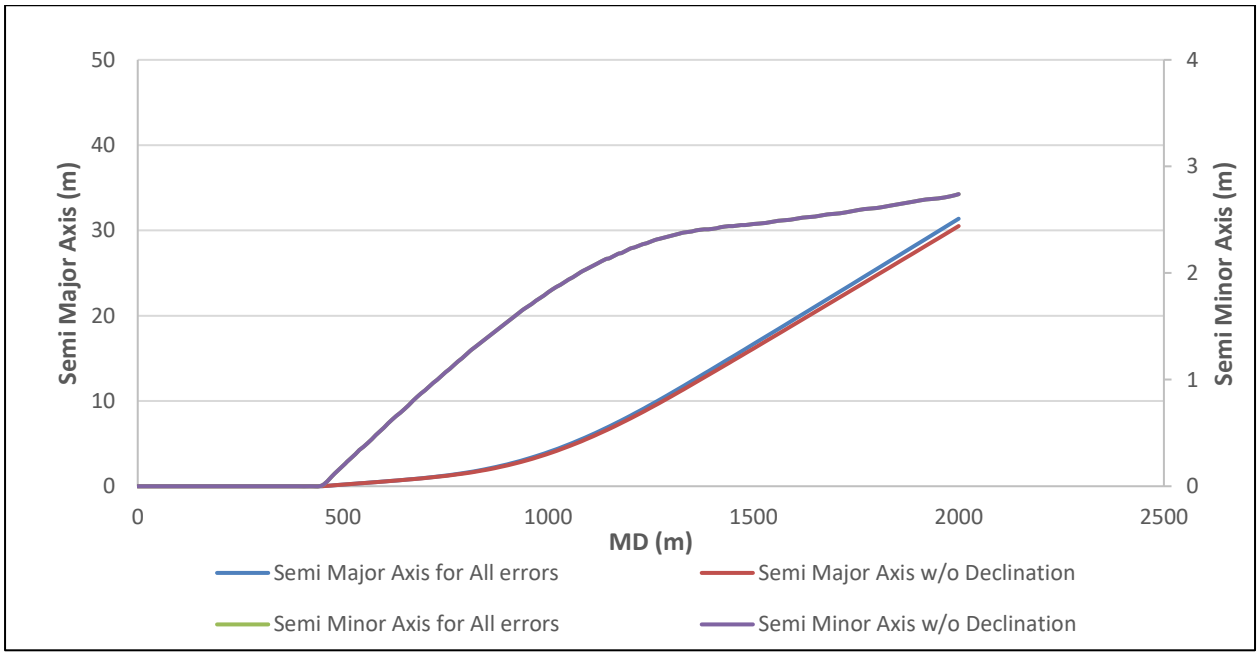

Figure 6.7 - Effect of Declination Error on Total Position Uncertainty at Azimuth = 45°

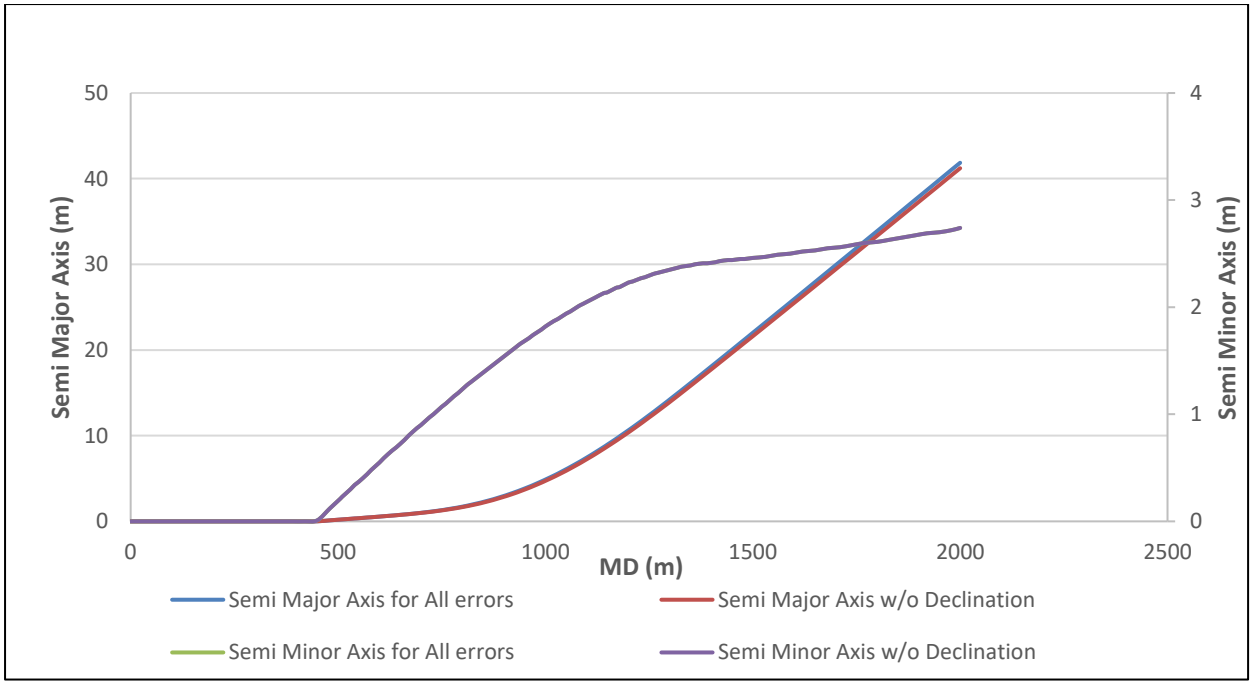

Figure 6.8 - Effect of Declination Error on Total Position Uncertainty at Azimuth = 75°

6.4 Tool Misalignment Errors

The ISCWSA Error model uses a total of six (6) error terms to incorporate the effect of tool misalignment on measurement and position uncertainty. Three of these affect the inclination uncertainty and the remaining three affect azimuth uncertainty. The effects on inclination and azimuth uncertainties will therefore be separately discussed in the following two sections based on their respective weighting functions. The error magnitudes used along with these weighting functions have been listed in Appendix D.

6.4.1 Effect on Inclination Uncertainty

Equations 6.7 - 6.9 are used to model the effect of tool misalignment on inclination uncertainties. Although inclination uncertainties are independent of drilling direction (azimuth) but the weighting functions for misalignment affecting inclination also involve azimuth. However, the inclination uncertainties still remain unchanged in North-South, North-East and East-West wells and therefore Figure 6.9 below has been considered sufficient to explain the effect of misalignment on inclination uncertainties in the three wells.

$$MAL_1 = \begin{pmatrix} 0 \\ \sin I \\ 0 \end{pmatrix} \tag{6.7}$$

$$MAL_2 = \begin{pmatrix} 0 \\ \cos(A)\sqrt{1-\sin^2(I)} \\ 0 \end{pmatrix} \tag{6.8}$$

$$MAL_3 = \begin{pmatrix} 0 \\ \sin(A)\sqrt{1-\sin^2(I)} \\ 0 \end{pmatrix} \tag{6.9}$$

Further, figure 6.9 shows that misalignment error induces a constant inclination error along the entire well length which does not change with changing hole inclination. In addition, the inclination uncertainties due to misalignment are exactly equal to the total inclination uncertainties in the vertical and near vertical section. This shows a predominant effect of misalignment in this part of the well. While in the deviated and horizontal sections, the inclination error due to misalignment is slightly less than the total inclination error making it relatively less effective at higher inclinations.

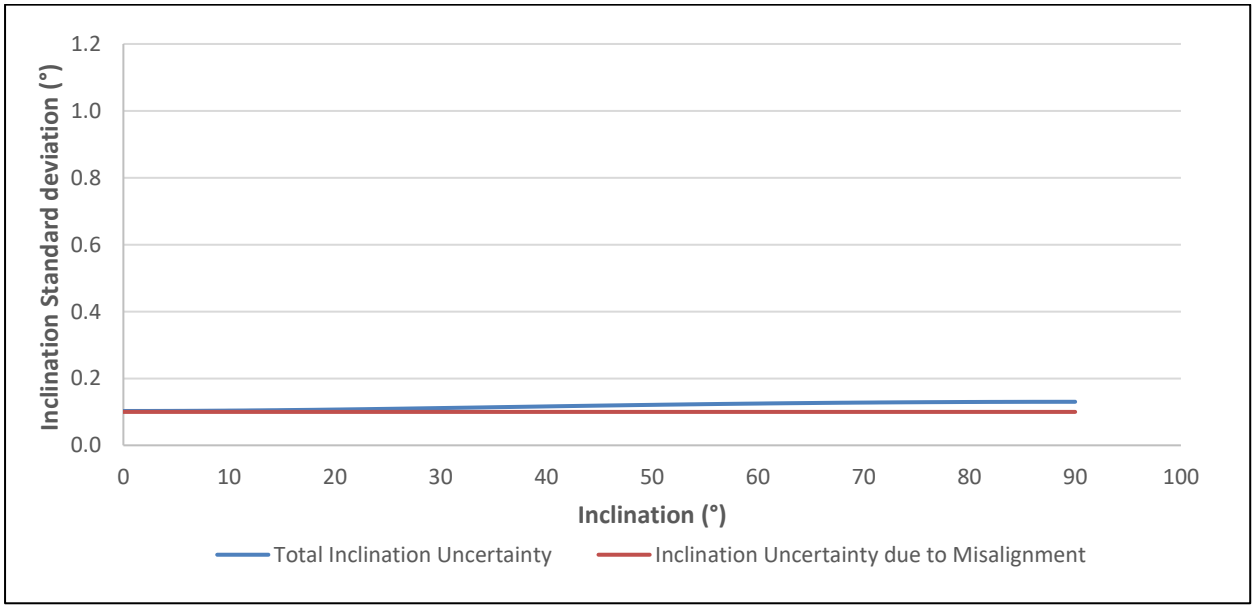

Figure 6.9 - Effect of Misalignment on Inclination Uncertainties

6.4.2 Effect on Azimuth Uncertainty

The effect of tool misalignment on azimuth uncertainties is modeled using equations 6.10-6.12. It is important to mention that these equations are originally used in the error model to predict lateral uncertainties. To convert these equations to estimate azimuth uncertainties *sin(I)* has been introduced in the denominator of all equations. Furthermore, from the weighting functions the azimuth uncertainties are a function of both hole inclination and azimuth. Therefore, the azimuth uncertainties are plotted as a function of hole inclination at three difference azimuths for North-South, North-East and East-West wells using the following equations.

$$MAL_4 = \begin{pmatrix} 0 \\ 0 \\ \dfrac{\sqrt{1-\sin^2(I)}}{\sin(I)} \end{pmatrix} \tag{6.10}$$

$$MAL_5 = \begin{pmatrix} 0 \\ 0 \\ \dfrac{-\sin(A)\sqrt{1-\sin^2(I)}}{\sin(I)} \end{pmatrix} \tag{6.11}$$

$$MAL_6 = \begin{pmatrix} 0 \\ 0 \\ \dfrac{\cos(A)\sqrt{1-\sin^2(I)}}{\sin(I)} \end{pmatrix} \tag{6.12}$$

From the three plots below, the behavior of misalignment error along the well is almost identical in all three wells. The azimuth uncertainties are extremely large in the vertical and near vertical sections but sharply decrease in the buildup section and remain unchanged up to the horizontal section. Due to these high azimuth uncertainties at lower inclinations, misalignment has the greatest impact on total azimuth error budget in the vertical and near vertical sections and relatively less impact in the buildup and horizontal sections of each well.

Misalignment error has therefore a uniform impact in the vertical and near vertical sections of the three wells. However, due to the different behavior of total azimuth uncertainties in the buildup and horizontal sections, its effectiveness towards total azimuth error is different. It is observed to be most effective in the buildup and horizontal sections of the North-South well while being least effective in the East-West well.

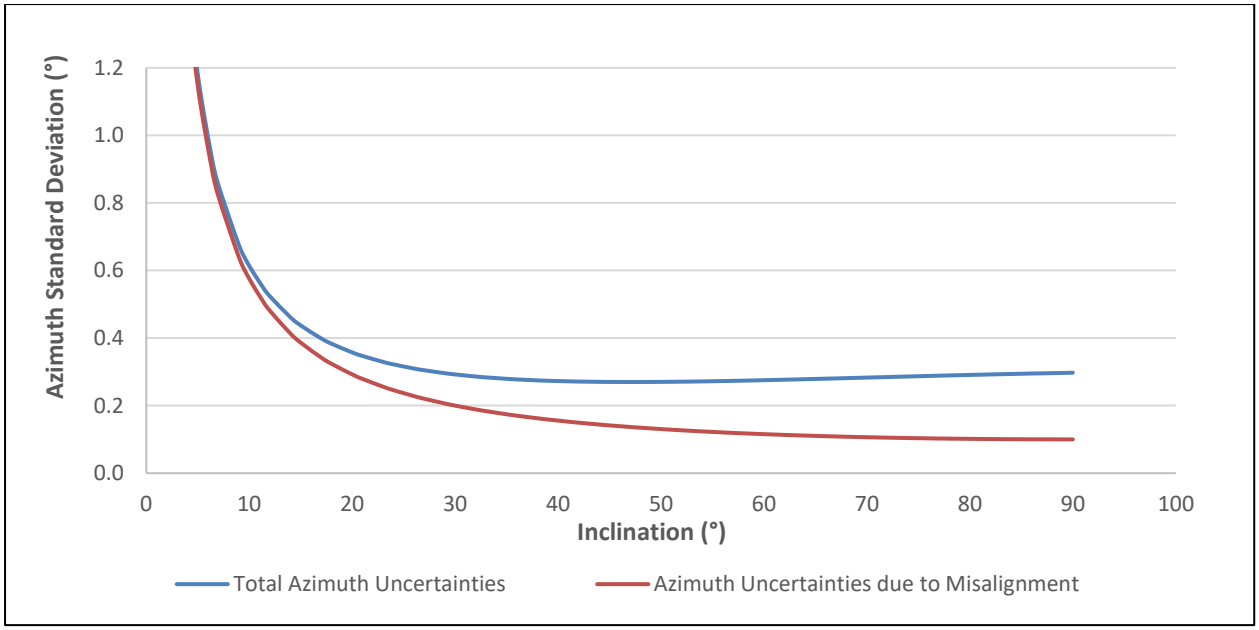

Figure 6.10 - Effect of Misalignment on Azimuth Uncertainties at Azimuth = 0°

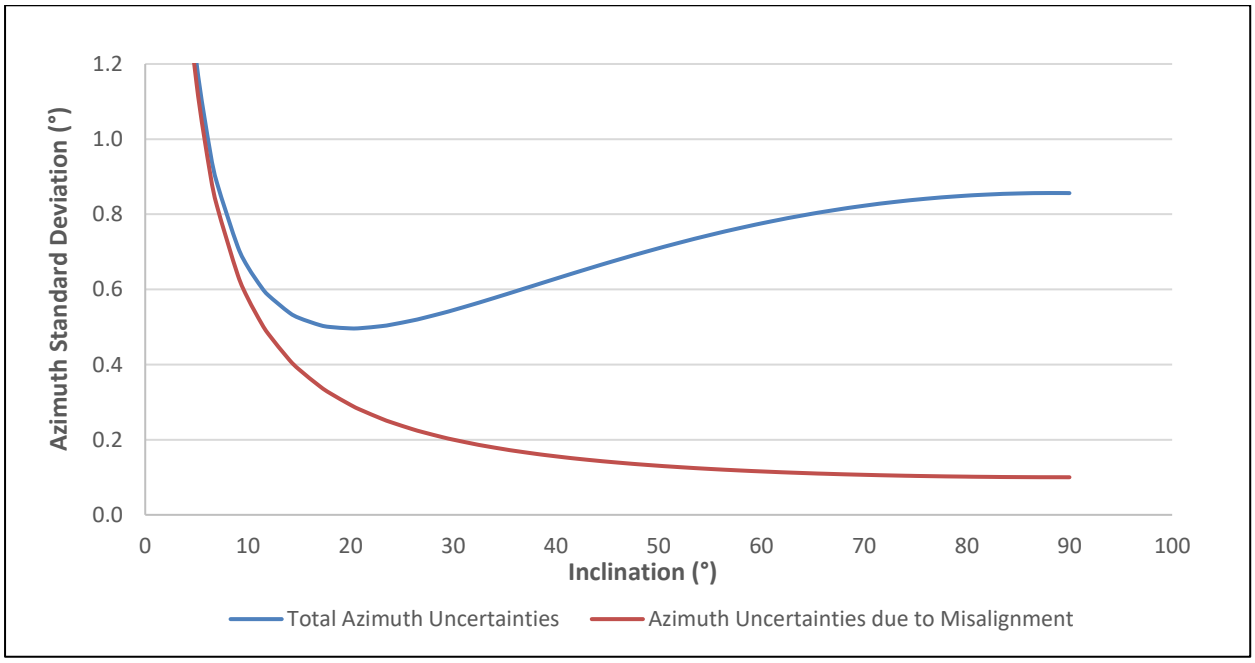

Figure 6.11 - Effect of Misalignment on Azimuth Uncertainties at Azimuth = 45°

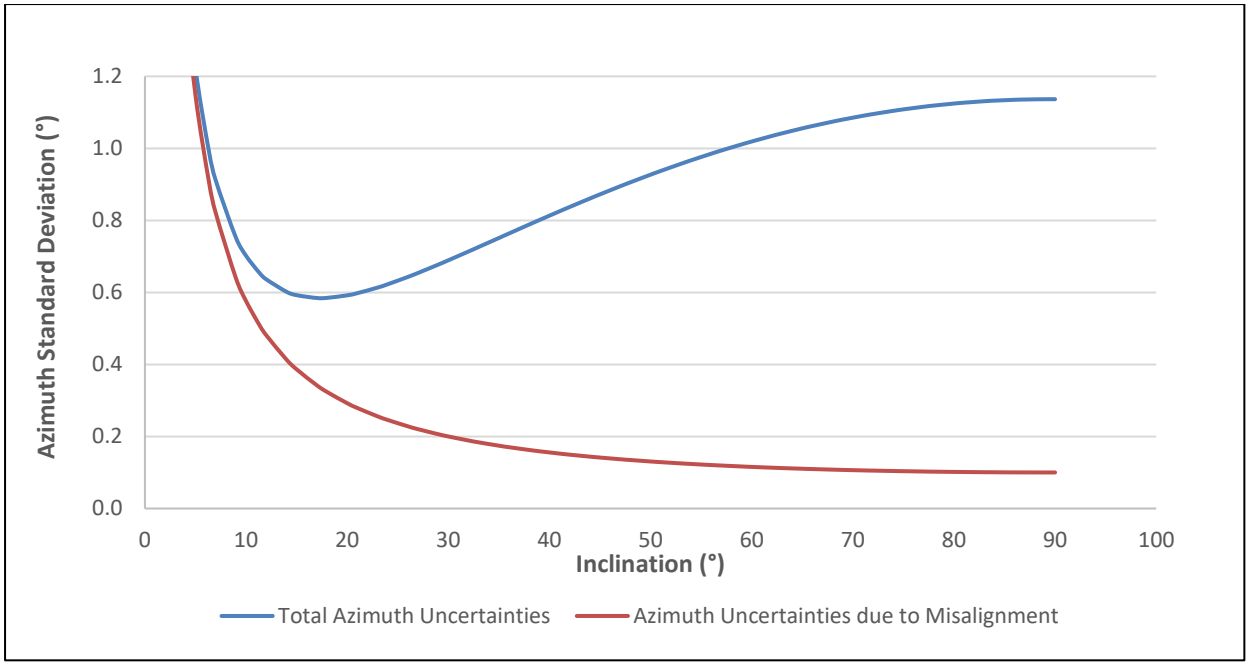

Figure 6.12 - Effect of Misalignment on Azimuth Uncertainties at Azimuth = 75°

6.4.3 Effect on Total Position Uncertainty

The size of position uncertainty ellipse in Appendix E only due to misalignment is same in each of the three wells used in this analysis. This section will demonstrate the effect of misalignment on total position uncertainty in all three wells. In each of the three wells, hardly any separation can be observed between the lengths of semi major axis for the two cases throughout the well. But the difference in the lengths of semi minor axis for the two cases is quite prominent below approximately 500m MD. This shows that misalignment adds significantly to the total position error in each well below this depth. Also, the difference in the lengths of semi minor axis is almost constant for all three wells which shows that it is equally affecting the total position error budget.

The above results show that although misalignment error is having greatest impact on inclination and azimuth uncertainties in the vertical and near vertical sections of all wells, but it is hardly having any influence on position uncertainties in these hole sections. Contrary to this, at higher depths corresponding to buildup and horizontal section, its impact on measurement uncertainties is observed to drop while that on position uncertainty increases. Also, among the three wells, its relative effect on total azimuth uncertainties decreases towards East-West drilling direction but remains constant for position uncertainty.

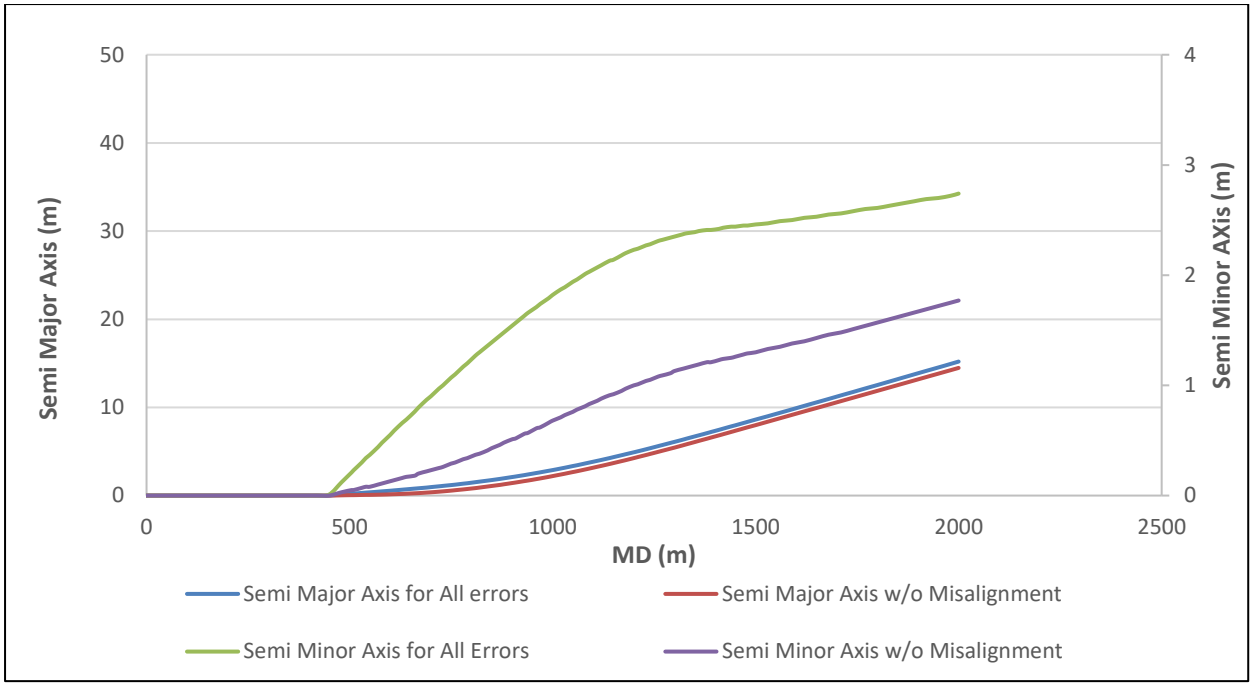

Figure 6.13 - Effect of Misalignment on Total Position Uncertainty at Azimuth = 0°

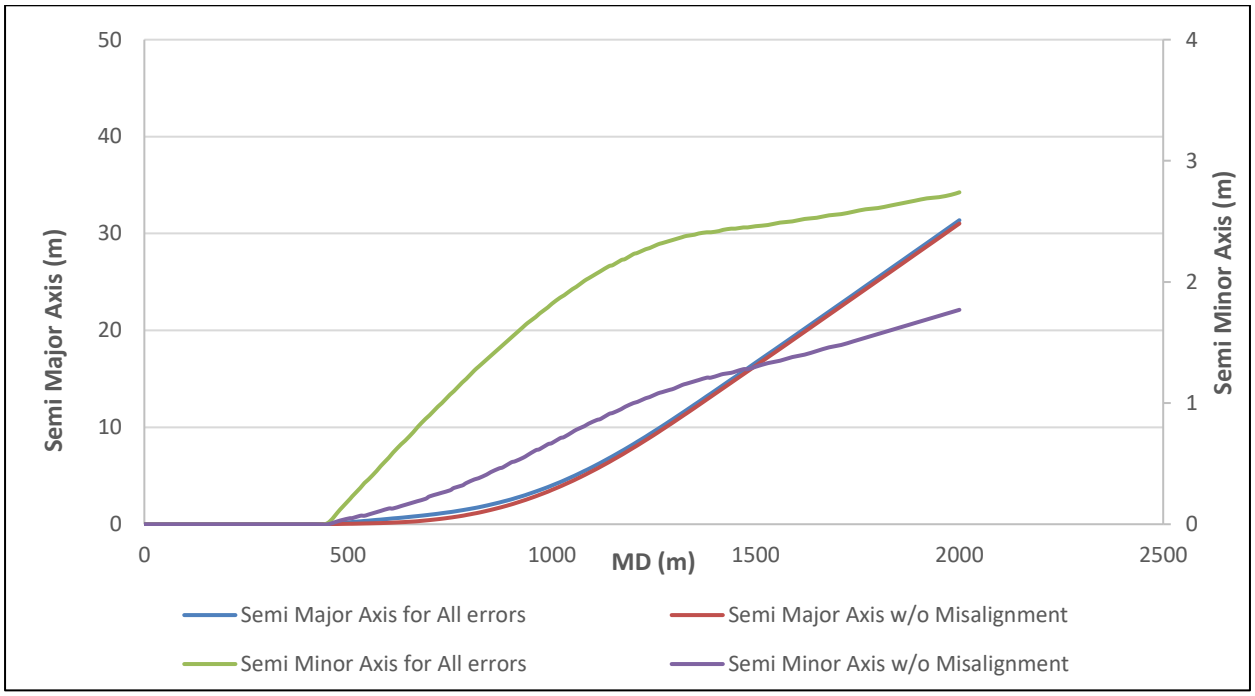

Figure 6.14 - Effect of Misalignment on Total Position Uncertainty at Azimuth = 45°

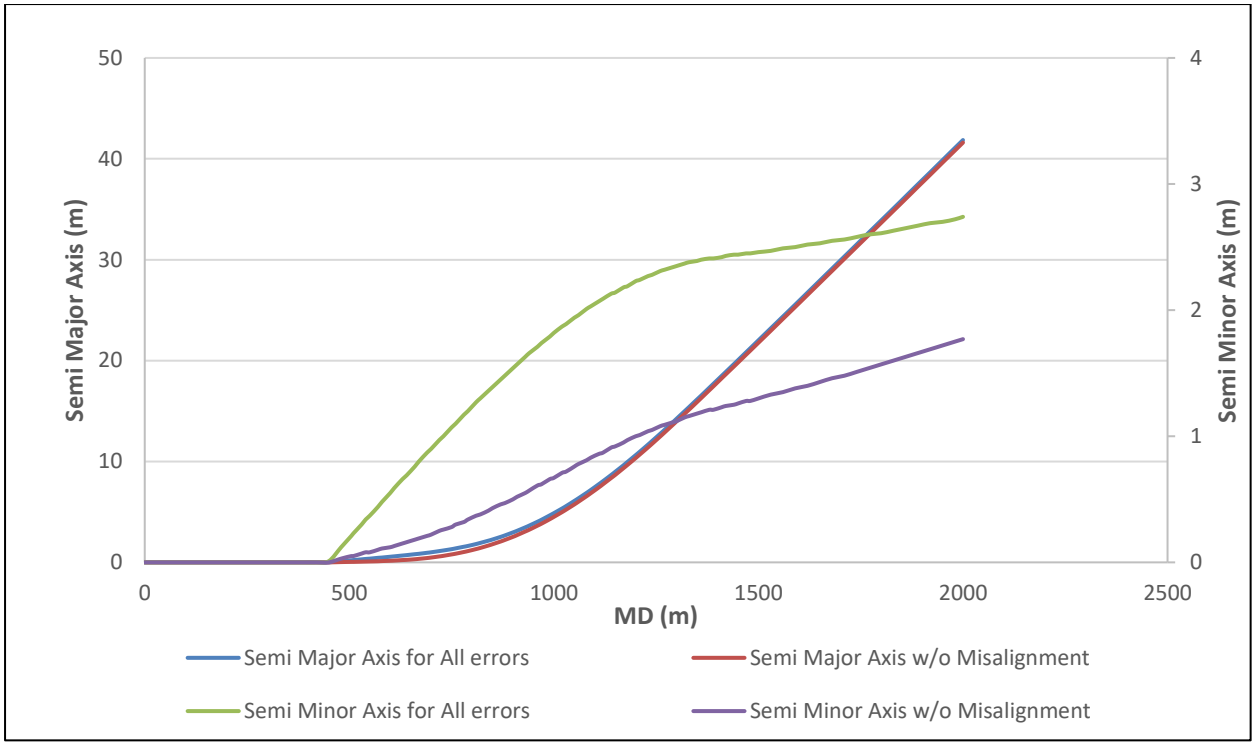

Figure 6.15 - Effect of Misalignment on Total Position Uncertainty at Azimuth = 75°

6.5 Magnetic Axial Drillstring Interference (AMIL)

This error term is included in the ISCWSA error model to include the effect of magnetic axial drillstring interference impacting azimuth measurements. From the weighting function given below, effect of this error source is dependent on well trajectory, direction and location where it is drilled. The corresponding error magnitude has been provided in Appendix D.

$$amil = \begin{pmatrix} 0 \\ 0 \\ \dfrac{\sin(I)\sin(A)}{B\cos(\Theta)} \end{pmatrix} \tag{6.13}$$

6.5.1 Effect on Azimuth Uncertainty

The effect of this error source on azimuth uncertainties has been evaluated in all three wells separately. The dip angle and magnetic field values have been used for typical North-sea conditions. The azimuth uncertainties in the North-South well are almost negligible throughout the well and remain independent of inclination. Therefore, they have no contribution towards the total azimuth uncertainties in any part of the well. For the North-East and East wells, the

effect on azimuth uncertainties is almost identical. The azimuth uncertainties increase as a function of inclination from being minimum in the vertical section to maximum in the horizontal section. Due to this increase, their contribution towards the total azimuth error budget also increases and is maximum in the horizontal section.

Comparing the azimuth uncertainties in the three wells based on the above analysis, this error source has therefore no influence at all in the North-South well. For the North-East and East-West wells, the effect is same in the vertical and near vertical section of the two wells. However, the error source has a slightly greater share towards the total azimuth uncertainties in the highly deviated and horizontal section of the East-West well.

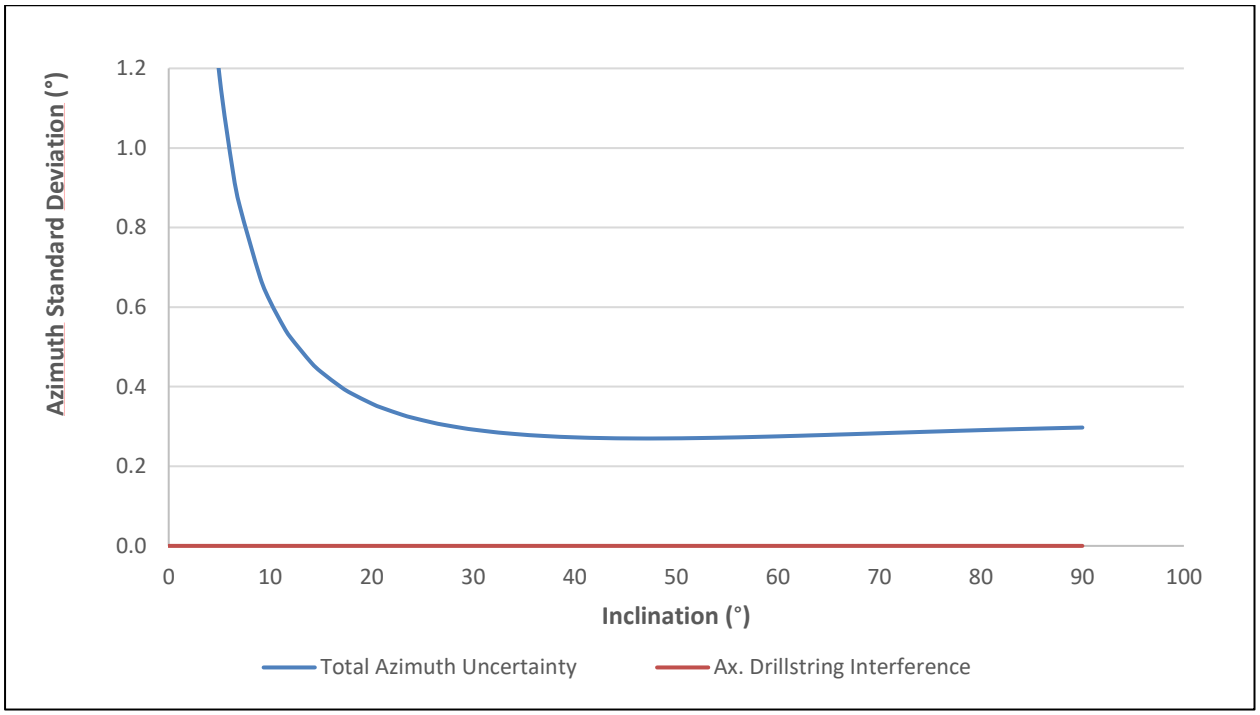

Figure 6.16 - Effect of AMIL on Azimuth Uncertainties at Azimuth = 0°

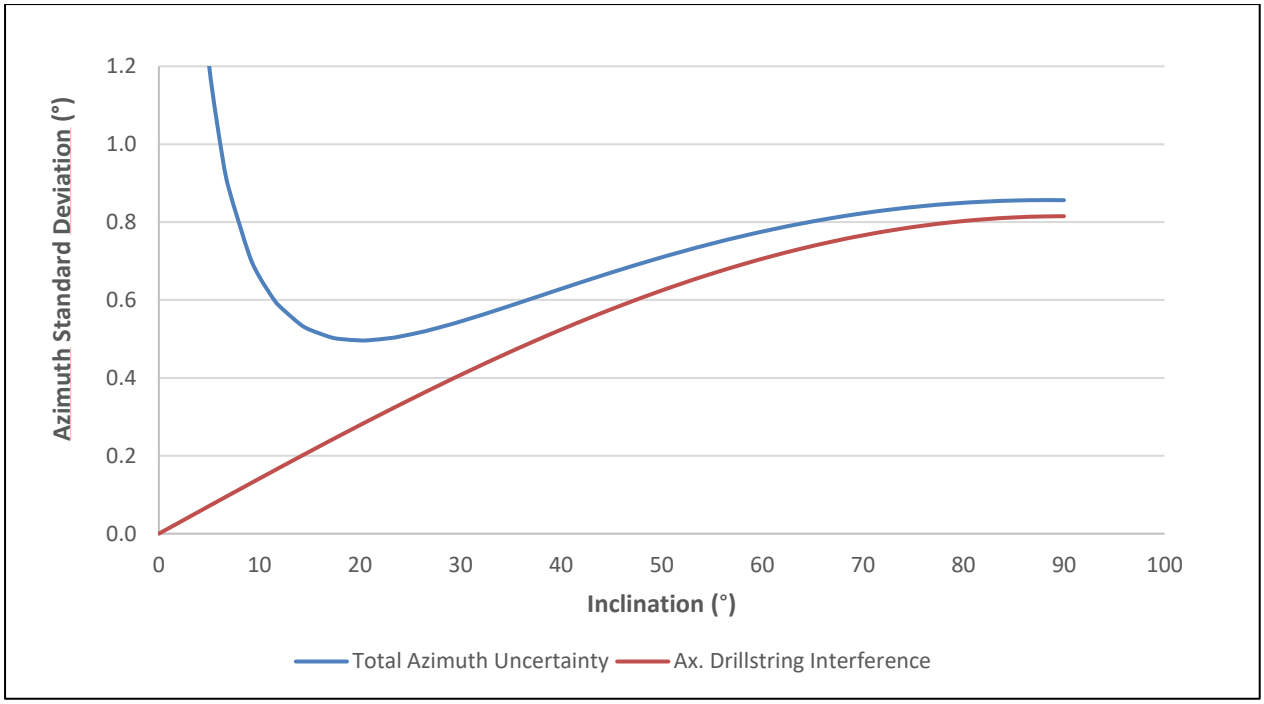

Figure 6.17 - Effect of AMIL on Azimuth Uncertainties at Azimuth = 45°

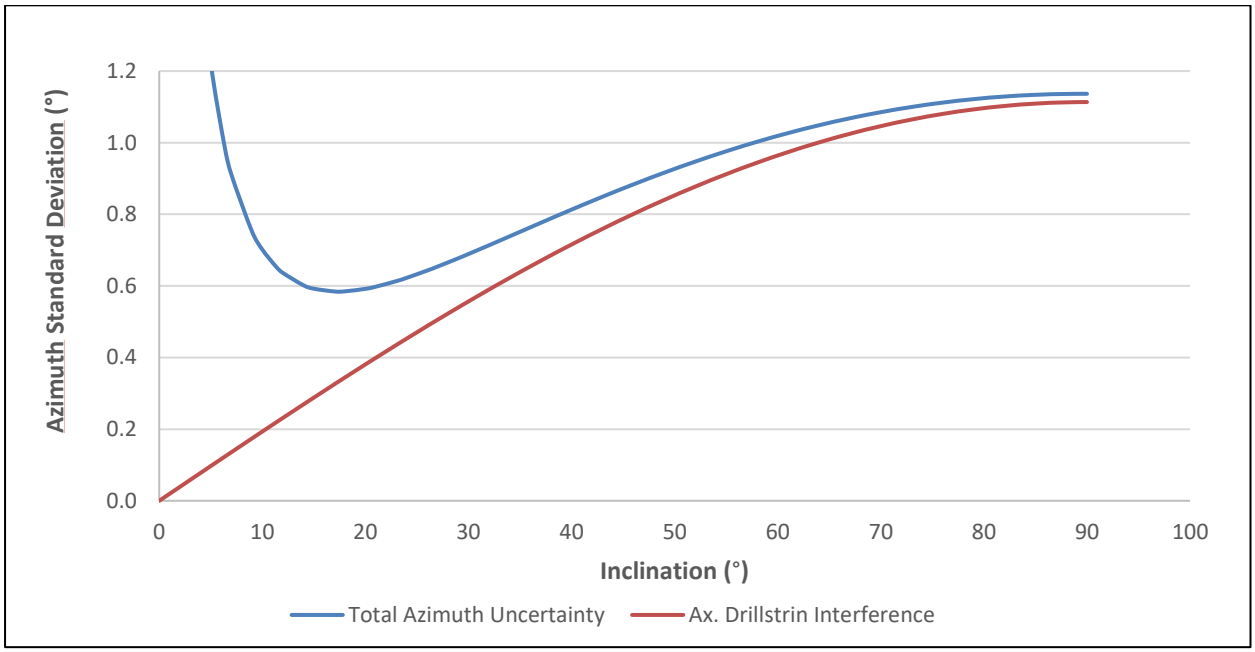

Figure 6.18 - Effect of AMIL on Azimuth Uncertainties at Azimuth = 75°

6.5.2 Effect on Total Position Uncertainty

Figures 6.19-6.21 show the effect of this error source on total position uncertainty. For the North-South well, the effect on total position uncertainty is also negligible throughout the well as observed in the case for azimuth uncertainties. But, the effect on total position uncertainties in the North-East and East-West well is quite similar along the well. The error source starts

affecting the total position uncertainty in both wells only below approximately 1000m MD and becomes more effective with increasing depth. However, between the two wells, removing this error source has a greater influence on total position uncertainty in the East-West well compared to North-East well.

From the above analysis of measurement and position uncertainties, it is possible to see if the error source has a similar effect on azimuth and position uncertainties for each hole section or not. For the North-South well, the error source neither adds to the total azimuth nor to the position error budget throughout the well. Similarly, in the North-East and East-West well, the contribution of this error source towards total azimuth and position uncertainties is minimum in the vertical section and maximum in the horizontal section. Therefore, this error source has a uniform effect on both measurement and position uncertainties.

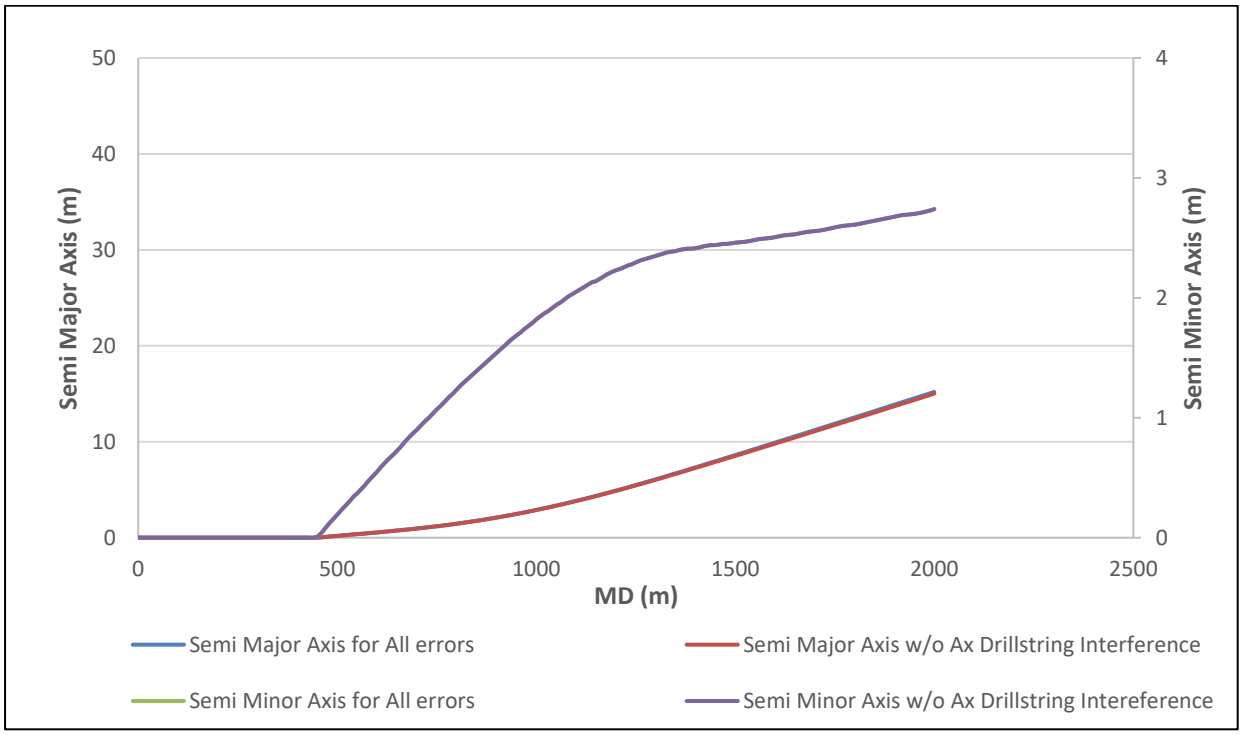

Figure 6.19 - Effect of AMIL on Total Position Uncertainty at Azimuth = 0°

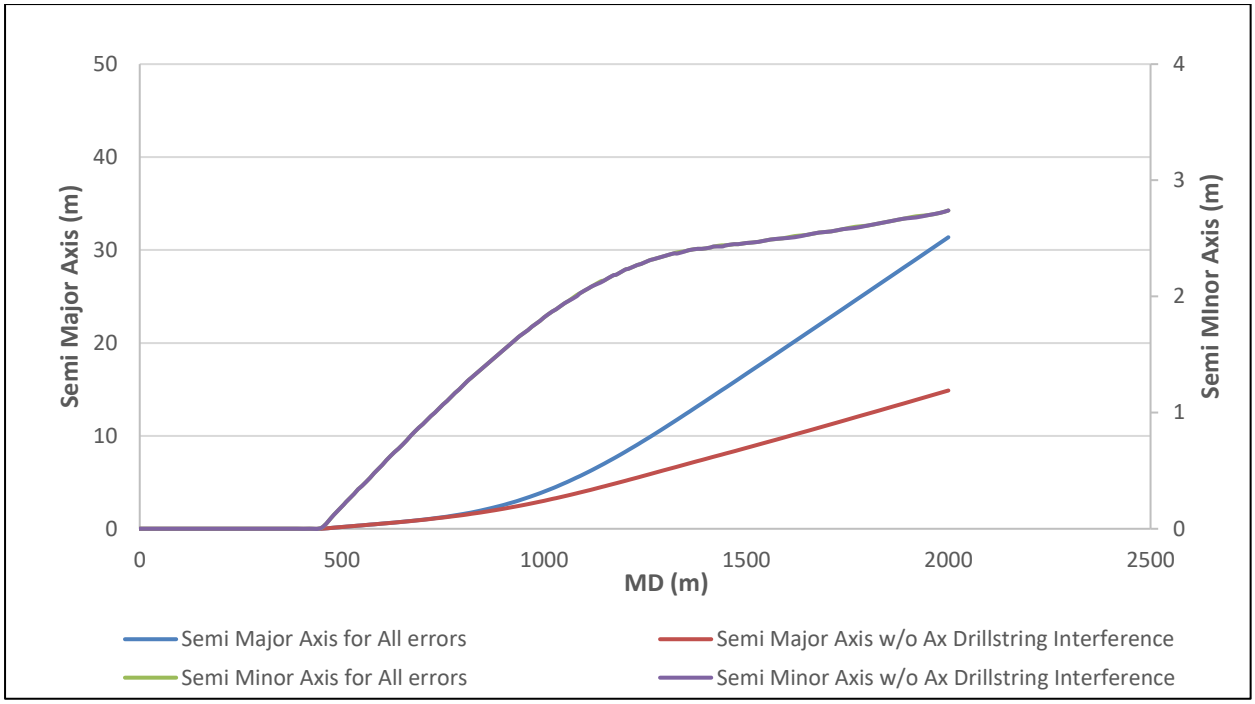

Figure 6.20 - Effect of AMIL on Total Position Uncertainty at Azimuth = 45°

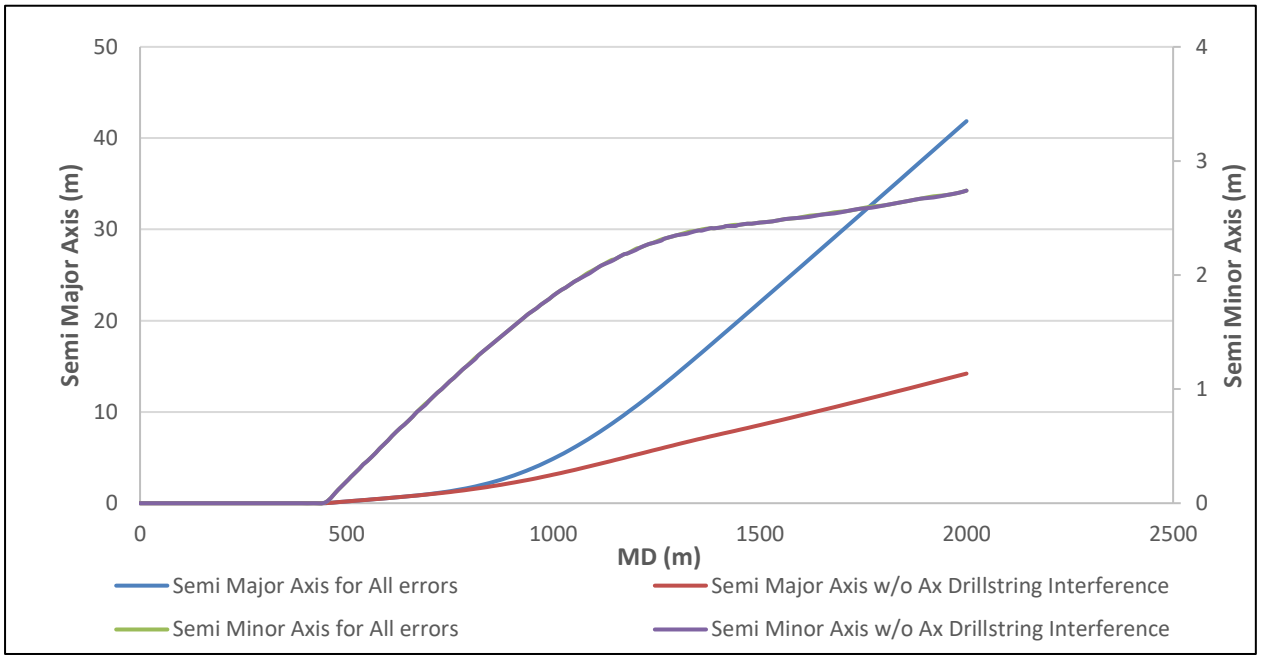

Figure 6.21 - Effect of AMIL on Total Position Uncertainty at Azimuth = 75°

6.6 Accelerometer Bias

Accelerometer Bias also affects both inclination and azimuth uncertainties. The ISCWSA error model has proposed a total of five different error terms to account for these effects which will be discussed separately in sections 6.6.1 and 6.6.2 along with their respective weighting

functions. When evaluating the effect on total position uncertainty however, all five equations will be used together in Compass along with their error magnitudes provided in Appendix D.

6.6.1 Effect on Inclination Uncertainty

Equations 6.14 & 6.15 have been used to calculate inclination uncertainties due to accelerometer bias. The combined effect of these two error terms has been used to demonstrate the effect on inclination uncertainty.

$$abxyi\_1 = \begin{pmatrix} 0 \\ \frac{-\cos(I)}{g_{tot}} \\ 0 \end{pmatrix} \tag{6.14}$$

$$abzi = \begin{pmatrix} 0 \\ \frac{-\sin(I)}{g_{tot}} \\ 0 \end{pmatrix} \tag{6.15}$$

The weighting functions show that the effect of accelerometer bias will be influenced only by hole inclination and total gravitational acceleration. Based on this, Figure 6.22 thus shows that accelerometer bias induces a very small constant inclination error along the well. Also, the contribution it makes to the total inclination error budget is very little and it remains to be an insignificant error source for almost entire well length.

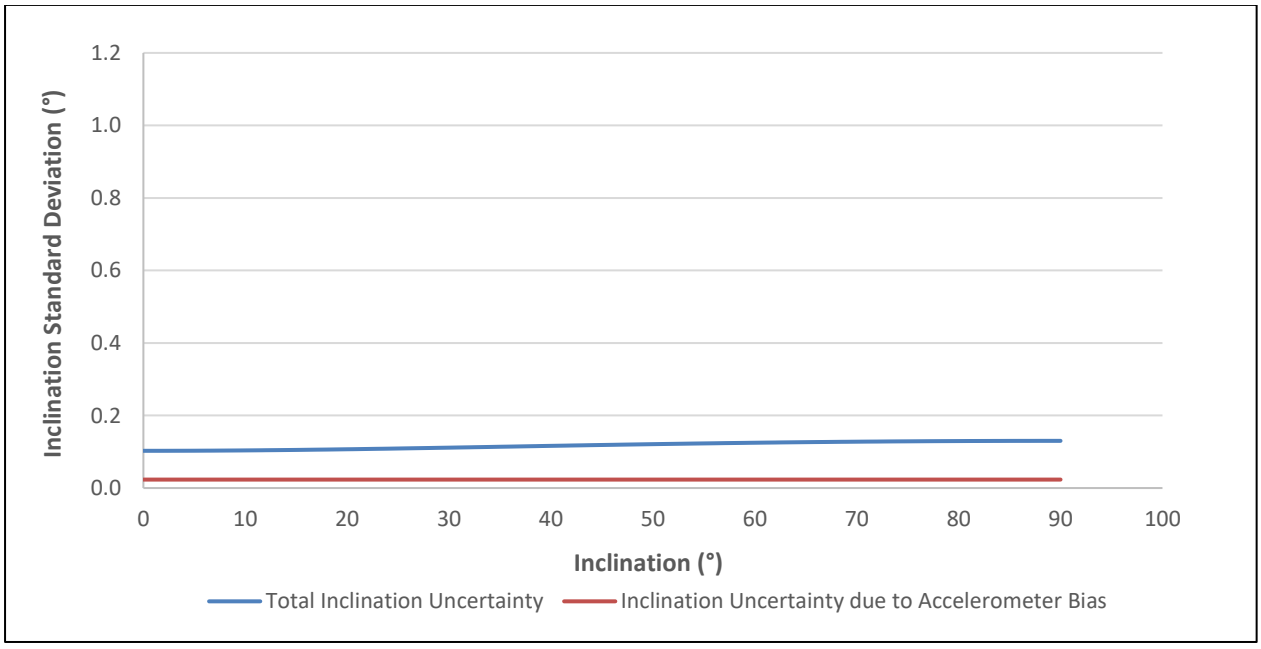

Figure 6.22 - Effect of Accelerometer Bias on Inclination Uncertainties

6.6.2 Effect on Azimuth Uncertainty

Azimuth uncertainties due to accelerometer bias have been calculated using equations 6.16-6.18 and are represented in Figures 6.23-6.25 for the three subject wells. The presence of *sin(I)* in equation 6.17 is intended to convert lateral uncertainties to azimuth uncertainties similar to misalignment azimuth errors. However, unlike the inclination uncertainties, azimuth uncertainties are also a function of drilling direction and well location in addition to hole inclination and total gravitational acceleration.

$$abxya\_1 = \begin{pmatrix} 0 \\ 0 \\ \dfrac{\tan(\Theta)\cos(I)\sin(A)}{g_{tot}} \end{pmatrix} \tag{6.16}$$

$$abxya\_2 = \begin{pmatrix} 0 \\ 0 \\ \dfrac{\cos(I) - \tan(\Theta)\cos(A)\sin(I)}{\sin(I)g_{tot}} \end{pmatrix} \tag{6.17}$$

$$abza = \begin{pmatrix} 0 \\ 0 \\ \dfrac{\tan(\Theta)\sin(I)\sin(A)}{g_{tot}} \end{pmatrix} \tag{6.18}$$

Based on the weighting functions above, all three wells experience very high azimuth uncertainties in the vertical and near vertical section primarily due to the error term *abxy_2* having *sin(I)* in the denominator. But in a very short span of 0 -15° the azimuth uncertainties drop to a minimum and maintain a constant trend for the rest of the well independent of the inclination. Due to this behavior of azimuth uncertainties, accelerometer bias has the greatest share towards total azimuth error budget from 0-15° inclination and is constant and minimum in the buildup and horizontal section of each well.

When comparing the effect of this error source in different wells, it is seen to have an almost uniform impact in the vertical and near vertical sections of each well. However, due to varying total azimuth uncertainties in the buildup and horizontal section it is observed to contribute most towards the total azimuth uncertainties in the buildup section of North-South well and minimum in the East-West well.

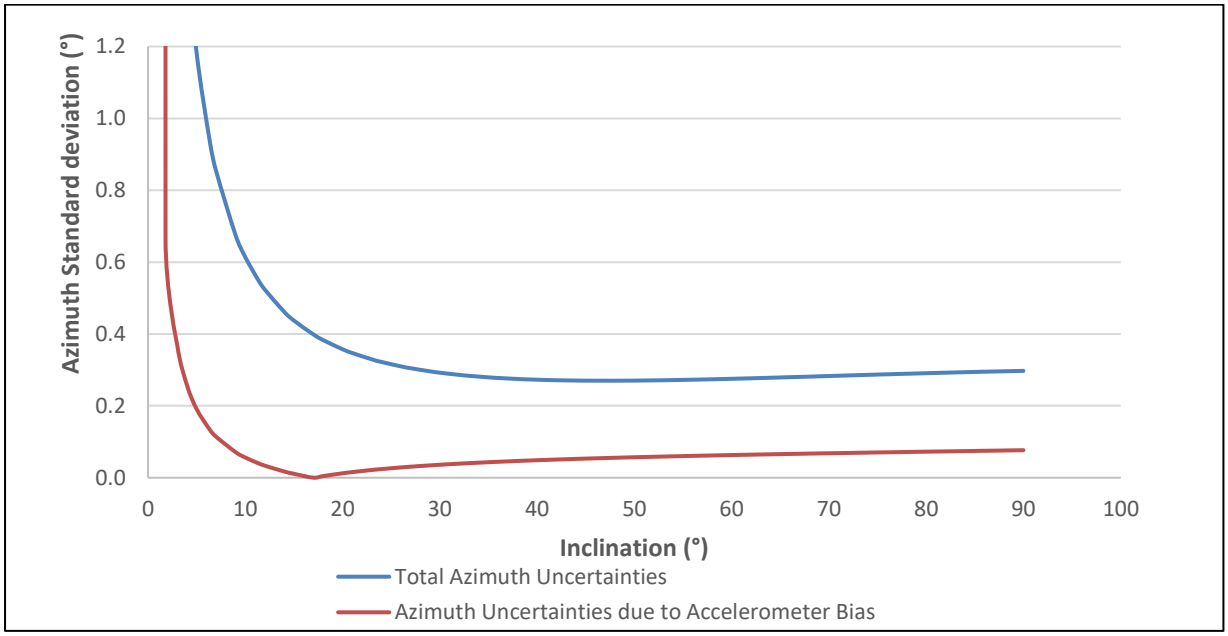

Figure 6.23 - Effect of Accelerometer Bias on Azimuth Uncertainties at Azimuth = 0°

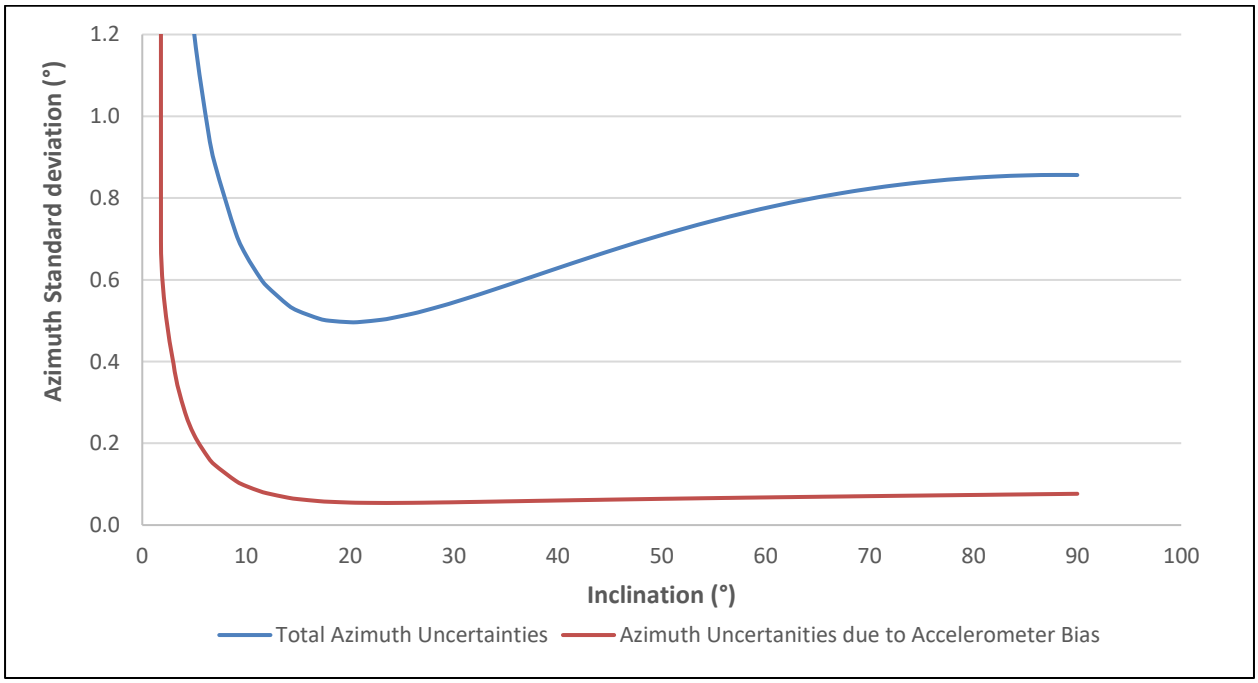

Figure 6.24 - Effect of Accelerometer Bias on Azimuth Uncertainties at Azimuth = 45°

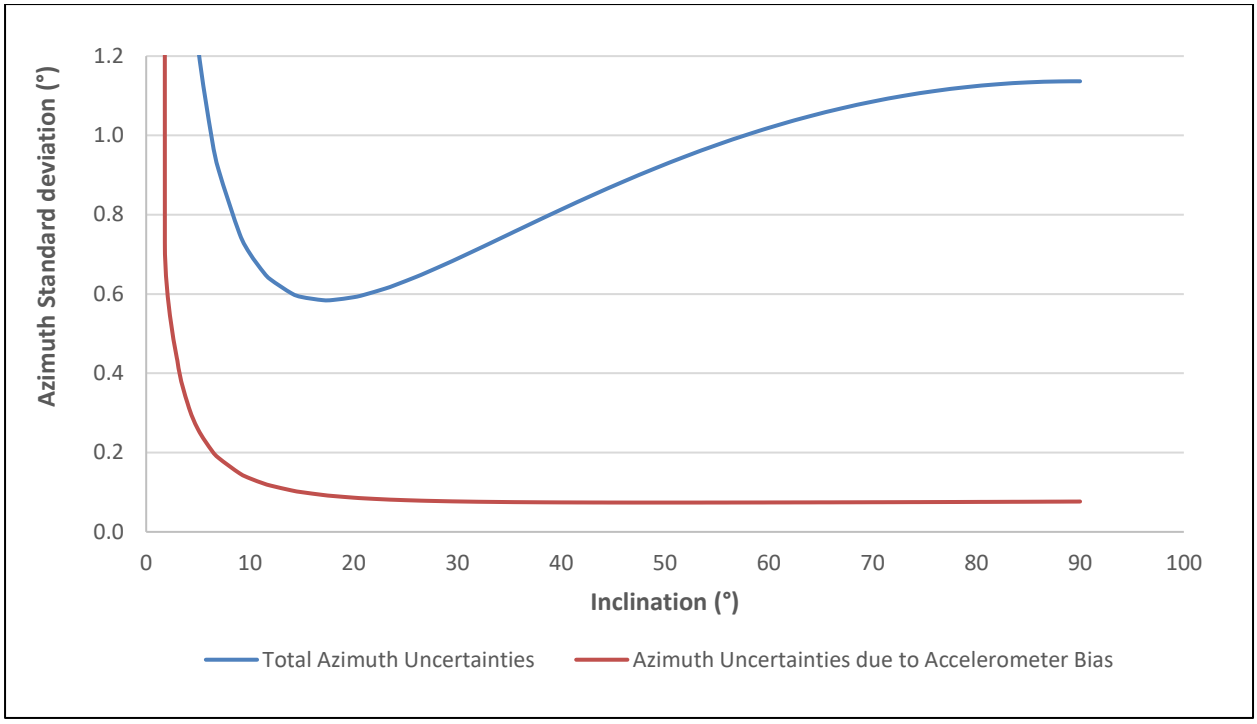

Figure 6.25- Effect of Accelerometer Bias on Azimuth Uncertainties at Azimuth = 75°

6.6.3 Effect on Total Position Uncertainty

The effect of accelerometer bias error on total position uncertainty is almost negligible throughout the well path in all three wells. No significant difference in lengths of either semi major or minor axis has been observed when accelerometer bias is removed from the error model. Only a very little deviation in the semi minor axis is observed in the horizontal section of all wells due to the *abxya_2* error term causing TVD errors.

The above results thus show that despite of accelerometer bias having large azimuth uncertainties in the vertical and near vertical section of the subject wells it still does not consequently affect position uncertainty in neither these nor any other hole sections. Also, the effect of accelerometer bias on measurement uncertainties is different in the buildup and horizontal section of the three wells but it has a uniform impact on position uncertainty for the corresponding hole sections.

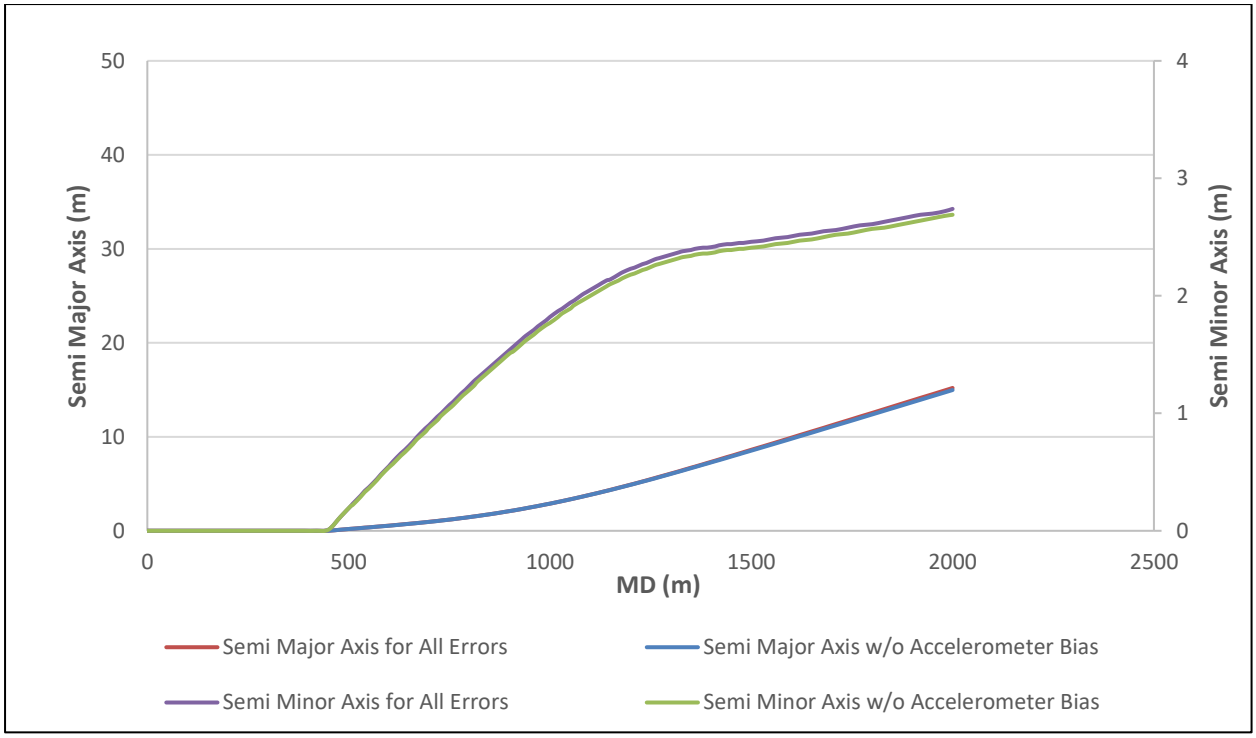

Figure 6.26 - Effect of Accelerometer Bias on Total Position Uncertainty at Azimuth = 0°

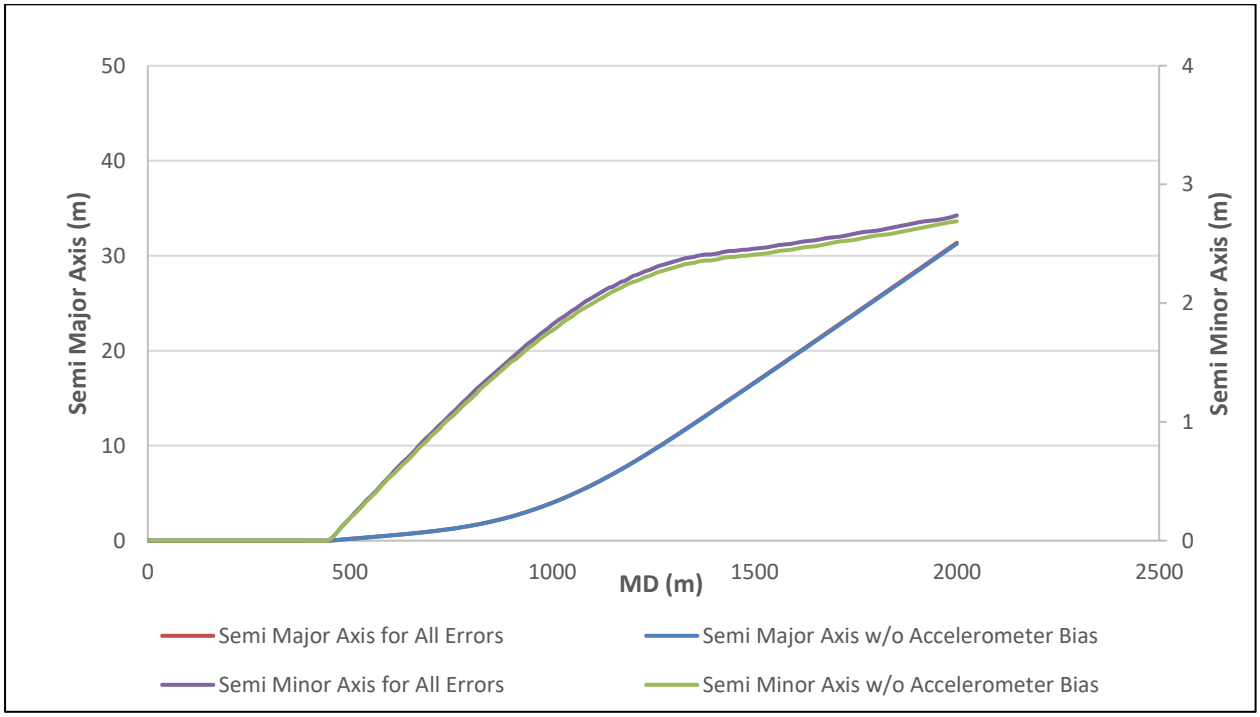

Figure 6.27 - Effect of Accelerometer Bias on Total Position Uncertainty at Azimuth = 45°

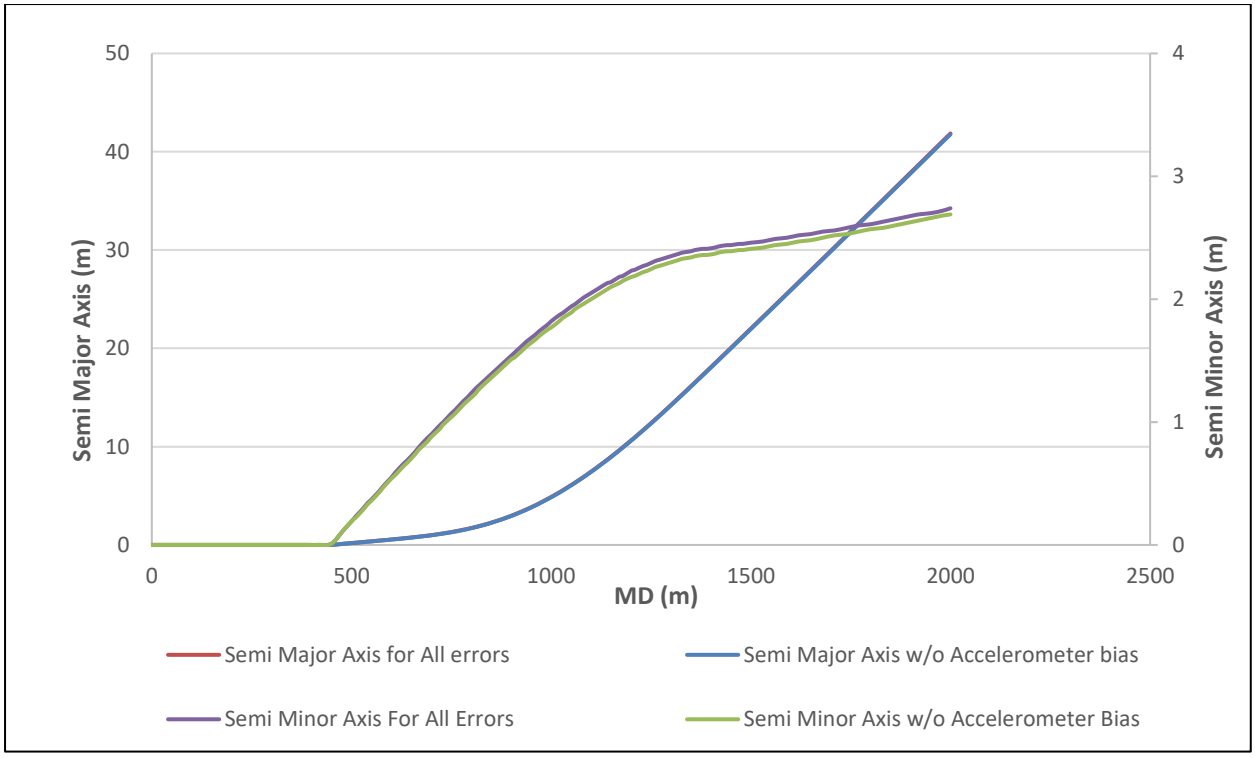

Figure 6.28- Effect of Accelerometer Bias on Total Position Uncertainty at Azimuth = 75°

6.7 Accelerometer Scale

The effect of accelerometer scale errors is accounted with a total of seven error terms in the ISCWSA error model. Three of them effect the inclination uncertainties while remaining four effect azimuth uncertainties. Sections 6.7.1 and 6.7.2 will discuss in detail the effects on each separately along with their weighting functions. Finally, the effect on position uncertainty will be determined combining all seven error terms for accelerometer scale.

6.7.1 Effect on Inclination Uncertainty

The effect of accelerometer scale on inclination uncertainties has been modeled using equations 6.19-6.21. Similar to accelerometer bias, the inclination uncertainty due to accelerometer scale is also a function of hole inclination only and not direction. The combined effect of the three equations below has been used to represent the effect of accelerometer scale on inclination uncertainties through Figure 32.

$$asxyi\_1 = \begin{pmatrix} 0 \\ \frac{\sin(I)\cos(I)}{\sqrt{2}} \\ 0 \end{pmatrix} \tag{6.19}$$

$$asxyi\_2 = \begin{pmatrix} 0 \\ \frac{\sin(I)\cos(I)}{2} \\ 0 \end{pmatrix} \tag{6.20}$$

$$asz = \begin{pmatrix} 0 \\ -\sin(I)\cos(I) \\ 0 \end{pmatrix} \tag{6.21}$$

Based on the above weighting functions, accelerometer scale hardly induces an inclination error along the well. This is because of the composition of above weighting functions. The functions *sin(I)* is minimum in the vertical and near vertical hole sections while *cos(I)* decreases at higher inclinations in the buildup and horizontal section. A product of these two functions always results in minimum inclination error almost for the entire well. Therefore, accelerometer scale hardly influences the total inclination error budget at any point along the well and cannot be regarded as an important contributor towards inclination uncertainties in any of the three wells.

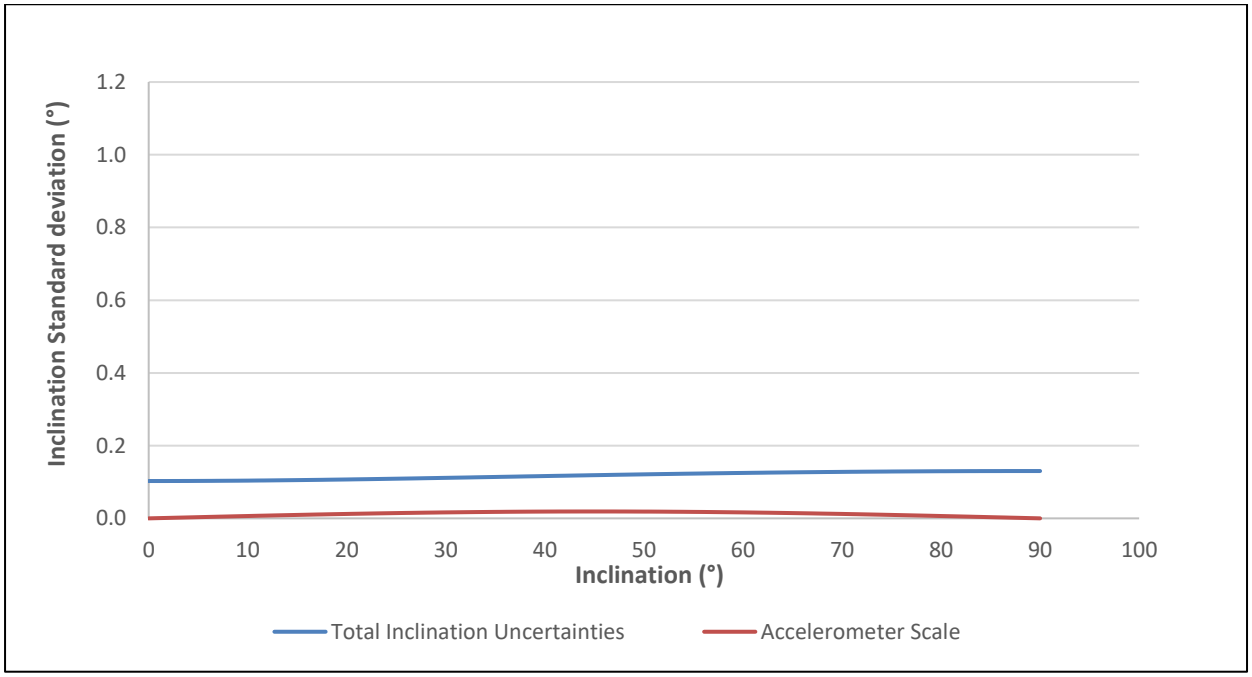

Figure 6.29 - Effect of Accelerometer Scale on Inclination Uncertainties

6.7.2 Effect on Azimuth Uncertainty

Azimuth uncertainties due to accelerometer scale are modeled using four equations 6.22 – 6.24. The weighting functions show that azimuth uncertainties for this error source are a function of hole inclination, azimuth and well location (dip angle).

$$asxya\_1 = \begin{pmatrix} 0 \\ 0 \\ \dfrac{-\tan(\Theta)\sin(I)\cos(I)\sin(A)}{\sqrt{2}} \end{pmatrix} \tag{6.22}$$

$$asxya\_2 = \begin{pmatrix} 0 \\ 0 \\ \dfrac{-\tan(\Theta)\sin(I)\cos(I)\sin(A)}{2} \end{pmatrix} \tag{6.23}$$

$$asxya\_3 = \begin{pmatrix} 0 \\ 0 \\ \dfrac{\tan(\Theta)\sin(I)\cos(A)-\cos(I)}{2} \end{pmatrix} \tag{6.24}$$

$$asza = \begin{pmatrix} 0 \\ 0 \\ \tan(\Theta)\sin(I)\cos(I)\sin(A) \end{pmatrix} \tag{6.25}$$

From the figures below the azimuth uncertainties are also extremely low throughout the three subject wells. In the vertical and near vertical section, the azimuth errors are almost zero in each well. The azimuth error slightly increases in the buildup and horizontal section of the North-South well and makes some contribution to the total azimuth error budget in these hole sections. While in the North-East and East-West wells, the azimuth error increases in the buildup section but again reduces to zero in the horizontal section. Due to this they make slightly contribute to total azimuth uncertainties only in the buildup section of the two wells.

Accelerometer scale thus does not have any impact on total azimuth uncertainties in the vertical and near vertical sections of all three wells. In the buildup section, it is seen to have relatively greater impact in the North-South well compared to North-East and East-West wells. This is again because of increase in total azimuth uncertainties and reducing accelerometer scale's percentage contribution. For the horizontal section, accelerometer scale does not have any

influence on total azimuth error budget for North-East and East-West wells but has a slight contribution in the North-South well.

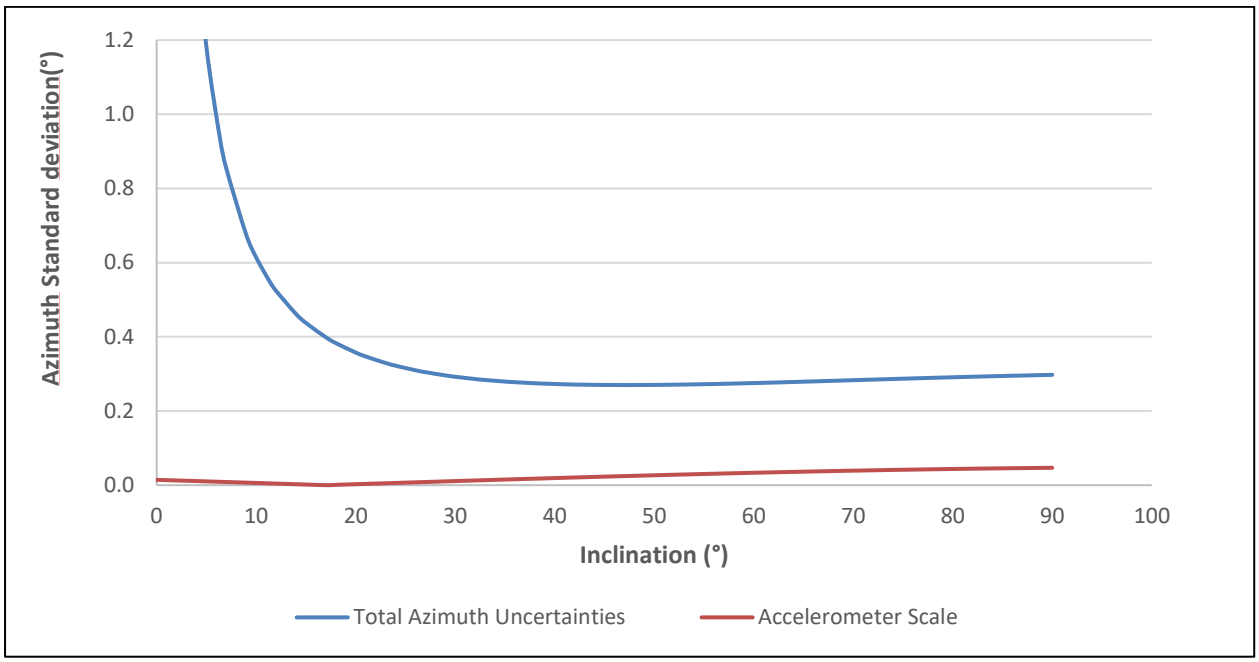

Figure 6.30 - Effect of Accelerometer Scale on Azimuth Uncertainties at Azimuth = 0°

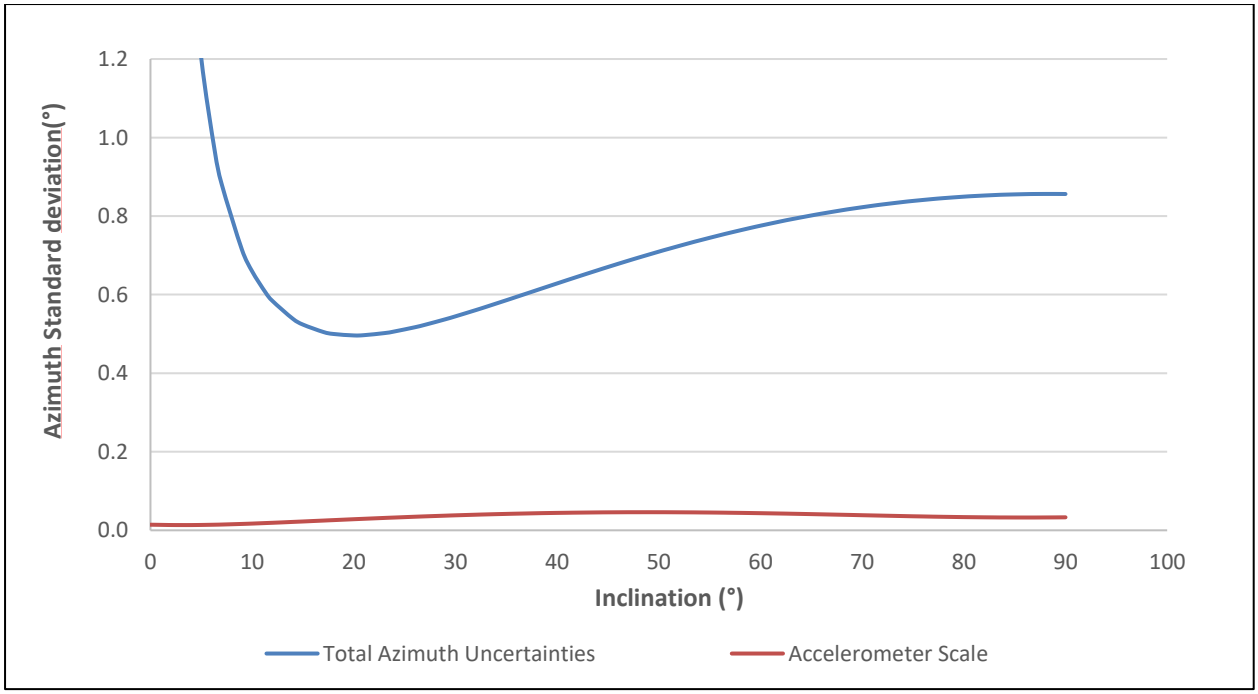

Figure 6.31 - Effect of Accelerometer Scale on Azimuth Uncertainties at Azimuth = 45°

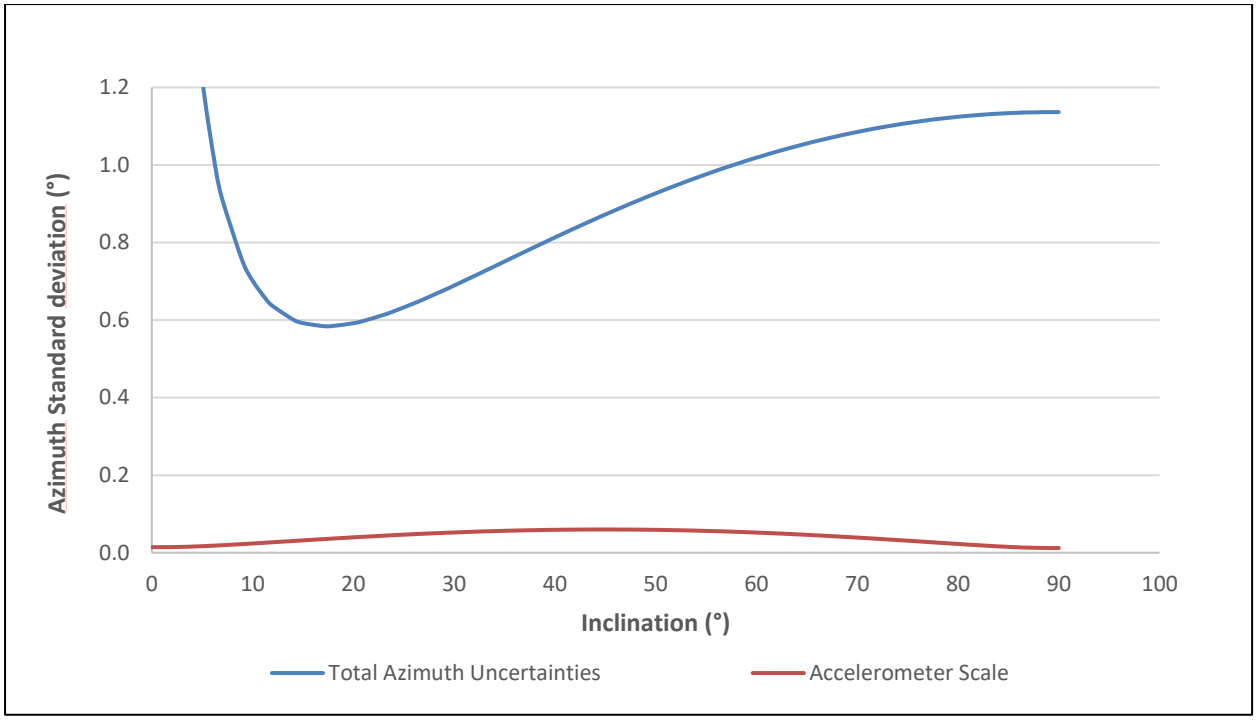

Figure 6.32 - Effect of Accelerometer Scale on Azimuth Uncertainties at Azimuth = 75°

6.7.3 Effect on Total Position Uncertainty

Figures 6.33-6.35 have been used to understand the effect of accelerometer scale errors on total position uncertainty. Neither a difference in lengths of semi major or minor axis is observed at any point in any of the three wells when accelerometer scale error has been ignored. This shows that even removing accelerometer scale error terms from the error model will not impact the total position uncertainty. Although accelerometer scale did induce very little measurement errors in some hole sections but they can be considered insufficient to cause a significant impact on wellbore position uncertainty.

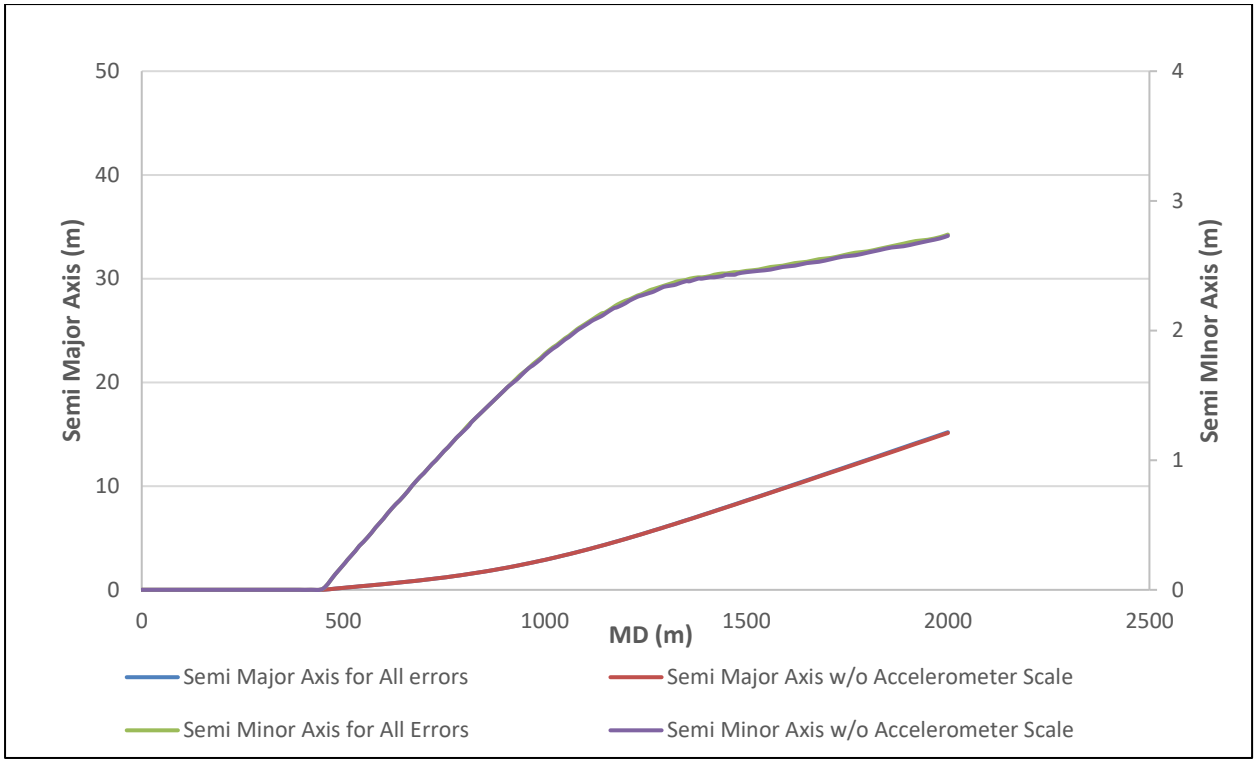

Figure 6.33 - Effect of Accelerometer Scale on Total Position Uncertainty at Azimuth = 0°

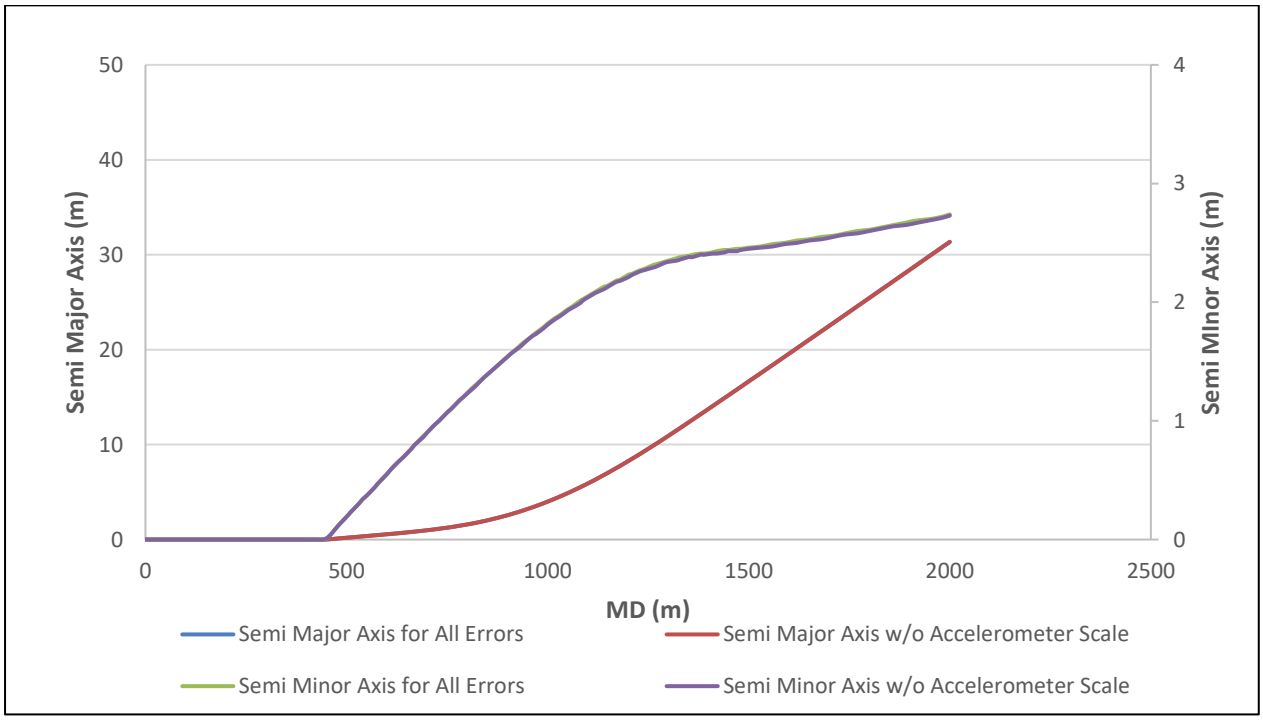

Figure 6.34 - Effect of Accelerometer Scale on Total Position Uncertainty at Azimuth = 45°

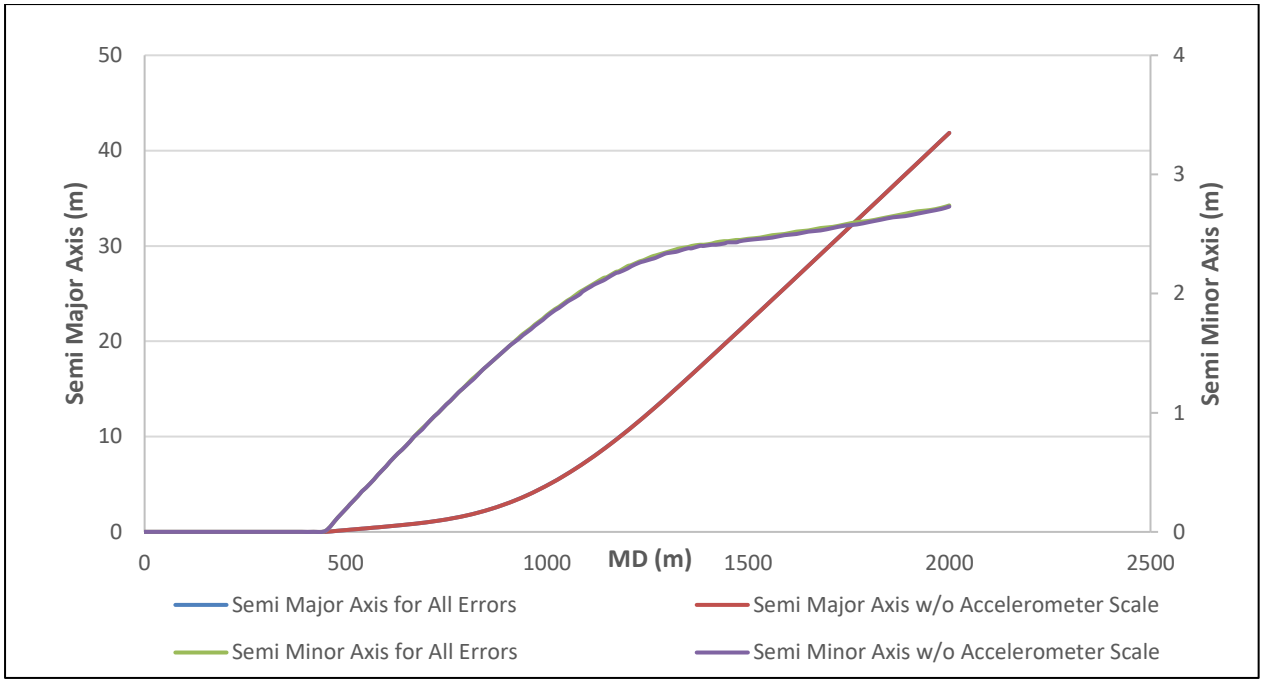

Figure 6.35 - Effect of Accelerometer Scale on Total Position Uncertainty at Azimuth = 75°

6.8 Magnetometer Cross-Axial Bias

To incorporate the effect of magnetometer bias on azimuth uncertainties, the ISCWSA error model has proposed a total of three error terms. All these error terms only effect the azimuthal part of measurements adding to the total azimuth uncertainty. Weighting functions of these error terms are listed in equations 6.26 – 6.28 and error magnitudes have been provided in Appendix D.

$$mbxy\_1 = \begin{pmatrix} 0 \\ 0 \\ \dfrac{-\cos(I)\sin(A)}{B_t \cos(\Theta)} \end{pmatrix} \tag{6.26}$$

$$mbxy\_2 = \begin{pmatrix} 0 \\ 0 \\ \dfrac{\cos(A)}{B_t \cos(\Theta)} \end{pmatrix} \tag{6.27}$$

$$mbz = \begin{pmatrix} 0 \\ 0 \\ \dfrac{-\sin(I)\sin(A)}{B_t \cos(\Theta)} \end{pmatrix} \tag{6.28}$$

6.8.1 Effect on Azimuth Uncertainty

Based on the above weighting functions, azimuth uncertainties due to Magnetometer Bias are very low and independent of inclination when drilling in the North-South direction. However, their trend is almost similar in the North-East and East-West wells respectively where the azimuth uncertainties are a maximum in the vertical and near vertical section of these wells but continuously drop as the inclination builds up before decreasing to a minimum in the horizontal section.

The relative contribution of this error source to the total azimuth error budget is minimum in the vertical and near vertical section and relatively greater in the buildup and horizontal section of the North-South well. But in the North-East and East-West wells it is observed to be most effective only within 15-20° inclination since the difference between the total azimuth uncertainties and those due to magnetometer bias is minimum in this inclination range. The effect of magnetometer bias continuously drops further in the buildup section above 20° inclination because the total azimuth uncertainties continuously increase and those due to magnetometer bias decrease to almost zero in the horizontal section.

Based on the above analysis, magnetometer bias has a greater influence on total azimuth uncertainties in the vertical, near vertical and buildup section of the East-West well and minimum throughout the North-South well. While its percentage contribution in the horizontal section is greatest in the North-South well and minimum in the East-West well. This is because of very high total azimuth uncertainties in North-East and East-West wells.

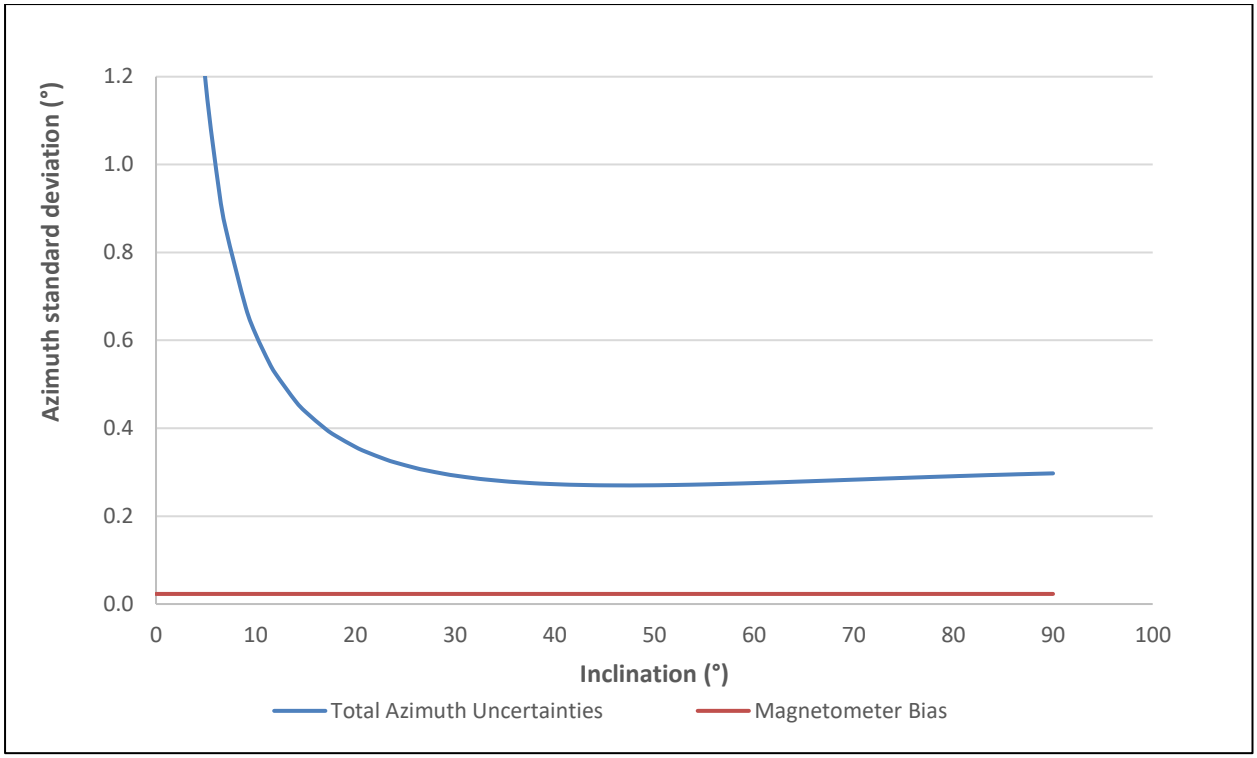

Figure 6.36 - Effect of Magnetometer Bias on Azimuth Uncertainties at Azimuth = 0°

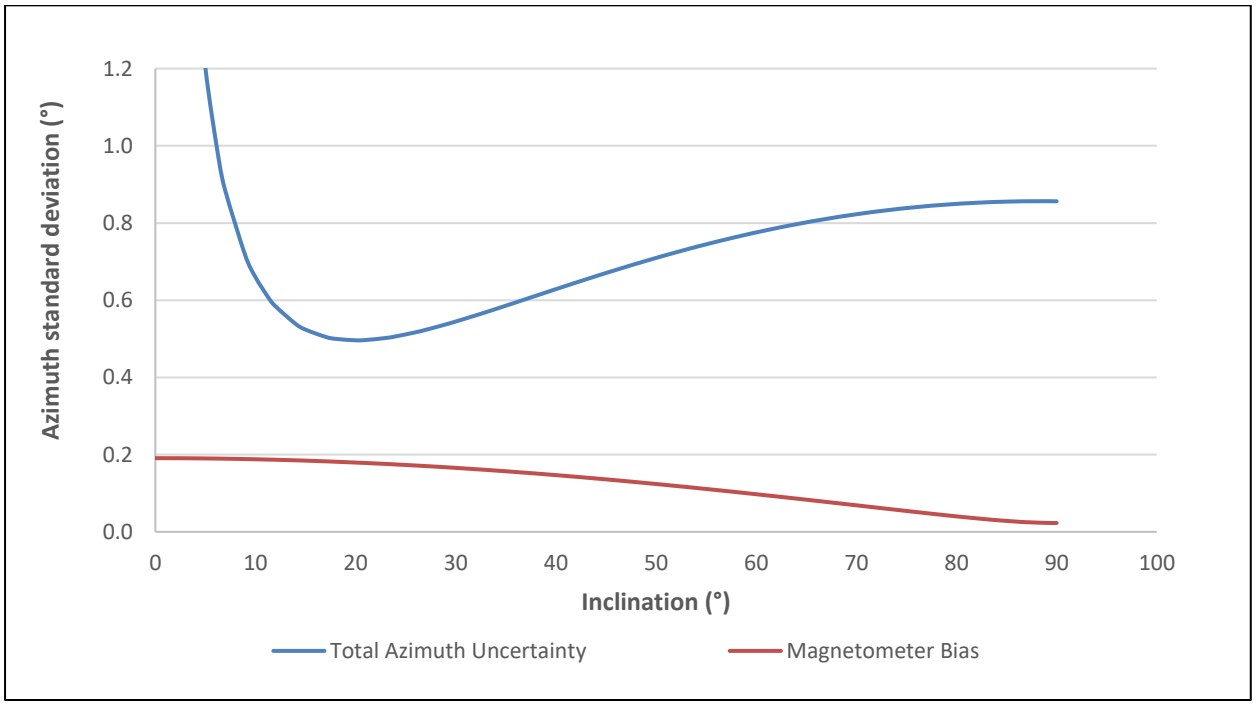

Figure 6.37 - Effect of Magnetometer Bias on Azimuth Uncertainties at Azimuth = 45°

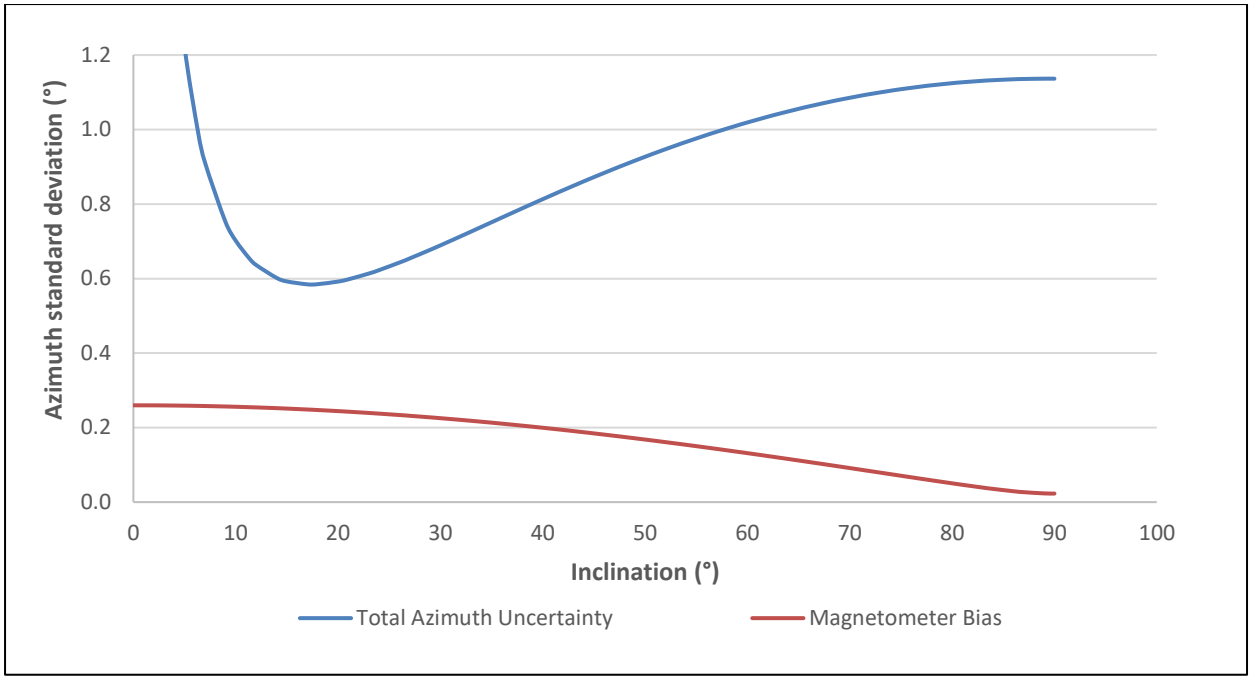

Figure 6.38 - Effect of Magnetometer Bias on Azimuth Uncertainties at Azimuth = 75°

6.8.2 Effect on Total Position Uncertainty

This section will demonstrate the effect of magnetometer bias on total position uncertainty in different hole sections of North-South, North-East and East-West wells. In all three wells the contribution of this error source towards total position error budget increases below approximately 1000-1200m MD. However, below this depth the error is observed to have the greatest effect on total position uncertainties in North-South well and minimum in the East-West well.

Combining the results of measurement and position uncertainties, the error source has minimum impact on total azimuth and position error budget at shallow depths or lower inclinations of the North-South well and maximum impact at higher depths corresponding to buildup and horizontal section. Contrary to this, the effect on azimuth and position uncertainties in the North-East and East-West wells is not the same in each hole section. The effect on azimuth uncertainties is greatest in the initial buildup section but has no influence on total position uncertainty for this hole section. It only slightly contributes to the total position error budget at higher depths close to and in the horizontal section while least influencing the total azimuth error budget for the same sections.

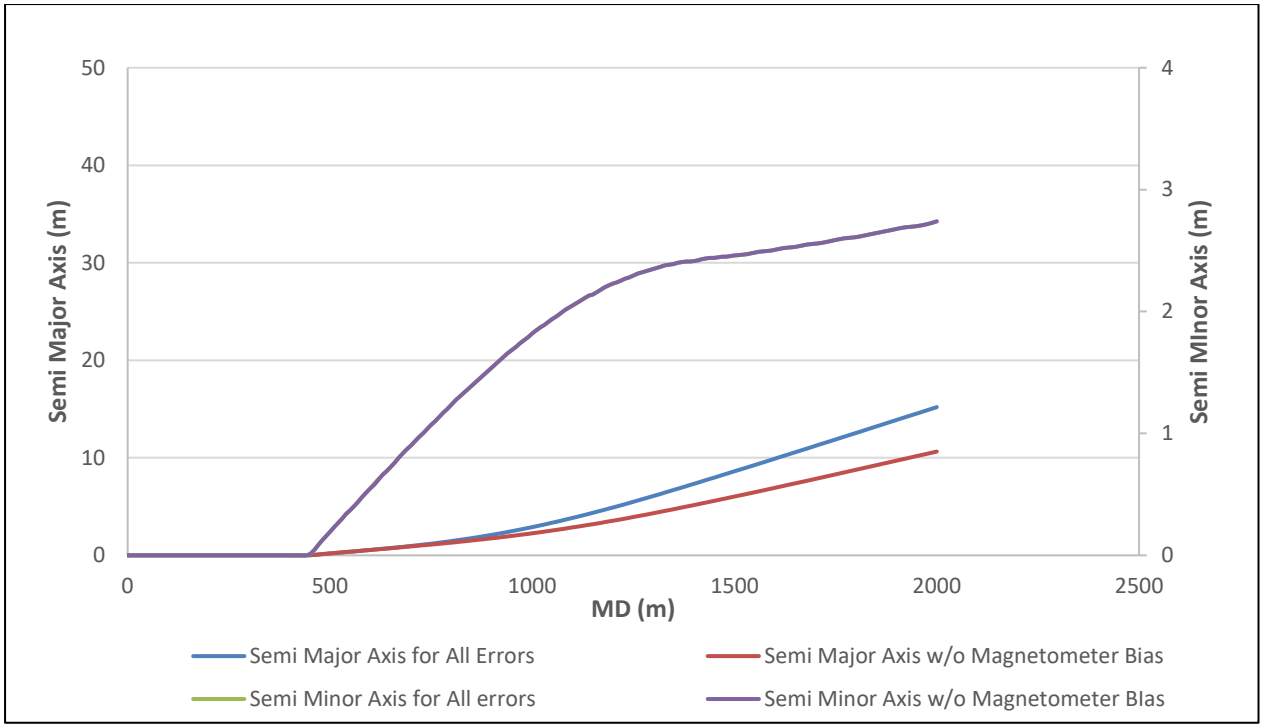

Figure 6.39 - Effect of Magnetometer Bias on Total Position Uncertainty at Azimuth = 0°

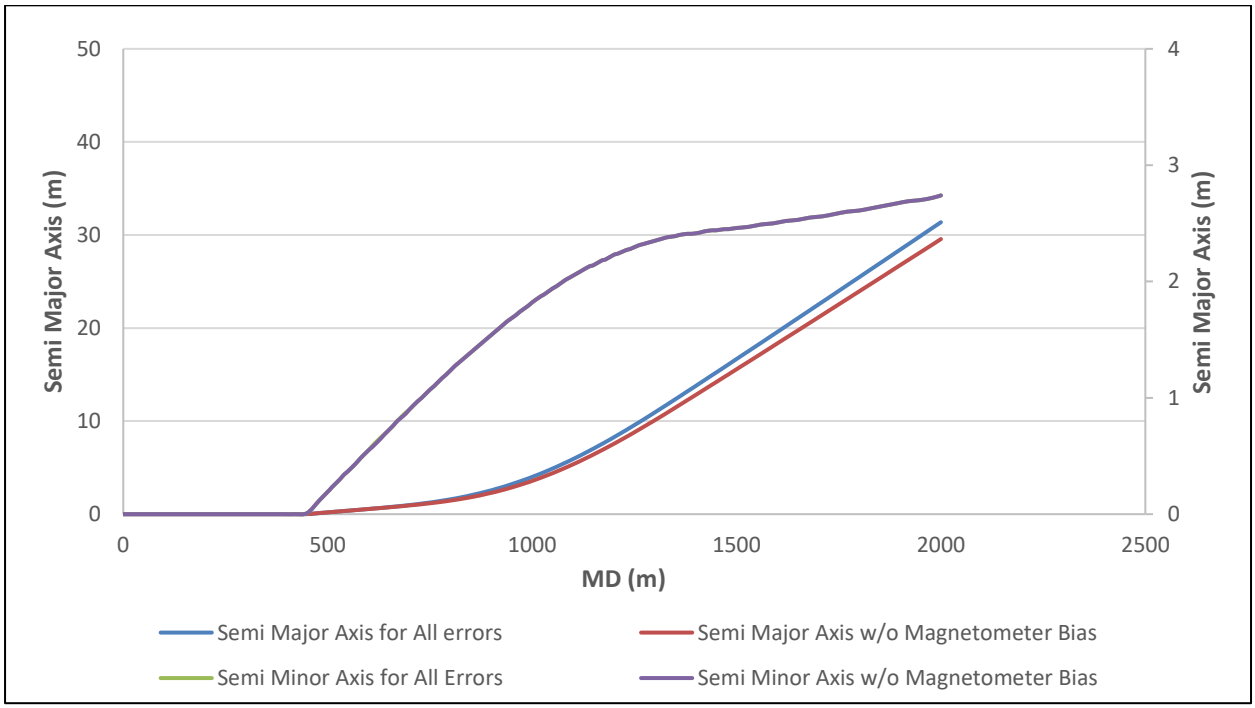

Figure 6.40 - Effect of Magnetometer Bias on Total Position Uncertainty at Azimuth = 45°

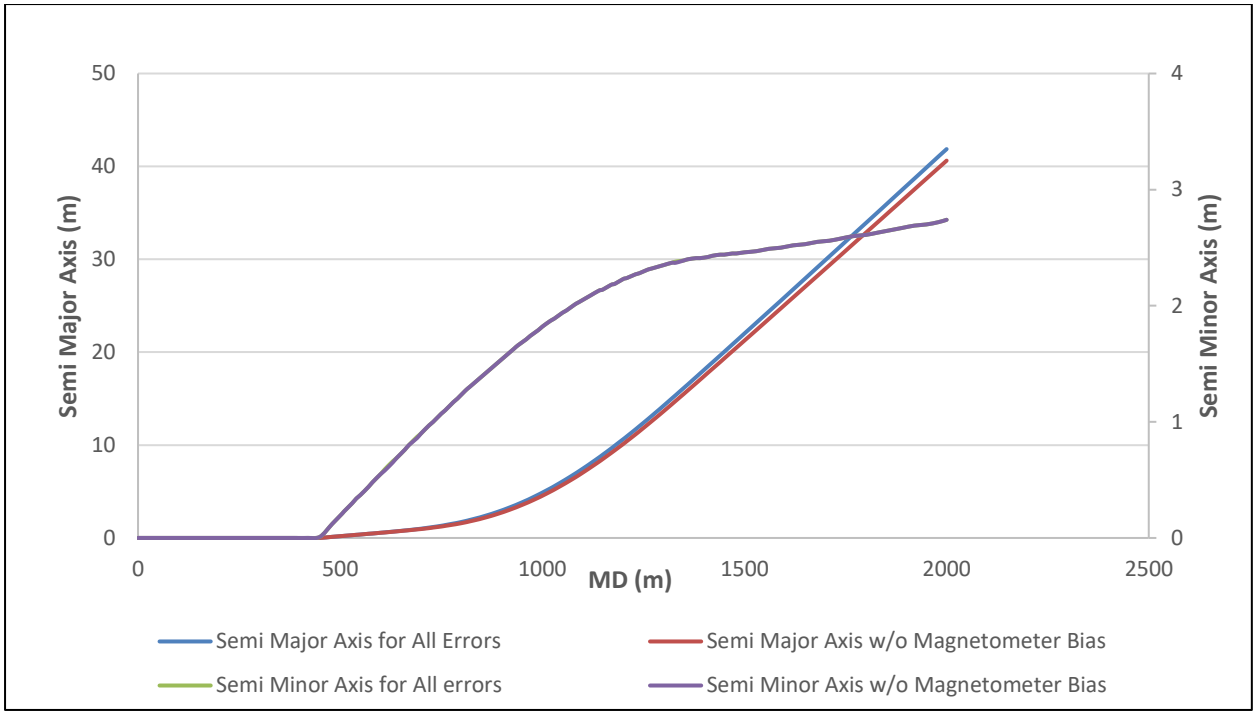

Figure 6.41- Effect of Magnetometer Bias on Total Position Uncertainty at Azimuth = 75°

6.9 Magnetometer Scale

The effect of magnetometer scale on azimuth and position uncertainties can be analyzed using the four error terms from the ISCWSA error model. From the weighting functions listed below, the effect of magnetometer scale is not only dependent on hole inclination or azimuth but also well location due to the presence of dip angle. The error magnitudes for these weighting functions have been listed in Appendix D.

$$msxy\_1 = \begin{pmatrix} 0 \\ 0 \\ \dfrac{\sin(I)\sin(A)\left[\tan(\Theta)\cos(I)+\sin(I)\cos(A)\right]}{\sqrt{2}} \end{pmatrix} \tag{6.29}$$

$$msxy\_2 = \begin{pmatrix} 0 \\ 0 \\ \dfrac{\sin(A)\left[\tan(\Theta)\sin(I)\cos(I)-\cos^2(I)\cos(A)-\cos(A)\right]}{2} \end{pmatrix} \tag{6.30}$$

$$msxy\_3 = \begin{pmatrix} 0 \\ 0 \\ \dfrac{\cos(I)\left[\cos^2(A) - \cos(I)\sin^2(A) - \tan(\Theta)\sin(I)\cos(A)\right]}{2} \end{pmatrix} \tag{6.31}$$

$$msz = \begin{pmatrix} 0 \\ 0 \\ -\left[\sin(I)\cos(A) + \tan(\Theta)\cos(I)\right]\sin(I)\sin(A) \end{pmatrix} \tag{6.32}$$

6.9.1 Effect on Azimuth Uncertainty

The azimuth uncertainties are quite high even in the vertical and near vertical sections of the North-South well and further increase above 30° inclination to a maximum of 0.2° in the horizontal section. When compared this with total azimuth uncertainties, magnetometer scale has a relatively greater impact in the buildup and horizontal section of this well.

The behavior of azimuth uncertainties in the North-East and East-West wells is almost identical. In the North-East well, the azimuth uncertainties increase from 0.06° to a maximum of 0.2° at 50° inclination and then decrease from there onwards till the horizontal section. Similarly, in the East-West well, the azimuth uncertainties increase from 0.05° to 0.2° at 50° inclination before dropping down to a minimum in the horizontal section. When analyzed along with total azimuth uncertainties magnetometer scale is observed to have maximum impact on total azimuth error budget in the buildup section and minimum in the vertical, near vertical and horizontal section.

Based on the above analysis, in every hole section magnetometer scale has the greatest percentage contribution to the total azimuth error budget of the North-South well compared to its effect in the corresponding hole sections of North-East and East-West wells.

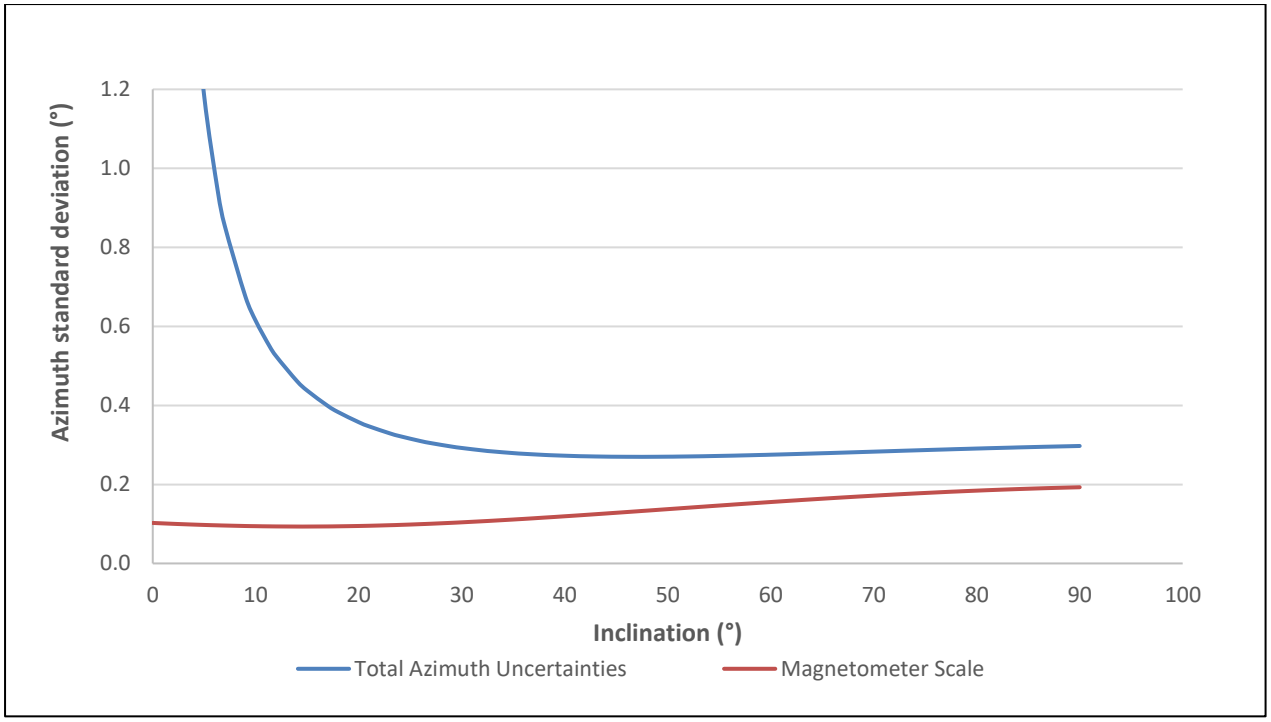

Figure 6.42 - Effect of Magnetometer Scale on Azimuth Uncertainties at Azimuth = 0°

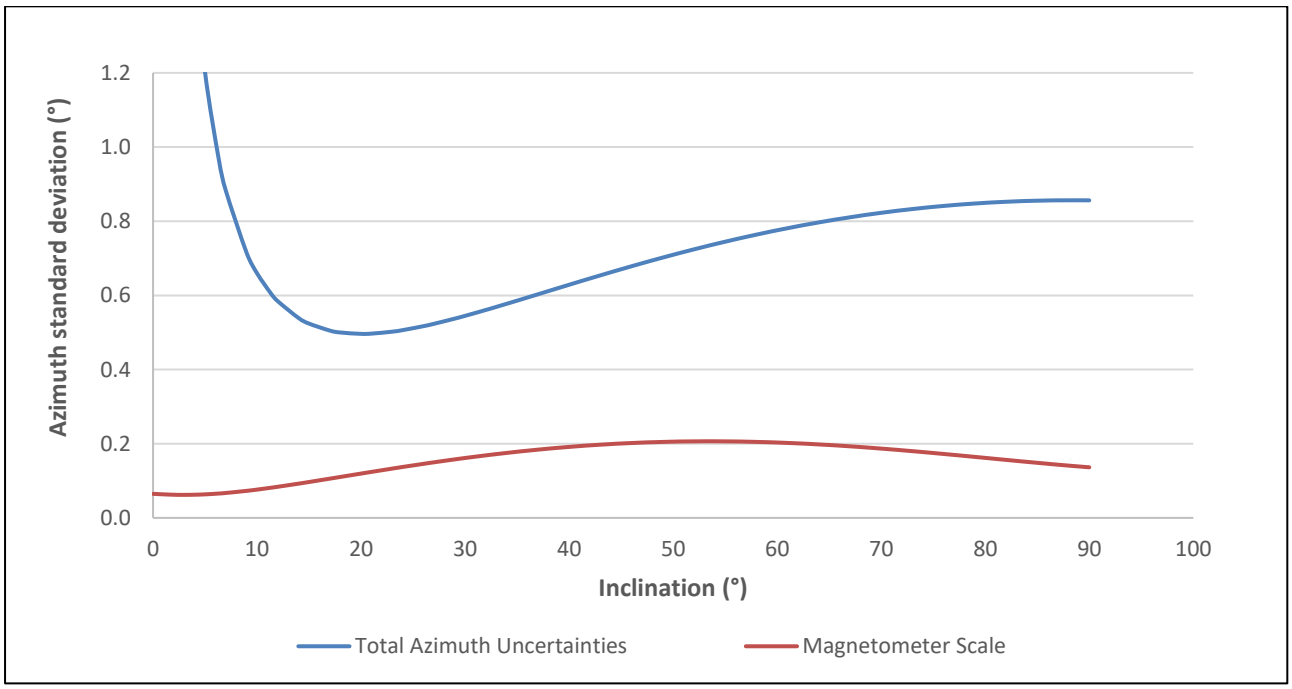

Figure 6.43 - Effect of Magnetometer Scale on Azimuth Uncertainties at Azimuth = 45°

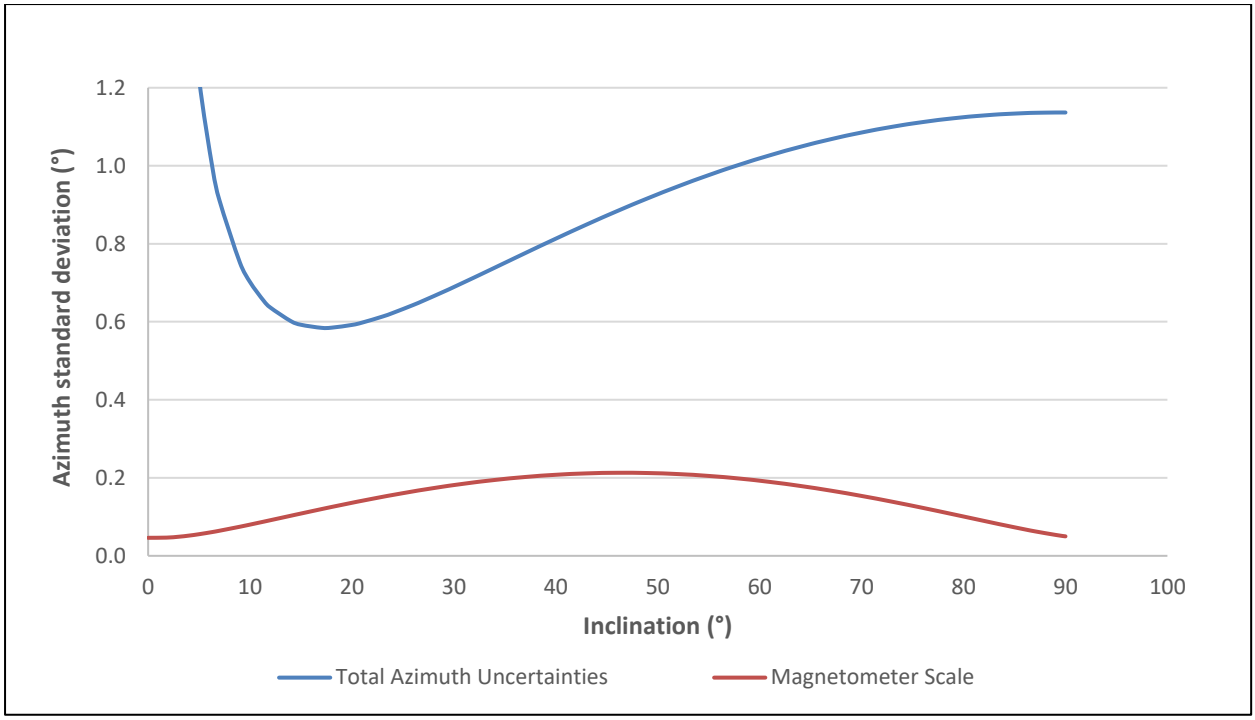

Figure 6.44 - Effect of Magnetometer Scale on Azimuth Uncertainties at Azimuth = 75°

6.9.2 Effect on Total Position Uncertainty

Magnetometer scale does not have a notable impact on total position uncertainty in any of the three wells. Only a very small reduction in total position uncertainty is observed in the horizontal section of North-South well. But otherwise, it cannot be seen to influence the position error budget at any other point along the three wells.

Concluding from above results, magnetometer scale has the greatest share towards total azimuth and position error budget in the horizontal section of the North-South well. While in the buildup sections of North-East and East-West wells although magnetometer scale did make some contribution to the total azimuth uncertainties, but it did not impact the total position uncertainty at all in this hole section.

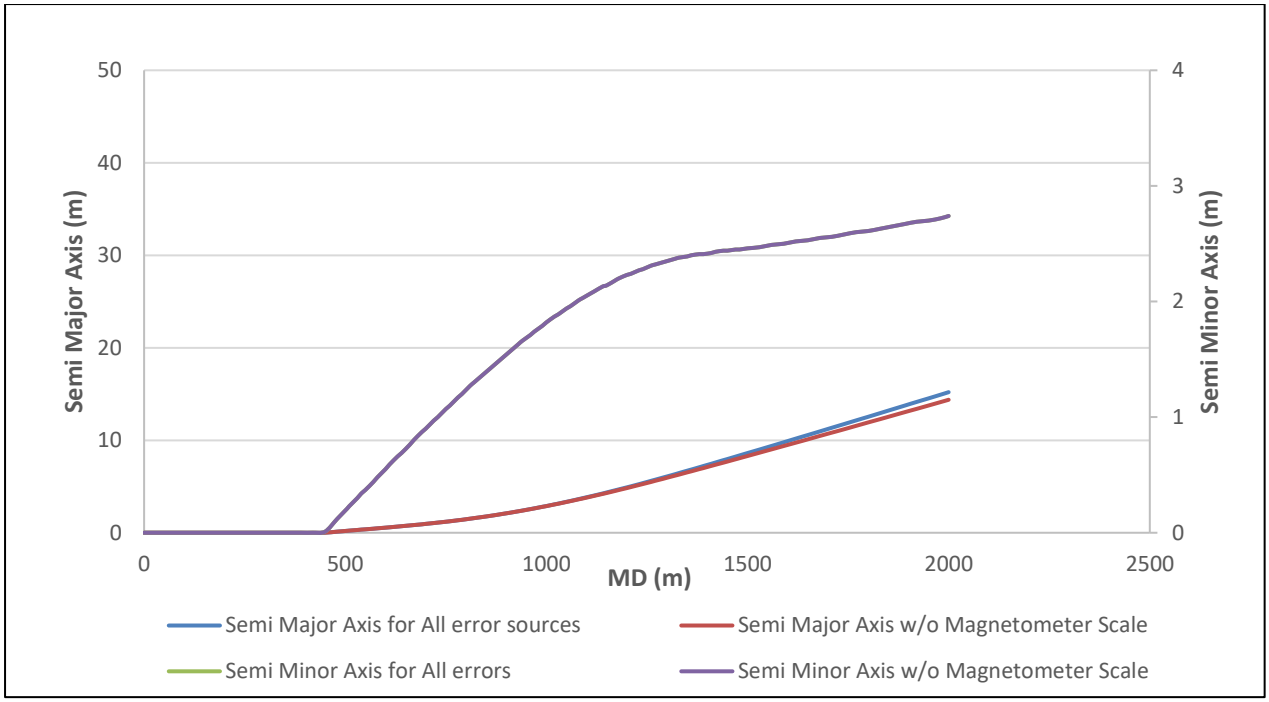

Figure 6.45 - Effect of Magnetometer Scale on Total Position Uncertainty at Azimuth = 0°

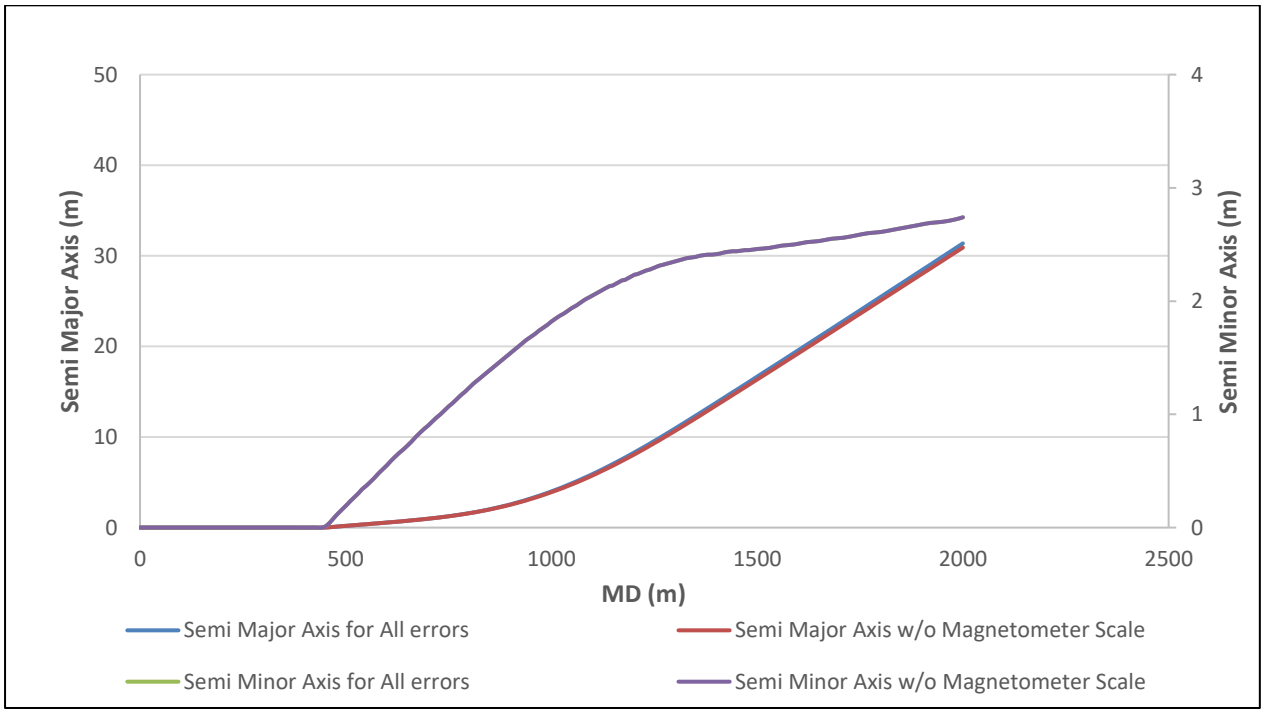

Figure 6.46 - Effect of Magnetometer Scale on Total Position Uncertainty at Azimuth = 45°

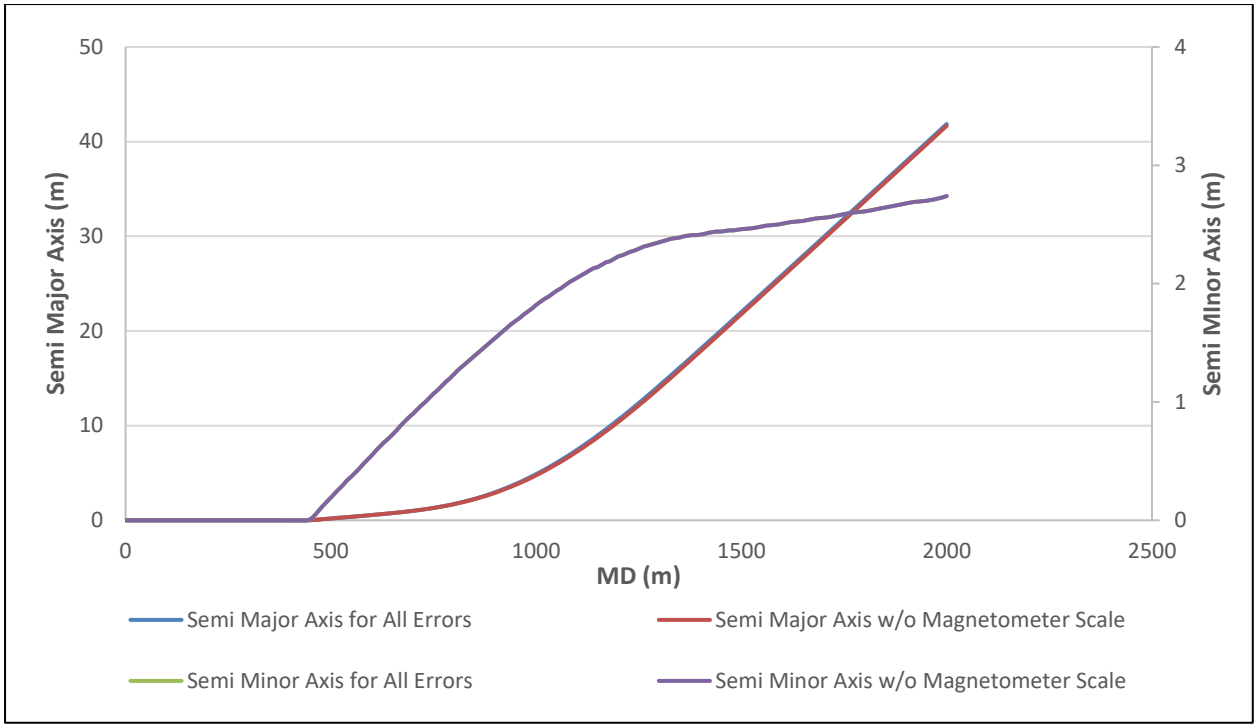

Figure 6.47 - Effect of Magnetometer Scale on Total Position Uncertainty at Azimuth = 75°

Chapter 7. Error Analysis of Mag-corr Error Model

In the Non-mag error model, the sensor error terms used for predicting the effect of accelerometer and magnetometer on azimuth uncertainties involve the dip angle and magnetic field measurements. These two parameters can be influenced by the magnetic axial drillstring interference giving inaccurate uncertainty estimates. So, it becomes important to modify the error terms accordingly to include the effect of axial drillstring interference and also have a quantitative estimate of the uncertainties introduced by these two parameters.

The Mag-corr error model thus uses modified sensor error terms corrected for magnetic axial drillstring interference. In addition, to have a much better understanding and estimate of the uncertainties introduced by magnetic dip angle and magnetic field measurements, two additional terms have been introduced in this error model. These error terms predict the uncertainties specifically due to magnetic dip angle and magnetic field measurements. This chapter will in detail discuss the impact of all these error terms on inclination, azimuth and position uncertainty for the three subject wells (North-South, North-East, East-West) under study.

7.1 Magnetic Dip Angle (MDI)

Insecurities due to magnetic dip angle are included in the Mag-corr error model through equation 7.1. Error magnitude used with this weighting function to calculate the respective azimuth and position uncertainty is listed in Appendix D.

$$mdi = \begin{pmatrix} 0 \\ 0 \\ \dfrac{\sin(I)\sin(A)\left[\tan(\Theta)\sin(I)\cos(A)-\cos(I)\right]}{1-\sin^2(I)\sin^2(A)} \end{pmatrix} \tag{7.1}$$

7.1.1 Effect on Azimuth Uncertainty

The weighting function above has been used to predict the azimuth uncertainties due to this error source in North-South, North-East and East-West wells. The azimuth uncertainties are almost negligible in the North-South well in Figure 7.1 and thus do not have any influence towards the total azimuth error budget at any point along the well. But for the North-East and East-West wells the azimuth uncertainties start to increase above 50° and 60° inclination

respectively and consequently their effect on total azimuth error budget also increases. However, the effect of *mdi* on total azimuth uncertainties is relatively greater in the East-West well compared to the North-East well.

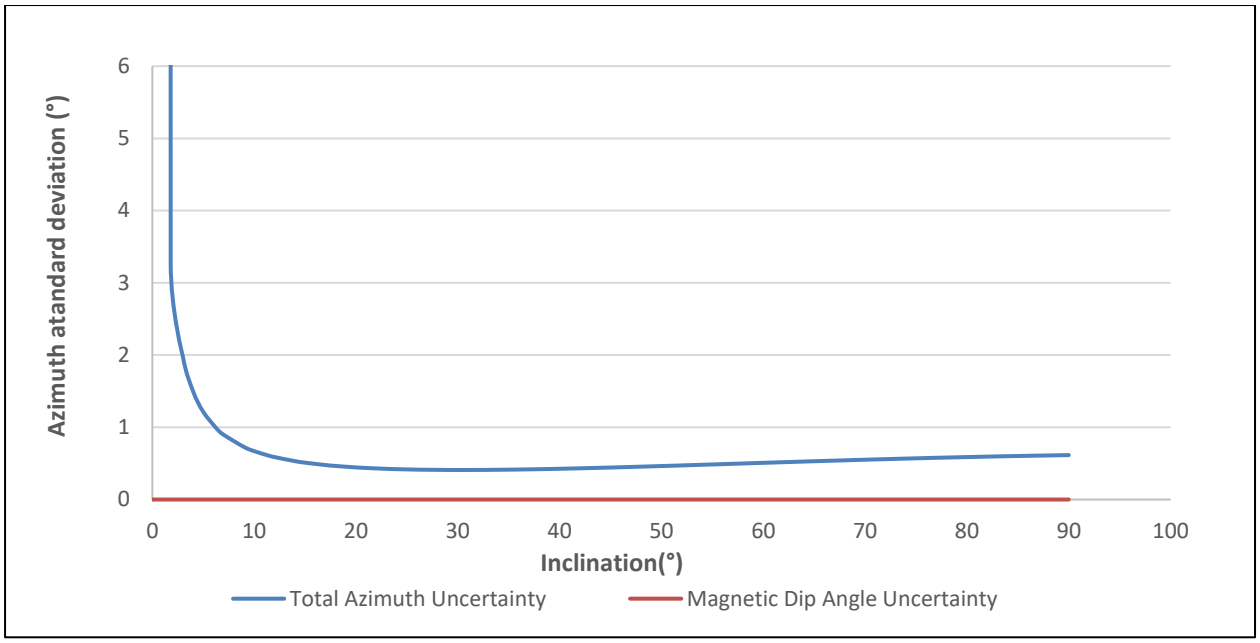

Figure 7.1 - Effect of Magnetic Dip Angle on Azimuth Uncertainties at Azimuth = 0°

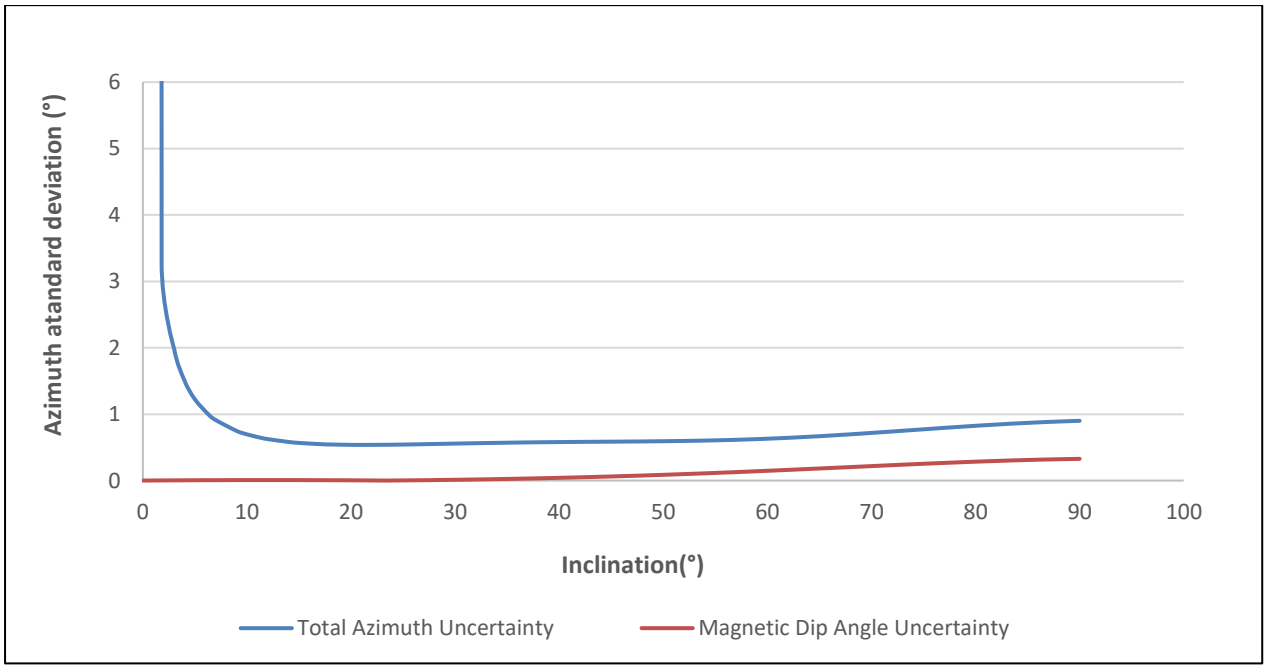

Figure 7.2 - Effect of Magnetic Dip Angle on Azimuth Uncertainties at Azimuth = 45°

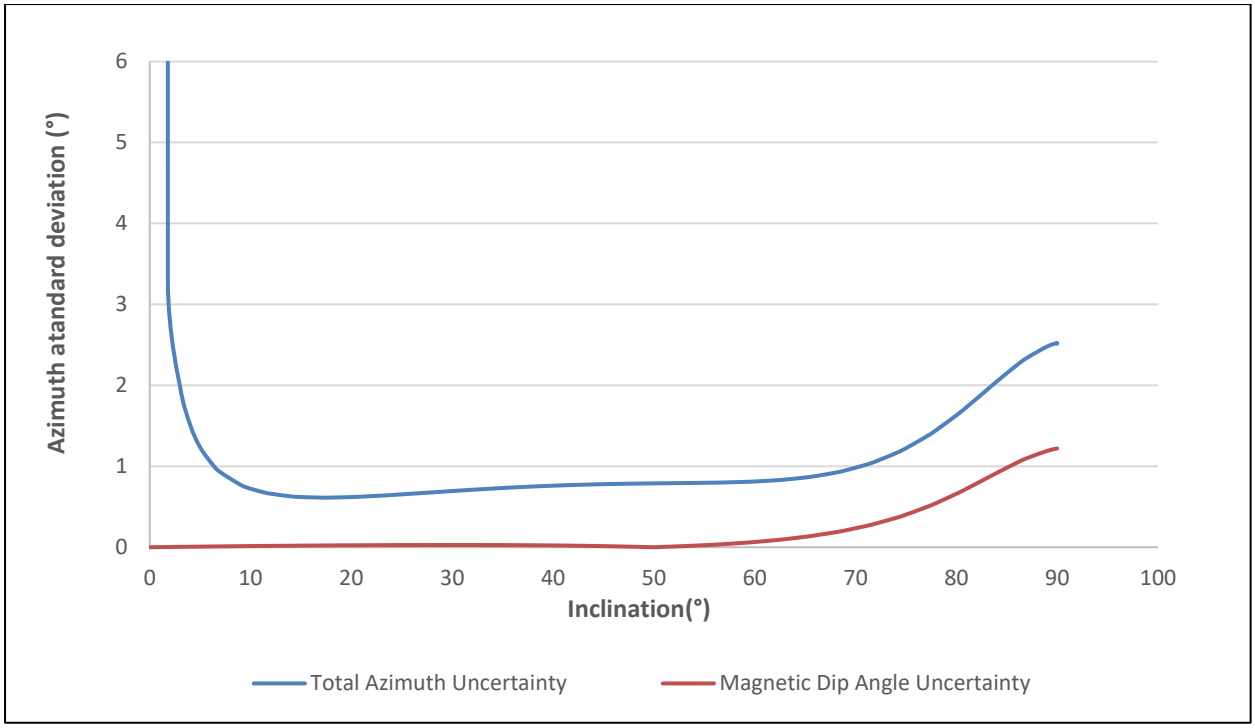

Figure 7.3 - Effect of Magnetic Dip Angle on Azimuth Uncertainties at Azimuth = 75°

7.1.2 Effect on Total Position Uncertainty

This section will explain the effect of magnetic dip angle on total position uncertainty. In all three wells *mdi* affects the total position uncertainty only below almost 1000m MD with the maximum impact in horizontal section. However, comparing its relative effect along different wells, it has the maximum influence on total position error budget of East-West well with the total position uncertainty reduced to almost 33m when *mdi* is excluded from the error model.

The above results show that although *mdi* did not have any effect on azimuth uncertainties in the North-South well but it is still seen to have some impact on total position error budget for this well. While the error source is having a notable contribution to both azimuth and position error budgets of North-East and East-West wells at higher depths. Also, this effect is maximum in the East-West well compared to the North-East well. Therefore, except for the North-South well *mdi* has a uniform impact on azimuth and position uncertainties.

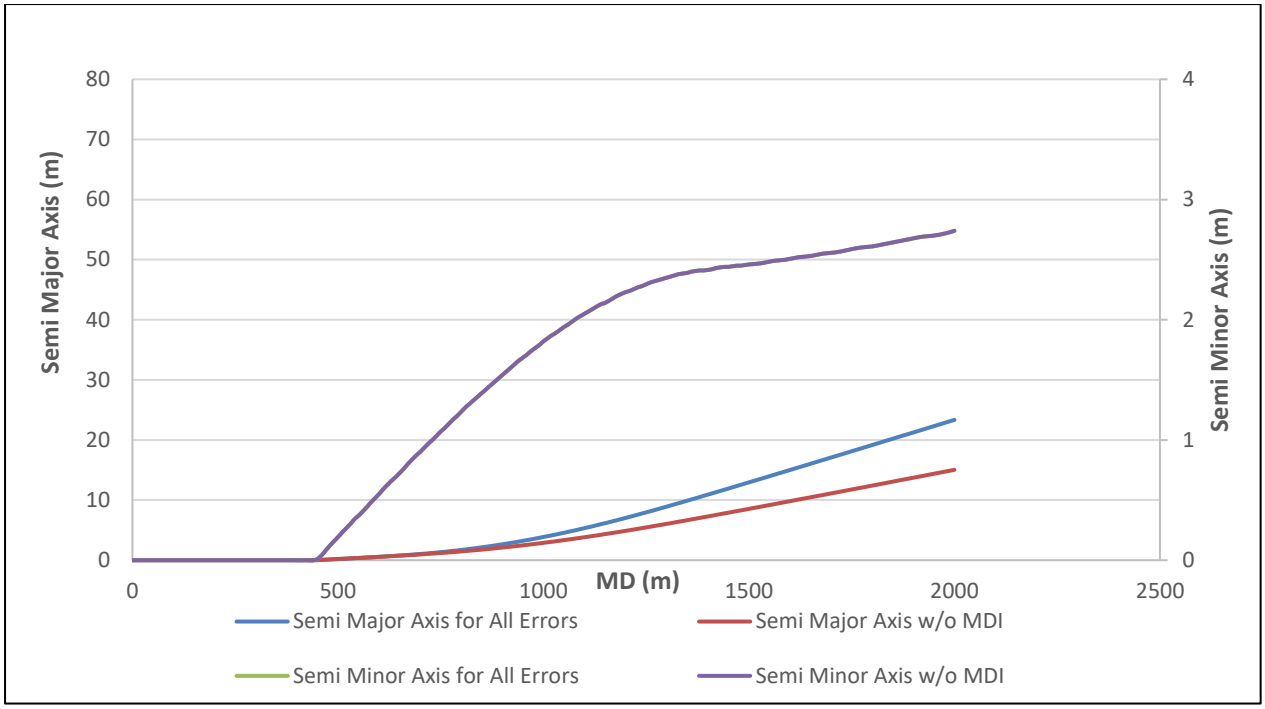

Figure 7.4 - Effect of Magnetic Dip Angle on Total Position Uncertainty at Azimuth = 0°

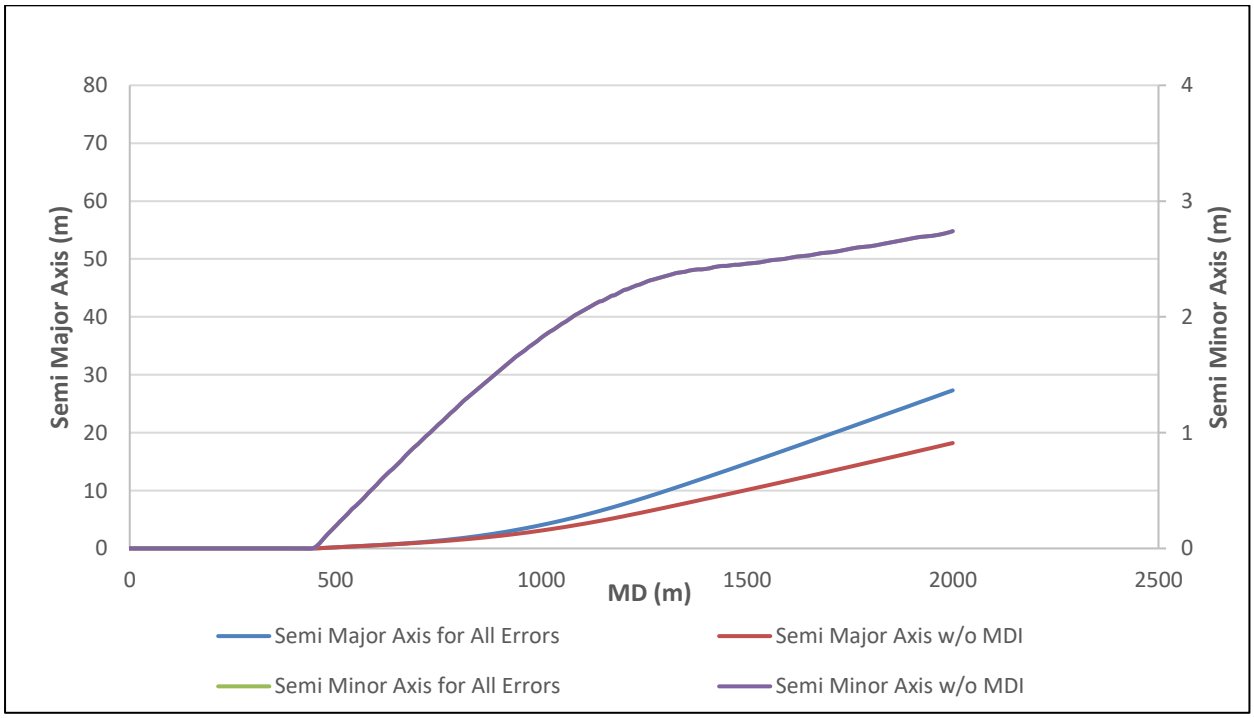

Figure 7.5 - Effect of Magnetic Dip Angle on Total Position Uncertainty at Azimuth =45 °

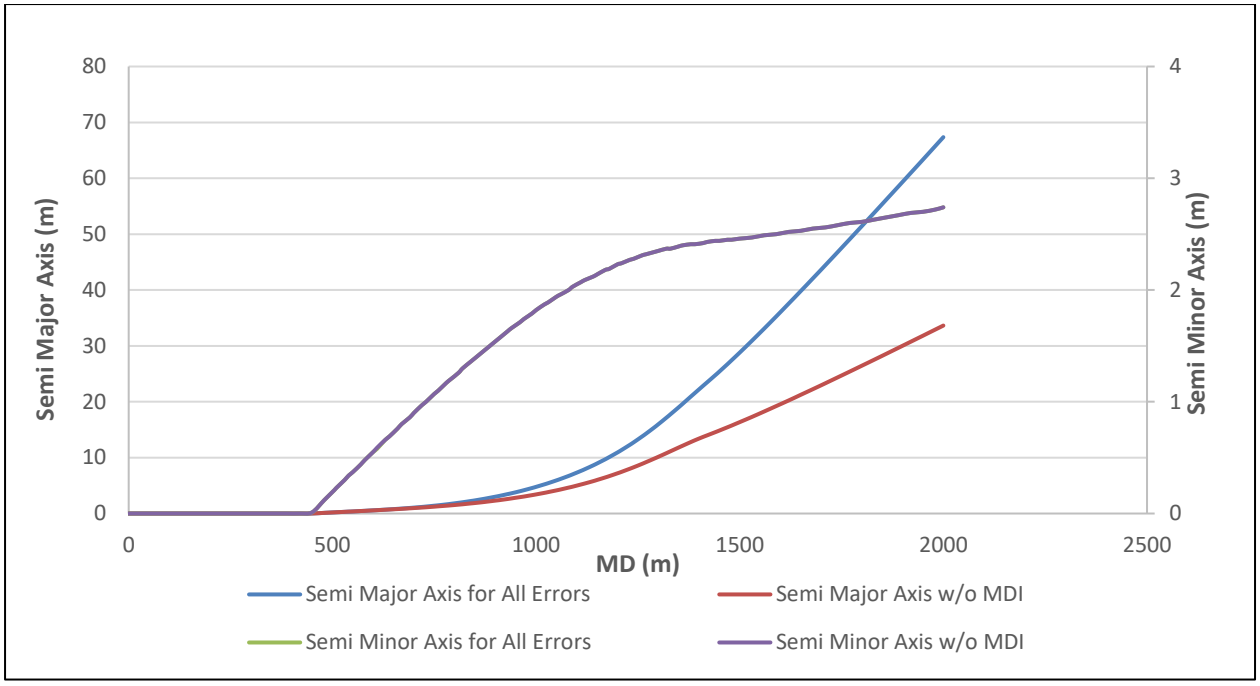

Figure 7.6 - Effect of Magnetic Dip Angle on Total Position Uncertainty at Azimuth = 75°

7.2 Magnetic Field Intensity (MFI)

Uncertainties introduced by magnetic field measurements are estimated using equation 7.2 and the error magnitude used for calculating azimuth and position uncertainty due to this error source is listed in Appendix D.

$$mfi = \begin{pmatrix} 0 \\ 0 \\ \dfrac{-\sin(I)\sin(A)\left[\tan(\Theta)\cos(I)+\sin(I)\cos(A)\right]}{B_t\left[1-\sin^2(I)\sin^2(A)\right]} \end{pmatrix} \tag{7.2}$$

7.2.1 Effect on Azimuth Uncertainty

Based on the weighting function in equation 7.2, azimuth uncertainties are dependent on hole inclination, azimuth, dip angle and magnetic field strength. In short, the effect of this error source will be determined by well trajectory, direction and its location.

The effect of *mfi* on azimuth uncertainties is negligible in the North-South well and does not change at all as a function of inclination. Due to this, the error source has no contribution to

the total azimuth uncertainties in the North-South well. Similarly, in the North-East well it does not induce any azimuth uncertainties for most part of the well except at inclinations from 50-70°. Therefore, it will only have a very little contribution to the total azimuth error budget in this part of well. In the East-West well the error starts affecting the azimuth measurements from approximately 30° inclination and causes a maximum of 0.4° azimuth error at 80° inclination. This drops down to 0.2° azimuth error in the horizontal section. Thus, the error contributes most to the total azimuth error budget between inclinations 40°-70° in this well.

Based on the above results, *mfi* remains totally ineffective in the vertical and near vertical part of all three wells. While it has a relatively large contribution to the total azimuth error in the buildup and horizontal section of East-West well compared to North-East and North-South wells mainly due to the presence of *sinI* term in the denominator.

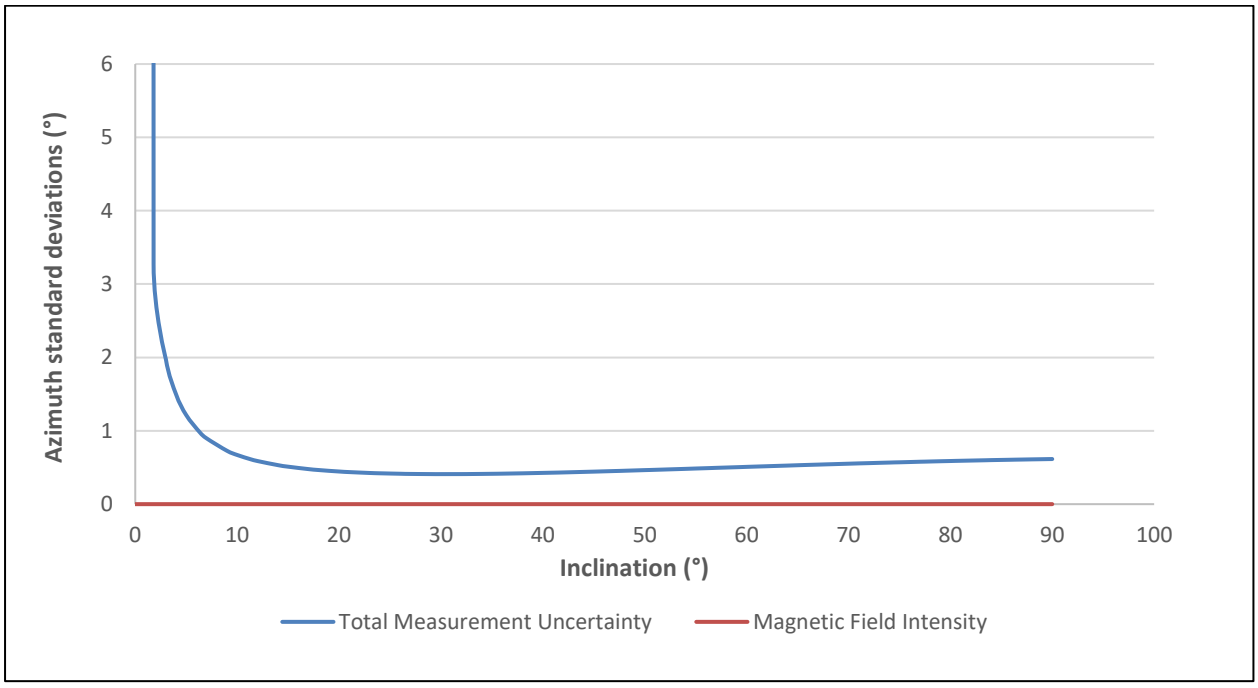

Figure 7.7 - Effect of Magnetic Field Intensity on Azimuth Uncertainties at Azimuth = 0

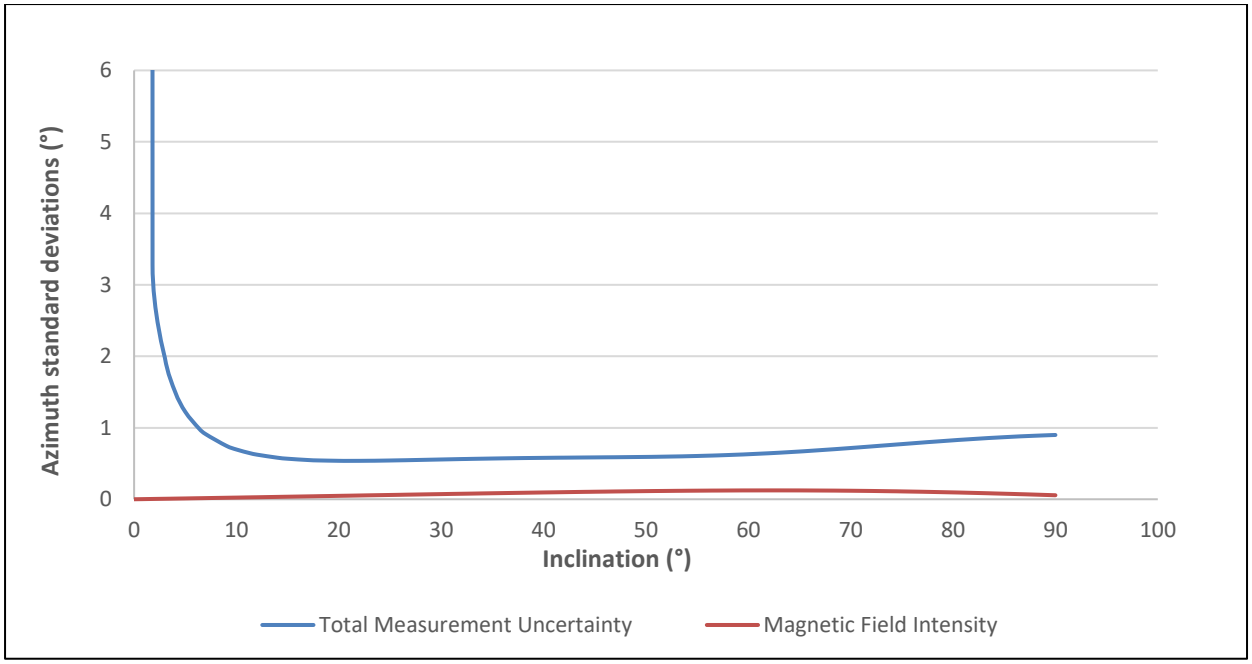

Figure 7.8 - Effect of Magnetic Field Intensity on Azimuth Uncertainties at Azimuth = 45°

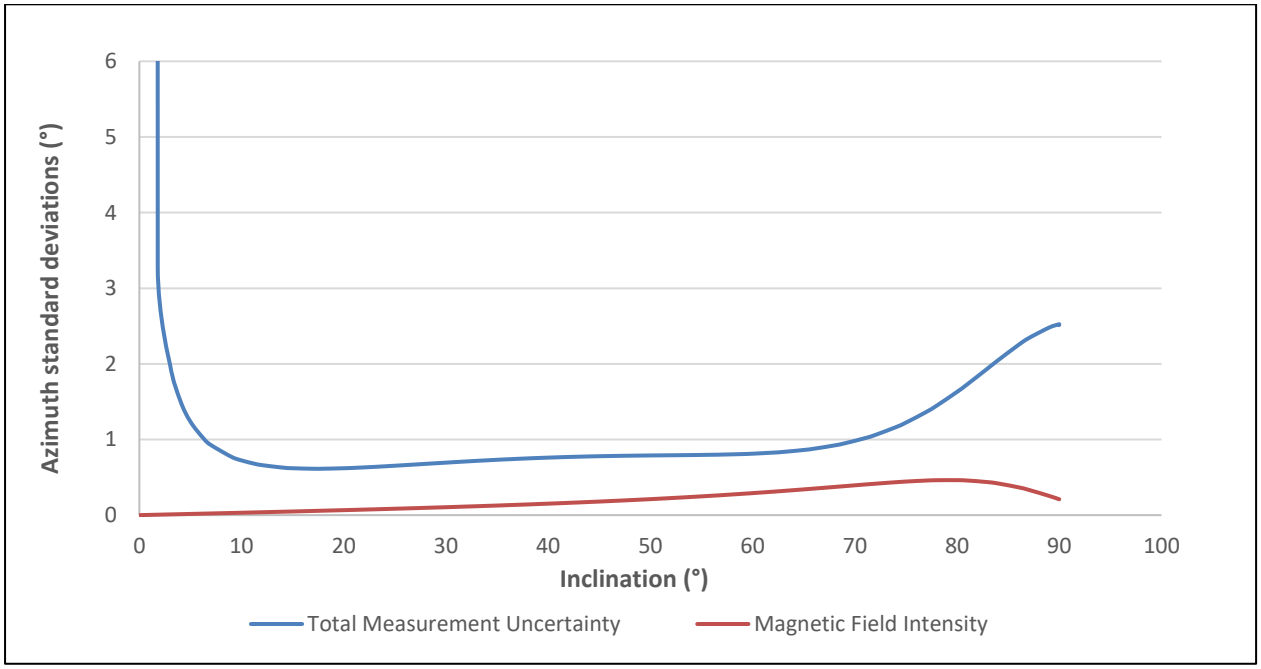

Figure 7.9 - Effect of Magnetic Field Intensity on Azimuth Uncertainties at Azimuth = 75°

7.2.2 Effect on Total Position Uncertainty

The analysis of Figures 7.10-7.12 provides an understanding of the effect of *mfi* on total position uncertainty. This error source also effects the total position uncertainty of all three wells only at depths below 1000m MD. Below this depth, the effect continuously increases and

is maximum at TD in the horizontal section. However, between the North-South, North-East and East-West wells, the total position uncertainty is reduced the most in the East-West well when this error source is excluded from the error model and an almost similar effect is observed in the North-South and North-East wells. This shows that below 1000m MD, *mfi* has the largest impact on total position error budget of the East-West well.

When the results of measurement and position uncertainties are combined, the error source has no effect at all on total azimuth uncertainties in the North-South well while it still adds to the total position uncertainty of this well at higher depths. But for the North-East and East-West wells it is impacting both the total azimuth and position error budgets in the buildup and horizontal section. The relative effect of *mfi* is however in the East-West well is greater with respect to both azimuth and position uncertainties.

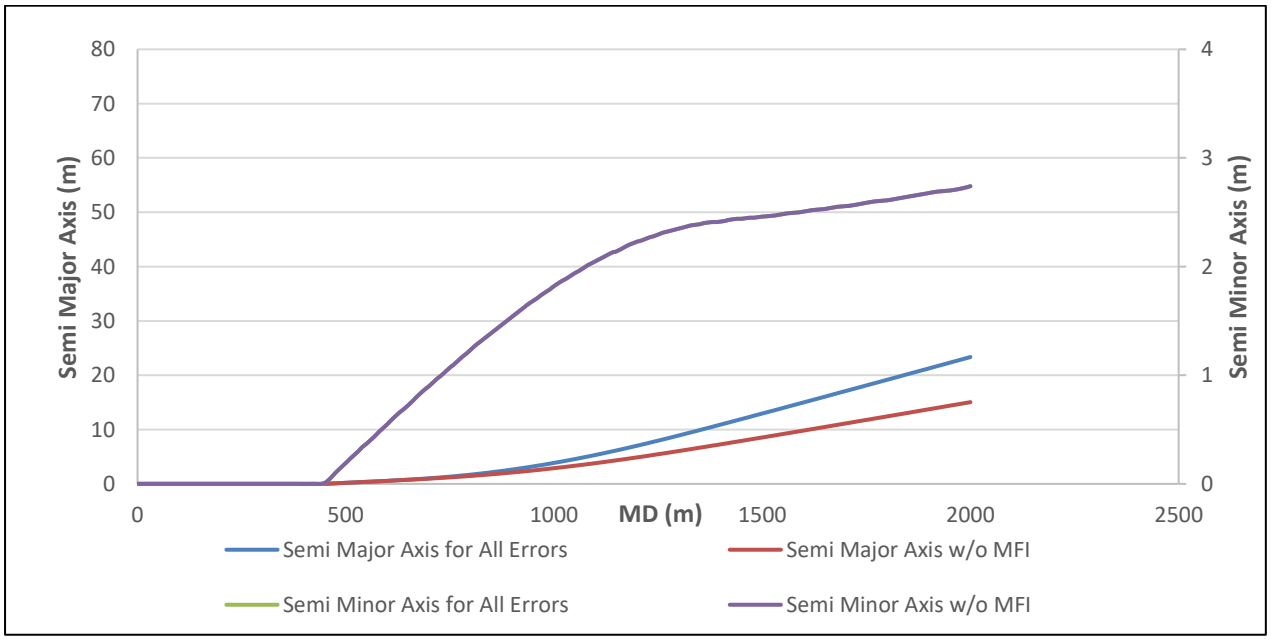

Figure 7.10 - Effect of Magnetic Field on Total Position Uncertainty at Azimuth = 0°

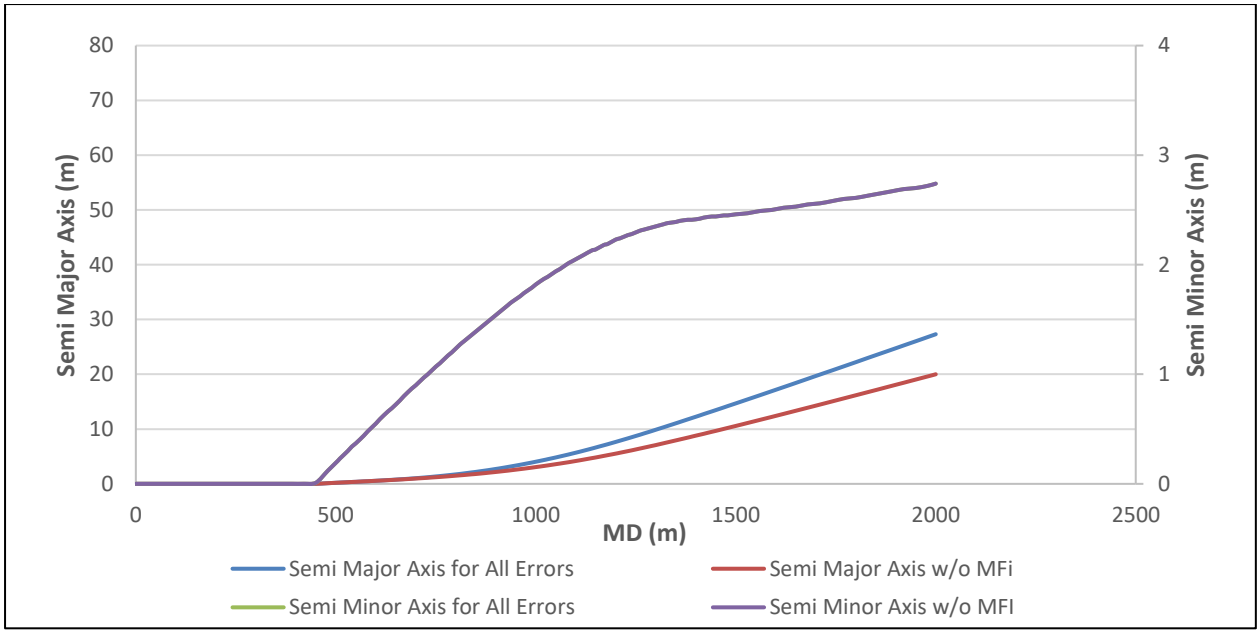

Figure 7.11 - Effect of Magnetic Field on Total Position Uncertainty at Azimuth = 45°

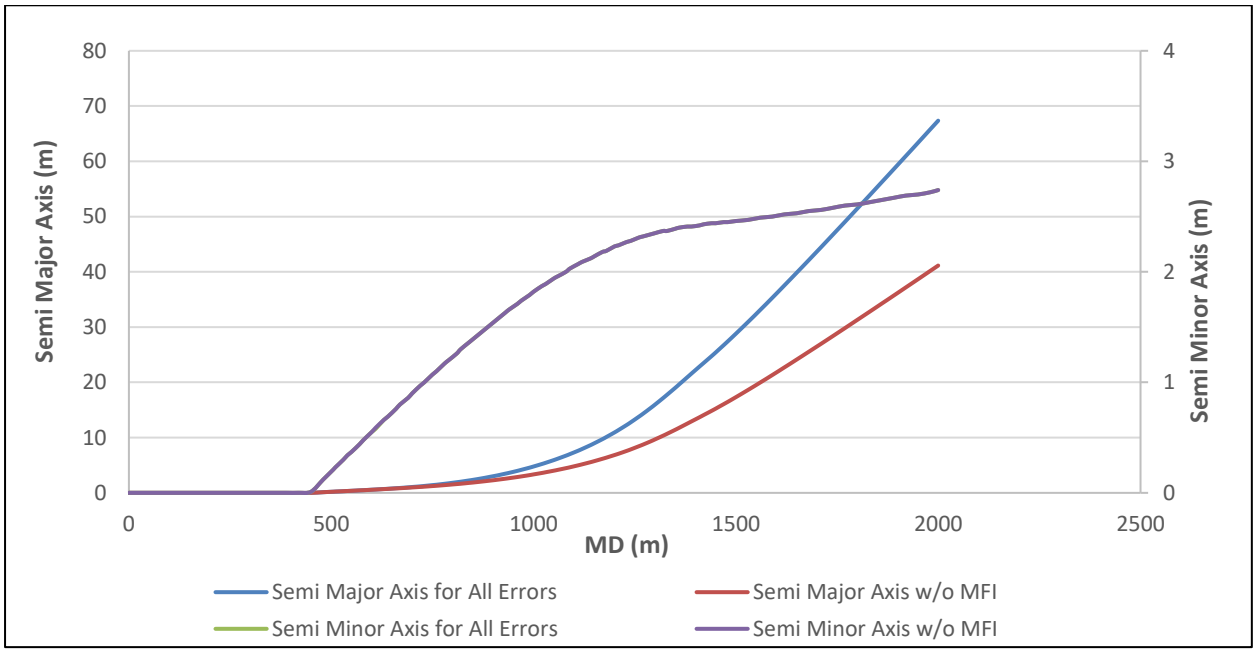

Figure 7.12 - Effect of Magnetic Field on Total Position Uncertainty at Azimuth = 75°

7.3 Accelerometer Bias

The modified weighting functions which also consider the effect of axial drillstring interference have been listed as equations 7.3-7.5. These are the accelerometer bias error terms affecting only the azimuth uncertainty since error terms used to predict inclination uncertainty are identical in both error models and have already been discussed in detail in Non-mag error

model. Therefore, the azimuth uncertainty plotted in Figures 7.13-7.15 has been calculated through following three equations. However, while estimating position uncertainty in Compass, the error terms impacting both inclination and azimuth uncertainty have been used together.

It is important to mention that the purpose of adding *sinI* in the denominator of equation 7.4 is to convert the lateral uncertainties to azimuth uncertainties. The original term without *sinI* is used to predict lateral uncertainties in Compass.

$$abixy\_1 = \begin{pmatrix} 0 \\ 0 \\ \dfrac{\cos^2(I)\sin(A)\left[\tan(\Theta)\cos(I)+\sin(I)\cos(A)\right]}{g_{tot}\left[1-\sin^2(I)\sin^2(A)\right]} \end{pmatrix} \tag{7.3}$$

$$abixy\_2 = \begin{pmatrix} 0 \\ 0 \\ \dfrac{-\left[\tan(\Theta)\sin(I)\cos(A)-\cos(I)\right]}{g_{tot}\sin(I)\left[1-\sin^2(I)\sin^2(A)\right]} \end{pmatrix} \tag{7.4}$$

$$abiz = \begin{pmatrix} 0 \\ 0 \\ \dfrac{[\sin(I)\cos(I0\sin(A)\{\tan(\Theta)\cos(I)+\sin(I)\cos)(A)\}]}{gt_{ot}\left[1-\sin^2(I)\sin^2(A)\right]} \end{pmatrix} \tag{7.5}$$

7.3.1 Effect on Azimuth Uncertainty

The effect of accelerometer bias on azimuth uncertainties is quite similar along the three wells. The azimuth uncertainties are extremely high in the vertical and near vertical section and sharply drop down as the wells are slightly deviated. The reason for these very high azimuth uncertainties is mainly because of *abixy_2* error term that involves *sinI* in its denominator. Because of such high azimuth uncertainties, the error source has a very high contribution to the total azimuth error budget in these two hole sections.

In the buildup and horizontal section of the three wells, the azimuth uncertainties remain very low throughout the three wells except close to and in the horizontal section of East-West well. The azimuth uncertainties in this well slightly increase above approximately 75° inclination to reach a maximum of almost 0.3° in the horizontal section. However, the effect on total azimuth

uncertainties is not much different in the buildup and horizontal section of the three wells. This is mainly because an increase in total azimuth uncertainties for East-West well is compensated with an almost equal increase in the total azimuth uncertainties in the horizontal section of this well. Therefore, the percentage contribution to the total azimuth error budget is almost the same as in North-South and North-East wells.

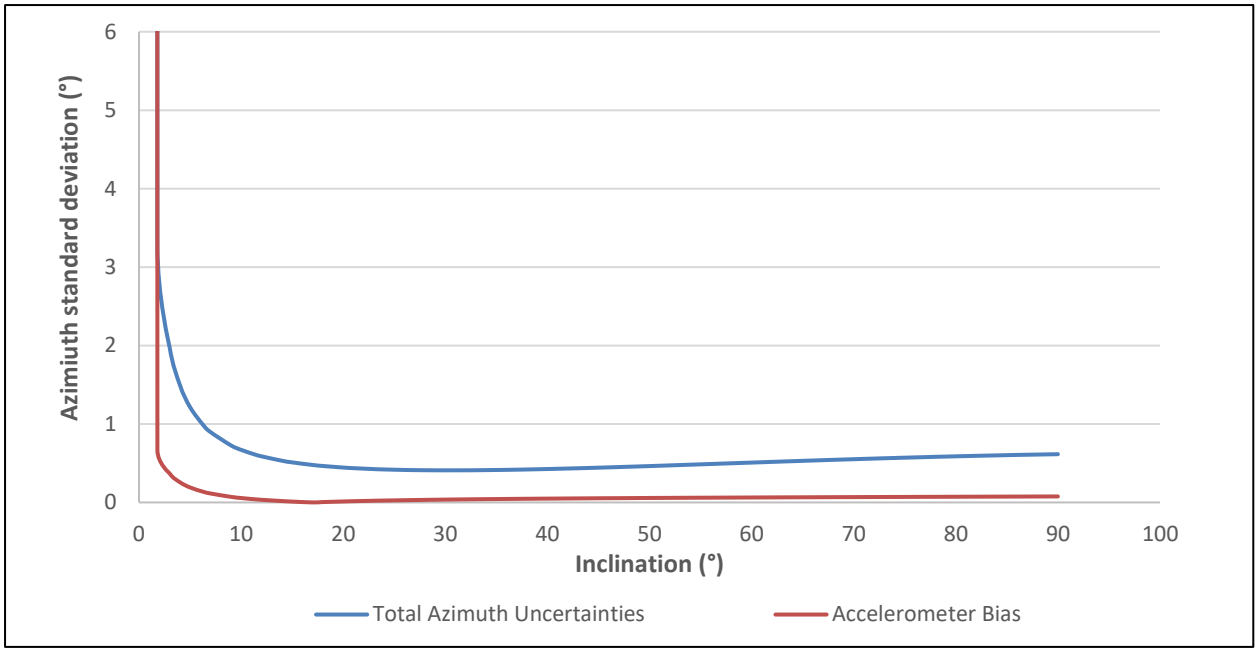

Figure 7.13 - Effect of Accelerometer Bias on Azimuth Uncertainties at Azimuth = 0°

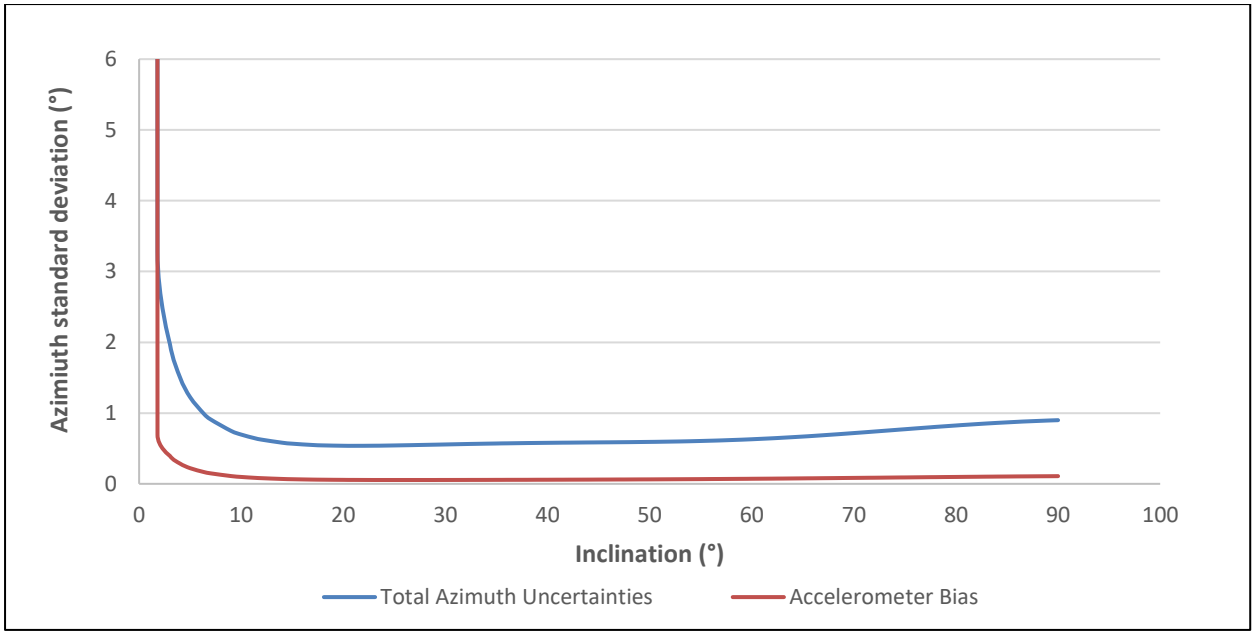

Figure 7.14 - Effect of Accelerometer Bias on Azimuth Uncertainties at Azimuth = 45°

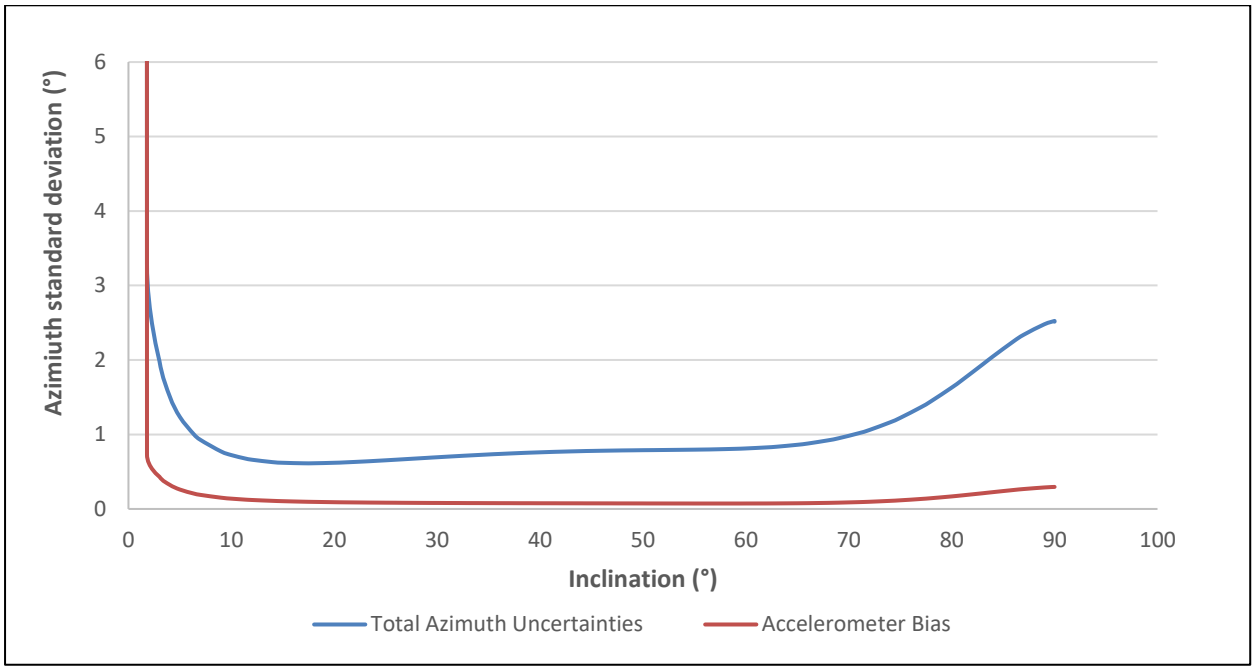

Figure 7.15 - Effect of Accelerometer Bias on Azimuth Uncertainties at Azimuth = 75°

7.3.2 Effect on Total Position Uncertainty

This section will analyze the effect of accelerometer bias on total position uncertainty. At shallow depths it does not have any effect on total position uncertainty in all three wells, but it seems to be quite effective at depths below 1000m MD. Below this depth, it has an almost

equal impact in the North-South and North-East wells but it influences the most in East-West well. For this well, the total position uncertainty is underestimated to almost 25m when accelerometer bias error is ignored.

Combining the results from measurement and position uncertainties, despite of having such high contribution to the total azimuth uncertainties in the vertical and near vertical section of each well it did not have any influence on total position error budget in these hole sections. Similarly, for the buildup and horizontal sections, when the error has minimum impact on total azimuth uncertainties it becomes a major contributor to the total position uncertainties. Therefore, the effect of accelerometer bias on azimuth and position uncertainties is totally opposite.

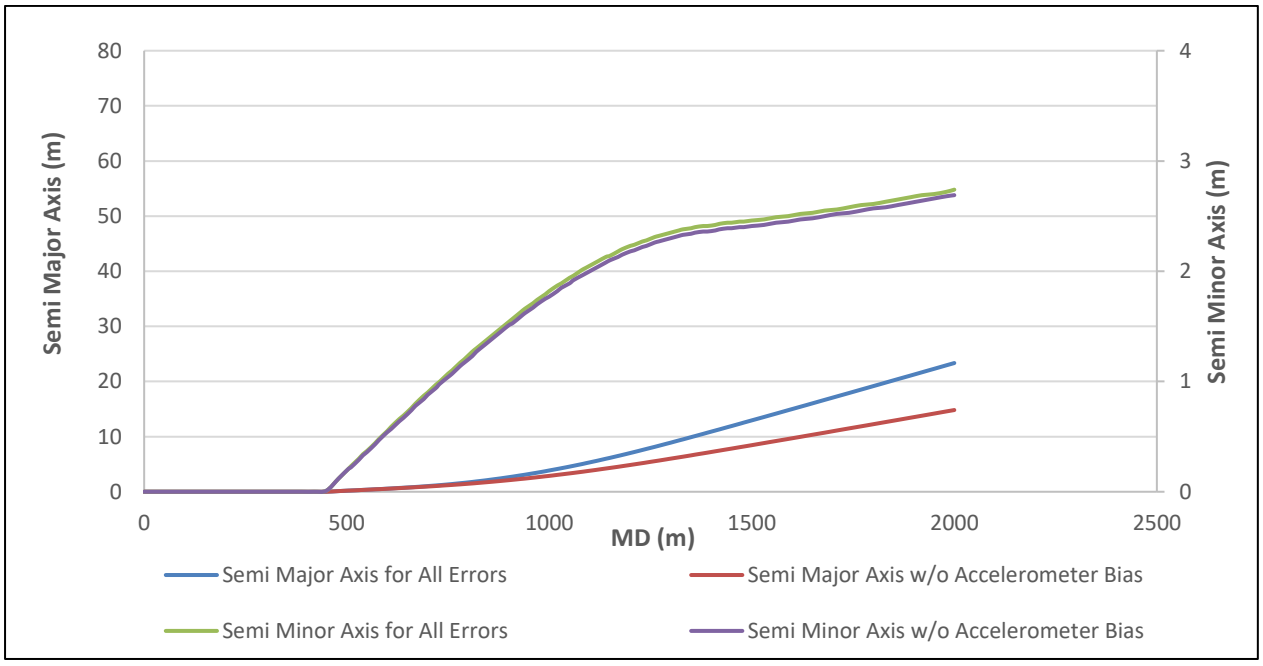

Figure 7.16 - Effect of Accelerometer Bias on Total Position Uncertainty at Azimuth = 0°

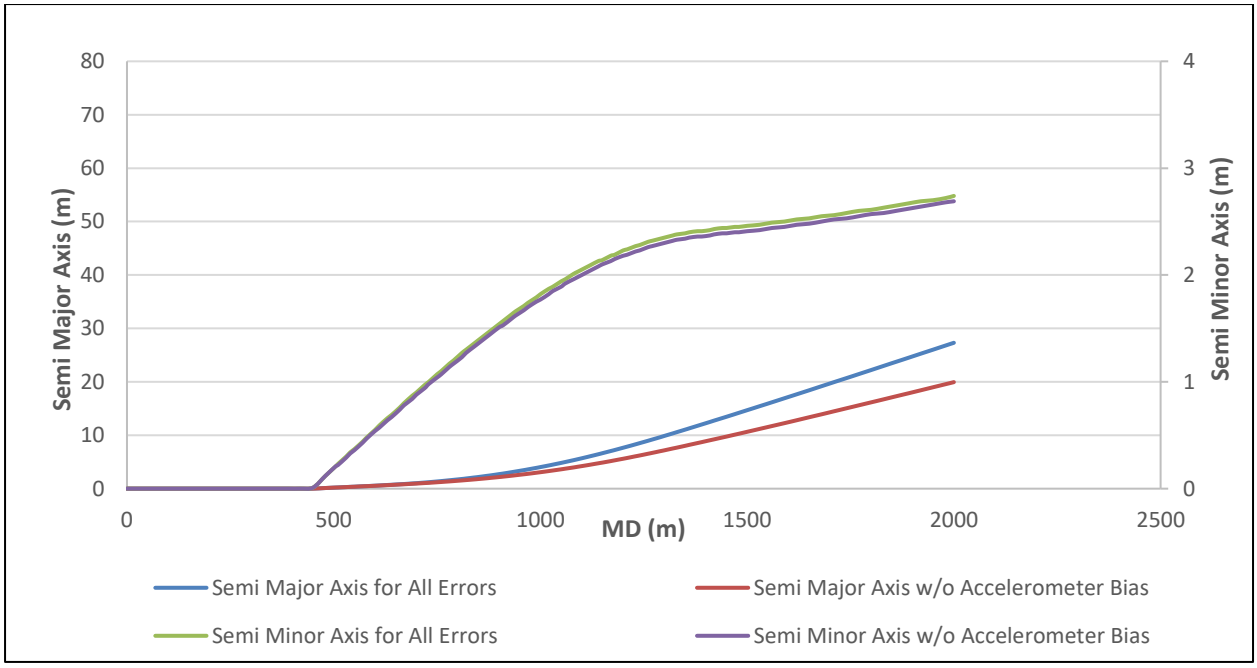

Figure 7.17 - Effect of Accelerometer Bias on Total Position Uncertainty at Azimuth = 45°

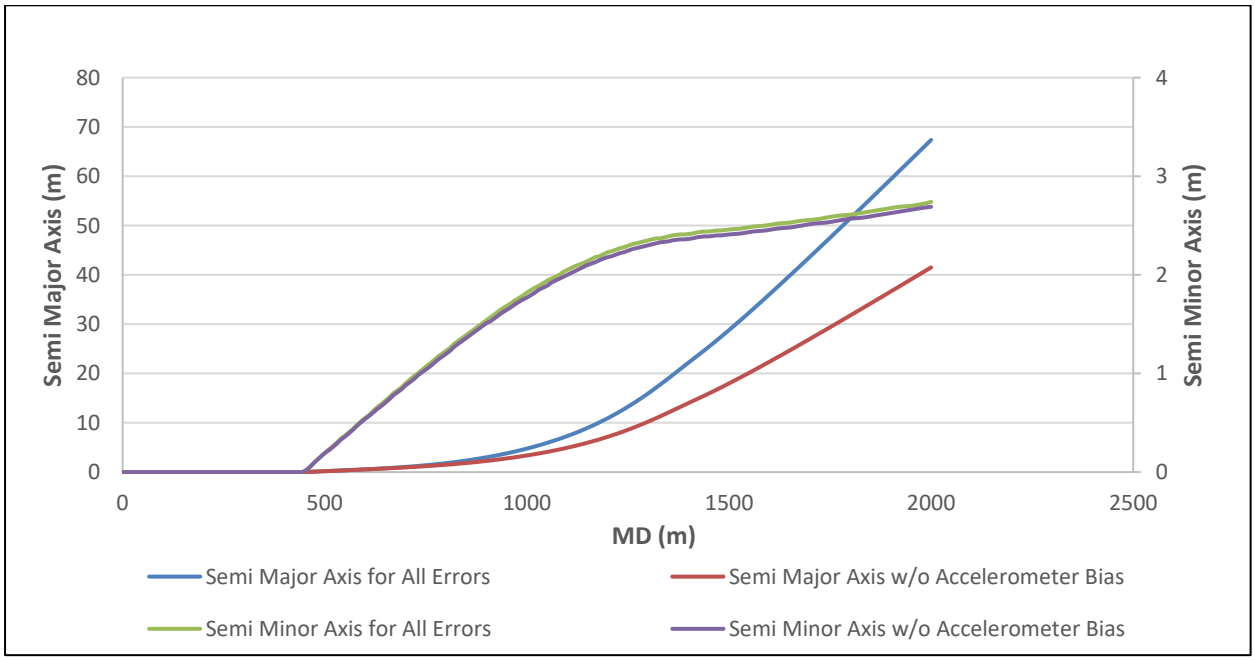

Figure 7.18 - Effect of Accelerometer Bias on Total Position Uncertainty at Azimuth = 75°

7.4 Accelerometer Scale

This section will analyze the impact of accelerometer scale on azimuth and position uncertainty using the modified error terms. Equations 7.6-7.9 list the weighting functions for accelerometer scale error terms impacting azimuth uncertainty only. Similar to accelerometer bias, since the

error terms used to estimate the inclination uncertainty due to accelerometer scale are identical in both error models, therefore error terms impacting only azimuth uncertainty will be used in the analysis. However, the position uncertainty will again be predicted using both inclination and azimuth related error terms.

$$asixy\_1 = \begin{pmatrix} 0 \\ 0 \\ \dfrac{-\sin(I)\cos^2(I)\sin(A)\left[\tan(\Theta)\cos(I)+\sin(I)\cos(A)\right]}{\sqrt{2}\left[1-\sin^2(I)\sin^2(A)\right]} \end{pmatrix} \tag{7.6}$$

$$asixy\_2 = \begin{pmatrix} 0 \\ 0 \\ \dfrac{-\sin(I)\cos^2(I)\sin(A)\left[\tan(\Theta)\cos(I)+\sin(I)\cos(A)\right]}{2\left[1-\sin^2(I)\sin^2(A)\right]} \end{pmatrix} \tag{7.7}$$

$$asixy\_3 = \begin{pmatrix} 0 \\ 0 \\ \dfrac{\tan(\Theta)\sin(I)\cos(A)-\cos(I)}{2\left[1-\sin^2(I)\sin^2(A)\right]} \end{pmatrix} \tag{7.8}$$

$$asiz = \begin{pmatrix} 0 \\ 0 \\ \dfrac{\left[\sin(I)\cos^2(I)\sin(A)\{\tan(\Theta)\cos(I)+\sin(I)\cos)(A)\}\right]}{1-\sin^2(I)\sin^2(A)} \end{pmatrix} \tag{7.9}$$

7.4.1 Effect on Azimuth Uncertainty

Using the weighting functions in above four equations, azimuth uncertainty is plotted as a function of hole inclination for the three subject wells in Figures 7.19-7.21. In the North-South well, accelerometer scale only induces azimuth uncertainties above 30° inclination but makes a good contribution to the total azimuth error budget above this inclination. The azimuth uncertainties in the North-East well do not change much as a function of inclination but are still enough to contribute to the total azimuth error budget in the buildup and horizontal section. In the East-West well, the azimuth uncertainties increase twice along the well. From being minimum in the vertical section, they continuously increase up to 50° inclination and then maintain a constant trend up to 70° inclination. Above this inclination, it sharply increases

while approaching the horizontal section to a maximum of 1.8° azimuth error. Despite of this large azimuth error, it has a relatively greater contribution to the total azimuth error budget in the buildup section compared to horizontal section. This is governed by the behavior of total azimuth uncertainties in this well.

Accelerometer scale also has an almost similar impact on azimuth uncertainties in different hole sections of all three wells. The error source does not seem to have any notable impact in the vertical and near vertical section of all three wells. While it is almost equally effective in the buildup and horizontal sections of the three wells.

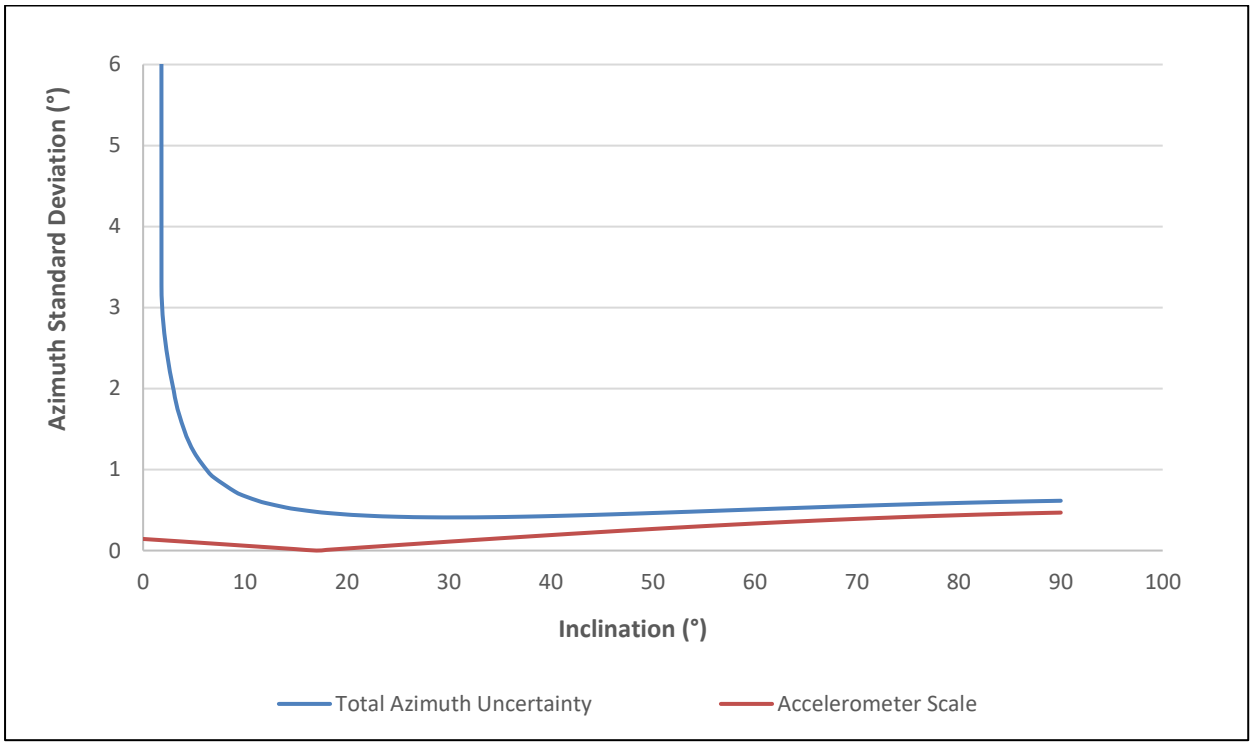

Figure 7.19 - Effect of Accelerometer Scale on Azimuth Uncertainties at Azimuth = 0°

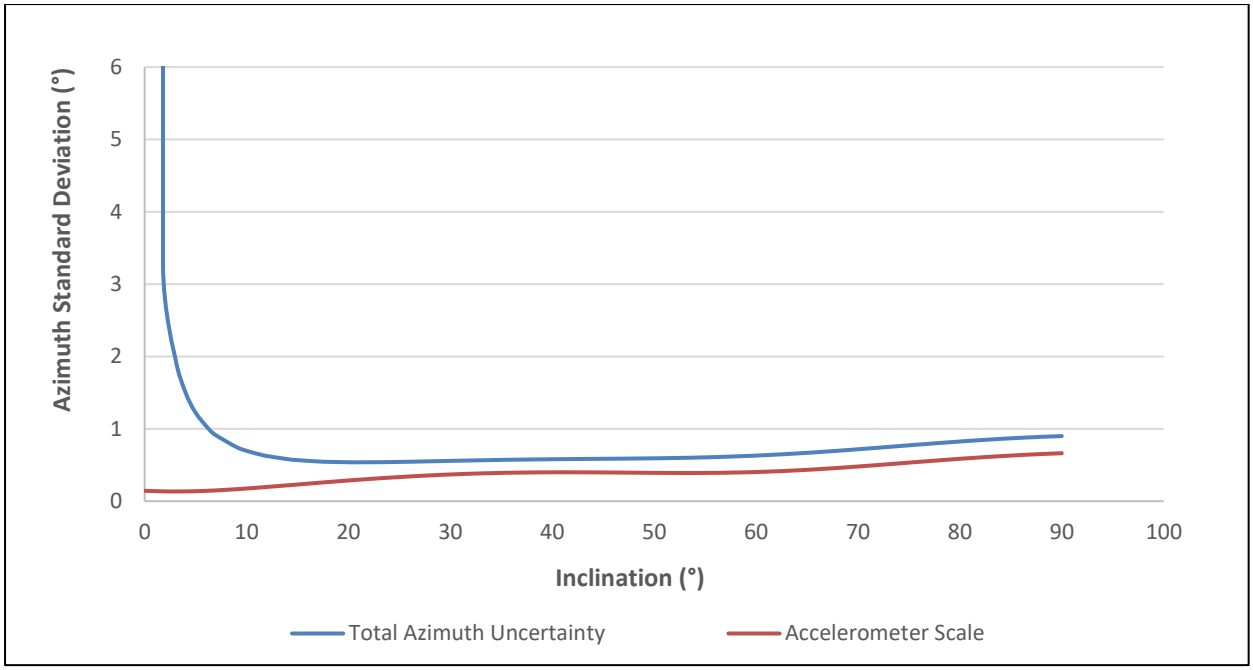

Figure 7.20 - Effect of Accelerometer Scale on Azimuth Uncertainties at Azimuth = 45°

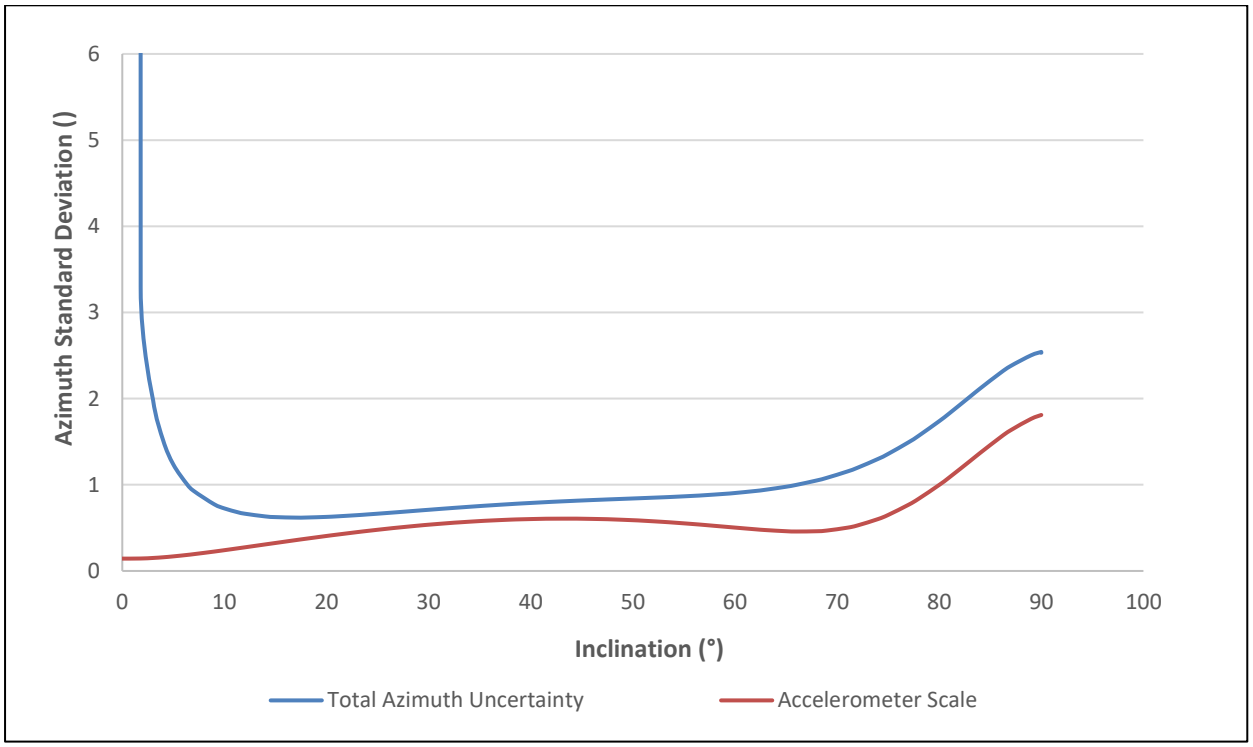

Figure 7.21 - Effect of Accelerometer Scale on Azimuth Uncertainties at Azimuth = 75°

7.4.2 Effect on Total Position Uncertainty

This section will explain the effect of accelerometer scale on total position uncertainty in the three wells through figures 7.22-7.24. The total position uncertainty in each well is again only influenced at higher depths approximately below 1000m MD. Further below this depth, the effect of accelerometer scale on total position uncertainty continuously increases and is maximum in the horizontal section. It is also observed to have an almost similar impact in the North-South and North-East wells where ignoring the accelerometer scale error terms result in a total position uncertainty reduced to 8m & 7m respectively for the East-West well, excluding this error source underestimates the position uncertainty by approximately 26m in the horizontal section.

Based on the analysis of measurement and position uncertainties above, accelerometer scale neither influences the azimuth nor position uncertainties in the vertical and near vertical sections of the three wells corresponding to shallow depths. But it affects both azimuth and position error budgets in the buildup and horizontal sections of all wells. This shows that the error has a uniform effect on measurement and position uncertainties in each hole section.

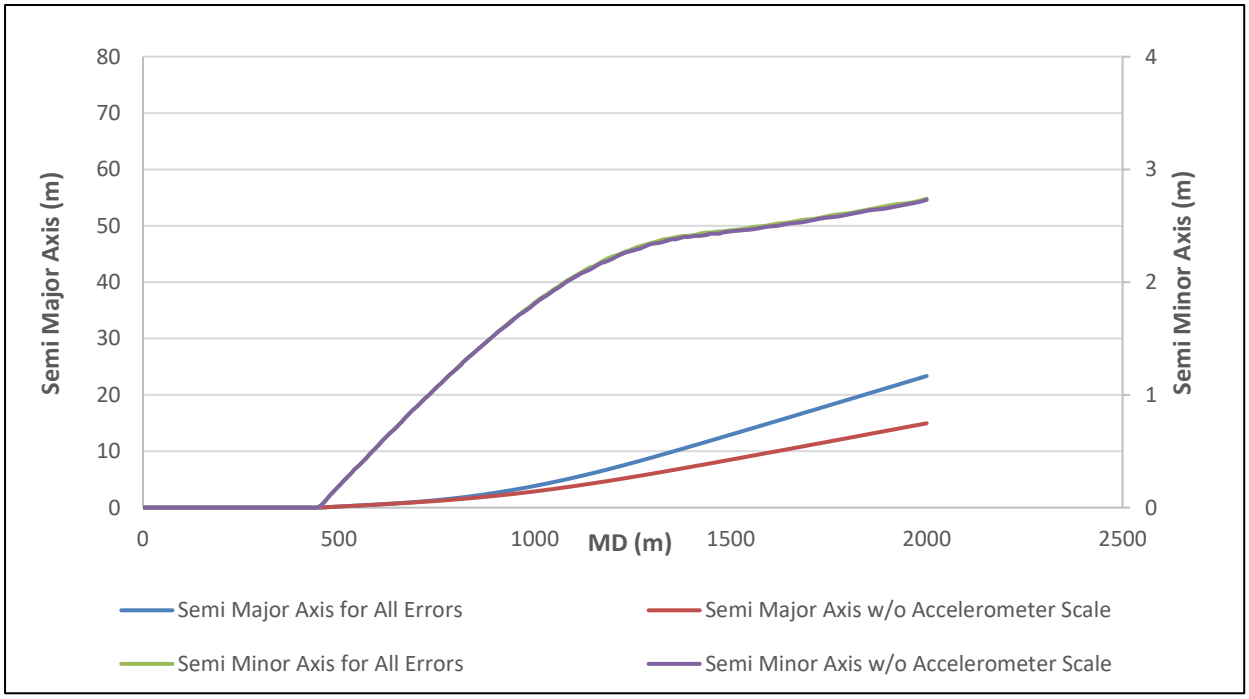

Figure 7.22 - Effect of Accelerometer Scale on Total Position Uncertainty at Azimuth = 0°

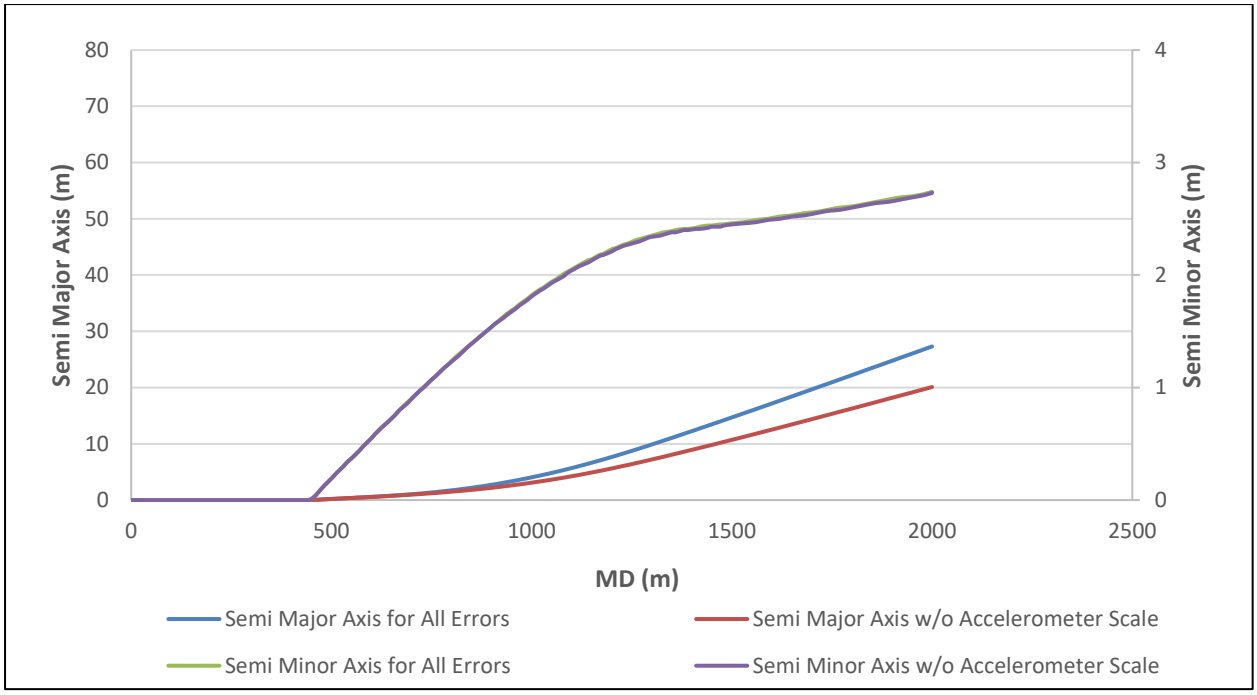

Figure 7.23 - Effect of Accelerometer Scale on Total Position Uncertainty at Azimuth = 45°

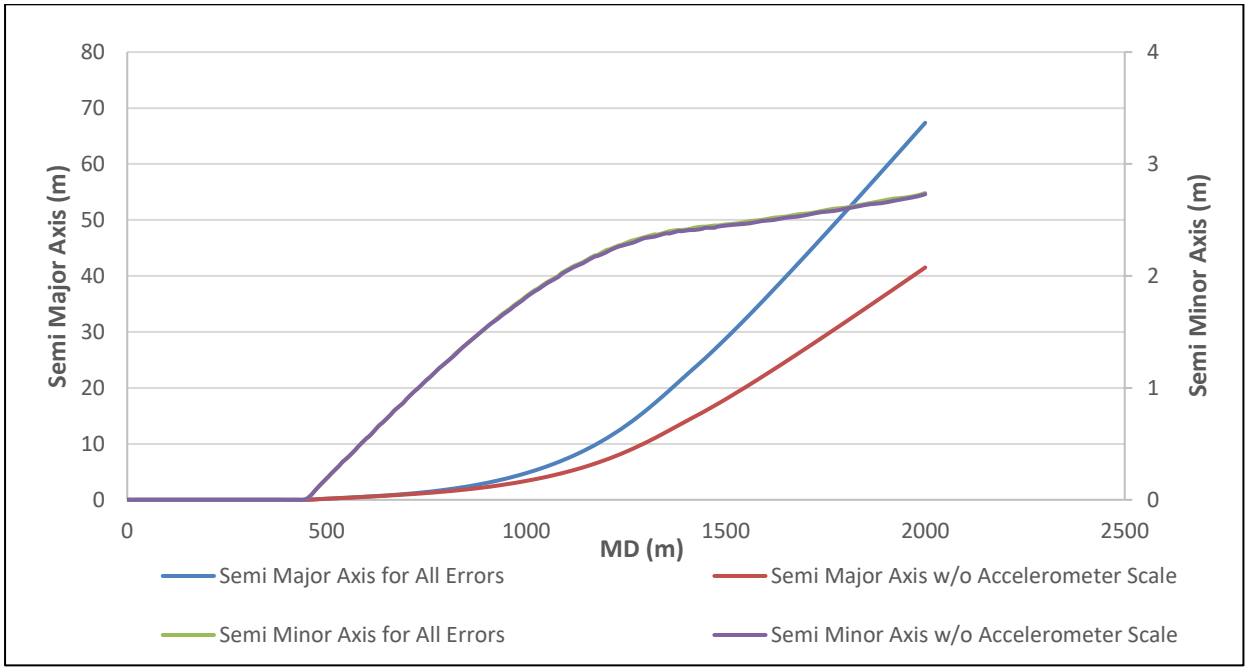

Figure 7.24 - Effect of Accelerometer Scale on Total Position Uncertainty at Azimuth = 75°

7.5 Magnetometer Cross- Axial Bias

The effect of magnetometer cross-axial bias on azimuth and position uncertainty has been analyzed using equations 7.10 & 7.11. Since the results of this error source are also influenced

by magnetic axial drillstring interference, therefore these error terms have been modified accordingly in the Mag-corr error model to cater this effect. The error magnitude used to calculate the effect has been listed in Appendix D.

$$mbixy\_1 = \begin{pmatrix} 0 \\ 0 \\ \dfrac{-\cos(I)\sin(A)}{B_t \cos(\Theta)\left[1-\sin^2(I)\sin^2(A)\right]} \end{pmatrix} \tag{7.10}$$

$$mbixy\_2 = \begin{pmatrix} 0 \\ 0 \\ \dfrac{\cos(A)}{B_t \cos(\Theta)\left[1-\sin^2(I)\sin^2(A)\right]} \end{pmatrix} \tag{7.11}$$

7.5.1 Effect on Azimuth Uncertainty

Based on the weighting functions above, the two error terms will result in large azimuth errors when drilling horizontal East-West because of the trigonometric identity [(1-sin^2(I)sin^2(A)] in the denominator of both weighting functions. This can be verified from figure 7.27 where the azimuth uncertainties are seen to suddenly increase while approaching the horizontal section of East-West well. For the rest of the well, its behavior is almost independent of inclination like North-South and North-East wells. Depending upon this behavior, the relative effect of this error source on total azimuth uncertainties is minimum in the vertical and near vertical section and maximum in the buildup section despite of having higher azimuth uncertainties in the horizontal section.

The azimuth uncertainties in the North-South and North-East wells remain completely independent of inclination throughout the well path. Therefore, their impact on total azimuth error budget will solely be determined by the total azimuth uncertainties in the two wells. Magnetometer bias thus has minimum affect in the vertical and near vertical section of these two wells and is most effective in the buildup section.

To compare the effect of this error source in the corresponding hole sections of different wells, it is seen to have an almost negligible effect in the vertical and near vertical sections of all wells. Similarly, it is observed to have an almost uniform impact in the horizontal sections of the three wells. It is only in the buildup section where the effect is different and magnetometer

bias has a relatively greater effect on total azimuth error budget of North-South well and less in North-East and East-West wells.

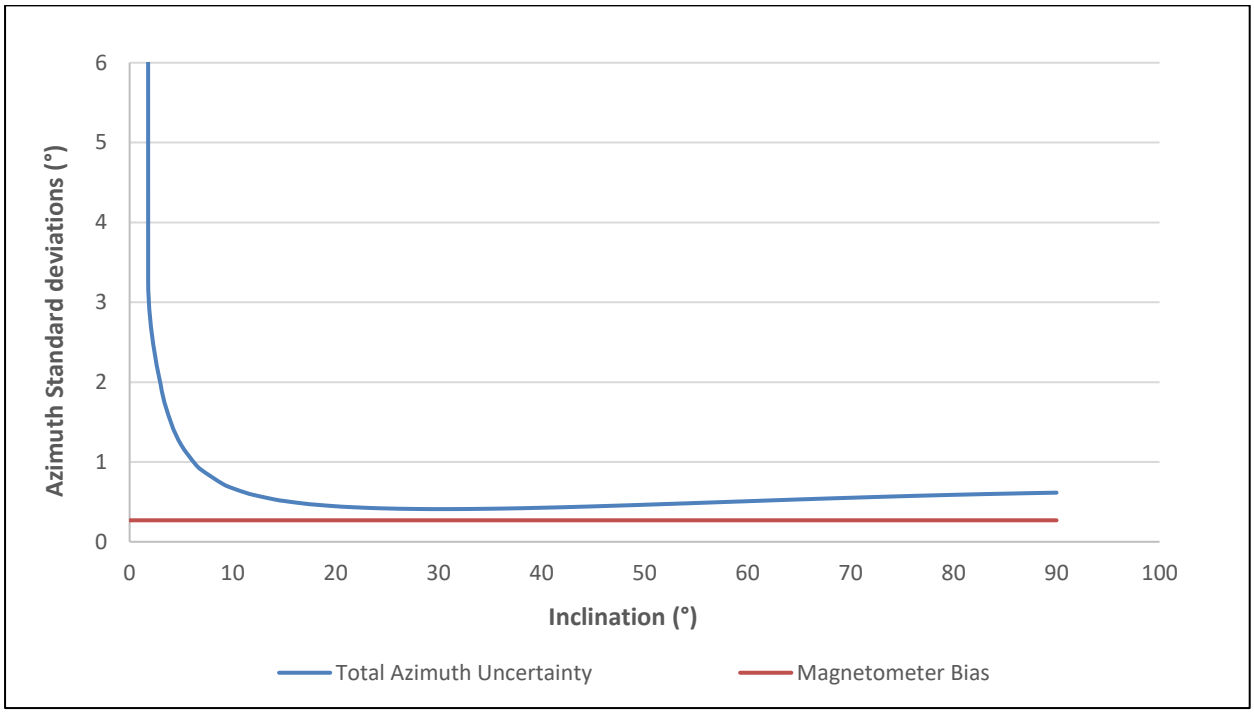

Figure 7.25 - Effect of Magnetometer Bias on Azimuth Uncertainties at Azimuth = 0°

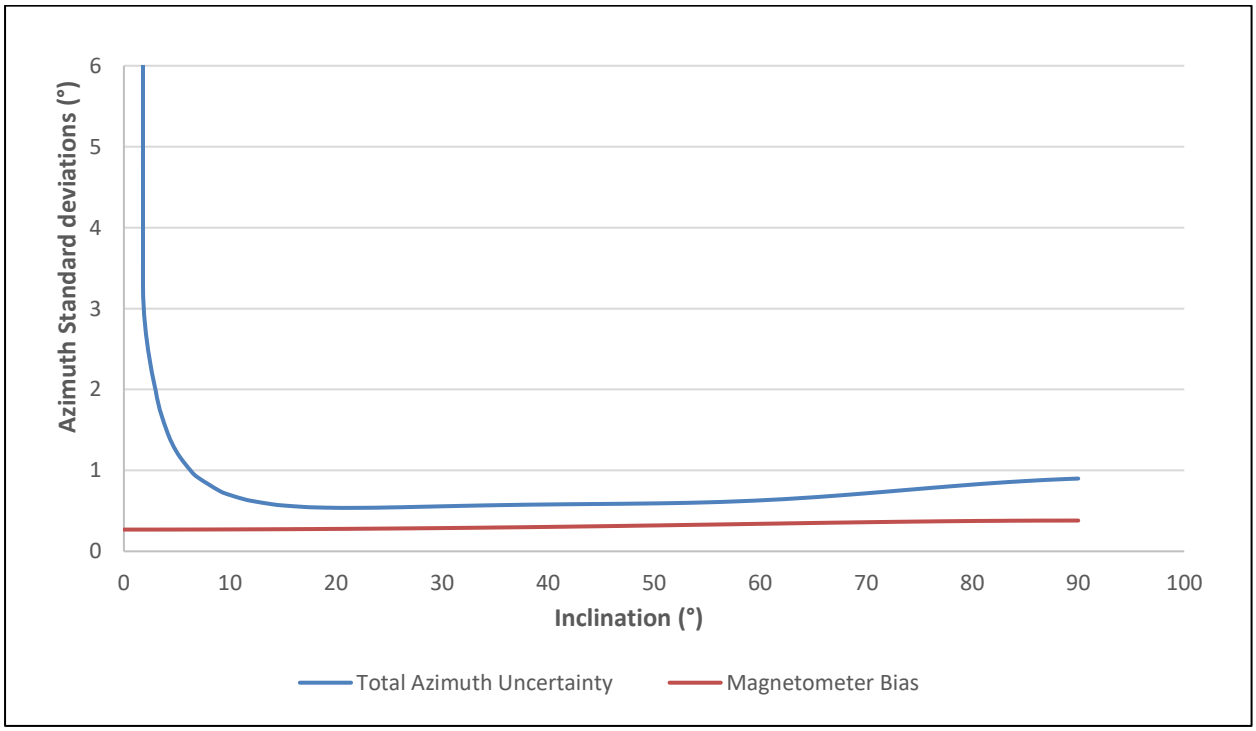

Figure 7.26 - Effect of Magnetometer Bias on Azimuth Uncertainties at Azimuth = 45°

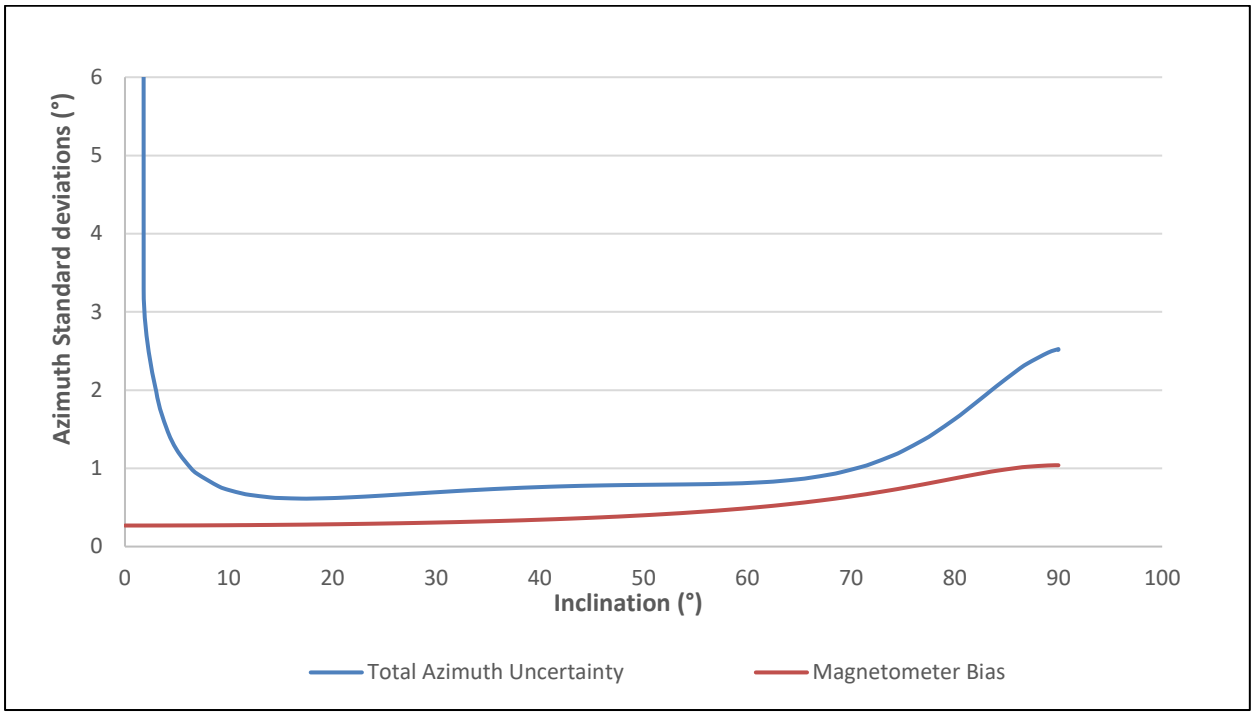

Figure 7.27 - Effect of Magnetometer Bias on Azimuth Uncertainties at Azimuth = 75°

7.5.2 Effect on Total Position Uncertainty

Figures 7.28-7.30 have been used to explain the effect of magnetometer cross-axial bias on total position uncertainty. Mainly, in the vertical and near vertical part of the three wells, the effect on total position uncertainty is almost negligible and ignoring the error does not change the total position uncertainty at all. But at greater depths, the separation between the two curves increases and reach to a maximum in the horizontal section at TD. At TD, ignoring the error term in North-South well underestimates the total position uncertainty to 12m while in North-East and East-West wells ignoring this error term will underestimate the total position uncertainty to almost 12m and 33m's respectively. Therefore, given its large impact on position uncertainty in East-West well this error becomes most important in this drilling direction.

The above measurement and position uncertainty results show that the error has no contribution to the total azimuth or position error budget in the vertical and near vertical section of the three wells. The error however makes contribution to both in buildup and horizontal sections of the three wells indicating a uniform effect on azimuth and position uncertainties for the corresponding hole sections in each well.

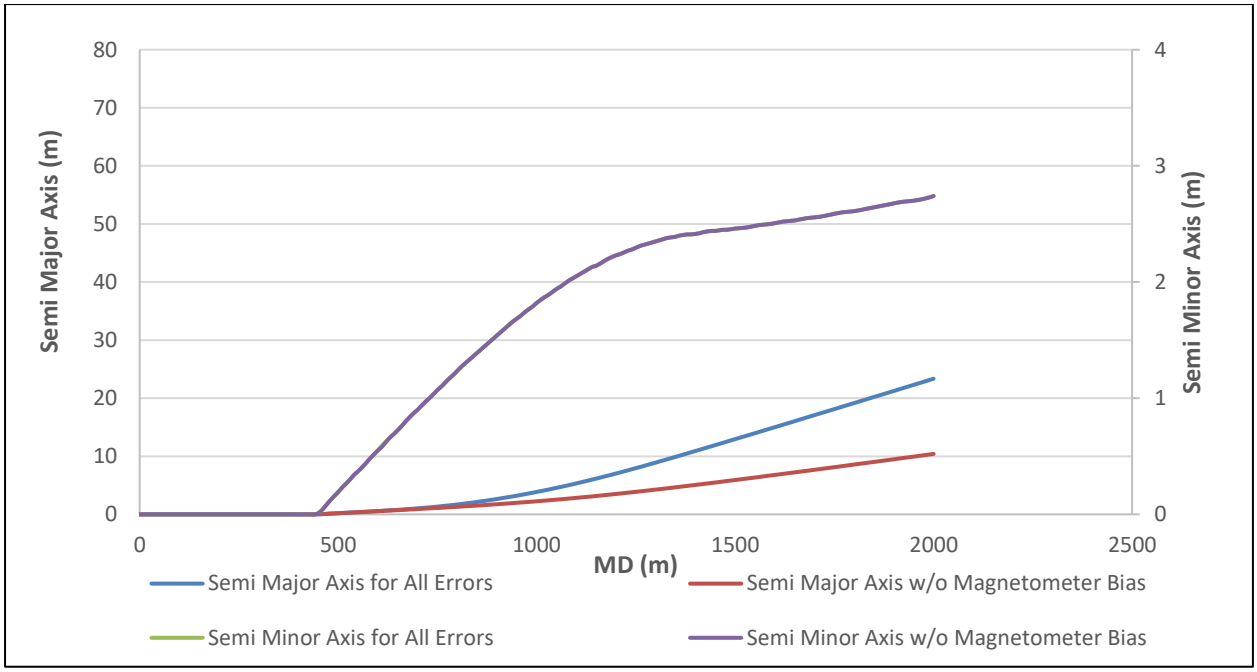

Figure 7.28 - Effect of Magnetometer Bias on Total Position Uncertainty at Azimuth = 0°

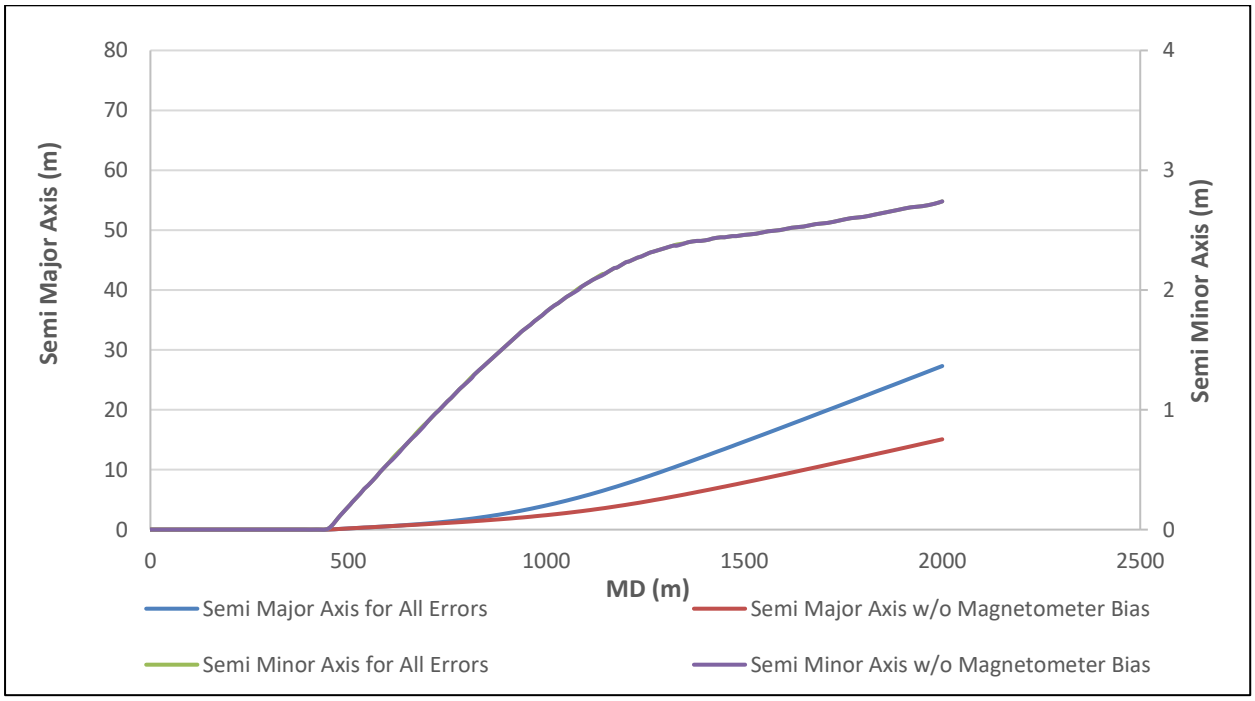

Figure 7.29 - Effect of Magnetometer Bias on Total Position Uncertainty at Azimuth = 45°

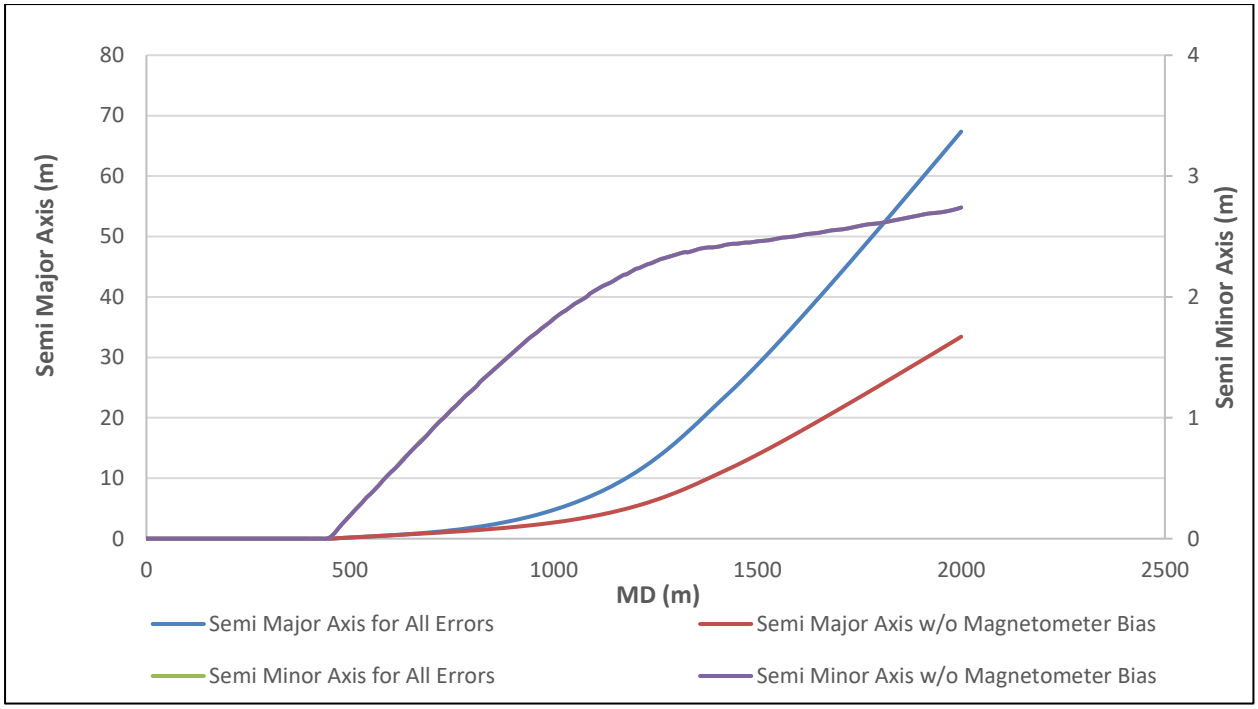

Figure 7.30 - Effect of Magnetometer Bias on Total Position Uncertainty at Azimuth = 75°

7.6 Magnetometer Scale

After suitable modification of the magnetometer scale error terms in the Mag-corr error model, equations 7.12-7.14 are used to calculate the measurement and position uncertainties for this error source. The presence of trigonometric identity *[(1-sin^2(I)sin^2(A)]* in the denominator of all equations indicates that this error should also have maximum impact when drilling a horizontal well in East-West direction. Figures 7.31-7.33 will in detail explain the effect of magnetometer scale on azimuth and position uncertainties in three wells drilled in different directions.

$$msixy\_1 = \begin{pmatrix} 0 \\ 0 \\ \dfrac{\sin(I)\sin(A)\left[\tan(\Theta)\cos(I)+\sin(I)\cos(A)\right]}{\sqrt{2}\left[1-\sin^2(I)\sin^2(A)\right]} \end{pmatrix} \tag{7.12}$$

$$msixy\_2 = \begin{pmatrix} 0 \\ 0 \\ \dfrac{\sin(I)\left[\tan(\Theta)\sin(I)\cos(I)-\cos^2(I)\cos(A)-\cos(A)\right]}{2\left[1-\sin^2(I)\sin^2(A)\right]} \end{pmatrix} \tag{7.13}$$

$$msixy\_3 = \begin{pmatrix} 0 \\ 0 \\ \dfrac{\cos(I)\cos^2(A) - \cos(I)\sin^2(A) - \tan(\Theta)\sin(I)\cos(A)}{2\left[1 - \sin^2(I)\sin^2(A)\right]} \end{pmatrix} \quad (7.14)$$

7.6.1 Effect on Azimuth Uncertainty

The effect of magnetometer scale on azimuth uncertainties in the three wells is not much different. In the North-South and North-East wells the azimuth error is negligible up to 50° and 20° inclination respectively. Only above these inclinations magnetometer scale has a constant azimuth error that does not change much as a function of hole inclination. Due to this, magnetometer scale makes a very little contribution to the total azimuth error budget in the buildup and horizontal sections but has no influence at all in the vertical and near vertical sections of the two wells.

The behavior in the East-West well as expected is slightly different in the horizontal section than in the North-South and North-East wells. A sudden increase in azimuth error is observed because of the trigonometric identity in the above equations. But even due to this increase, its relative effect on total azimuth uncertainties in the horizontal section is not different compared with other hole sections.

Therefore, magnetometer scale has no impact in the vertical and near vertical section of each well. But it does have a little influence in the buildup and horizontal sections and the relative effect in each buildup and horizontal sections is also almost same.

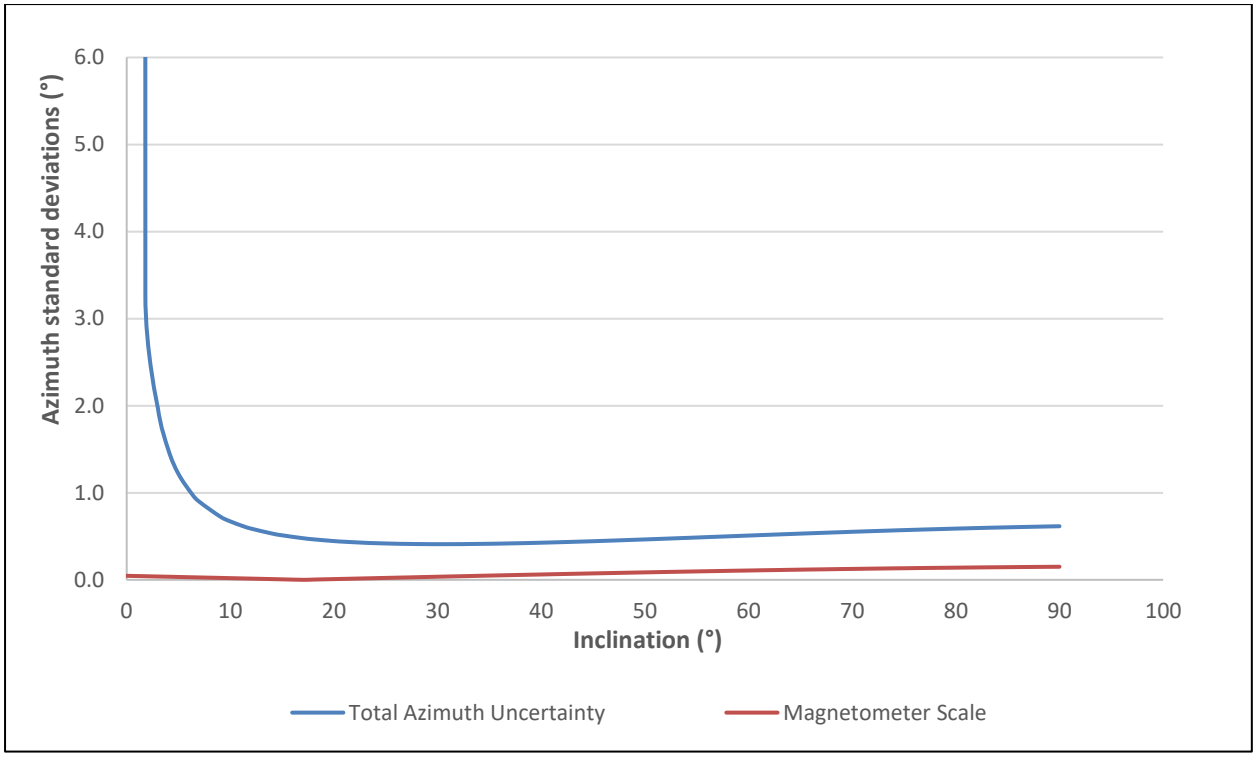

Figure 7.31 - Effect of Magnetometer Scale on Azimuth Uncertainties at Azimuth = 0°

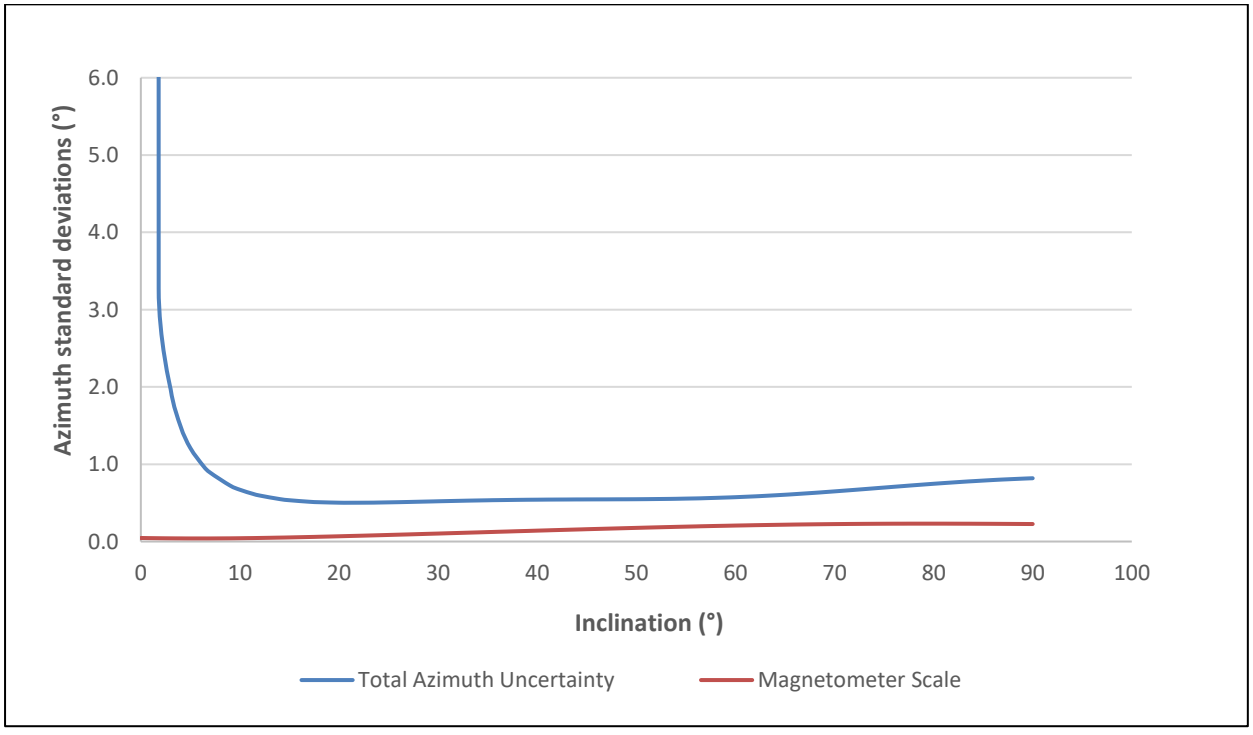

Figure 7.32 - Effect of Magnetometer Scale on Azimuth Uncertainties at Azimuth = 45°

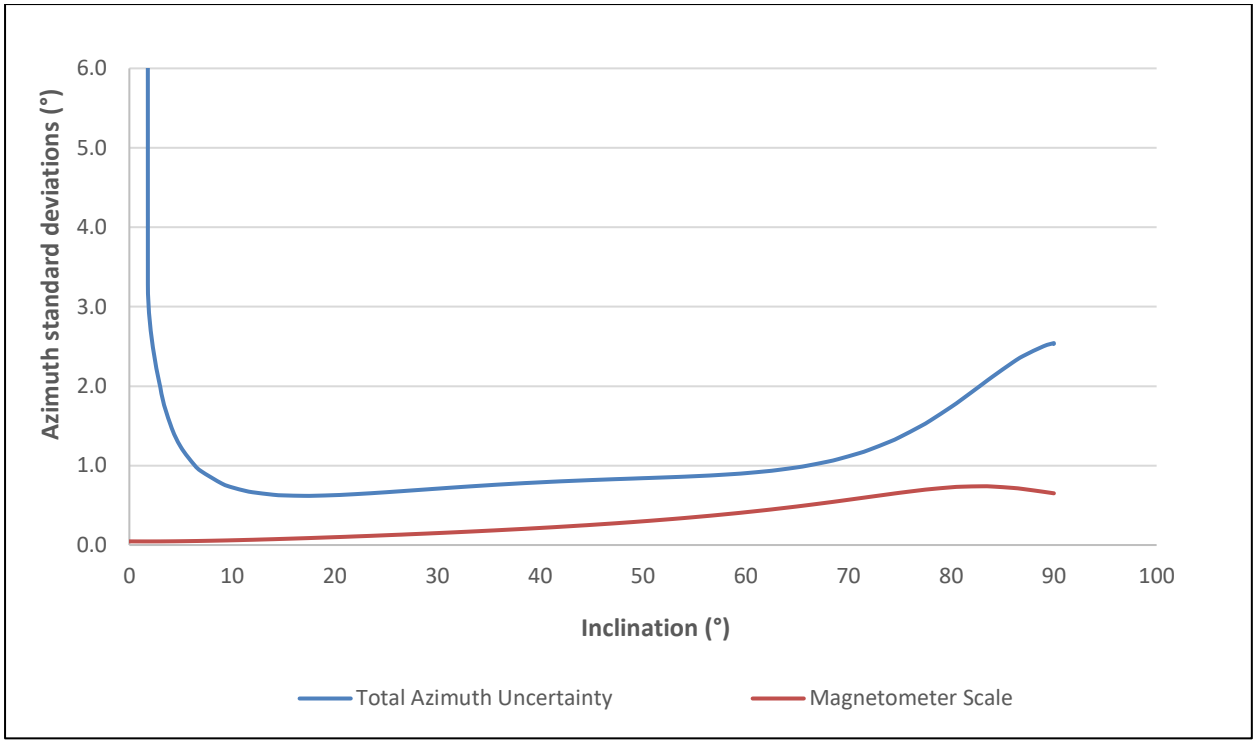

Figure 7.33 - Effect of Magnetometer Scale on Azimuth Uncertainties at Azimuth = 75°

7.6.2 Effect on Total Position Uncertainty

Magnetometer scale also affects the total position uncertainties only below 1000m MD and the effect continuously increases along with depth in all three wells. Thus, the error source does not have any contribution to the total position error budget in the vertical and near vertical sections while it increases in the buildup section and is maximum in the horizontal section. The relative effect of this error source is same for vertical, near vertical and buildup sections of the three wells but among the horizontal sections, it has the largest effect in East-West well. Ignoring this error source in East-West well underestimates the total position uncertainty to almost 30m.

Magnetometer scale therefore has a similar impact on measurement and position uncertainties. In the three subject wells, it neither adds to the total azimuth error nor to the total position error budget. While it's effect on azimuth and position uncertainties increases in the buildup and horizontal sections respectively.

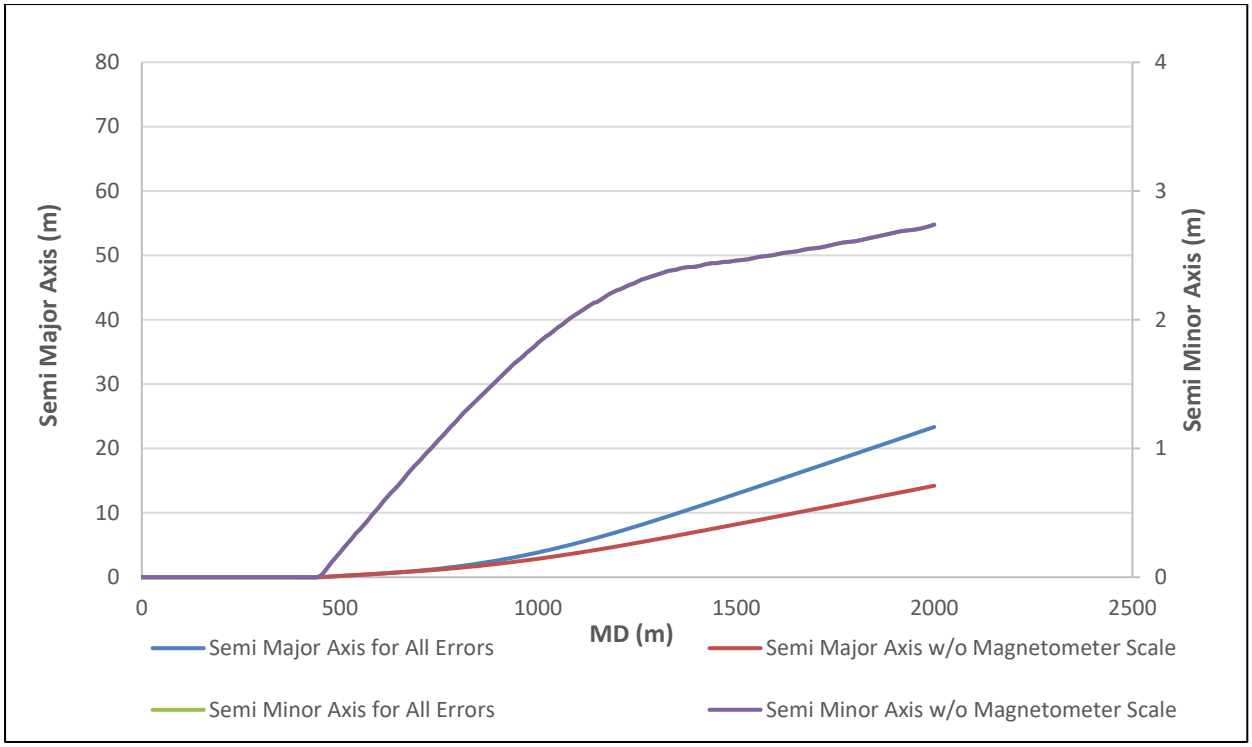

Figure 7.34 - Effect of Magnetometer Scale on Total Position Uncertainty at Azimuth = 0°

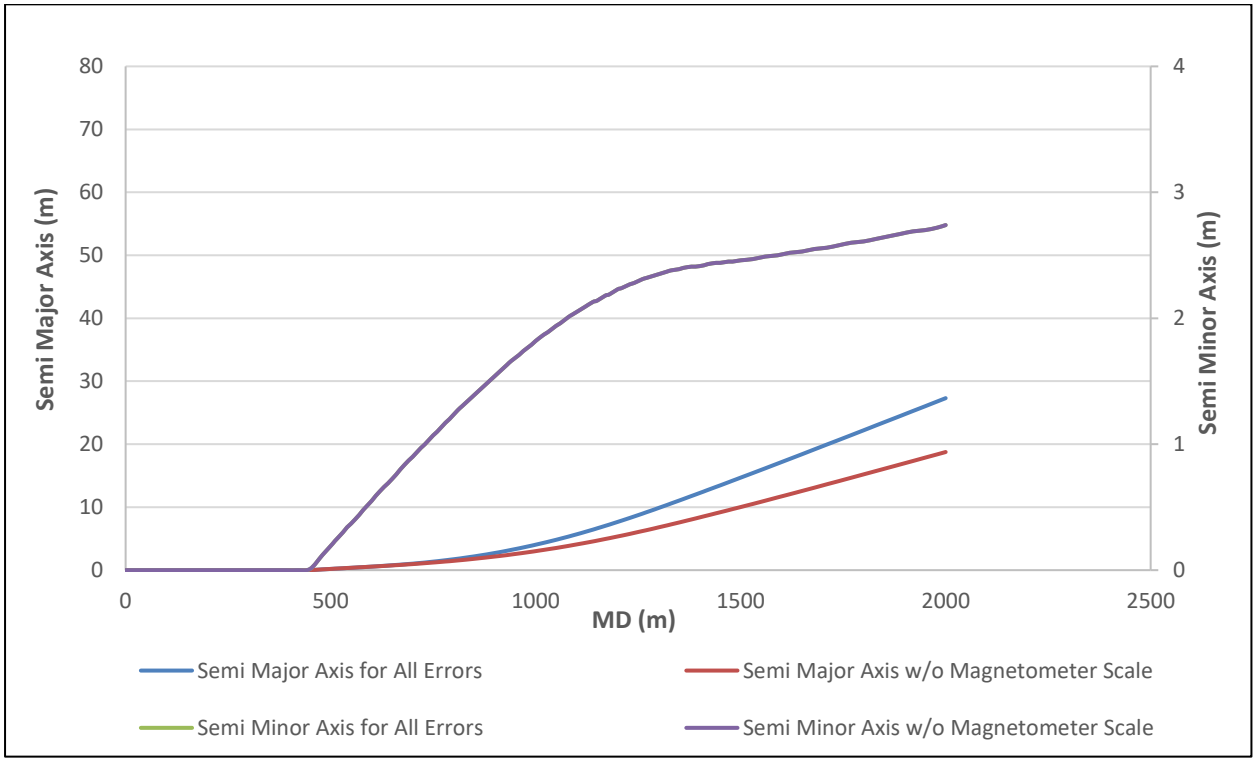

Figure 7.35 - Effect of Magnetometer Scale on Total Position Uncertainty at Azimuth = 45°

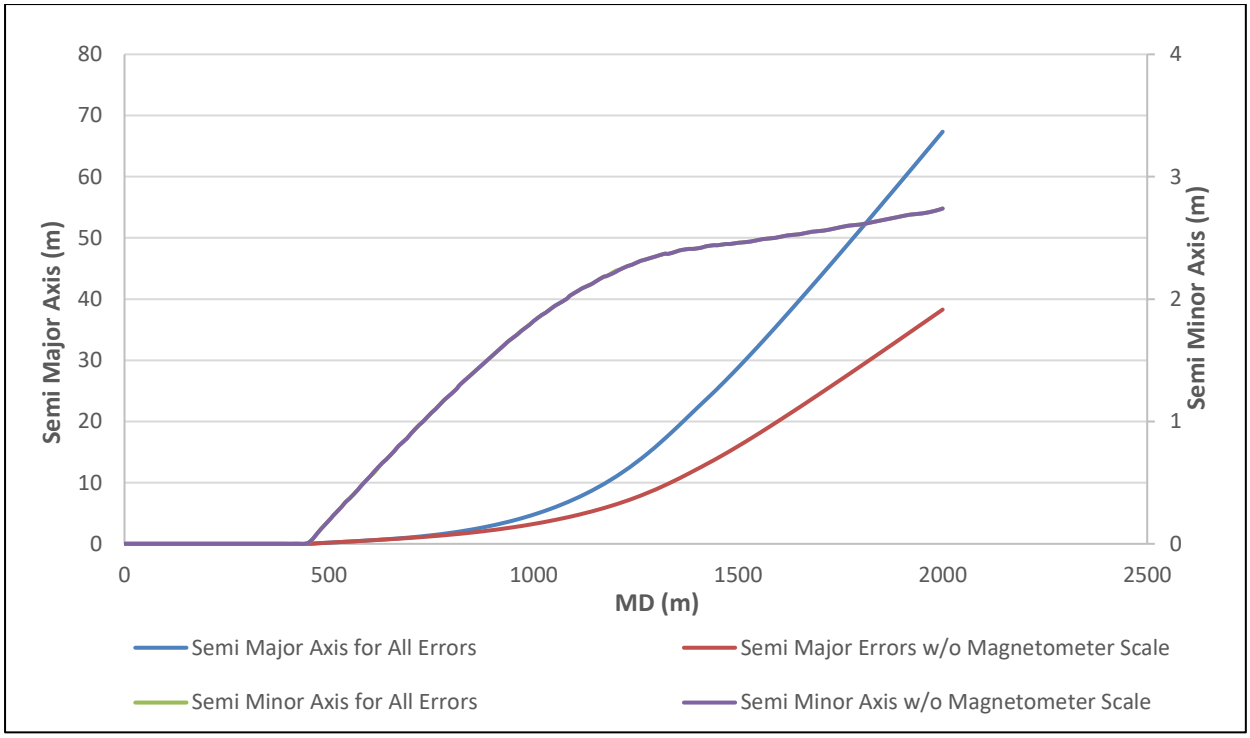

Figure 7.36 - Effect of Magnetometer Scale on Total Position Uncertainty at Azimuth = 75°

Chapter 8. Comparison of Non-mag and Mag-corr Error Models

This chapter will present a comparison between sensor error terms in the two error models since they only carry different weighting functions. The plots will illustrate the difference in the azimuth and position errors predicted from the two models.

8.1 Accelerometer Bias

8.1.1 Effect on Azimuth Uncertainty

Figures 8.1-8.3 represent the effect of AMIL correction on azimuth uncertainties due to accelerometer bias. Both Non-mag and Mag-corr error models predict almost equal azimuth errors along all three wells. This shows, that using either set of error terms the resultant azimuth uncertainties do not change in any of the three wells. Only a very small deviation is observed in the horizontal section of East-West well but is not too significant.

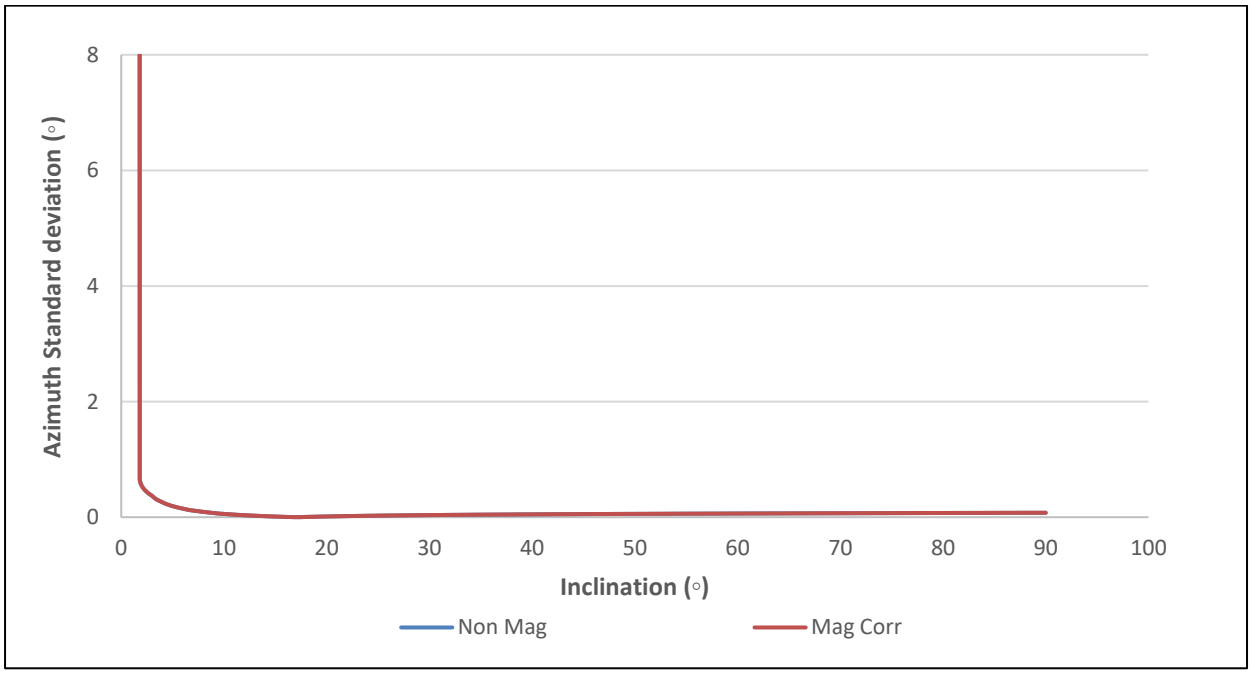

Figure 8.1 – Comparison of Azimuth Uncertainties due to Accelerometer Bias at Azimuth = 0°

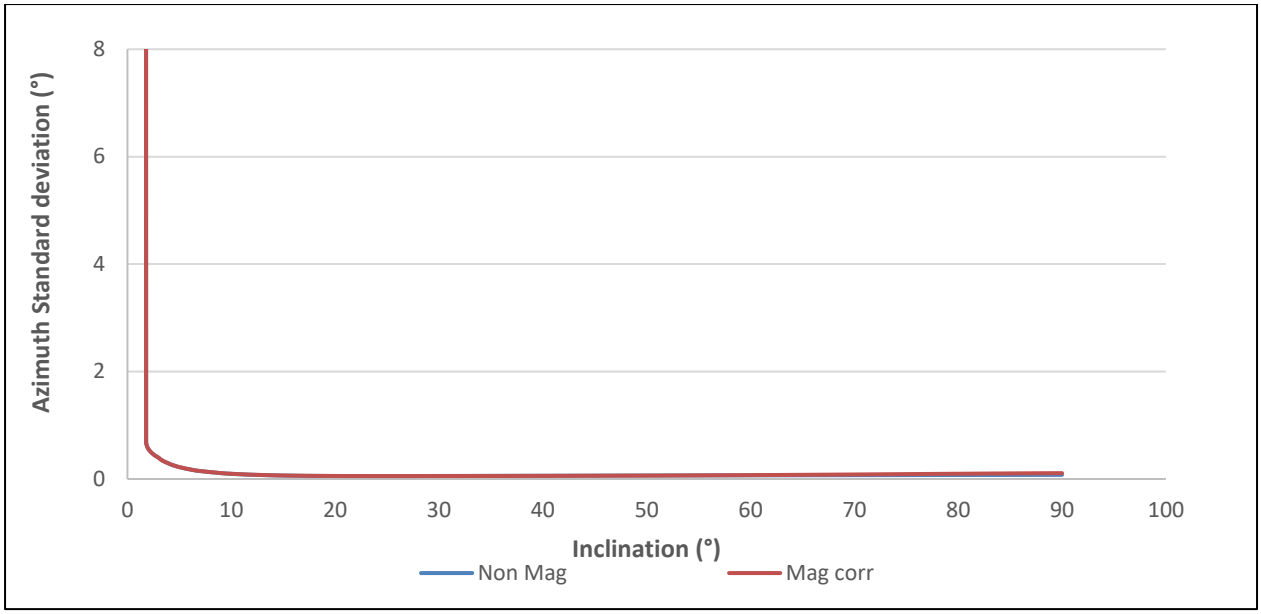

Figure 8.2 - Comparison of Azimuth Uncertainties due to Accelerometer Bias at Azimuth = 45°

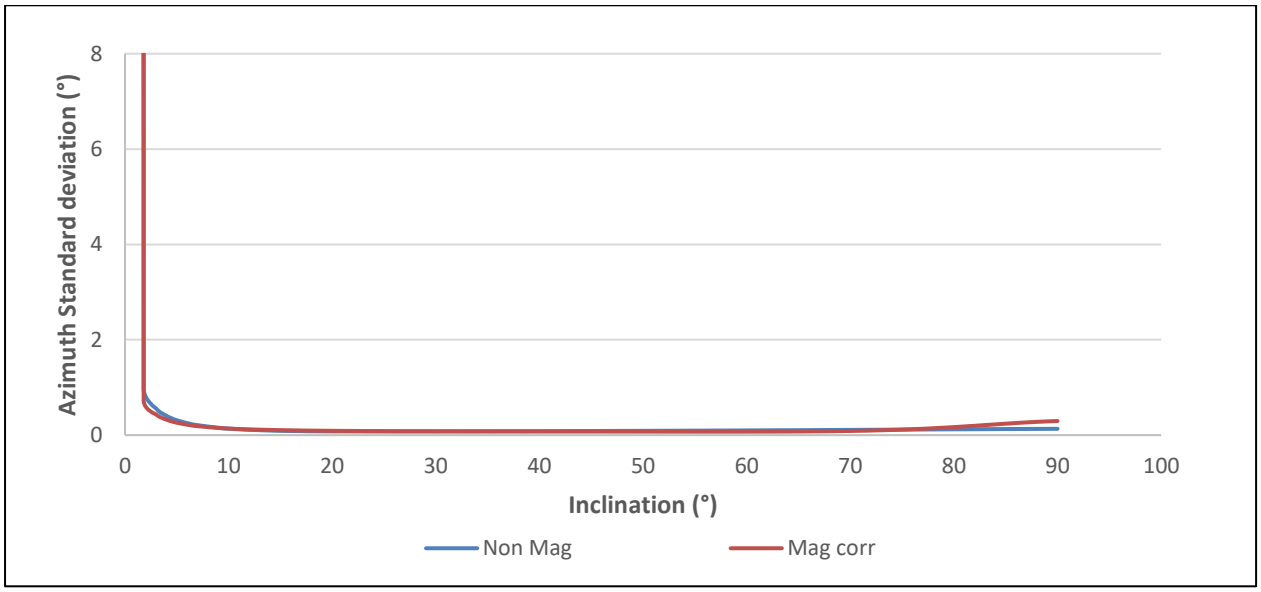

Figure 8.3 – Comparison of Azimuth Uncertainties due to Accelerometer Bias at Azimuth = 75°

8.1.2 Effect on Position Uncertainty

Position uncertainties predicted from the Non-mag and Mag-corr error models are exactly the same throughout the North-South well. But in the horizontal sections of the North-East and East-West wells, Mag-corr error model results in significantly large position uncertainty compared to the Non-mag error model. This difference between the two is relatively greater in the East-West well than in North-East well.

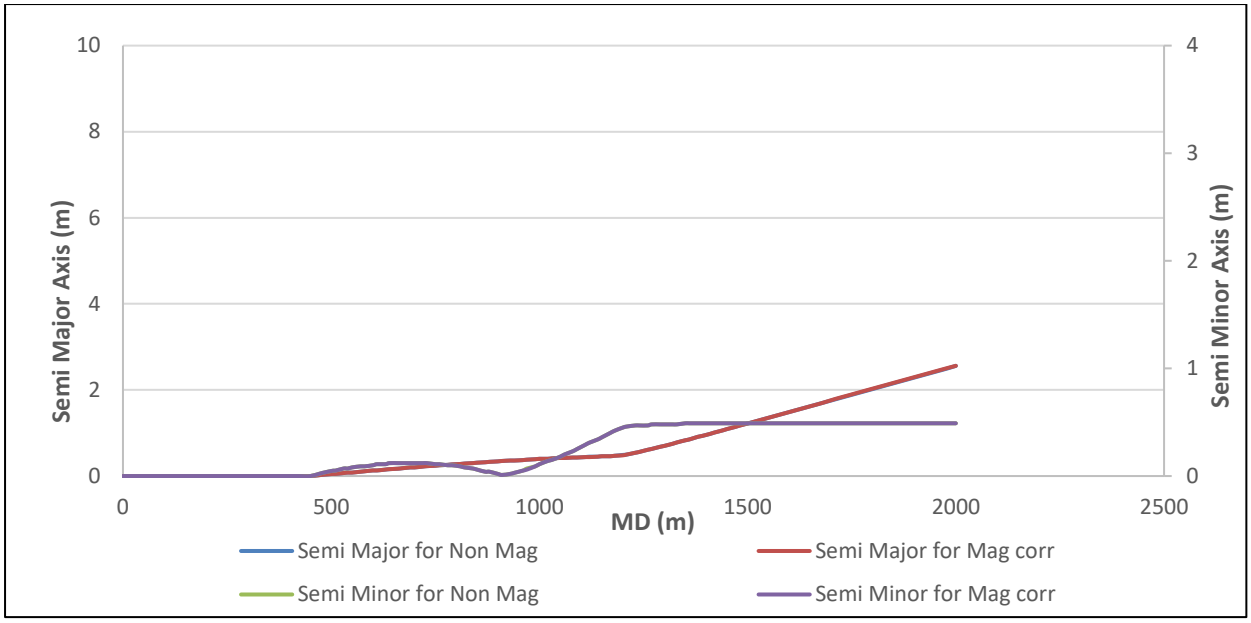

Figure 8.4 – Comparison of Position Uncertainty due to Accelerometer Bias at Azimuth = 0°

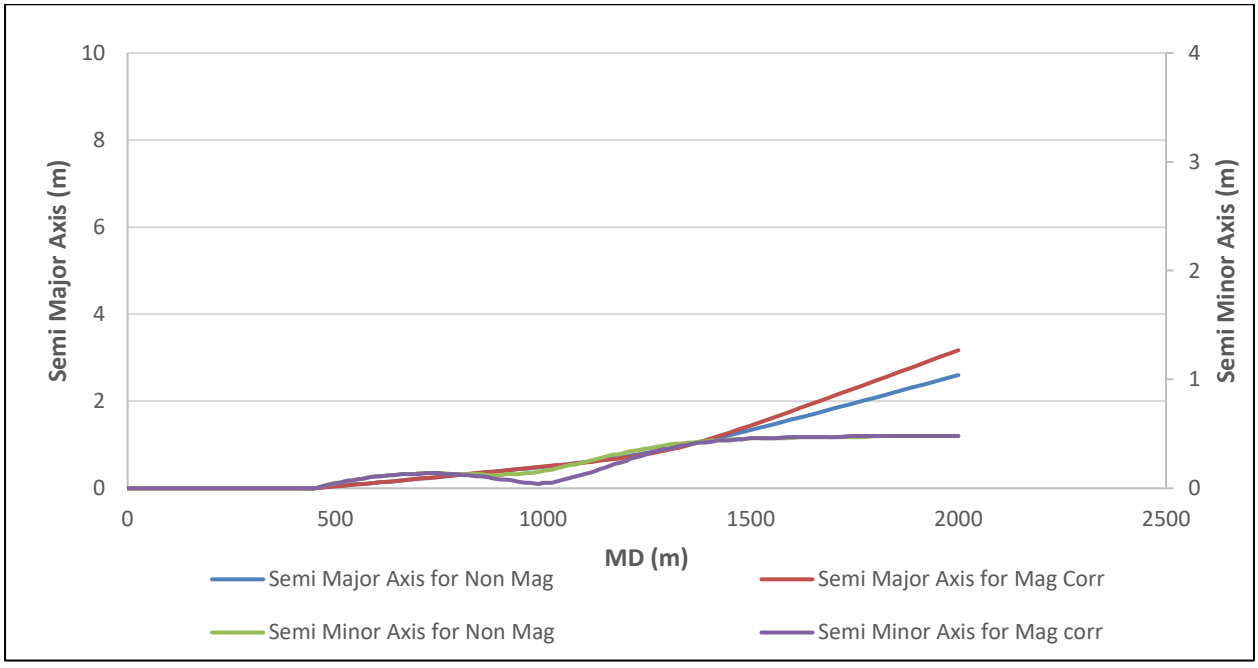

Figure 8.5 – Comparison of Position Uncertainty due to Accelerometer Bias at Azimuth = 45°

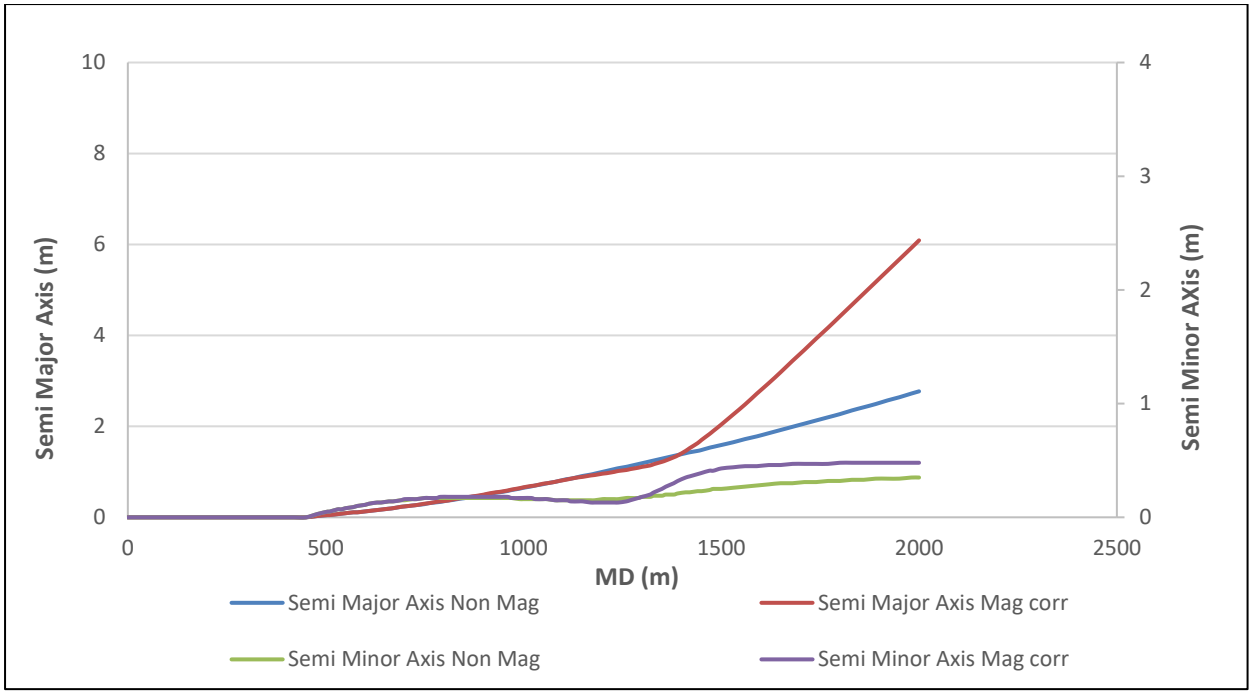

Figure 8.6 – Comparison of Position Uncertainty due to Accelerometer Bias at Azimuth = 75°

8.2 Accelerometer Scale

8.2.1 Effect on Azimuth Uncertainty

Figures 8.7-8.9 present a comparison between azimuth uncertainties calculated using Non-mag and Mag-corr error models. In the North-South well, the deviation is observed above 30° inclination. The azimuth uncertainties from the Mag-corr error model increase above this inclination while those due to Non-mag are negligible. The azimuth uncertainties in the North-East well are slightly different almost throughout the well, with Mag-corr predicting greater azimuth error compared to Non-mag error model. Similarly, azimuth uncertainties are also different in the East-West well and the greatest deviation is observed while approaching the horizontal section. Therefore, AMIL correction clearly effects azimuth errors in all three subject wells but the greatest difference between the azimuth uncertainties predicted through the two models is in the East-West well.

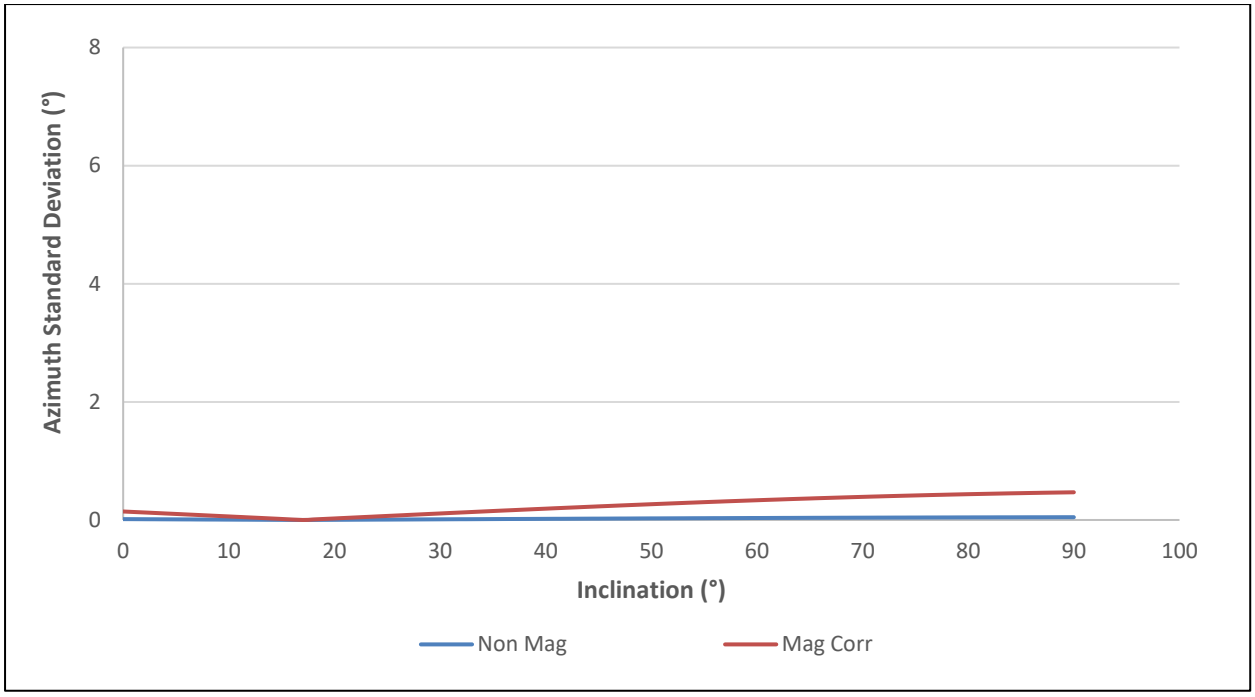

Figure 8.7 – Comparison of Azimuth Uncertainties due to Accelerometer Scale at Azimuth = 0°

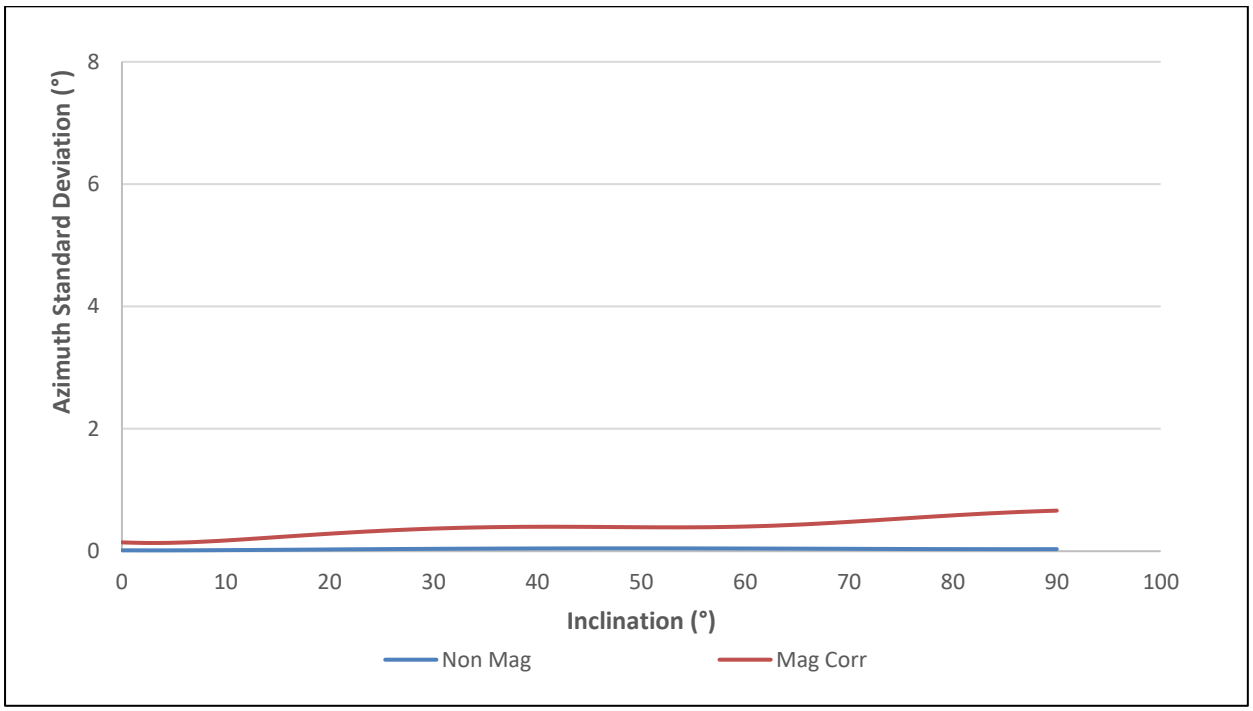

Figure 8.8 – Comparison of Azimuth Uncertainties due to Accelerometer Scale at Azimuth = 45°

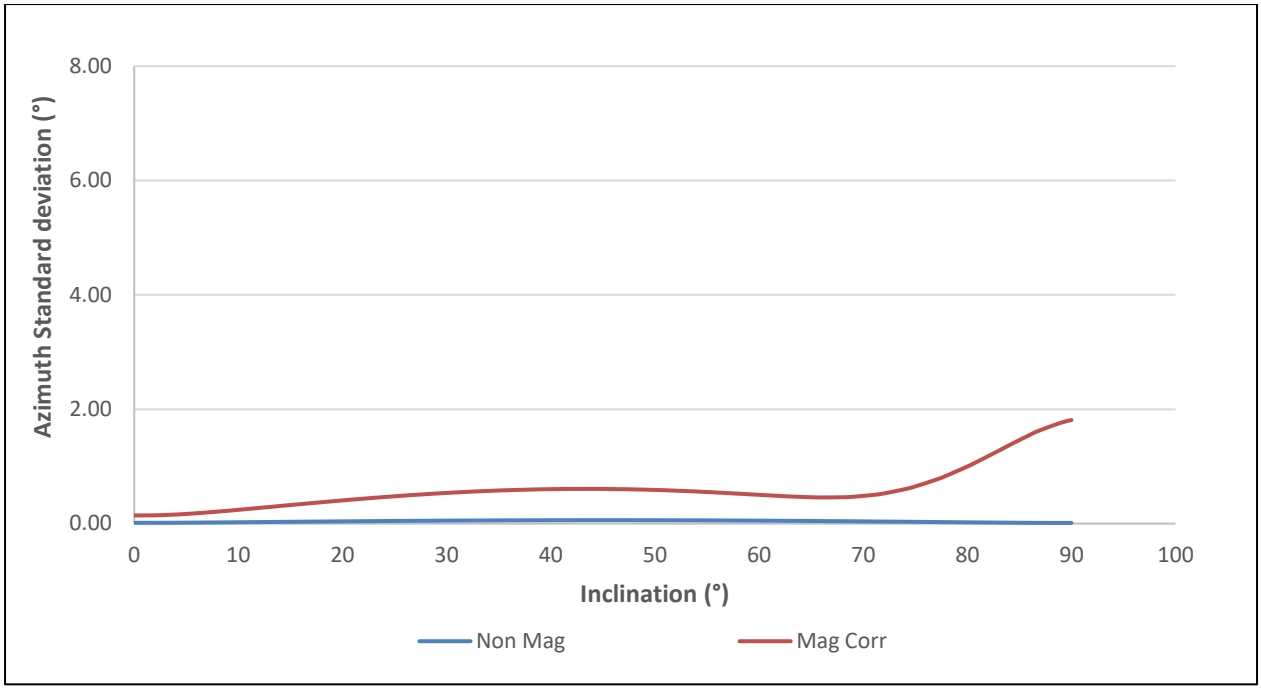

Figure 8.9 – Comparison of Azimuth Uncertainties due to Accelerometer Scale at Azimuth = 75°

8.2.2 Effect on Position Uncertainty

The position uncertainty calculated from the Non-mag and Mag-corr error models is the same in the North-South well since no difference in either the lengths of semi major or minor axis have been observed. In the North-East well, the difference in the lengths of semi major axis though small but exists only in the horizontal section of the well. When moving to the East-West well this difference between the two cases further increases but again only in the horizontal section. Therefore, the position uncertainties predicted using the two error models is different only in the horizontal sections of North-East and East-West wells.

The analysis shows that although azimuth uncertainties calculated from the two error models are different in the buildup and horizontal section of the North-South well but the position uncertainties are still alike. Contrary to this, in the North-East and East-West wells, both azimuth and position uncertainties are different from the two models for each hole section.

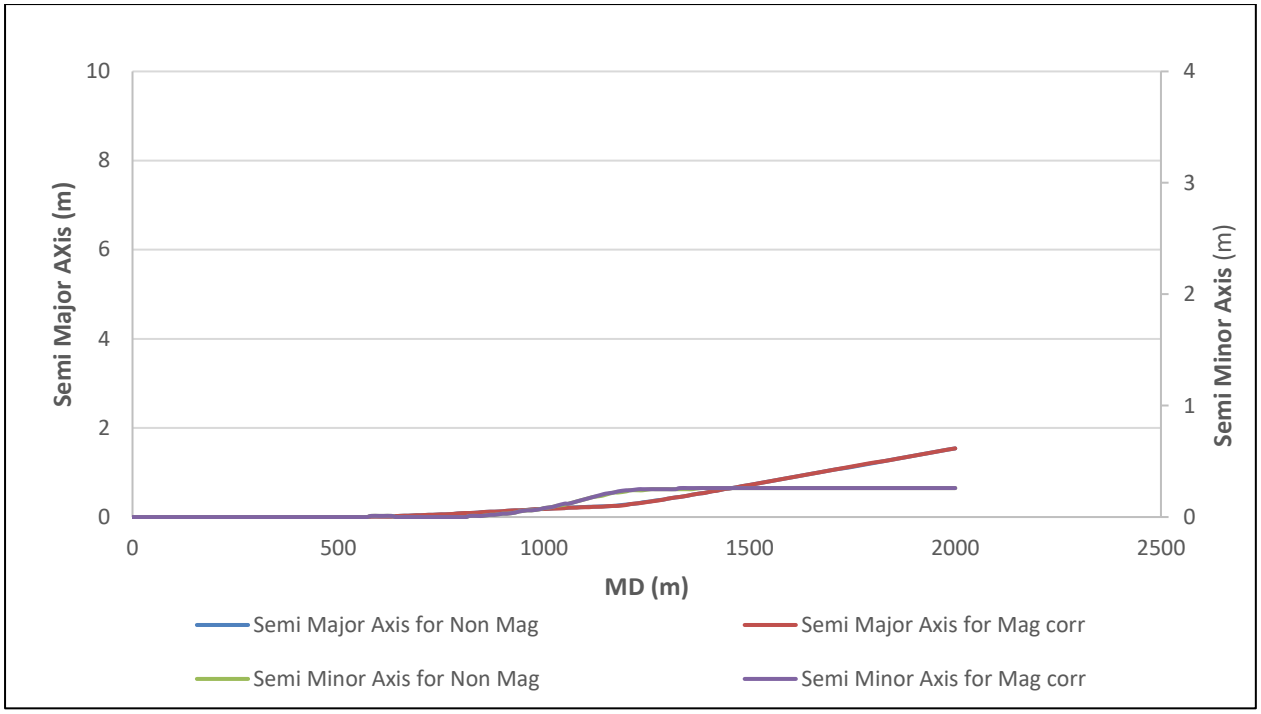

Figure 8.10 – Comparison of Position Uncertainty due to Accelerometer Scale at Azimuth =0°

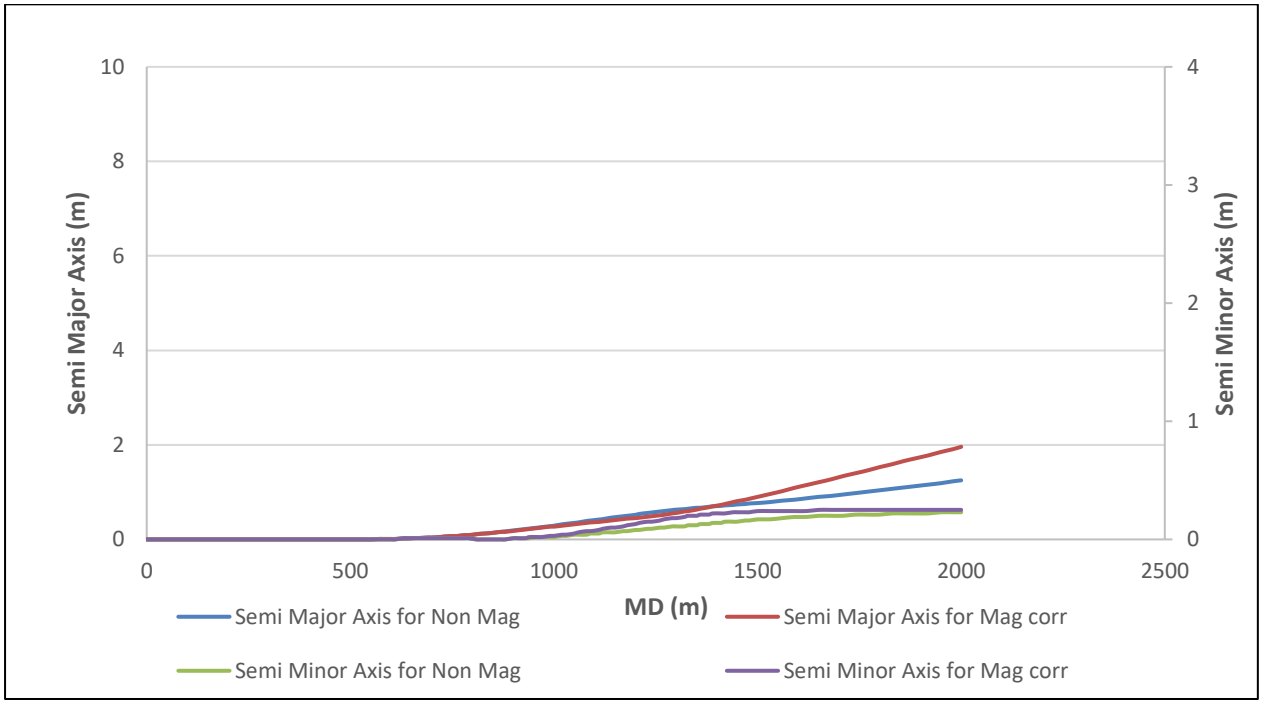

Figure 8.11 – Comparison of Position Uncertainty due to Accelerometer Scale at Azimuth = 45°

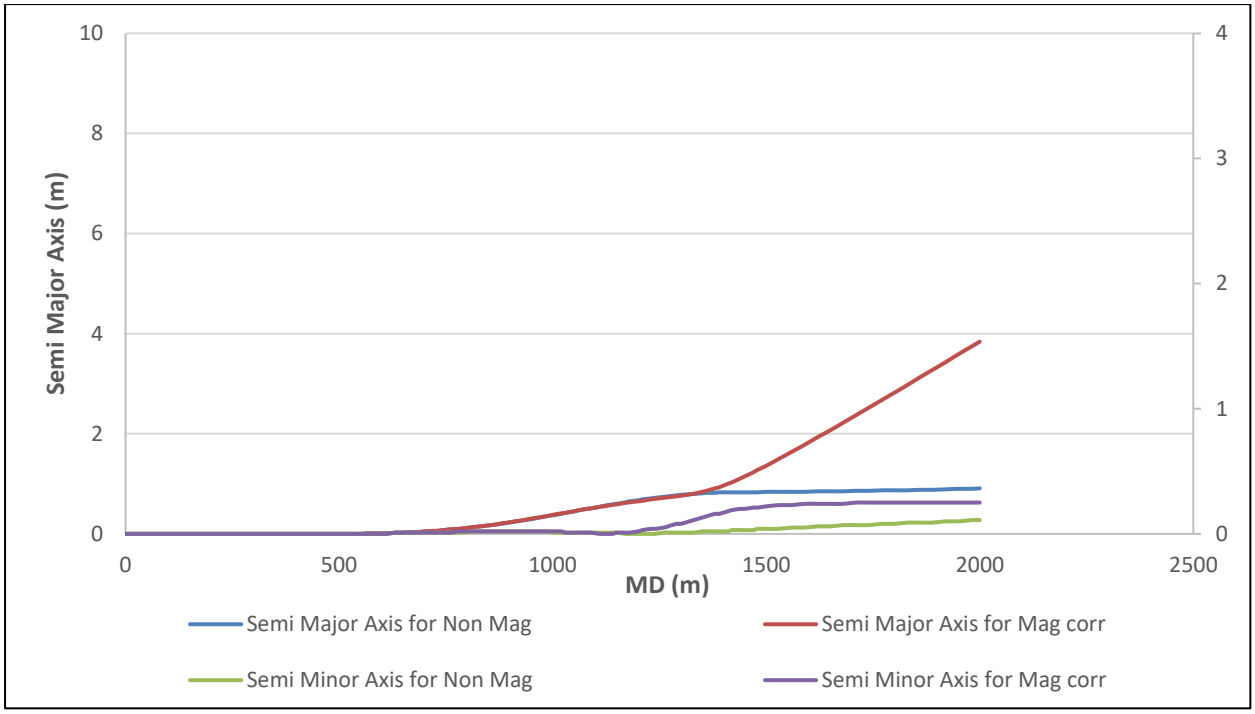

Figure 8.12 – Comparison of Position Uncertainty due to Accelerometer Scale at Azimuth = 75°

8.3 Magnetometer Cross-Axial Bias

8.3.1 Effect on Azimuth Uncertainty

Figures 8.13-8.15 represent a comparison of azimuth uncertainties predicted by Non-mag and Mag-corr error models for magnetometer cross-axial bias. In the North-South well, a constant separation exists throughout the well between the azimuth uncertainties calculated with the Non-mag and Mag-corr error models. For the North-East well, the difference between the two is initiated above 30° inclination and is maximum in the horizontal section. Above this inclination, the azimuth error in the Mag-corr error model remains constant while that in the Non-mag drops. Similar to the North-East well, the split between azimuth uncertainties in the East-West well also begins above 30° inclination and is maximum in the horizontal section.

Therefore, the azimuth uncertainties calculated from the two error models are different in each well especially in the buildup and horizontal sections. The difference is observed to be highest in the horizontal section of East-West well.

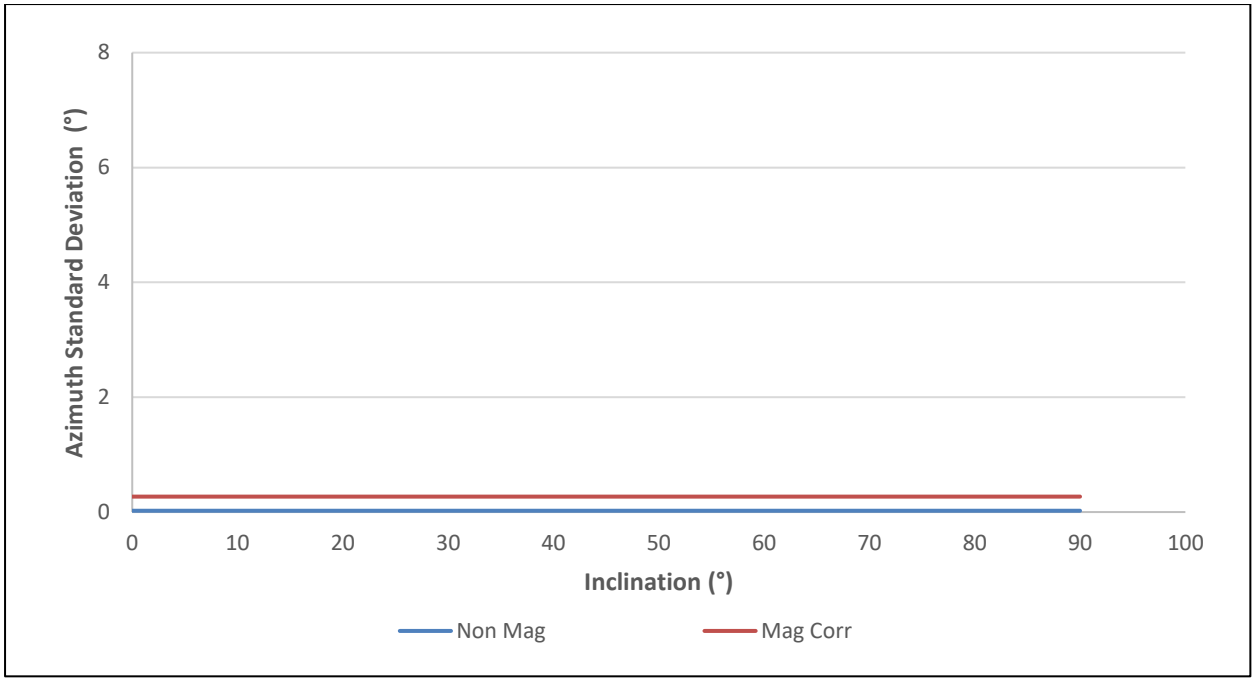

Figure 8.13 – Comparison of Azimuth Uncertainties due to Magnetometer Cross-Axial Bias at Azimuth = 0°

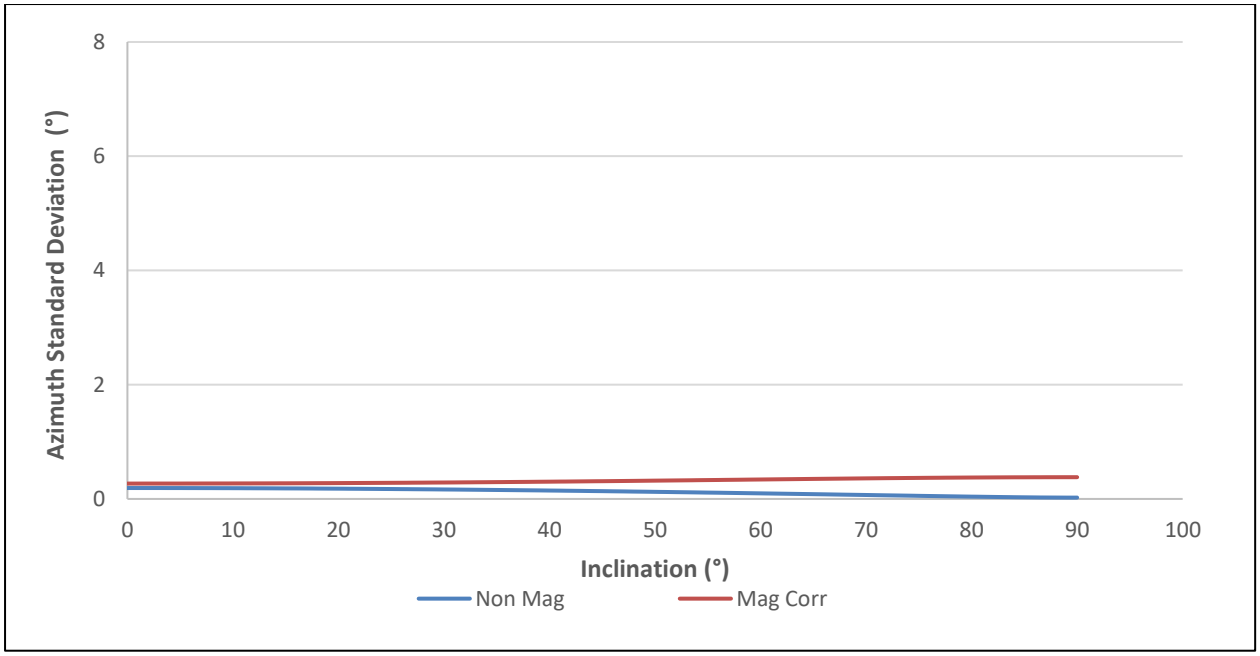

Figure 8.14 – Comparison of Azimuth Uncertainties due to Magnetometer Cross-Axial Bias at Azimuth = 45°

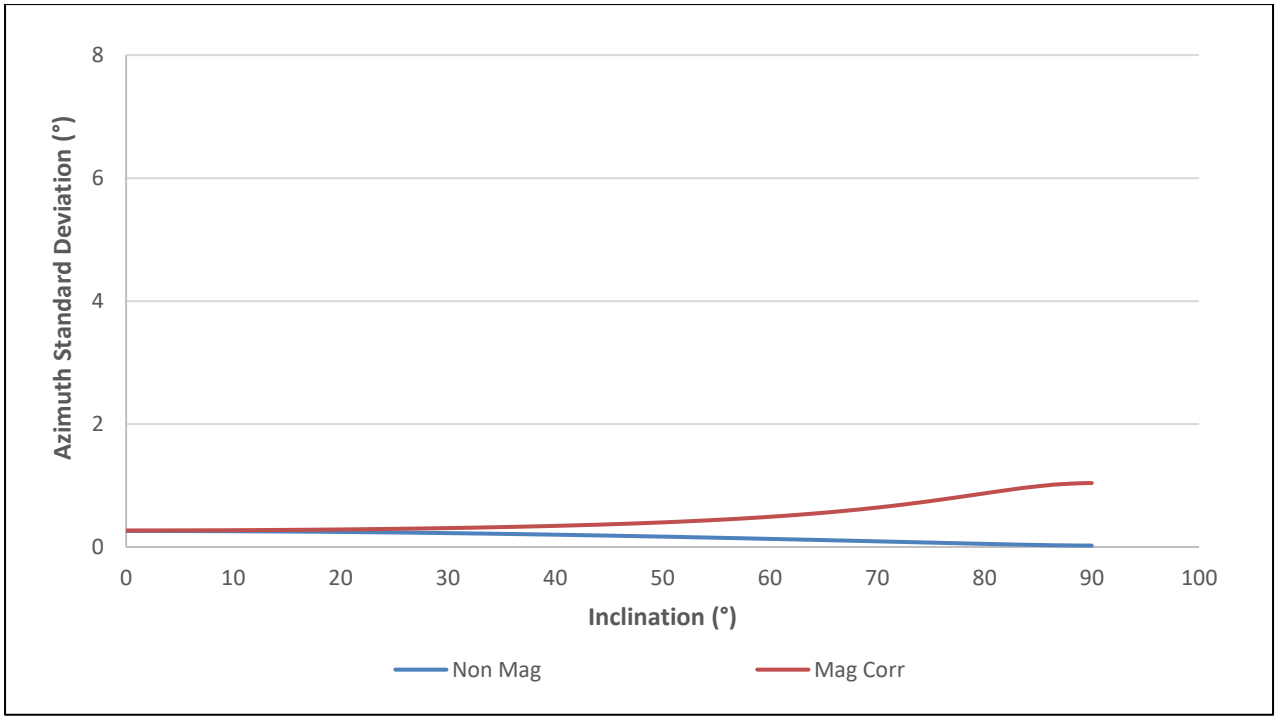

Figure 8.15 – Comparison of Azimuth Uncertainties due to Magnetometer Cross-Axial Bias at Azimuth = 75°

8.3.2 Effect on Position Uncertainty

AMIL correction has no influence on position uncertainty estimates in the entire North-South well. For the North-East and East-West wells however, it has a quite similar trend. At shallow depths, the position uncertainty predicted by both Non-mag and Mag-corr error models is same, but at higher depths primarily while approaching the horizontal section the difference between the two is quite clear. The Mag-corr error model in both wells predicts position uncertainty greater than in Non-mag error model. However, the relative difference between the two is greater in the East-West well compared to North-East well.

Difference in azimuth and position uncertainties are again not in agreement in the North-South well. Despite of different azimuth errors calculated in the two models, the position uncertainties are still the same. But the difference is notable in both azimuth and position errors for the North-East and East-West wells at corresponding depths.

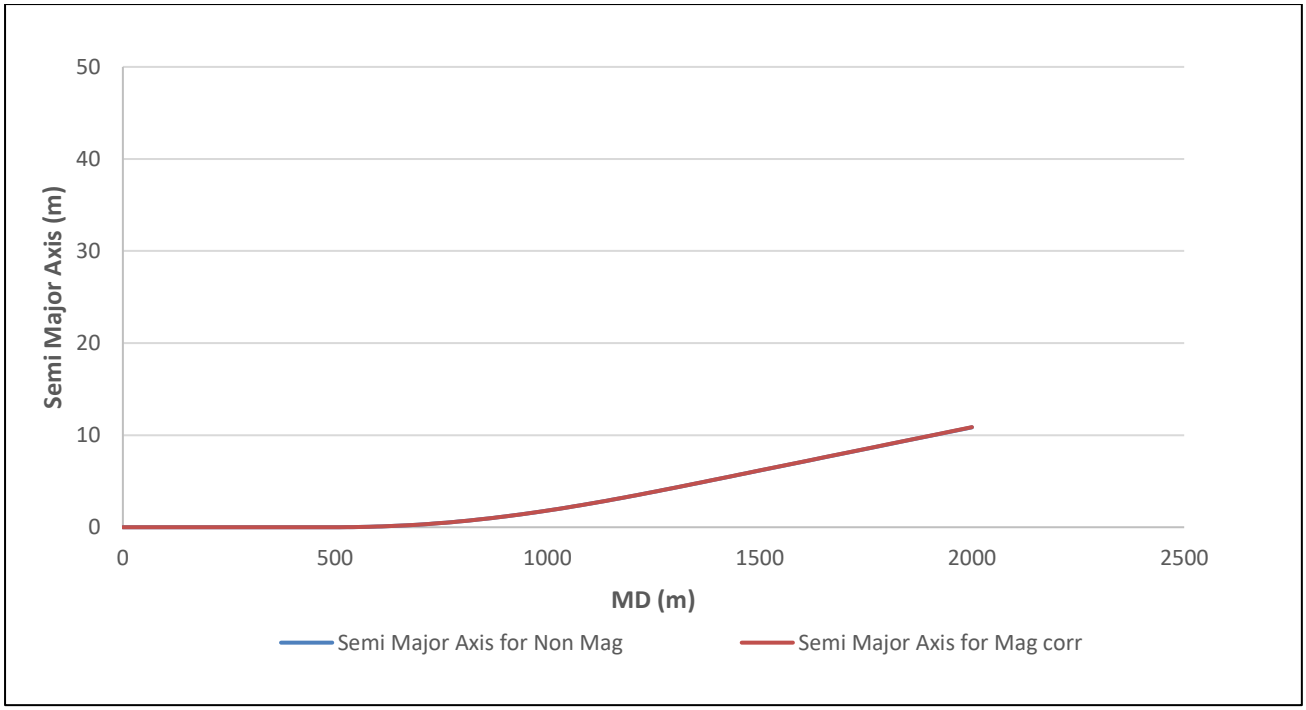

Figure 8.16 – Comparison of Position Uncertainty due to Magnetometer Cross-Axial Bias at Azimuth = 0°

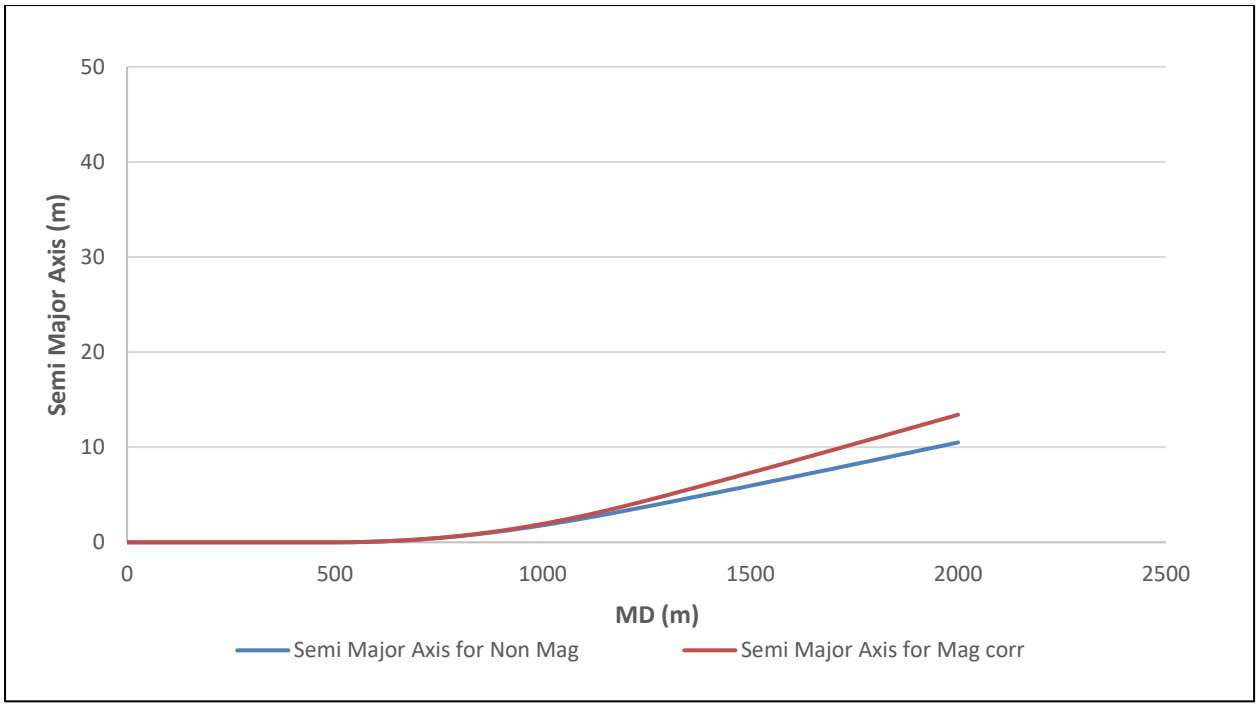

Figure 8.17 – Comparison of Position Uncertainty due to Magnetometer Cross-Axial Bias at Azimuth = 45°

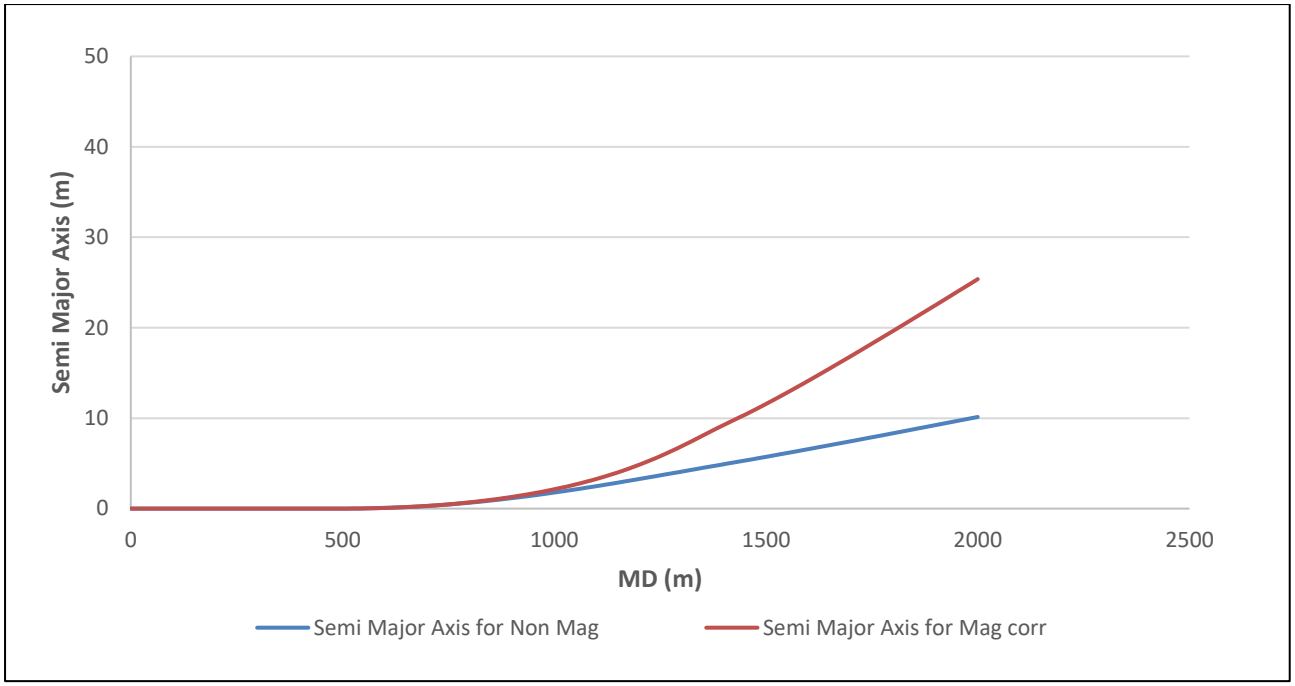

Figure 8.18 – Comparison of Position Uncertainty due to Magnetometer Cross-Axial Bias at Azimuth = 75°

8.4 Magnetometer Scale

8.4.1 Effect on Azimuth Uncertainty

The azimuth uncertainties predicted by the Non-mag and Mag-corr error models due to magnetometer scale are analyzed in this section. From figures 8.19 & 8.20, the azimuth uncertainties are identical throughout the North-South and North-East wells. Only some deviation close to and in the horizontal section of East-West well is noted.

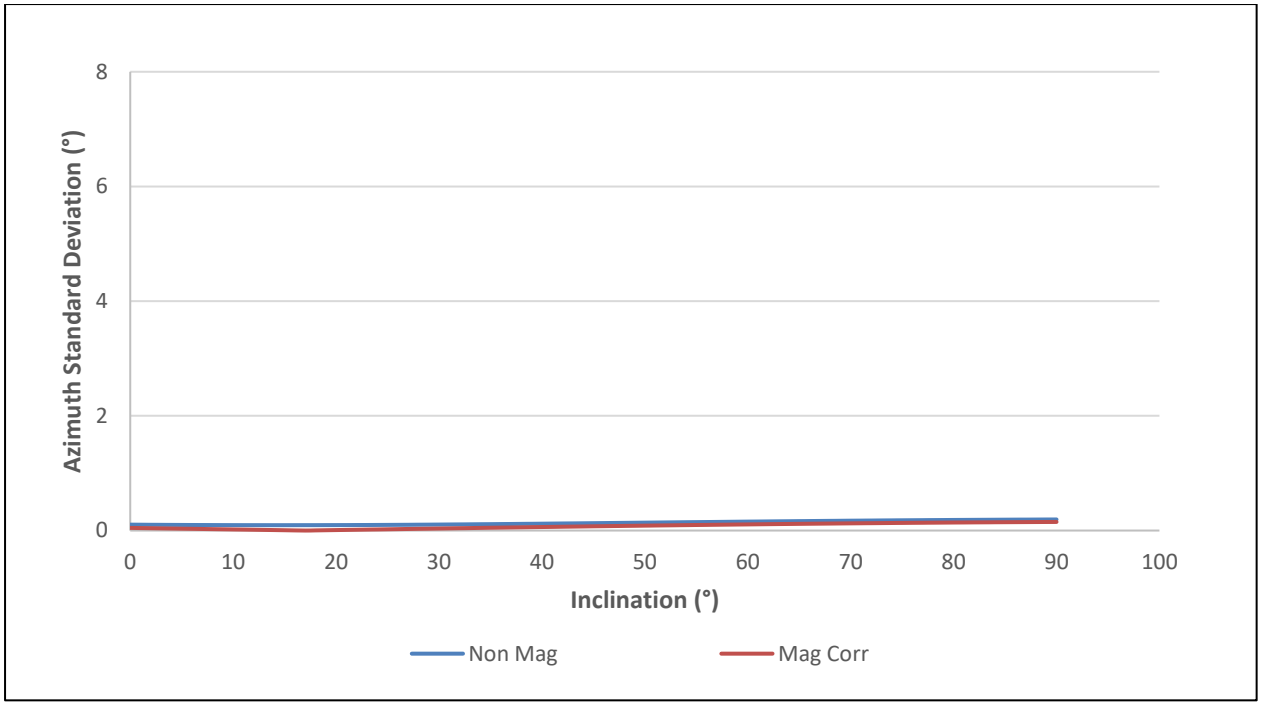

Figure 8.19 – Comparison of Azimuth Uncertainties due to Magnetometer Scale at Azimuth = 0°

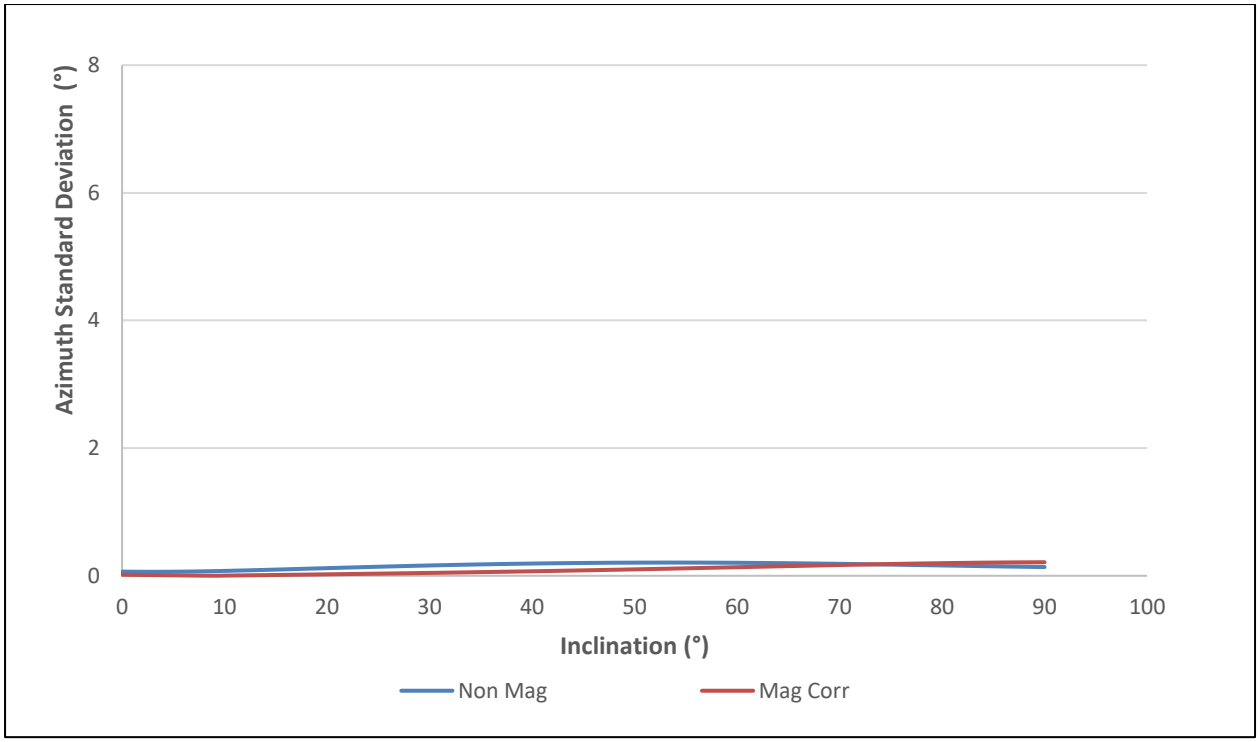

Figure 8.20 Comparison of Azimuth Uncertainties due to Magnetometer Scale at Azimuth = 45°

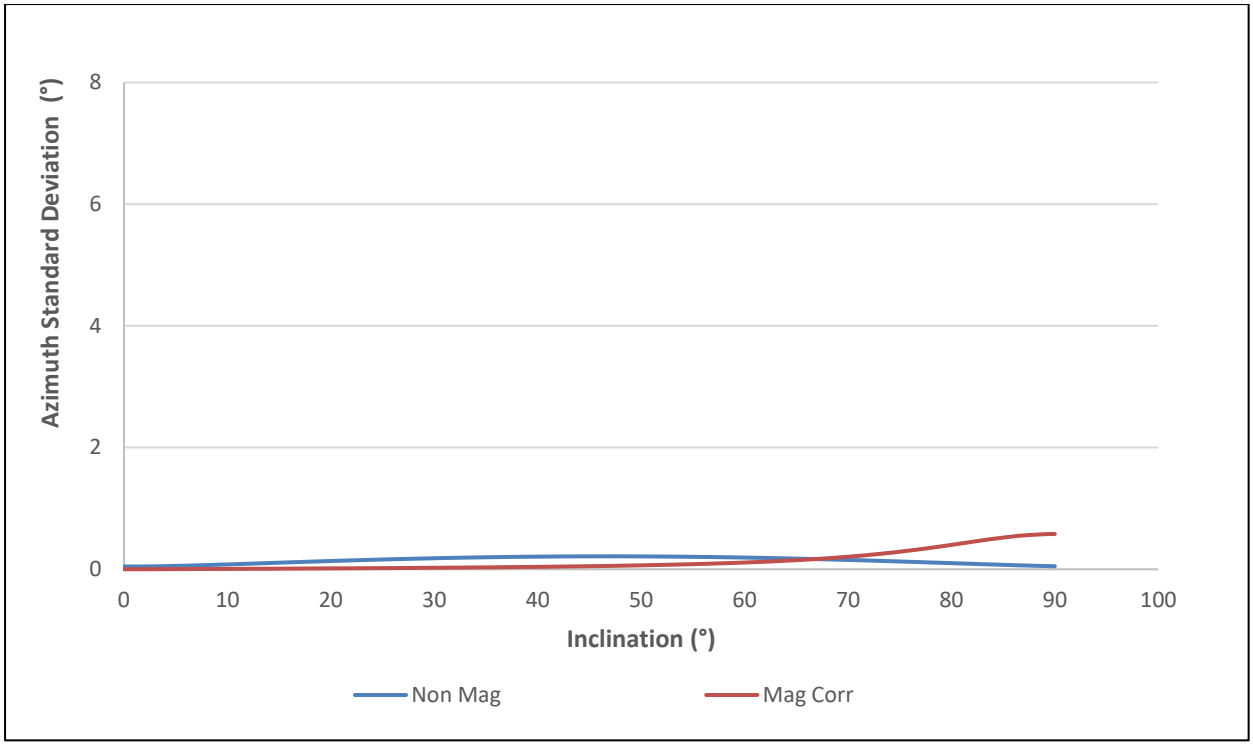

Figure 8.21 Comparison of Azimuth Uncertainties due to Magnetometer Scale at Azimuth = 75°

8.4.2 Effect on Position Uncertainty

The position uncertainty predicted from the two error models is the same for the entire North-South well. At shallow depths of North-East and East-West well the position uncertainty predicted from the two error models is almost the same but slightly different in the horizontal section of North-East well and the difference further increases in the horizontal section of East-West well.

From the analysis above, neither any difference in azimuth or position errors is observed in the North-South well. But for the North-East well, despite of having negligible difference in azimuth errors in the horizontal section, the position uncertainty predicted from the two models is still slightly different. In the East-West well however, both azimuth and position errors are clearly different in the horizontal section.

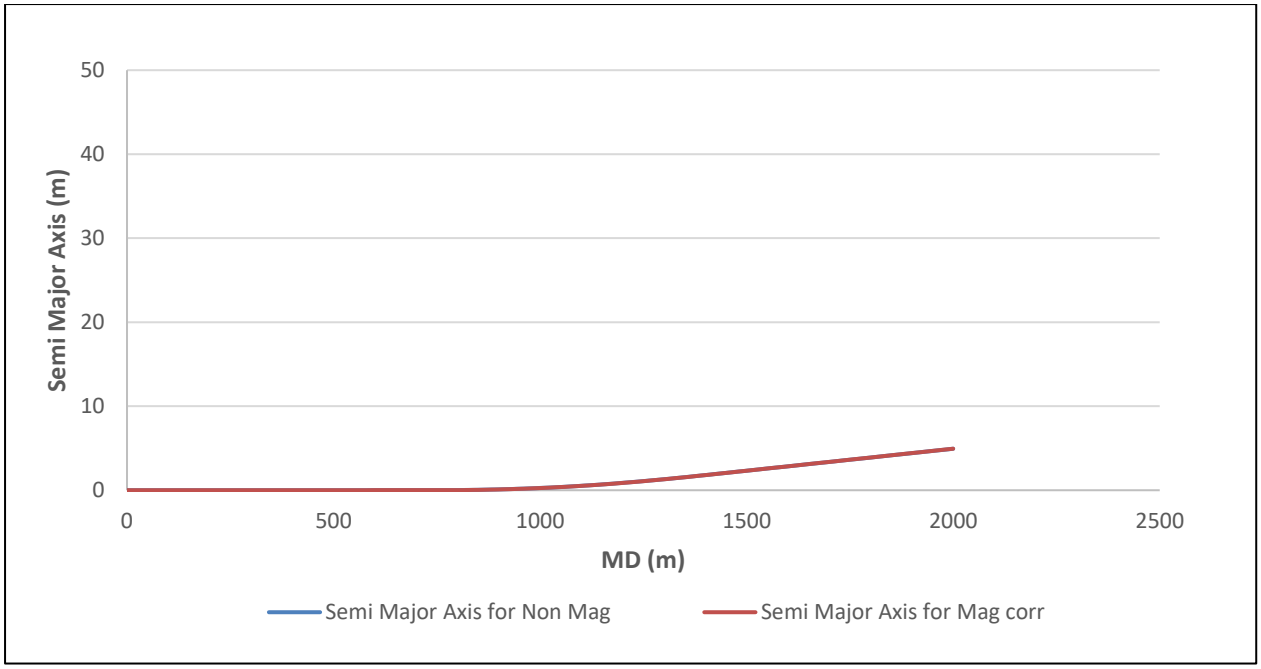

Figure 8.22 – Comparison of Position Uncertainty due to Magnetometer Scale at Azimuth = 0°

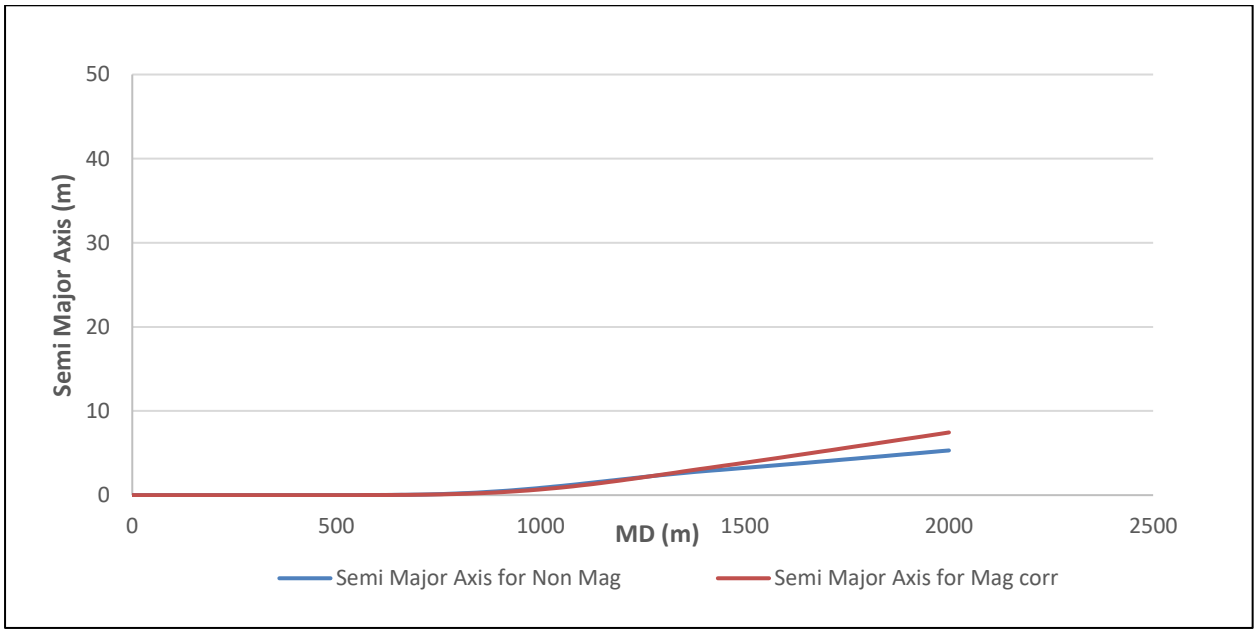

Figure 8.23 – Comparison of Position Uncertainty due to Magnetometer Scale at Azimuth = 45°

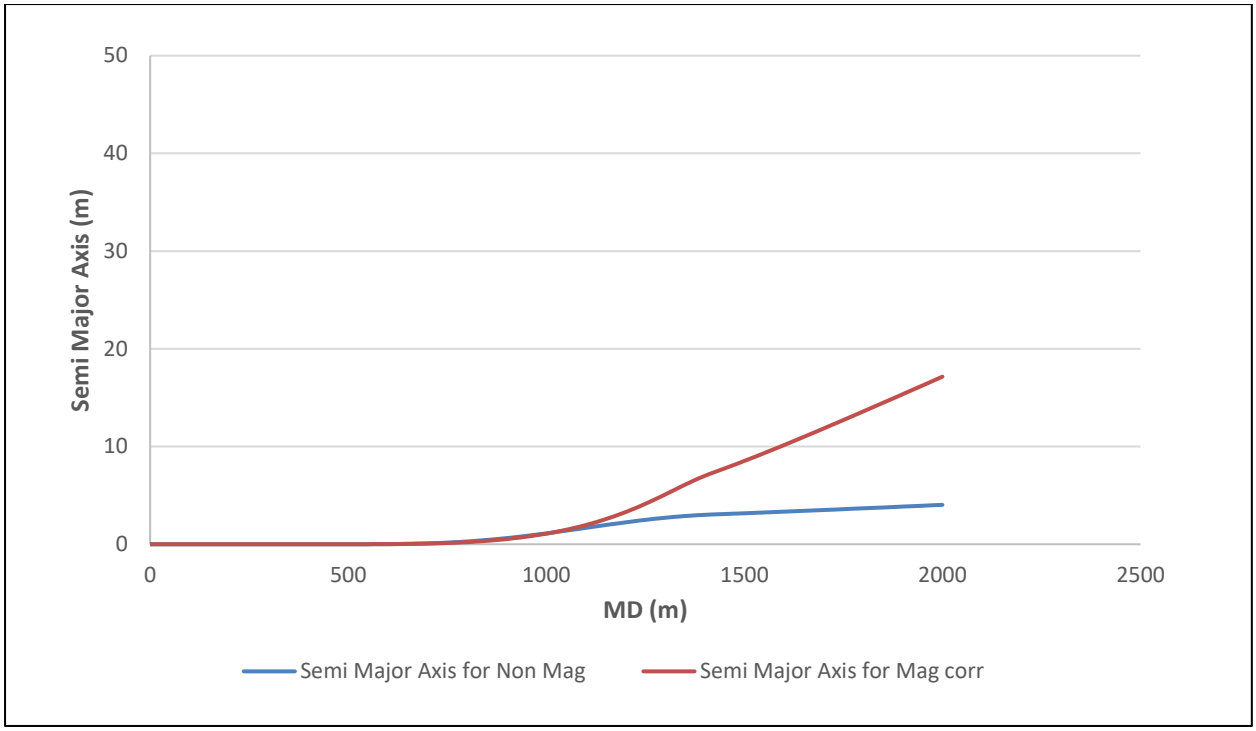

Figure 8.24 – Comparison of Position Uncertainty due to Magnetometer Scale at Azimuth = 75°

8.5 Total Error Sources

8.5.1 Effect on Azimuth Uncertainty

This section will present a comparison between total azimuth uncertainties resulting from all error sources in the Non-mag and Mag-corr error model. In the North-South well, total azimuth uncertainties are same in the vertical and near vertical section and slightly different in the buildup and horizontal sections. In the North-East well a very small difference is observed in some part of buildup section while in the East-West well, the total azimuth errors are slightly different in a part of buildup section and significantly different in the horizontal section. In fact among all different sections of the three wells, the greatest difference between the azimuth uncertainties is in the East-West well's horizontal section.

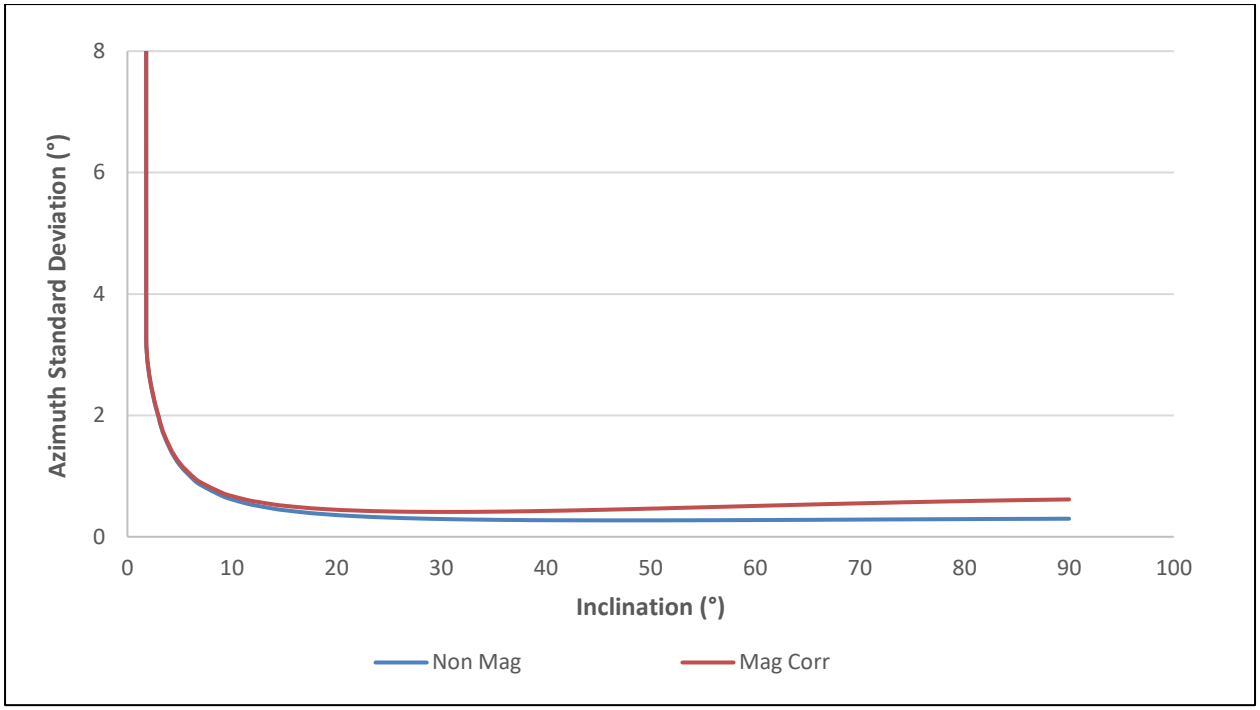

Figure 8.25 – Comparison of Total Azimuth Uncertainties at Azimuth = 0°

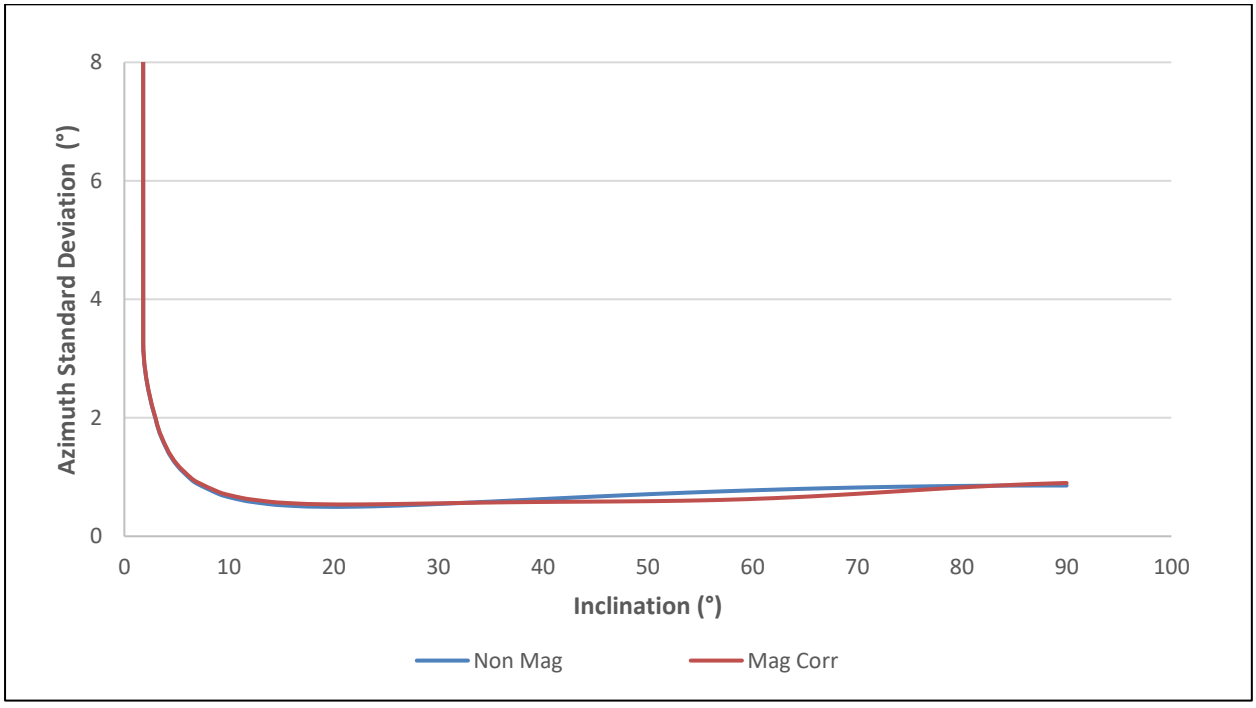

Figure 8.26 – Comparison ofTotal Azimuth Uncertainties at Azimuth = 45°

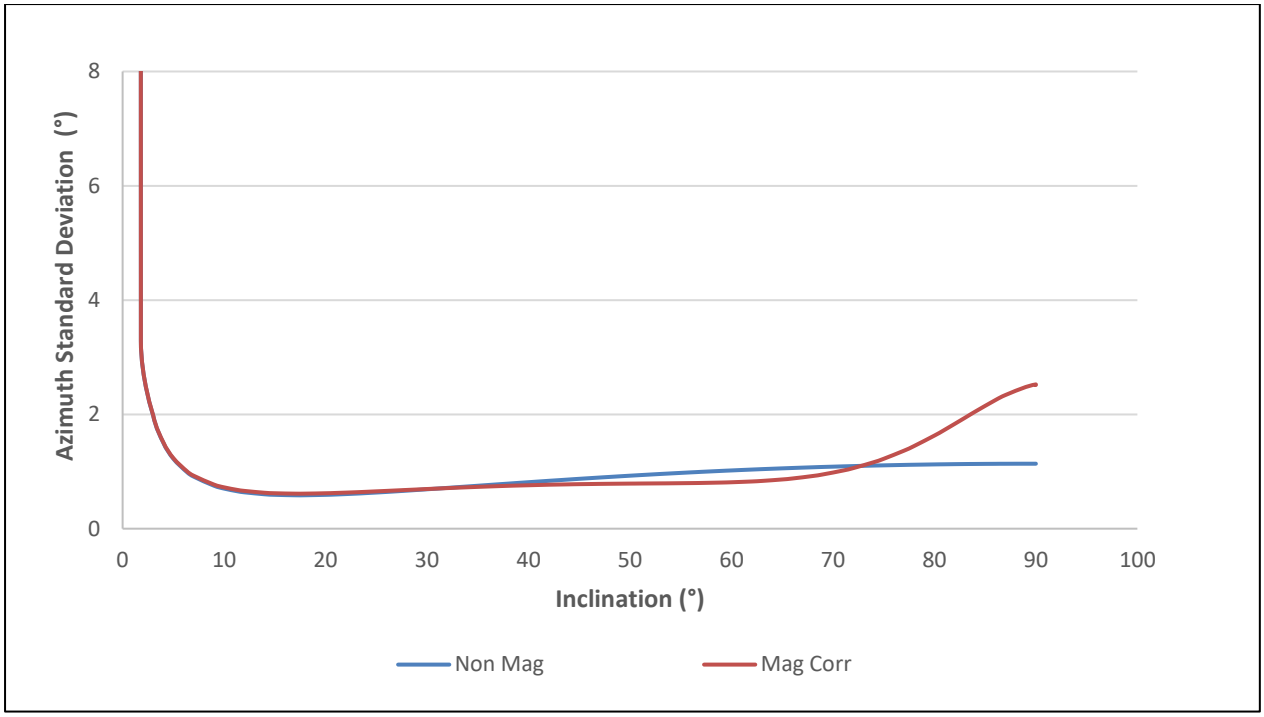

Figure 8.27 – Comparison of Total Azimuth Uncertainties at Azimuth = 75°

8.5.2 Effect on Total Position Uncertainty

The difference in position errors from the two error models is negligible for the entire North-South well and increases only below 1000m MD in the North-East and East-West wells. Below this depth in the North-East well, the difference continuously increases and is maximum in the horizontal section. But in the East-West well, the difference increases between approximately 1000-1500m MD and again slightly decreases while approaching the horizontal section. Therefore, the greatest difference in position errors for this well is most likely in the buildup sections.

Combining the above measurement and position uncertainty results, although azimuth errors are different in the buildup and horizontal sections, but position errors are the same in the North-South well. Similarly, in the North-East well, there is no difference in azimuth errors in the horizontal section, but position errors are different. For the East-West well, when azimuth errors are the same in the buildup section, the position errors have the greatest difference in this section and when azimuth errors are a lot different in the horizontal section, the difference in position errors decreases. Therefore, for almost all wells the effect on azimuth and position errors is different.

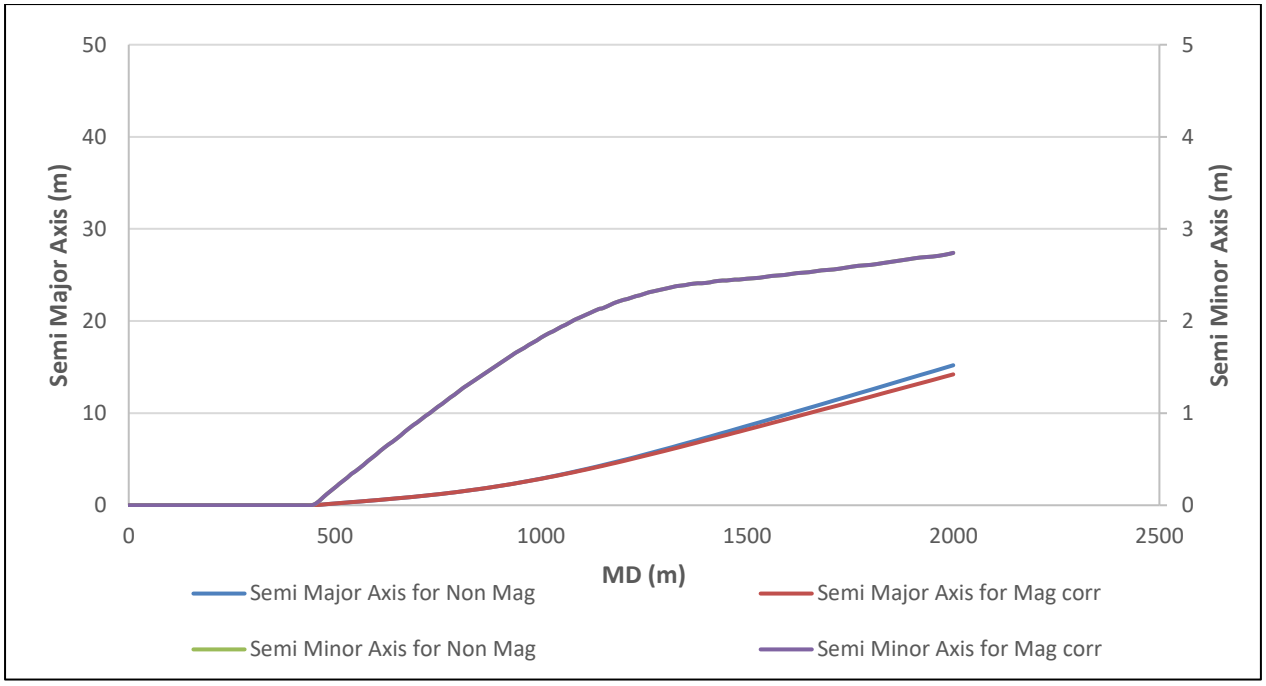

Figure 8.28 – Comparison of Total Position Uncertainties at Azimuth = 0°

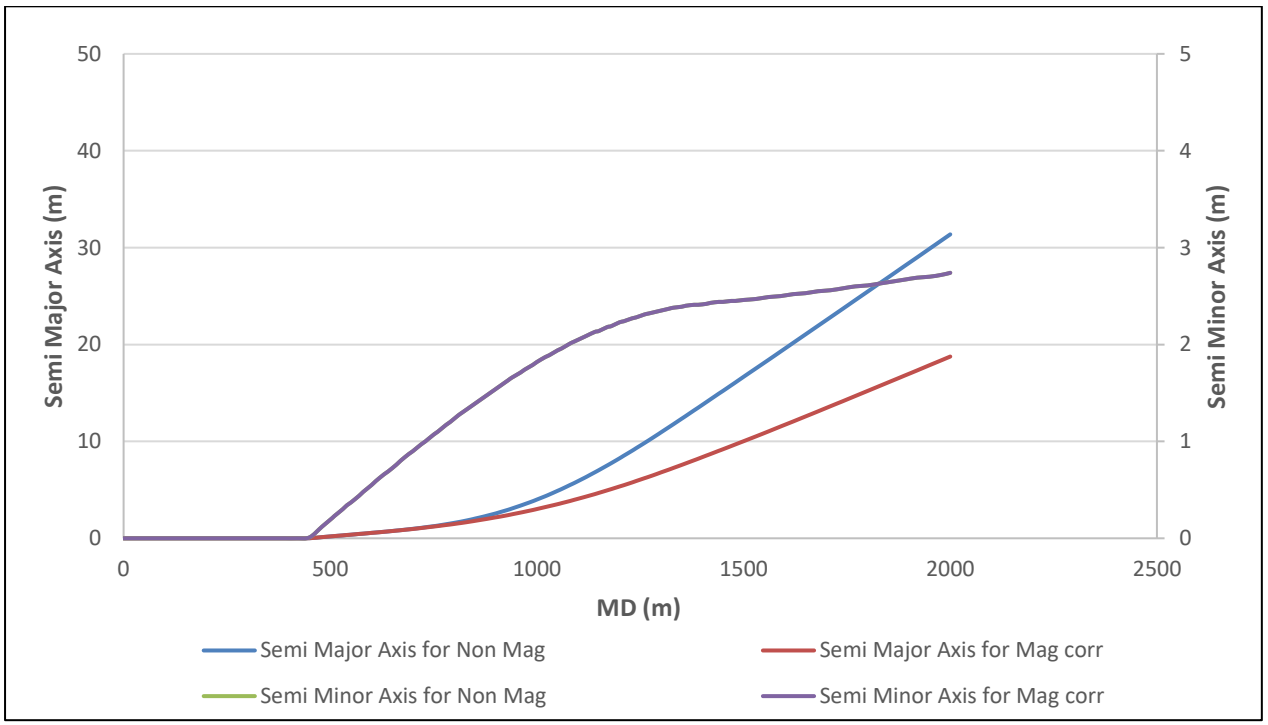

Figure 8.29 – Comparison of Total Position Uncertainties at Azimuth = 45°

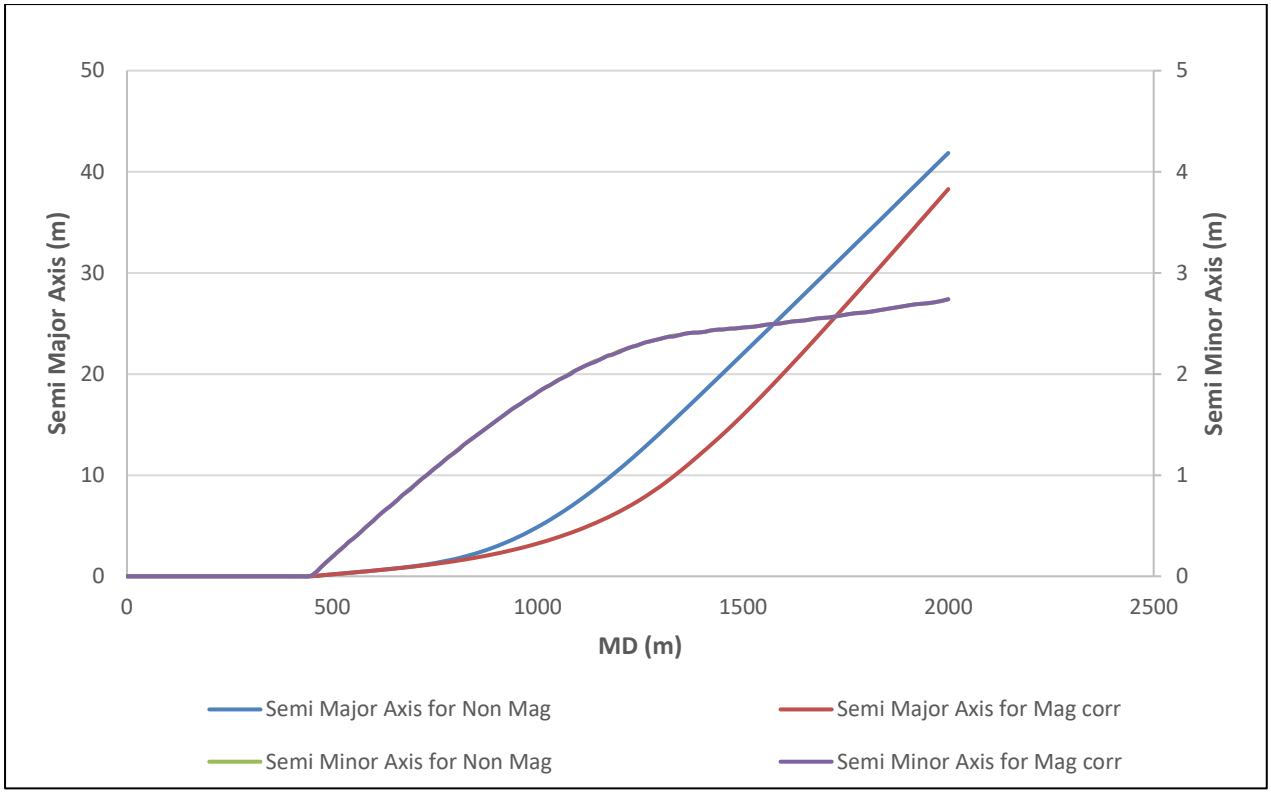

Figure 8.30 Comparison of Total Position Uncertainties at Azimuth = 75°

Chapter 9. Conclusions

- Depth errors, BHA sag and MAL errors are the major sources of TVD uncertainty. MAL and Depth errors are more effective in vertical well while Sag has more influence on TVD in horizontal well.
- Errors in Magnetometer sensors have significantly smaller influence than external errors such as geomagnetic interference, AMIL, MAL etc. Sensor errors generally have the smallest effect on position uncertainties.
- Sensor errors do not have any contribution to the total inclination uncertainties but are a major source of total azimuth uncertainties in the vertical and near vertical hole sections.
- MAL has the greatest contribution to the total inclination and azimuth error budgets in the vertical and near vertical hole sections. It also induces largest TVD errors.
- The effect of global errors on the total measurement or position error budget depends on the behavior of total measurement and position uncertainties along the well. Same is true for errors independent of hole inclination.
- Large measurement or position errors from a specific error source do not necessarily have an equally large impact on total measurement or position error budgets.
- An error source can have a completely different effect on total measurement and position error budgets. An example is a large azimuth error in the vertical well which does not have any influence on position uncertainty for the hole section.
- The effect of an error source might increase along the well in a North/South well and decrease in an East/West well. For example, Magnetometer Cross-Axial Bias.
- The resultant azimuth and position uncertainties from all Mag-corr error terms except that of MDI are highest in horizontal East-West drilling direction.
- Each error source in the Mag-corr error model has an identical effect on total position uncertainty in the North/South and North/East wells. For improved accuracy, it is preferable to stay +/- 45° North/South.
- An error source might be dependent on inclination in one drilling direction while completely independent of inclination in another drilling direction. For example, AMIL.

- Some error sources have identical impact in North/South and East/West directions despite of being a function of direction. For example, MAL.
- Azimuth errors due to accelerometer bias are identical in the Non-mag and Mag-corr error models irrespective of drilling direction.
- Position errors from all different error sources are same in the Mag-corr and Non-mag error models for the North/South well.
- An error source cannot be completely ignored in a specific drilling direction. Either it contributes to the measurement uncertainty or to the position uncertainty.

Chapter 10. Further Work

- Gyroscopic tools are also used by the industry for wellbore surveying. Therefore, a similar analysis can be extended utilizing the error terms from ISCWSA Gyro error model.
- Unwanted magnetic particles in the mud is considered a significant source of distorting wellbore survey data. Specific error terms dealing with this error source need to be formulated in the current MWD error model to determine its impact on measurement and position uncertainty.
- The behavior of error terms can assist during anticollision analysis, relief well drilling and occasions where wellbore positioning is critical. A better understanding of these error sources will help mitigate the problem of WPU for safe drilling operations.
- The effect of individual error terms can also be investigated without combining them together as one error source. This will help screen out the most effective error terms contributing to the total uncertainties.
- There are several error sources which cannot be mathematically modeled. An experience based approach should be devised to handle such error sources so a quantitative effect on WPU is determined.
- Errors such as poor survey management plan, human errors etc cannot be mathematically modeled but are consequential towards WPU. An experience based approach should be devised to quantify the effect of these error sources on WPU.

Bibliography

1. Jamieson, A., *Introduction to Wellbore Positioning*. Vol. V06.02.17. 2012, University of Highlands and Islands (UHI): Research Office of UHI. 197.
2. Gjerde, T., *A heavy tailed statistical model applied in anti-collision calculations for petroleum wells*. 2008, Institutt for matematiske fag.
3. Schlumberger. *Oilfield Glossary*. 2017 [cited 2017 08/05/2017]; Available from: http://www.glossary.oilfield.slb.com/Terms/b/borehole_orientation.aspx.
4. Williamson, H.S., *Accuracy Prediction for Directional MWD*. Society of Petroleum Engineers.
5. Macmillan, S. and S. Grindrod, *Confidence Limits Associated With Values of the Earth's Magnetic Field Used for Directional Drilling.*
6. ADMINISTRATION, N.O.A.A. *The World Magnetic Model*. 2015 [cited 2017 12/05/2017]; Available from: https://www.ngdc.noaa.gov/geomag/WMM/DoDWMM.shtml.
7. Arnaud Chulliat., S.M., Patrick Alken., Ciaran Beggan., Manoj Nair., Brian Hamilton., Adam Woods., Victoria Ridley., Stefan Maus., Alan Thomson, *The US/UK World Magnetic Model for 2015-2020*. National Geophysical Data Center, NOAA.
8. Nyrnes, E., *Error analyses and quality control of wellbore directional surveys*. 2006, NTNU: Norway.
9. Brechan, B., *Drilling Engineering Compendium.* 2015.
10. Sawaryn, S.J. and J.L. Thorogood, *A Compendium of Directional Calculations Based on the Minimum Curvature Method.*
11. Yu, X. and J. Jie, *Relief Well Drilling Technology*. Society of Petroleum Engineers.
12. Wolff, C.J.M. and J.P. de Wardt, *Borehole Position Uncertainty - Analysis of Measuring Methods and Derivation of Systematic Error Model.*
13. Priest, J., T. Quinn, and E. Frost, Jr., *Magnetic Interference Effects on Accelerometer and Magnetometer Data: Detection, Quality Control and Correction*. Society of Petrophysicists and Well-Log Analysts.

14. Torkildsen, T., et al., *Drilling Fluid affects MWD Magnetic Azimuth and Wellbore Position*. Society of Petroleum Engineers.

15. Wilson, H. and A.G. Brooks, *Wellbore Position Errors Caused by Drilling Fluid Contamination*. Society of Petroleum Engineers.

16. Sunny. *Art of Directional Drilling - Magnetic Interference*. 2015; Available from: https://directionaldrillingart.blogspot.com/2015/10/magnetic-interference.html.

17. Endevco, *Practical understanding of key accelerometer specifications*.

18. Ekseth, R., et al., *The reliability problem related to directional survey data*. Society of Petroleum Engineers.

19. SensorWiki.org. *Gyroscope*. [cited 2017 18/05/2017]; Available from: http://sensorwiki.org/doku.php/sensors/gyroscope.

20. Torkildsen, T., et al., *Prediction of Wellbore Position Accuracy When Surveyed With Gyroscopic Tools.*

21. Ekseth, R., et al., *Improving the Quality of Ellipse of Uncertainty Calculations in Gyro Surveys to Reduce the Risk of Hazardous Events like Blow Outs or Missing Potential Production Through Incorrect Well Bore Placement*. Society of Petroleum Engineers.

22. Langaker, I., *Causes for Wellbore Position Uncertainty*, R. Hassan, Editor. 2017.

23. Studer, R.E. and L.P.Y. Macresy, *Improved BHA Sag Correction and Uncertainty Evaluation Brings Value to Wellbore Placement*. Society of Petroleum Engineers.

24. Bang, J., et al., *Targeting Challenges in Northern Areas due to Degradation of Wellbore Positioning Accuracy*. Society of Petroleum Engineers.

Appendix A

This Appendix provides the equations in [6] for calculating Wellbore Position Uncertainty (WPU). The total position covariance is the sum of random, systematic, global and well errors.

Randomly propagating errors are calculated from the following two equations.

$$C_{i,l}^{\ rand} = \sum_{k=1}^{K_l} (e_{i,l,k}).(e_{i,l,k})^T \tag{A.1}$$

$$C_{i,K}^{\ rand} = \sum_{i=1}^{L-1} C_{i,l}^{\ rand} + \sum_{k=1}^{K-1} (e_{i,L,k}).(e_{i,L,k})^T + (\bar{e}_{i,L,K}).(\bar{e}_{i,L,K})^T \tag{A.2}$$

Similarly, systematic errors are calculated in the following way.

$$C_{i,l}^{\ syst} = \left[\sum_{k=1}^{K_l} e_{i,l,k}\right].\left[\sum_{k=1}^{K_l} e_{i,l,k}\right]^T \tag{A.3}$$

$$C_{i,l}^{\ syst} = \sum_{l=1}^{L-1} C_{i,l}^{\ syst} + \left[\sum_{k=1}^{K-1} e_{i,L,k} + \bar{e}_{i,L,K}\right].\left[\sum_{k=1}^{K-1} e_{i,L,k} + \bar{e}_{i,L,K}\right]^T \tag{A.4}$$

The behavior of each of the above error types is systematic between all survey stations in a well. Therefore, the total vector error from the slot to survey station is a sum of these individual errors and can be calculated from the following equation.

$$E_{i,K} = \sum_{l=1}^{L-1}\left[\sum_{k=1}^{K_l} e_{i,l,k}\right] + \sum_{k=1}^{K-1} e_{i,L,k} + \bar{e}_{i,L,K} \tag{A.5}$$

The total uncertainty at the survey station K is calculated as:

$$C_{i,K}^{\ well} = E_{i,K} E^T{}_{i,K} \tag{A.6}$$

Finally, the total position covariance at the survey station K is the sum of all different error sources and is calculated using equation (7).

$$C_K^{svy} = \sum_{i \in R} C_{i,K}^{rand} + \sum_{i \in S} C_{i,K}^{syst} + \sum_{i \in \{W,G\}} C_{i,K}^{well} \quad \text{(A.7)}$$

Where,

C is the Wellbore Position Uncertainty Covariance Matrix

e is 1 s.d vector error at an intermediate survey station

e is 1 s.d vector error at the station of interest

E is the sum of vector errors from slot to the station of interest

Appendix B

$$CV = \begin{bmatrix} a11 & a12 & a13 \\ a21 & a22 & a23 \\ a31 & a32 & a33 \end{bmatrix}$$

Eigen Values

Consider the above CV matrix. An n×n symmetric matrix will have n eigen values as λ_1, λ_2, $\lambda 3 \ldots$ λ_n which are obtained by the following equation.

$$\mathbf{|(CV- \lambda I)|= 0}$$

Determinant of the above equation will yield a polynomial equation, roots of which will give the eigen values. The standard polynomial equation which can be compared to find the roots of the polynomial equation is given below.

$$\mathbf{ax^2 + bx +c}$$

Eigen Vectors

The direction of ellipse of uncertainty is defined by these eigen vectors which can be calculated from the equation given below.

$$\mathbf{(CV- \lambda_i I)\, e_i = 0}$$

The above equation shows that the product of the bracket function with the eigen vector (e_i) will give the eigen vector corresponding to eigen value $\boldsymbol{\lambda_i}$. However, it has been noticed that this does not yield a unique solution unless the following expression presented below is used.

$$\mathbf{e_i\, e_i^T = 1}$$

Appendix C

Survey Data of North/South Well

Survey Station	MD (m)	Inc (°)	Azi (°)	TVD (m)	NS (m)	EW (m)
1	30	0	0	30	0	0
2	60	0	0	60	0	0
3	90	0	0	90	0	0
4	120	0	0	120	0	0
5	150	0	0	150	0	0
6	180	0	0	180	0	0
7	210	0	0	210	0	0
8	240	0	0	240	0	0
9	270	0	0	270	0	0
10	300	0	0	300	0	0
11	330	0	0	330	0	0
12	360	0	0	360	0	0
13	390	0	0	390	0	0
14	420	0	0	420	0	0
15	450	0	0	450	0	0
16	480	0	0	480	0	0
17	505	0	0	505	0	0
18	510	1.8	0	510	0.08	-0.02
19	530	3	0	529.98	0.88	-0.24
20	540	4	0	539.96	1.47	-0.4
21	550	5	0	549.93	2.23	-0.6
22	570	6.33	0	569.83	4.14	-1.11
23	580	7	0	579.77	5.26	-1.41
24	600	9	0	599.57	7.95	-2.13
25	610	10	0	609.43	9.54	-2.56
26	630	11.33	0	629.09	13.12	-3.52

Survey Station	MD (m)	Inc (°)	Azi (°)	TVD (m)	NS (m)	EW (m)
27	640	12	0	638.88	15.07	-4.04
28	660	14	0	658.37	19.42	-5.2
29	670	15	0	668.05	21.84	-5.85
30	690	17	0	687.27	27.16	-7.28
31	700	18	0	696.81	30.07	-8.06
32	720	20	0	715.72	36.36	-9.74
33	730	21	0	725.09	39.74	-10.65
34	750	23	0	743.63	46.97	-12.59
35	760	24	0	752.8	50.83	-13.62
36	780	26	0	770.92	58.99	-15.81
37	790	27	0	779.87	63.3	-16.96
38	810	29	0	797.53	72.37	-19.39
39	820	30	0	806.23	77.13	-20.67
40	840	32	0	823.38	87.07	-23.33
41	850	33	0	831.81	92.26	-24.72
42	870	35	0	848.39	103.07	-27.62
43	880	36	0	856.53	108.68	-29.12
44	900	38	0	872.5	120.3	-32.23
45	910	39	0	880.33	126.31	-33.85
46	930	41	0	895.65	138.73	-37.17
47	940	42	0	903.14	145.13	-38.89
48	960	44	0	917.77	158.31	-42.42
49	970	45	0	924.9	165.08	-44.23
50	990	47	0	938.79	178.97	-47.96
51	1000	48	0	945.55	186.09	-49.86
52	1020	50	0	958.67	200.67	-53.77
53	1030	51	0	965.03	208.13	-55.77
54	1050	53	0	977.34	223.35	-59.85

Survey Station	MD (m)	Inc (°)	Azi (°)	TVD (m)	NS (m)	EW (m)
55	1060	54	0	983.29	231.11	-61.93
56	1080	56	0	994.76	246.94	-66.17
57	1090	57	0	1000.28	254.99	-68.32
58	1110	59	0	1010.88	271.37	-72.71
59	1120	60	0	1015.95	279.7	-74.94
60	1140	62	0	1025.65	296.59	-79.47
61	1150	63	0	1030.26	305.16	-81.77
62	1170	65	0	1039.03	322.52	-86.42
63	1180	66	0	1043.18	331.31	-88.77
64	1200	68	0	1050.99	349.09	-93.54
65	1210	69	0	1054.66	358.08	-95.95
66	1230	71	0	1061.5	376.23	-100.81
67	1240	72	0	1064.67	385.39	-103.27
68	1260	74	0	1070.52	403.87	-108.22
69	1270	75	0	1073.19	413.17	-110.71
70	1290	77	0	1078.03	431.92	-115.73
71	1300	78	0	1080.19	441.35	-118.26
72	1320	80	0	1084.01	460.31	-123.34
73	1330	81	0	1085.66	469.84	-125.89
74	1350	83	0	1088.44	488.97	-131.02
75	1360	84	0	1089.57	498.56	-133.59
76	1380	86	0	1091.32	517.81	-138.75
77	1390	87	0	1091.93	527.45	-141.33
78	1410	89	0	1092.63	546.75	-146.5
79	1420	90	0	1092.71	556.41	-149.09
80	1440	90	0	1092.71	575.73	-154.27
81	1450	90	0	1092.71	585.39	-156.86
82	1470	90	0	1092.71	604.71	-162.03

Survey Station	MD (m)	Inc (°)	Azi (°)	TVD (m)	NS (m)	EW (m)
83	1480	90	0	1092.71	614.37	-164.62
84	1500	90	0	1092.71	633.69	-169.8
85	1530	90	0	1092.71	662.67	-177.56
86	1560	90	0	1092.71	691.64	-185.33
87	1590	90	0	1092.71	720.62	-193.09
88	1620	90	0	1092.71	749.6	-200.85
89	1650	90	0	1092.71	778.58	-208.62
90	1680	90	0	1092.71	807.55	-216.38
91	1710	90	0	1092.71	836.53	-224.15
92	1740	90	0	1092.71	865.51	-231.91
93	1770	90	0	1092.71	894.49	-239.68
94	1800	90	0	1092.71	923.47	-247.44
95	1830	90	0	1092.71	952.44	-255.21
96	1860	90	0	1092.71	981.42	-262.97
97	1890	90	0	1092.71	1010.4	-270.74
98	1920	90	0	1092.71	1039.38	-278.5
99	1950	90	0	1092.71	1068.35	-286.26
100	1980	90	0	1092.71	1097.33	-294.03
101	2000	90	0	1092.71	1116.65	-299.21

Survey Data for North East well

Survey Station	MD (m)	Inc (°)	Azi (°)	TVD (m)	NS (m)	EW (m)
1	30	0	75	30	0	0
2	60	0	75	60	0	0
3	90	0	75	90	0	0
4	120	0	75	120	0	0
5	150	0	75	150	0	0
6	180	0	75	180	0	0

Survey Station	MD (m)	Inc (°)	Azi (°)	TVD (m)	NS (m)	EW (m)
7	210	0	75	210	0	0
8	240	0	75	240	0	0
9	270	0	75	270	0	0
10	300	0	75	300	0	0
11	330	0	75	330	0	0
12	360	0	75	360	0	0
13	390	0	75	390	0	0
14	420	0	75	420	0	0
15	450	0	75	450	0	0
16	480	0	75	480	0	0
17	505	0	75	505	0	0
18	510	1.8	75	510	0.08	-0.02
19	530	3	75	529.98	0.88	-0.24
20	540	4	75	539.96	1.47	-0.4
21	550	5	75	549.93	2.23	-0.6
22	570	6.33	75	569.83	4.14	-1.11
23	580	7	75	579.77	5.26	-1.41
24	600	9	75	599.57	7.95	-2.13
25	610	10	75	609.43	9.54	-2.56
26	630	11.33	75	629.09	13.12	-3.52
27	640	12	75	638.88	15.07	-4.04
28	660	14	75	658.37	19.42	-5.2
29	670	15	75	668.05	21.84	-5.85
30	690	17	75	687.27	27.16	-7.28
31	700	18	75	696.81	30.07	-8.06
32	720	20	75	715.72	36.36	-9.74
33	730	21	75	725.09	39.74	-10.65
34	750	23	75	743.63	46.97	-12.59

Survey Station	MD (m)	Inc (°)	Azi (°)	TVD (m)	NS (m)	EW (m)
35	760	24	75	752.8	50.83	-13.62
36	780	26	75	770.92	58.99	-15.81
37	790	27	75	779.87	63.3	-16.96
38	810	29	75	797.53	72.37	-19.39
39	820	30	75	806.23	77.13	-20.67
40	840	32	75	823.38	87.07	-23.33
41	850	33	75	831.81	92.26	-24.72
42	870	35	75	848.39	103.07	-27.62
43	880	36	75	856.53	108.68	-29.12
44	900	38	75	872.5	120.3	-32.23
45	910	39	75	880.33	126.31	-33.85
46	930	41	75	895.65	138.73	-37.17
47	940	42	75	903.14	145.13	-38.89
48	960	44	75	917.77	158.31	-42.42
49	970	45	75	924.9	165.08	-44.23
50	990	47	75	938.79	178.97	-47.96
51	1000	48	75	945.55	186.09	-49.86
52	1020	50	75	958.67	200.67	-53.77
53	1030	51	75	965.03	208.13	-55.77
54	1050	53	75	977.34	223.35	-59.85
55	1060	54	75	983.29	231.11	-61.93
56	1080	56	75	994.76	246.94	-66.17
57	1090	57	75	1000.28	254.99	-68.32
58	1110	59	75	1010.88	271.37	-72.71
59	1120	60	75	1015.95	279.7	-74.94
60	1140	62	75	1025.65	296.59	-79.47
61	1150	63	75	1030.26	305.16	-81.77
62	1170	65	75	1039.03	322.52	-86.42

Survey Station	MD (m)	Inc (°)	Azi (°)	TVD (m)	NS (m)	EW (m)
63	1180	66	75	1043.18	331.31	-88.77
64	1200	68	75	1050.99	349.09	-93.54
65	1210	69	75	1054.66	358.08	-95.95
66	1230	71	75	1061.5	376.23	-100.81
67	1240	72	75	1064.67	385.39	-103.27
68	1260	74	75	1070.52	403.87	-108.22
69	1270	75	75	1073.19	413.17	-110.71
70	1290	77	75	1078.03	431.92	-115.73
71	1300	78	75	1080.19	441.35	-118.26
72	1320	80	75	1084.01	460.31	-123.34
73	1330	81	75	1085.66	469.84	-125.89
74	1350	83	75	1088.44	488.97	-131.02
75	1360	84	75	1089.57	498.56	-133.59
76	1380	86	75	1091.32	517.81	-138.75
77	1390	87	75	1091.93	527.45	-141.33
78	1410	89	75	1092.63	546.75	-146.5
79	1420	90	75	1092.71	556.41	-149.09
80	1440	90	75	1092.71	575.73	-154.27
81	1450	90	75	1092.71	585.39	-156.86
82	1470	90	75	1092.71	604.71	-162.03
83	1480	90	75	1092.71	614.37	-164.62
84	1500	90	75	1092.71	633.69	-169.8
85	1530	90	75	1092.71	662.67	-177.56
86	1560	90	75	1092.71	691.64	-185.33
87	1590	90	75	1092.71	720.62	-193.09
88	1620	90	75	1092.71	749.6	-200.85
89	1650	90	75	1092.71	778.58	-208.62
90	1680	90	75	1092.71	807.55	-216.38

Survey Station	MD (m)	Inc (°)	Azi (°)	TVD (m)	NS (m)	EW (m)
91	1710	90	75	1092.71	836.53	-224.15
92	1740	90	75	1092.71	865.51	-231.91
93	1770	90	75	1092.71	894.49	-239.68
94	1800	90	75	1092.71	923.47	-247.44
95	1830	90	75	1092.71	952.44	-255.21
96	1860	90	75	1092.71	981.42	-262.97
97	1890	90	75	1092.71	1010.4	-270.74
98	1920	90	75	1092.71	1039.38	-278.5
99	1950	90	75	1092.71	1068.35	-286.26
100	1980	90	75	1092.71	1097.33	-294.03
101	2000	90	75	1092.71	1116.65	-299.21

Survey Data for East West well

Survey Station	MD (m)	Inc (°)	Azi (°)	TVD (m)	NS (m)	EW (m)
1	30	0	45	30	0	0
2	60	0	45	60	0	0
3	90	0	45	90	0	0
4	120	0	45	120	0	0
5	150	0	45	150	0	0
6	180	0	45	180	0	0
7	210	0	45	210	0	0
8	240	0	45	240	0	0
9	270	0	45	270	0	0
10	300	0	45	300	0	0
11	330	0	45	330	0	0
12	360	0	45	360	0	0
13	390	0	45	390	0	0

Survey Station	MD (m)	Inc (°)	Azi (°)	TVD (m)	NS (m)	EW (m)
14	420	0	45	420	0	0
15	450	0	45	450	0	0
16	480	0	45	480	0	0
17	505	0	45	505	0	0
18	510	1.8	45	510	0.04	0
19	530	3	45	530	0.39	0
20	540	4	45	540	0.57	0
21	550	5	45	549.99	0.74	0
22	570	6.33	45	569.99	1.09	0
23	580	7	45	579.99	1.27	0
24	600	9	45	599.99	1.61	0
25	610	10	45	609.98	1.79	0
26	630	11.33	45	629.98	2.14	0
27	640	12	45	639.98	2.31	0
28	660	14	45	659.98	2.66	0
29	670	15	45	669.98	2.84	0
30	690	17	45	689.97	3.19	0
31	700	18	45	699.97	3.36	0
32	720	20	45	719.97	3.71	0
33	730	21	45	729.97	3.88	0
34	750	23	45	749.96	4.23	0
35	760	24	45	759.96	4.41	0
36	780	26	45	779.96	4.76	0
37	790	27	45	789.96	4.93	0
38	810	29	45	809.95	5.28	0
39	820	30	45	819.95	5.45	0
40	840	32	45	839.95	5.8	0

Survey Station	MD (m)	Inc (°)	Azi (°)	TVD (m)	NS (m)	EW (m)
41	850	33	45	849.95	5.98	0
42	870	35	45	869.94	6.33	0
43	880	36	45	879.94	6.5	0
44	900	38	45	899.94	6.85	0
45	910	39	45	909.94	7.02	0
46	930	41	45	929.94	7.37	0
47	940	42	45	939.93	7.55	0
48	960	44	45	959.93	7.9	0
49	970	45	45	969.93	8.07	0
50	990	47	45	989.93	8.42	0
51	1000	48	45	999.93	8.6	0
52	1020	50	45	1019.92	8.94	0
53	1030	51	45	1029.92	9.12	0
54	1050	53	45	1049.92	9.47	0
55	1060	54	45	1059.92	9.64	0
56	1080	56	45	1079.91	9.99	0
57	1090	57	45	1089.91	10.17	0
58	1110	59	45	1109.91	10.52	0
59	1120	60	45	1119.91	10.69	0
60	1140	62	45	1139.9	11.04	0
61	1150	63	45	1149.9	11.21	0
62	1170	65	45	1169.9	11.56	0
63	1180	66	45	1179.9	11.74	0
64	1200	68	45	1199.89	12.09	0
65	1210	69	45	1209.89	12.26	0
66	1230	71	45	1229.89	12.61	0
67	1240	72	45	1239.89	12.78	0

Survey Station	MD (m)	Inc (°)	Azi (°)	TVD (m)	NS (m)	EW (m)
68	1260	74	45	1259.89	13.13	0
69	1270	75	45	1269.88	13.31	0
70	1290	77	45	1289.88	13.66	0
71	1300	78	45	1299.88	13.83	0
72	1320	80	45	1319.88	14.18	0
73	1330	81	45	1329.87	14.35	0
74	1350	83	45	1349.87	14.7	0
75	1360	84	45	1359.87	14.88	0
76	1380	86	45	1379.87	15.23	0
77	1390	87	45	1389.87	15.4	0
78	1410	89	45	1409.86	15.75	0
79	1420	90	45	1419.86	15.93	0
80	1440	90	45	1439.86	16.27	0
81	1450	90	45	1449.86	16.45	0
82	1470	90	45	1469.85	16.8	0
83	1480	90	45	1479.85	16.97	0
84	1500	90	45	1499.85	17.32	0
85	1530	90	45	1529.84	17.85	0
86	1560	90	45	1559.84	18.37	0
87	1590	90	45	1589.84	18.89	0
88	1620	90	45	1619.83	19.42	0
89	1650	90	45	1649.83	19.94	0
90	1680	90	45	1679.82	20.46	0
91	1710	90	45	1709.82	20.99	0
92	1740	90	45	1739.81	21.51	0
93	1770	90	45	1769.81	22.03	0
94	1800	90	45	1799.8	22.56	0

Survey Station	MD (m)	Inc (°)	Azi (°)	TVD (m)	NS (m)	EW (m)
95	1830	90	45	1829.8	23.08	0
96	1860	90	45	1859.79	23.6	0
97	1890	90	45	1889.79	24.13	0
98	1920	90	45	1919.78	24.65	0
99	1950	90	45	1949.78	25.18	0
100	1980	90	45	1979.78	25.7	0
101	2000	90	45	1999.77	26.05	0

Well Paths

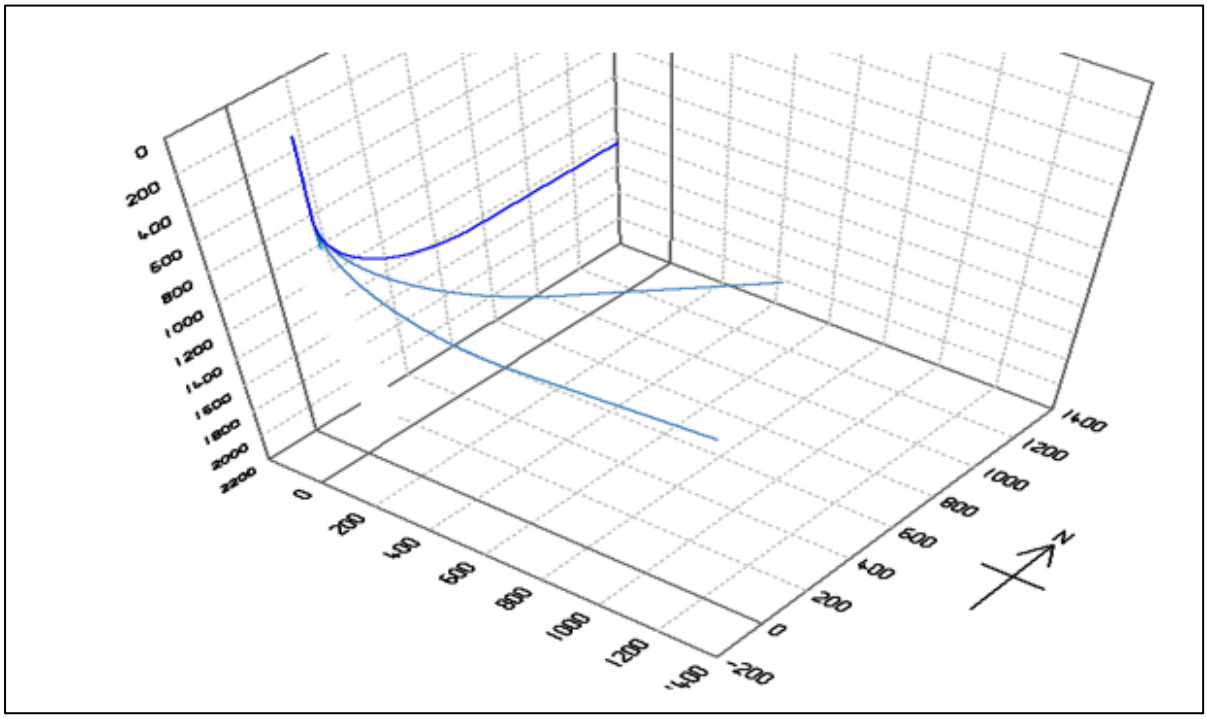

Figure C.10.1 - Well Paths from Compass

Appendix D

	Error Code	Propagation Mode	Error Magnitude	Units
1	drfs	S	1	m
2	dstg	G	0.00056	m
3	dsfs	S	2.5e-007	im
4	sag	S	0.08	deg
5	decg	G	0.15	dnt
6	dbhg	G	1500	dnt
7	MAL_1	S	0.1	deg
8	MAL_2	S	0.1	deg
9	MAL_3	S	0.1	deg
10	MAL_4	S	0.1	deg
11	MAL_5	S	0.1	deg
12	MAL_6	S	0.1	deg
13	Amil	S	300	nT
14	abxi	S	0.004	m/s^2
15	abzi	S	0.004	m/s^2
16	abxya_1	S	0.004	m/s^2
17	abxya_2	S	0.004	m/s^2
18	abza	S	0.004	m/s^2
19	asxyi_1	S	0.005	m/s^2
20	asxyi_2	S	0.005	m/s^2
21	asz	S	0.005	m/s^2
22	asxya_1	S	0.005	m/s^2
23	asxya_2	S	0.005	m/s^2
24	asxya_3	S	0.005	m/s^2

25	asz	S	0.005	m/s^2
26	mbxy_1	S	70	nT
27	mbxy_2	S	70	nT
28	mbz	S	70	nT
29	msxy_1	S	0.0016	
30	msxy_2	S	0.0016	
31	msxy_3	S	0.0016	
32	msz	S	0.0016	
33	mdi	G	0.1	deg
34	mfi	G	50	nT
35	abixy_1	S	0.004	m/s^2
36	abixy_2	S	0.004	m/s^2
37	abiz	S	0.004	m/s^2
38	asixy_1	S	0.0005	m/s^2
39	asixy_2	S	0.0005	m/s^2
40	asiz	S	0.0005	m/s^2
41	mbixy_1	S	70	nT
42	mbizy_2	S	70	nT
43	msixy_1	S	0.0016	
44	msixy_2	S	0.0016	
45	msixy_3	S	0.0016	

Appendix E

This Appendix provides the plots for Position Uncertainty resulting from individual error sources. The Semi major and Semi minor axis of the EOU's for all error sources have been plotted as a function of MD.

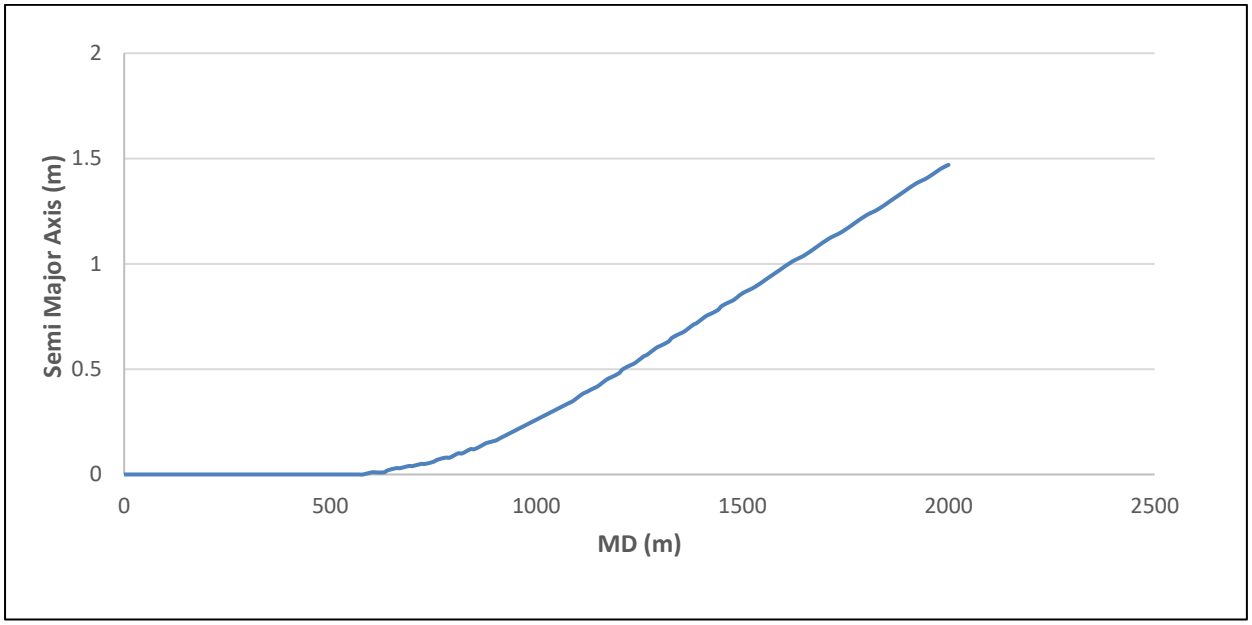

Figure E. 1 - Position Uncertainty due to Depth Errors

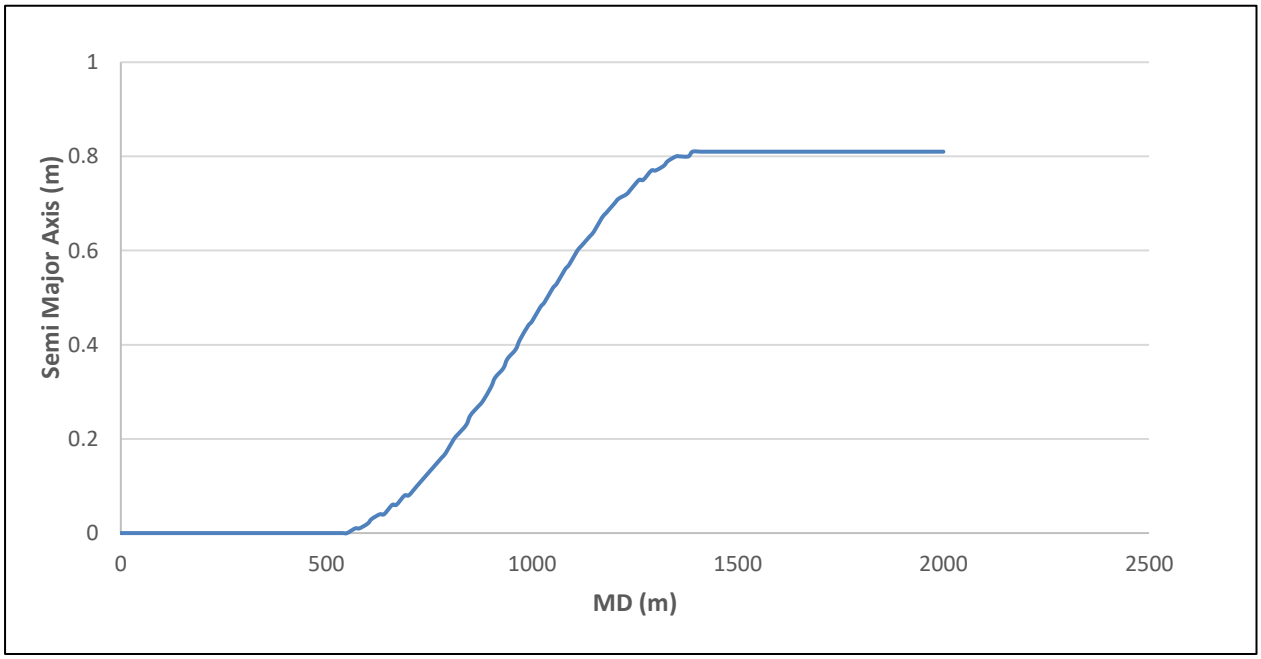

Figure E. 2- Position Uncertainty due to BHA Sag

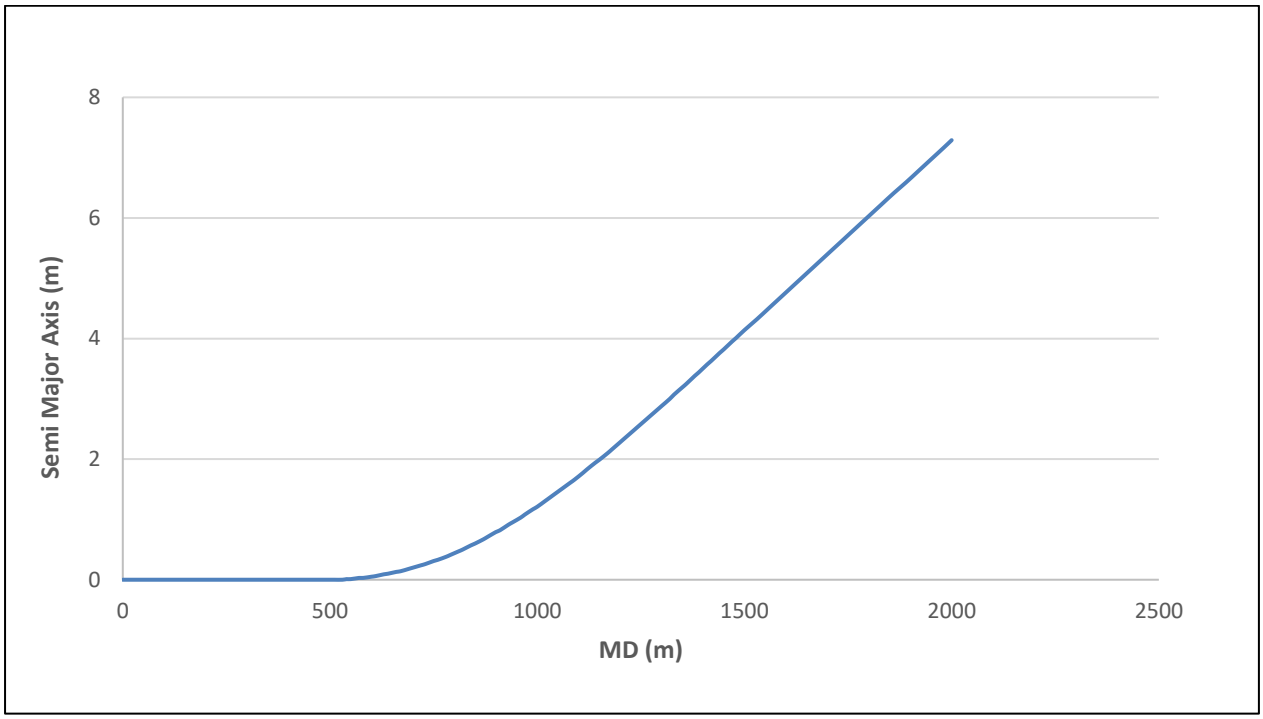

Figure E. 3- Position Uncertainty due to Declination Error

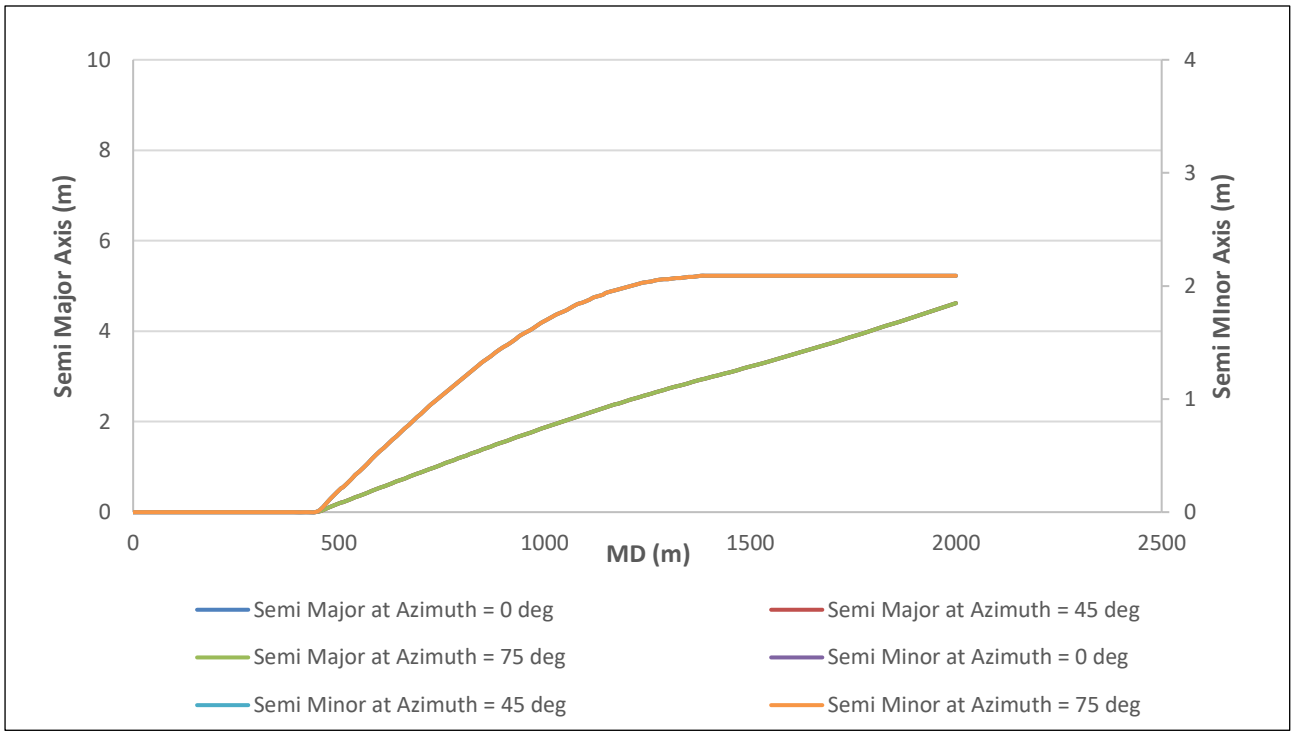

Figure E. 4- Position Uncertainty due to Tool Misalignment Errors

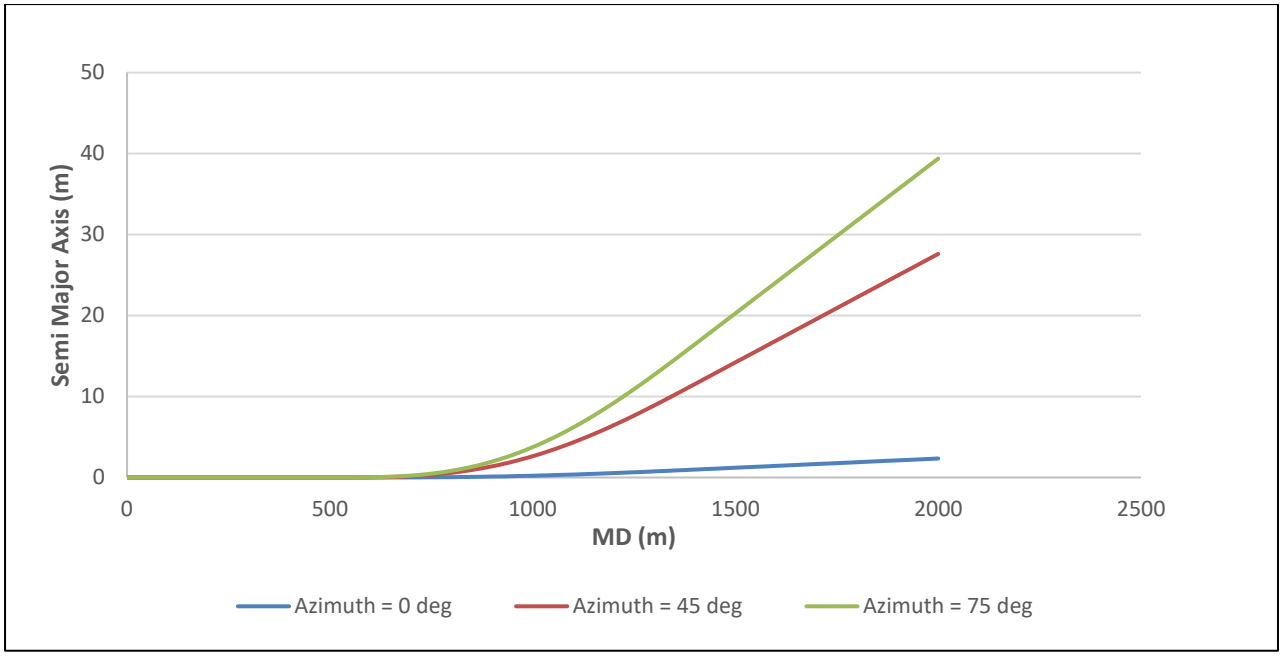

Figure E. 5- Position Uncertainty due to Magnetic Axial Drillstring Interference (AMIL)

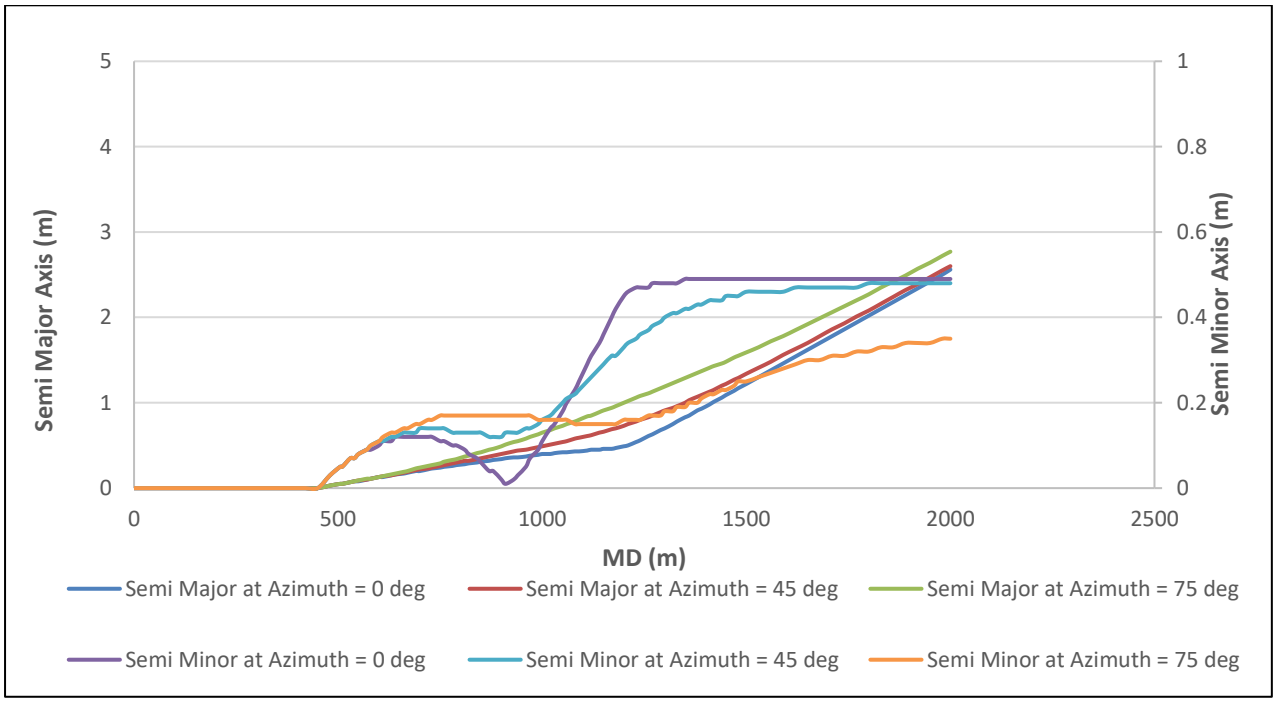

Figure E. 6- Position Uncertainty due to Accelerometer Bias (Non-mag)

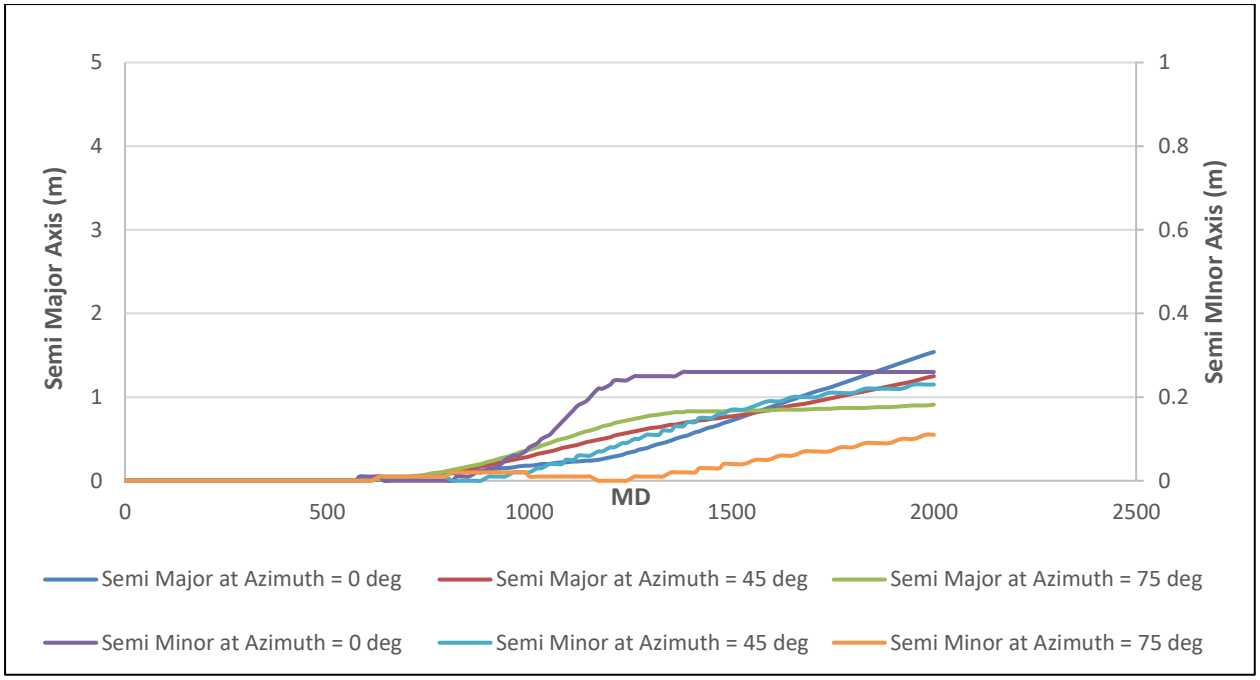

Figure E. 7 - Position Uncertainty due to Accelerometer Scale (Non-mag)

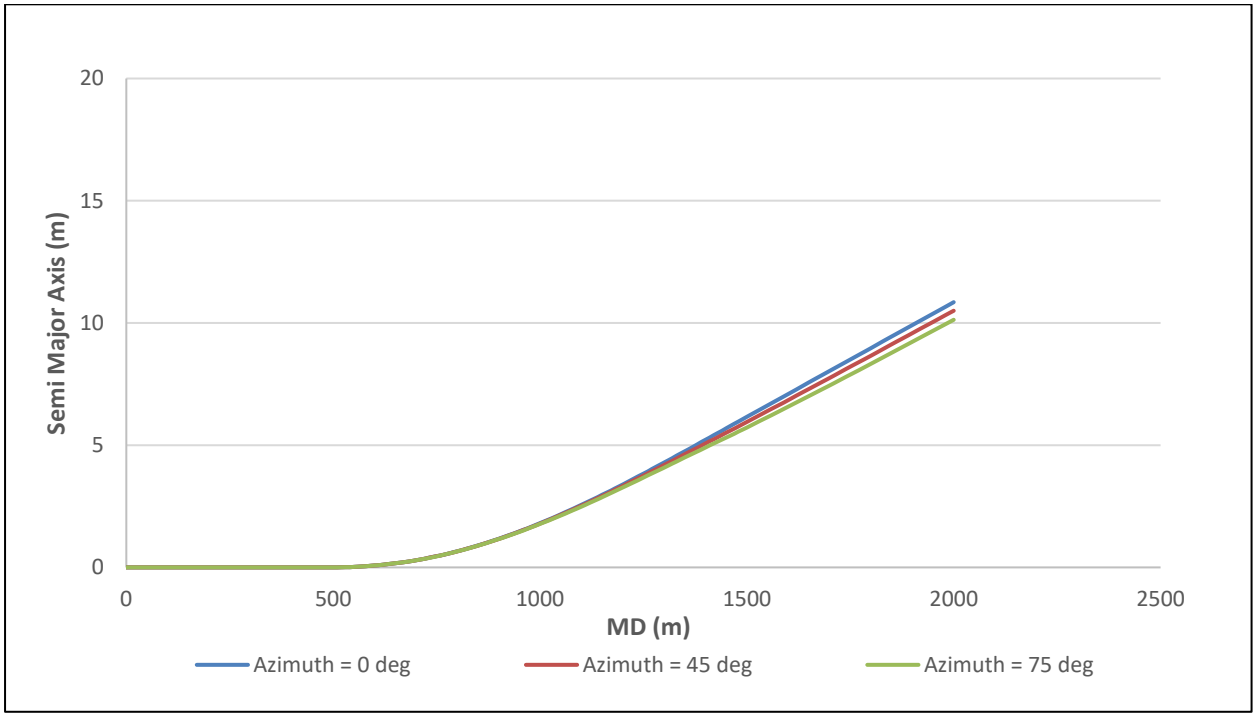

Figure E. 8- Position Uncertainty due to Magnetometer Bias (Non-mag)

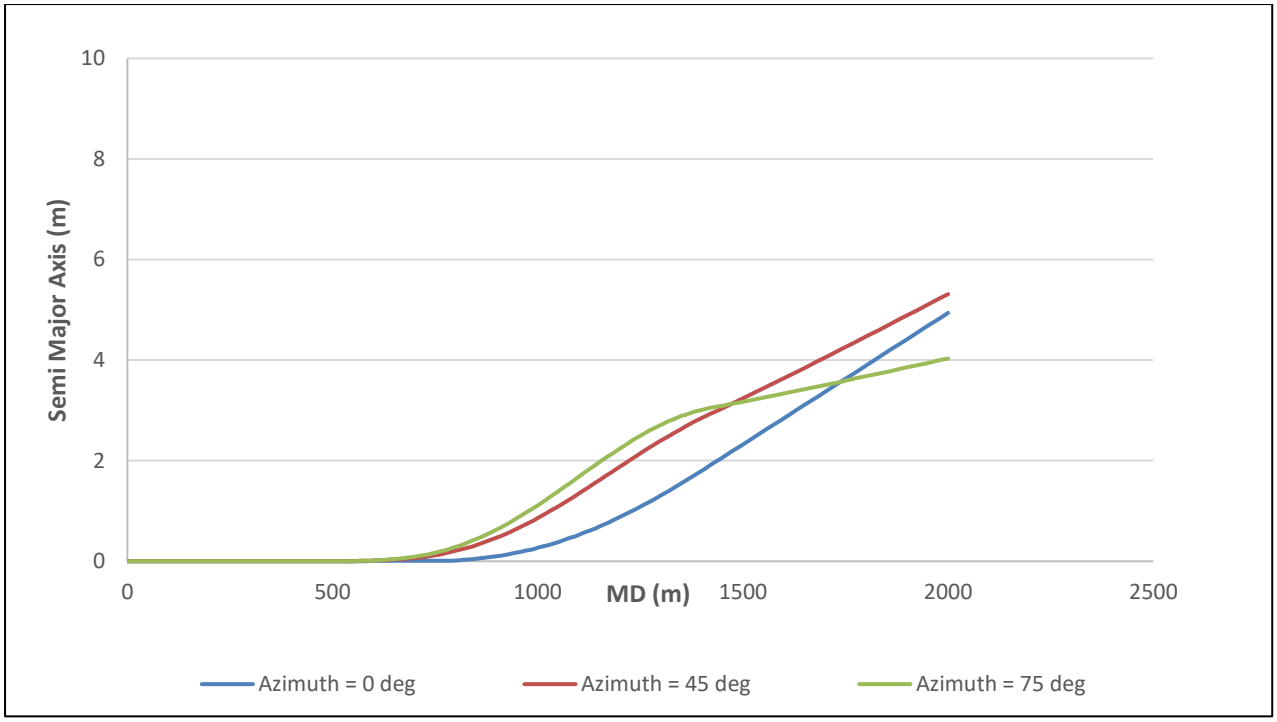

Figure E. 9 - Position Uncertainty due to Magnetometer Scale (Non-mag)

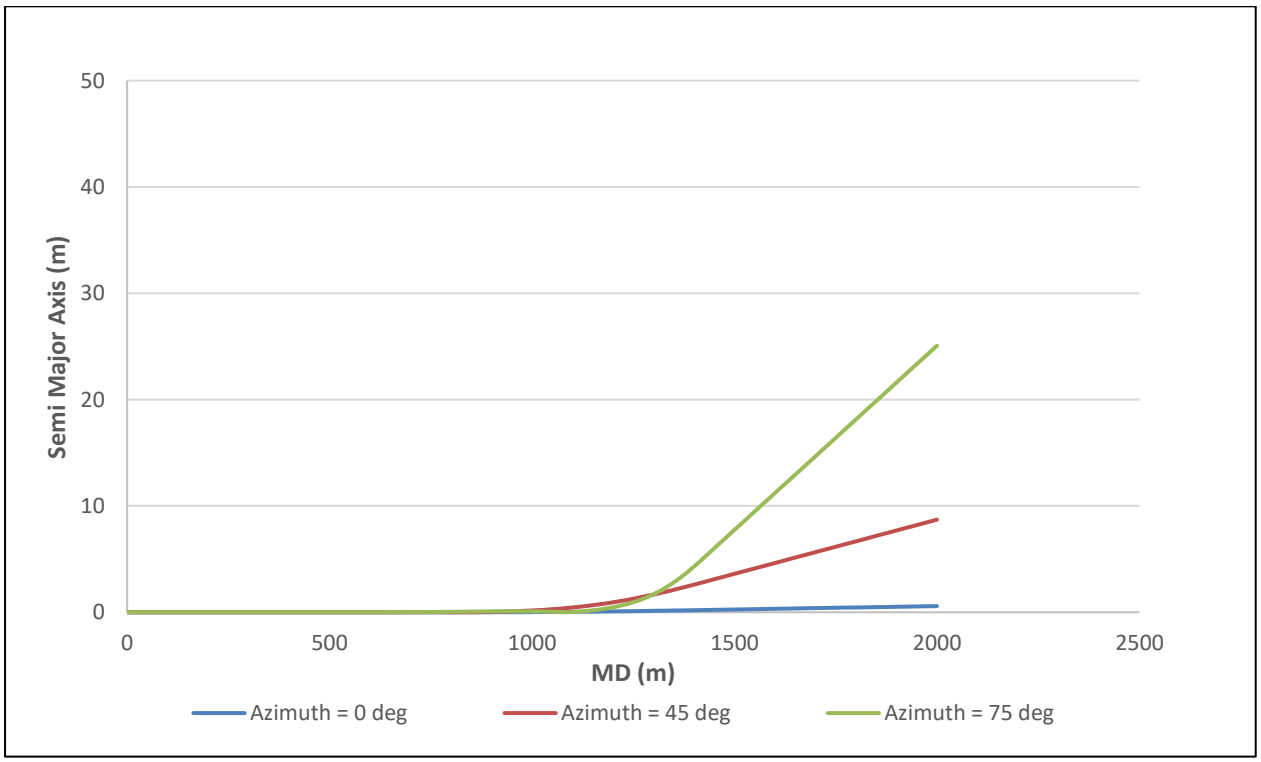

Figure E. 10- Position Uncertainty due to Magnetic Dip Angle (MDI)

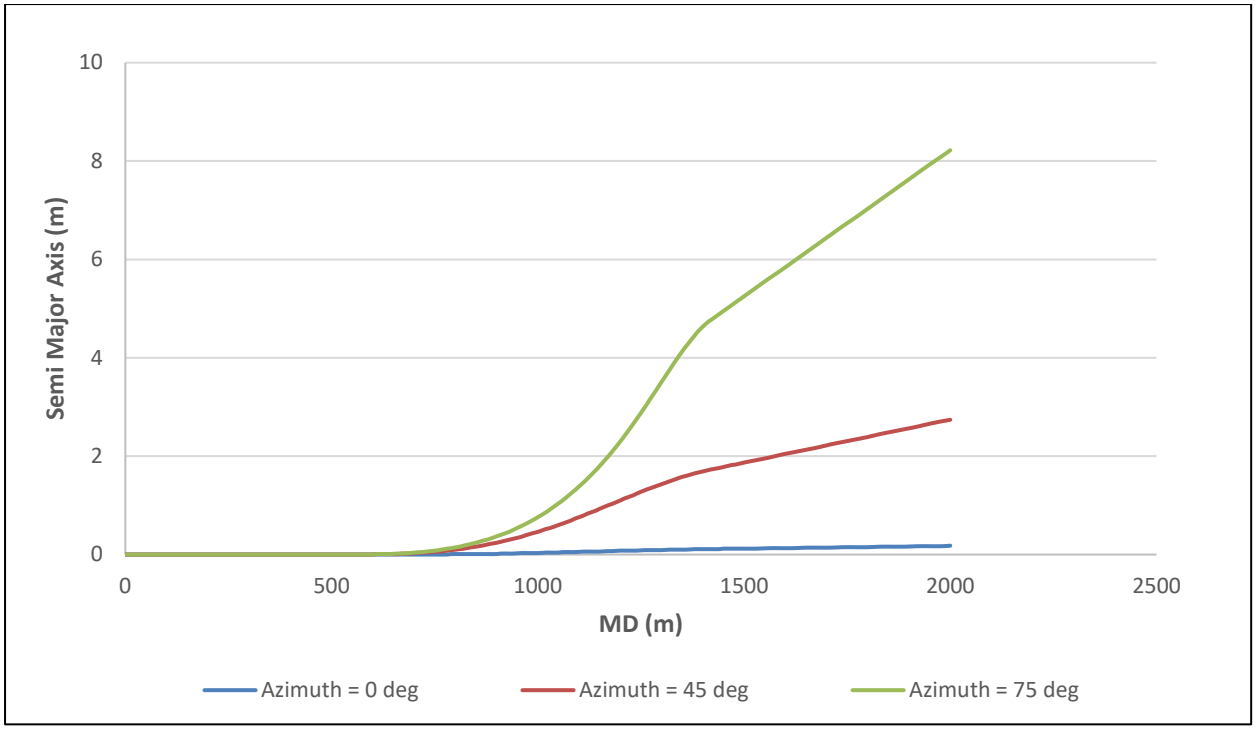

Figure E. 11- Position Uncertainty due to Magnetic Field Intensity (MFI)

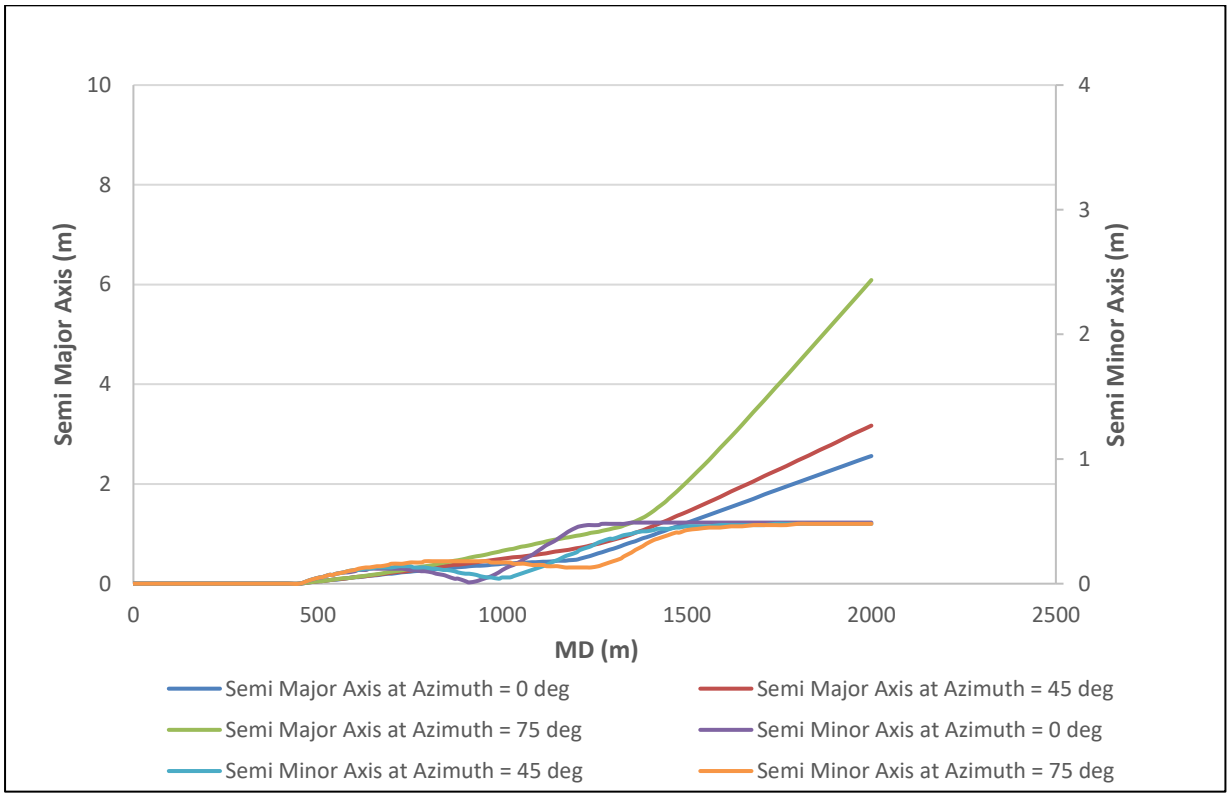

Figure E. 12 - Position Uncertainty due to Accelerometer Bias (Mag-corr)

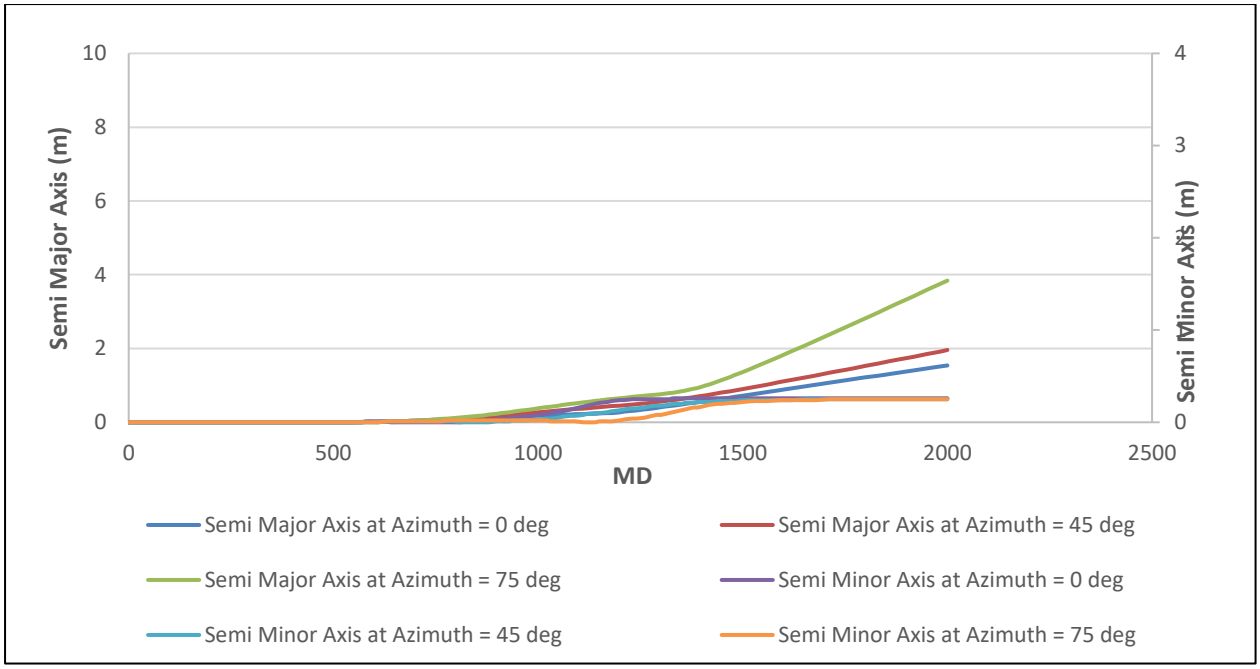

Figure E. 13- Position Uncertainty due to Accelerometer Scale (Mag-corr)

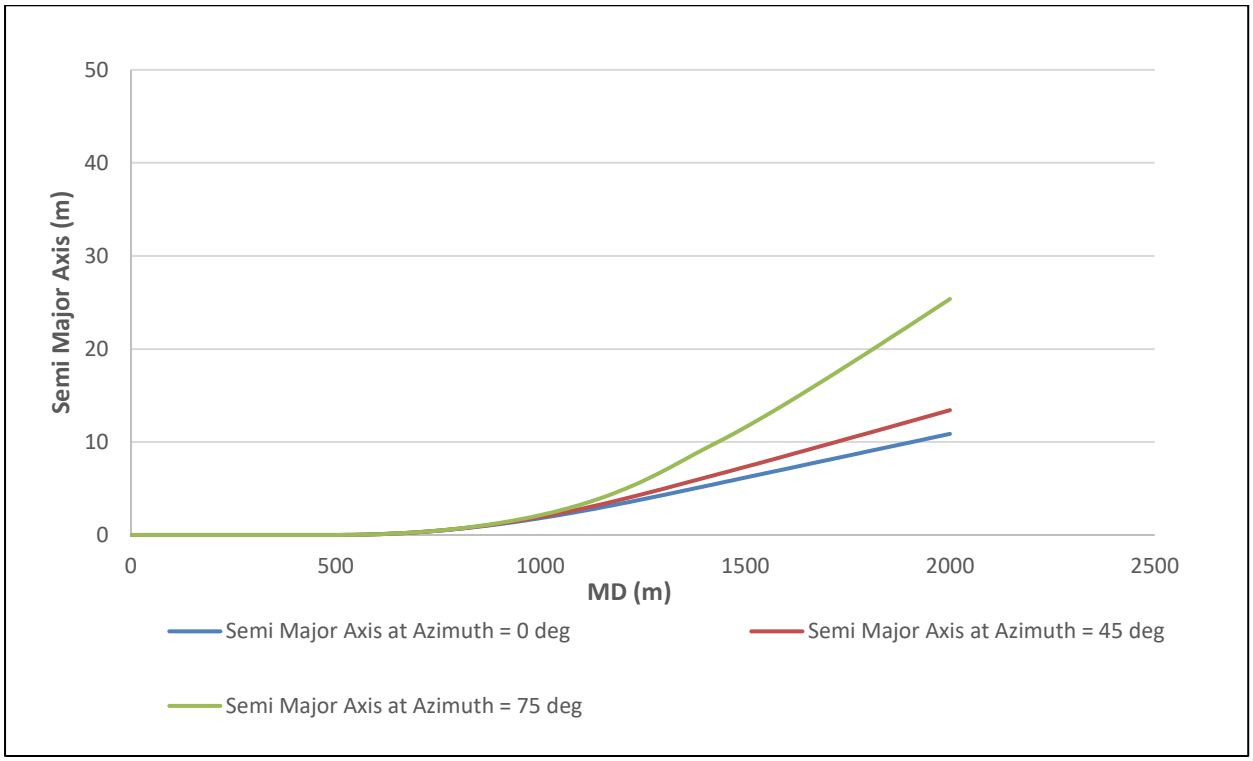

Figure E. 14- Position Uncertainty due to Magnetometer Bias (Mag-corr)

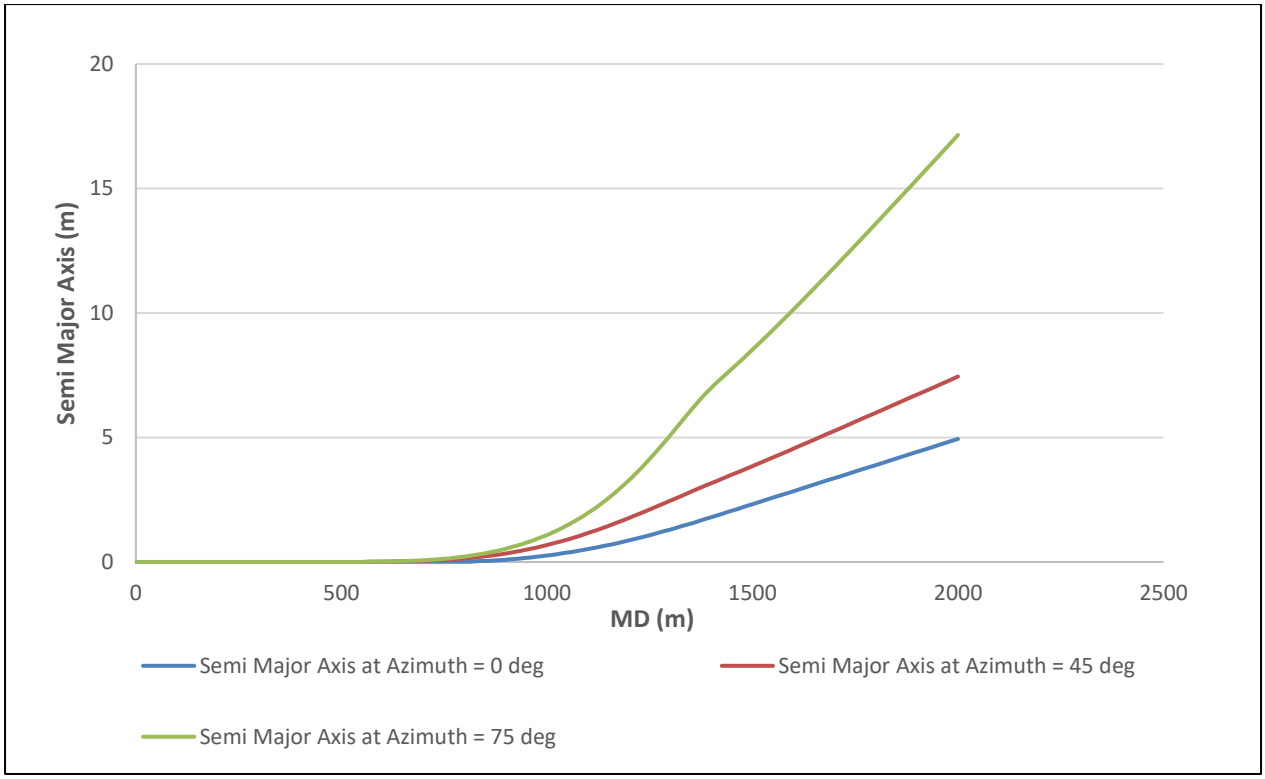

Figure E. 15- Position Uncertainty due to Magnetometer Scale (Mag-corr)

Appendix F

This Appendix will show step wise calculations of measurement errors resulting from different error sources. In this thesis, the errors with either global or systematic propagation modes have been used, therefore an example of each will be used to illustrate the calculation process.

Global Errors

Declination error will be used as an example to show how global measurement errors are calculated. Declination error is the resultant of two error terms, a constant declination error and B_h dependent declination error. The weighting functions and error magnitudes listed below are also provided in section 6.3 and Appendix D respectively.

Table F.1 - Weighting Function and Error Magnitude for Declination Error

Error Source	Weighting function	Error Magnitude
Constant Declination Error	1	0.15
B_h dependent Declination Error	$\frac{1}{B_t \cos(\Theta)}$	1500

General Approach

Measurement Error = Weighting function × Error Magnitude

Step 1:

Measurement Error of Constant Declination Error = $1 \times 0.15 = 0.15°$

Step 2:

Measurement Error of B_h dependent declination error = $\frac{1}{51000 \times \cos(75)} \times 1500 = 0.10°$

Where,

B_t = 51000 nt

$\Theta = 75°$

Step 3:

Total Dec Error = $\sqrt{0.15^2 + 0.10^2} = 0.18°$

Table F.2 - Calculation of Total Declination Error from two error terms

Survey Station	MD (m)	Inc (°)	Decg (°)	Dbhg (°)	Total Dec Error (°)
1	30	0	0.15	0.10	0.18
2	60	0	0.15	0.10	0.18
3	90	0	0.15	0.10	0.18
….	….	….	….	….	….
….	….	….	….	….	….
….	….	….	….	….	….
100	1980	90	0.15	0.10	0.18
101	2000	90	0.15	0.10	0.18

Note: Being a global error, declination error will have the same error magnitude throughout the well path and is independent of hole inclination or azimuth.

Systematic Errors

Magnetometer Cross-Axial Bias errors in the Non-mag error model will be used as an example to explain the calculation process of systematic errors. The weighting functions and error magnitudes have been listed in the table below.

Table F.3 - Weighting Function and Error Magnitude for Magnetometer Cross-Axial Bias

Error Source	Weighting function	Error Magnitude
Magnetometer Cross Axial Bias 1	$mbxy\_1 = \frac{-\cos(I)\sin(A)}{B_t \cos(\Theta)}$	70
Magnetometer Cross Axial Bias 2	$mbxy\_2 = \frac{\cos(A)}{B_t \cos(\Theta)}$	70
Magnetometer Cross Axial Bias along z-axis	$mbz = \frac{-\sin(I)\sin(A)}{B_t \cos(\Theta)}$	70

Using the weighting functions and error magnitudes above, the calculation process similar to global errors is also followed for systematic errors. The measurement errors will first be calculated for the three error terms separately and the final measurement error will be the statistical sum of the above three terms. The survey data for a North-South well will be used to illustrate the calculations for this error source in Table 3.

Table F.4 – Calculation of Magnetometer Cross Axial Bias in North-South well for Non-mag error model

Survey Station	MD (m)	Inc (°)	Azi (°)	mbxy_1	mbxy_2	mbz	Total Measurement Error
1	30	0	0	0	0.023	0.00	0.023
2	60	0	0	0	0.023	0	0.023
3	90	0	0	0	0.023	0	0.023
….	….	….	….	….	….	….	….
….	….	….	….	….	….	….	….
….	….	….	….	….	….	….	….
100	1980	90	0	0	0.023	0	0.023
101	2000	90	0	0	0.023	0	0.023

Note: Since a single tool is used for measurements throughout the well, therefore the resultant measurement errors are exactly same along the well. In case if different tools are used for different hole sections then the errors behave systematically along the respective hole sections.